



universität
wien

DISSERTATION / DOCTORAL THESIS

Titel der Dissertation /Title of the Doctoral Thesis

Wnt/ β -catenin signaling in the early development of
Nematostella vectensis.

verfasst von / submitted by

Isabell Niedermoser, MSc BSc

angestrebter akademischer Grad / in partial fulfilment of the requirements for the degree of

Doctor of Philosophy (PhD)

Wien, 2023 / Vienna 2023

Studienkennzahl lt. Studienblatt /
degree programme code as it appears on the student
record sheet:

UA 794 685 437

Dissertationsgebiet lt. Studienblatt /
field of study as it appears on the student record sheet:

Biologie / Biology

Betreut von / Supervisor:

Mag. Dr. Grigory Genikhovich, Privatdoz.

Acknowledgements	1
Abstract.....	2
Zusammenfassung	3
Introduction	4
Axial patterning.....	4
Body axes in development	4
cWnt in axis development	6
cWnt outside of early development	7
The membrane signaling complex of Wnt, Frizzled and LRP5/6	8
Wnt.....	8
Frizzled	9
LRP5/6.....	10
The canonical and the non-canonical Wnt signaling pathways and the promiscuity of the signaling components	12
<i>Nematostella</i> cWnt/ β -catenin dependent axis formation	15
<i>Nematostella vectensis</i> as a model organism	15
<i>Nematostella vectensis</i> cWnt signaling	16
Aims of the PhD project.....	17
Results.....	18
Chapter I: Analysis of the <i>Nematostella</i> Wnt-Fz signaling preferences in cell-culture	18
Results of the cell culture experiments.....	18
Proof of concept	19
<i>Nematostella</i> Fz+Wnt assays	21
Discussion	22
Conclusion.....	23
Materials and Methods.....	23
Paper I "Sea anemone Frizzled receptors play partially redundant roles in oral-aboral axis patterning."	26
Paper II "Cnidarian-bilaterian comparison reveals the ancestral regulatory logic of the β -catenin dependent axial patterning."	27
Paper III " β -catenin-dependent endomesoderm specification appears to be a Bilateria-specific co-option."	28
Discussion	29
Summary	29
Gastrulation and axial patterning.....	29
Endoderm specification.....	30

Receptor and ligand redundancy	32
Unresolved phenotypes	33
Enhanced β -catenin target gene expression at the midbody/aboral boundary.....	33
Simultaneous weakening and expansion of <i>Brachyury</i> expression	34
Outlook.....	34
Scientific contribution of the PhD project	35
References	36

Acknowledgements

First and foremost, I thank my parents for their unwavering support and love. None of this would have been possible without them. I cannot put into words how grateful and lucky I feel to have such fun and caring people in my life who provide such an incredible support system and safe haven I can rely on. They mean the world to me.

Thank you so very, very much.

I sincerely thank Grisha, my supervisor, mentor and the Brain to my Pinky, for giving me this chance and entrusting me with my project. I am truly grateful for his ceaseless support and incredible patience. I have learned so incredibly much from him that will continue to help me in all my future work and life in science and research. His wealth of knowledge, passion for his research, encouragement and humor fostered a group that felt like family.

I would also like to thank all the other past and current members of the Genikhovich group and the Technau group who made this experience so much more enjoyable.

In particular I would like to thank Paul, for being so welcoming from the very beginning and for being the person I could always run to, no matter how ridiculous the mishap or question. Special thanks to Tanya for dancing in the lab with me and special thanks to David for all his kind support and level-headedness.

I would also like to repeat my thanks to Johnathan Cooper-Knock who first allowed me to discover my love for wet-lab work and whose kind support gave me the confidence to follow my passion for science and research.

Many thanks to the FWF for funding this project and my TAC committee members Prof. Dr. Anna Kicheva and Prof. Dr. Elke Heiß. Special thanks to Prof. Dr. Elke Heiß and her team at the Department of Pharmacognosy, for supporting me in all my cell culture endeavors, especially Scarlet for teaching and helping me throughout the process. Special thanks also to the Vanhollebeke-lab for generously sharing their Fz-KO cells with us.

And finally, thanks to the magnificent LRP5/6, Frizzleds and Wnts for being such thrilling and beautiful research subjects. I will miss them dearly. I wish I could've continued studying them indefinitely. I know how special it is that I can say I had such a fun job and was excited to come to work in the lab every day.

Abstract

Canonical Wnt (cWnt) signaling fulfills critical roles in tissue and cell homeostasis, cell proliferation, cell fate determination and cancer. Importantly, it is also responsible for the patterning of the main body axis throughout Metazoa. cWnt signaling is initiated by binding of the Wnt ligand to Fz and LRP5/6 on the cell membrane, which represses β -catenin degradation and leads to its accumulation in the cell nucleus and transcriptional response. However, there is a bewildering variety of Wnt ligands and Fz receptors in Metazoa, and their individual functions are often unknown.

In this PhD thesis, I analyzed the roles of the cWnt signaling components in the axial patterning of the sea anemone *Nematostella vectensis*. As a member of the evolutionary sister group to Bilateria, the Cnidaria, this animal has become a powerful EvoDevo model for understanding the evolution of the axial patterning and germ layer formation mechanisms. This is why we wanted to understand the functions of the extremely wide *Nematostella* Wnt and Fz complement.

In cell culture, I analyzed preferential binding between all *Nematostella* Wnt ligands and Fz receptors. I also performed individual and combined knockdowns of all Wnt and Fz genes to understand their roles in the germ layer formation and axial patterning in the early embryos of my model sea anemone. I showed that Wnt/Fz/LRP5/6-mediated signaling is not required for the endomesoderm specification. This contradicts an accepted view that β -catenin signaling plays a conserved role in the definition of the endomesoderm in Cnidaria and Bilateria. However, strikingly, we showed by tagging the endogenous *Nematostella* β -catenin via a CRISPR/Cas9-mediated knock-in that, unlike in Bilateria, endomesoderm specification happens in the β -catenin-negative domain in *Nematostella*. In contrast, Wnt/Fz/LRP5/6-mediated signaling proved to be crucial for the axial patterning. I showed that all four *Nematostella* Fz receptors are involved in cWnt signaling and play partially redundant roles in the axial patterning. I also identified Wnt3 and Wnt4 as the most potent ligands responsible for the oral-aboral patterning in the early embryo of *Nematostella*. Finally, I contributed to the analysis of the patterning logic downstream of cWnt signaling.

Taken together, the results of this PhD significantly expand our understanding of the cWnt-dependent axial patterning in our model sea anemone and provide important comparative information. They suggest that cWnt signaling function in the axial patterning likely predated the cnidarian-bilaterian divergence, while β -catenin-dependent endomesoderm specification may have emerged as a bilaterian novelty.

Zusammenfassung

Die kanonische Wnt-Signalübertragung (cWnt) spielt eine entscheidende Rolle bei der Gewebe- und Zellhomöostase, der Zellproliferation, der Bestimmung des Zellschicksals und bei Krebs. Wichtig ist, dass sie auch für die Musterbildung der Körperachse in Metazoa verantwortlich ist. Das cWnt-Signal wird durch die Bindung des Wnt-Liganden durch Fz Rezeptoren und den Co-Rezeptor LRP5/6 an der Zellmembran ausgelöst, was die Degradation von β -catenin unterdrückt und zu dessen Akkumulation im Zellkern und einer transkriptionellen Reaktion führt. Allerdings gibt es eine verwirrende Vielfalt von Wnt-Liganden und Fz-Rezeptoren in Metazoa, und ihre individuellen Funktionen sind oft unbekannt.

In dieser Dissertation habe ich die Rolle der cWnt-Signalkomponenten bei der axialen Musterbildung der Seeanemone *Nematostella vectensis* untersucht. Als Mitglied der Nesseltiere (Cnidaria), der evolutionären Schwestergruppe zu Zweiseitentiere (Bilateria), ist dieses Tier ein wichtiges EvoDevo-Modell für die Evolution der Mechanismen der Achsenmusterbildung und der Keimschichtbildung geworden. Aus diesem Grund wollten wir die Funktionen des extrem breiten Wnt- und Fz-Komplements von *Nematostella* besser verstehen.

In Zellkultur analysierte ich die bevorzugten Bindungspartner zwischen allen *Nematostella* Wnt-Liganden und Fz-Rezeptoren. Außerdem habe ich in *Nematostella* einzelne und kombinierte Knockdowns aller Wnt- und Fz-Gene durchgeführt, um ihre Rolle bei der Bildung der Keimschicht und der axialen Musterbildung in den frühen Embryonen meiner Modellseeanemone zu verstehen. Ich konnte zeigen, dass die Wnt/Fz/LRP5/6-vermittelte Signalübertragung für die Endomesoderm-spezifikation nicht erforderlich ist. Dies widerspricht der gängigen Meinung, dass die β -catenin-Signalübertragung eine konservierte Rolle bei der Definition des Endomesoderms in Cnidaria und Bilateria spielt. Im Gegensatz konnten wir durch die Markierung des endogenen β -catenins in *Nematostella* mittels CRISPR/Cas9-Knock-in zeigen, dass die Endomesoderm Spezifikation in *Nematostella*, anders als bei Bilateria, in der β -catenin-negativen Domäne stattfindet. Allerdings erwies sich das Wnt/Fz/LRP5/6-vermittelte Signal als entscheidend für die axiale Musterbildung. Ich zeigte, dass alle vier Fz-Rezeptoren von *Nematostella* an der cWnt-Signalübertragung beteiligt sind und teilweise redundante Rollen bei der axialen Musterbildung spielen. Außerdem identifizierte ich Wnt3 und Wnt4 als die stärksten Liganden, die für die oral-aborale Musterung im frühen Embryo von *Nematostella* verantwortlich sind. Schließlich war ich an der Analyse der Transkriptionsfaktor basierten Musterbildungslogik beteiligt, die auf die cWnt-Signalaktivierung an der Membran folgt.

Insgesamt erweitern die Ergebnisse dieser Doktorarbeit unser Verständnis der cWnt-abhängigen axialen Musterbildung in unserer Modell-Seeanemone erheblich und liefern wichtige vergleichende Informationen. Sie deuten darauf hin, dass die Beteiligung des cWnt-Signals an der axialen Musterbildung wahrscheinlich der evolutionären Trennung von Cnidaria und Bilateria vorausging, während die β -catenin-abhängige Endomesoderm-Spezifikation als eine Neuheit innerhalb der Bilateria entstanden sein könnte.

Introduction

Axial patterning

Body axes in development

Complex networks of cell signaling pathways drive the appropriate spatiotemporal arrangement of cells during the development of multicellular organisms. Gene regulatory networks (GRNs) coordinate these pathways in the establishment of embryonic body plans and are governed by mechanochemical cues from the oocyte and environment (Hannezo & Heisenberg, 2019). Many of the signaling pathways employed by these gene regulatory networks are highly conserved across Metazoa. The conserved repertoire of cell signaling pathways which engineer metazoan development encompasses the Notch, TGF β (Transforming growth factor β), Wnt, Hedgehog, JAK/STAT (Janus kinase/Signal transducer and activator of transcription), RTK (Receptor tyrosine kinase) and nuclear hormone signaling pathways (Erwin & Davidson, 2009; Pires-daSilva & Sommer, 2003).

When the body of an organism forms, one of the first emerging features in embryonic development is an axis running from one given pole to another. This primary axis is the AV (animal-vegetal) axis of the unfertilized egg (Gilbert, 2000). In the developing zygote it usually corresponds to the AP (anterior-posterior) and OA (oral-aboral) axes of the respective organism (Anlas & Trivedi, 2020). Confusingly, this main definitive body axis of the animal is also called the primary body axis - the term I will also be using below for simplicity. One of the best-known pathways involved in the primary axis development is canonical Wnt/ β -catenin signaling (cWnt/ β -catenin). It is responsible for the formation of the posterior and patterning of the primary axis (Petersen & Reddien, 2009). It is also a common feature that Wnt ligand expression is at a maximum at one of the axis poles in early development, the pole at which gastrulation occurs (Isaeva & Kasyanov, 2021; Petersen & Reddien, 2009) (Fig. 1.). In bilaterally symmetric organisms such as Bilateria or anthozoan Cnidaria (sea anemones, corals), a secondary body axis can emerge. In Bilateria, this secondary axis is called the dorso-ventral (D-V) axis, and it arises simultaneously with the A-P axis (Beddington & Robertson, 1999). In contrast, in anthozoan Cnidaria the secondary, "directive" axis arises after the formation of the primary, oral-aboral axis (Genikhovich et al., 2015). Although both the DV and the directive axis are patterned by BMP (Bone morphogenetic protein) signaling, it remains disputed whether they are homologous to each other (Genikhovich et al., 2015; Greenfeld et al., 2021). This thesis, however, will only consider the primary, cWnt-dependent body axis.

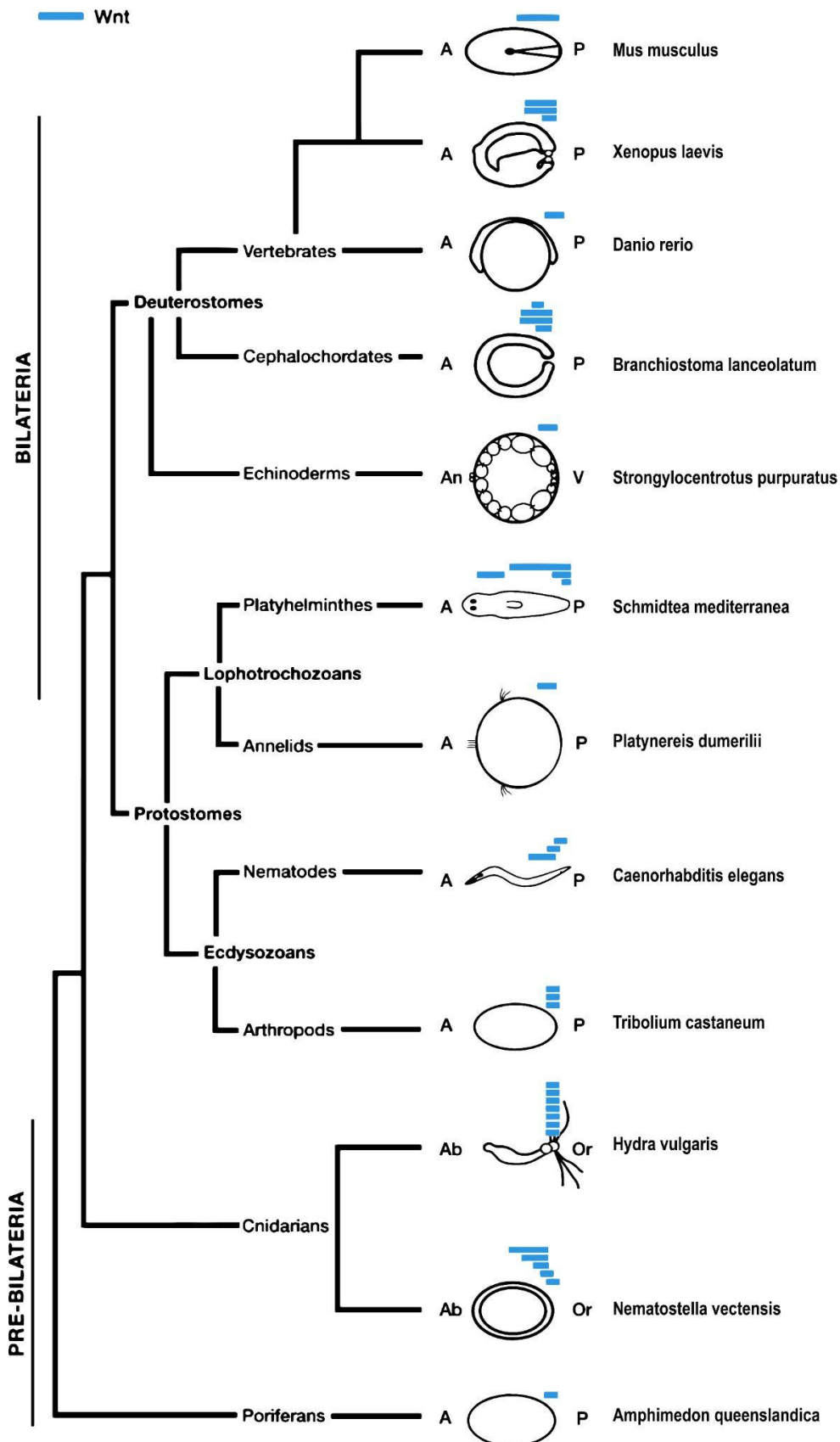


Figure 1. Wnt expression maxima at the pole of gastrulation is a common theme across Metazoa. Blue rectangles indicate Wnt expression domains along the A-P axis. A=anterior, P=posterior, An=animal, V=vegetal, Or=oral, Ab= aboral. Reproduced from Petersen & Reddien (2009).

cWnt in axis development

It has been demonstrated in multiple organisms that manipulation of Wnt and β -catenin leads to aberrations of the primary axis (Hikasa & Sokol, 2013; Petersen & Reddien, 2009; Sumanas et al., 2000; Wylie et al., 2014). Local cWnt signal enhancement commonly results in formation of ectopic or duplicated axes (McMahon & Moon, 1989; Petersen & Reddien, 2009; Sumanas et al., 2000; Tamai et al., 2000; Wu et al., 2009), whereas a loss-of-function (LOF) commonly results in the failure to form a viable axis (Huelsenken et al., 2000; P. Liu et al., 1999). In many organisms, the upregulation of β -catenin signaling leads to a posteriorized phenotype (Darras et al., 2018; Duffy et al., 2010), whereas the downregulation of cWnt leads to an anteriorized phenotype (Darras et al., 2018; Iglesias et al., 2008; Loh et al., 2016; Mao et al., 2001). Axis determination as well as initiation of gastrulation and cell fate specification often rely on maternally deposited components (Momose et al., 2008; Swartz et al., 2021; Tao et al., 2005; Vastenhouw et al., 2019), which is also the case for some cWnt mediated processes. The most well-known axis modulatory and maternally deposited Wnts are the *Xenopus* Wnt11 (Tao et al., 2005), zebrafish Wnt8a (Lu et al., 2011), sea urchin Wnt16 (Martinez-Bartolomé & Range, 2019) and, for cnidarians, CheWnt3 in *Clytia hemispherica* (Momose et al., 2008). In *Xenopus* maternal Wnt11, one of the earliest Wnts identified as critical to early development (Tao et al., 2005), is positioned vegetally in the egg, yet post fertilization this Wnt11 mRNA moves to the dorsal side and allows for β -catenin stabilization there (Weaver & Kimelman, 2004). Cha et al. (2009) found that complexes of Wnt5a/Wnt11 are responsible for *Xenopus* primary axis formation, whereas in zebrafish maternal Wnt8a was found to play this role (Lu et al., 2011). CheWnt3 is the only maternally deposited Wnt mRNA in *Clytia hemispherica*, and it is also the Wnt required for O-A axis patterning in this animal (Momose et al., 2008). Cell adhesion tension, (i. e. mechanical stretching) can cue gastrulation and β -catenin signaling as well (Brunet et al., 2013; Muncie et al., 2021). Mechanosensory modes of axis induction have been demonstrated in various species, including *Nematostella* (Pukhlyakova et al., 2018; Schwarz & Hadjantonakis, 2020). Röper and colleagues (2018) found that mechanical stretching facilitated access to the highly conserved Src-kinase target site of β -catenin at Tyrosine 654 in mouse, the subsequent phosphorylation of which can trigger β -catenin nuclearization and signaling (Brunet et al., 2013; Röper et al., 2018). The other monumental event in body plan formation, next to the formation of a primary axis, is the specification of the germ layers. In Bilateria, this refers to the differentiation and development of endo-, meso- and ecto-derm and in diploblastic metazoa the ecto- and endomesoderm, although other views on the identities of the cnidarian germ layers exist (Steinmetz et al., 2017). The body axis related role of cWnt is closely linked to ectodermal regulation, and in many Bilateria it has been shown that Wnt plays a role in the endodermal development as well (Darras et al., 2011; Hudson et al., 2013; McCauley et al., 2015; Range et al., 2013). In many organisms, not only does cWnt demarcate the site of gastrulation, it also regulates the EMT (Epithelial to Mesenchymal Transition) (Debnath et al., 2021). The exact mechanisms by which cWnt regulates endoderm development can vary, depending on organism and tissue context. For example, in *Xenopus*, nuclear β -catenin can act together with the transcription factor (TF) SOX17 to activate endoderm GRNs at certain enhancers yet be suppressed by SOX17 at other enhancer sites (Mukherjee et al., 2020). In zebrafish, correct SOX2 and Wnt interactions are responsible for EMT and proper mesoderm formation (Kinney et al., 2020). β -catenin can act together with some FOX TFs in driving EMT (Zheng et al., 2019) or be acted upon by other FOX TFs, suppressing EMT (Liu et al., 2015).

Though individual co-factors and mechanistic function may differ in these contexts, in Bilateria the general sequence of events of the primary tissue differentiations has been demonstrated in many organisms (Hudson et al., 2013). Firstly, the split between ectoderm and endomesoderm takes place; where the ectoderm is characterized by the lack of β -catenin nuclearization (Hudson et al., 2013). The endomesoderm is initially defined by β -catenin activity which remains active in the endoderm whilst being turned off in the resulting mesoderm in many phyla (Hudson et al., 2013), with some exceptions (Favarolo & López, 2018).

cWnt outside of early development

cWnt-mediated patterning is not only a key regulator of the establishment and patterning of the body axes, germ layer formation and other crucial processes during embryogenesis. Adult tissue homeostasis and repatterning are also driven by it (Pond et al., 2020). Thus, another avenue of study concerning body axis patterning mediated by cWnt signaling is that of regeneration (Warner et al., 2020). There are now numerous studies that have demonstrated the involvement of cWnt signaling in wound healing and regeneration of wound induced loss of body parts (Gufler et al., 2018; Hobmayer et al., 2000; Kawakami et al., 2006; Owlarn & Bartscherer, 2016; Whyte et al., 2012). As is the case in axial patterning, cWnt factors promote a posterior identity whilst Wnt-antagonists support anterior identities in regeneration as well (Duffy et al., 2010; Gurley et al., 2008; Petersen & Reddien, 2008). Wnt inhibition is presumed to perturb recruitment of cells to the wound blastema, inhibiting regeneration in various tissues and species, including mammals (Whyte et al., 2012). On the contrary, overexpression of Wnt in wounding/amputative processes can incur above-average healing/regenerative processes in tissue which otherwise would not display such regenerative capacity (Whyte et al., 2012).

Wound infliction triggers Wnt expression. This immediate response can be caused by hypoxia induced HIF1 α (Whyte et al., 2012), MAPK/ERK activation through reactive oxygen species and Ca⁺ (Tursch et al., 2022), Hedgehog signaling (De Robertis, 2010), the triggering of FOX TFs (Scimone et al., 2014) or also through a mechanical mode via wound constriction (Sinigaglia et al., 2020). Tursch et al. (2022) proposed that the Wnt response is a positionally independent injury-response, and the consequent regeneration of posterior versus anterior structures/tissues depends on the inherent β -catenin background level of the wound-adjacent tissue. Factors proposed to drive cWnt expression in early development, such as FOX TFs, also appear to drive cWnt in the context of regeneration (Pascual-Carreras et al., 2023), which is a feature found in the context of cancer as well (Koch, 2021).

The Wnt response is specifically linked to wound induced regeneration. This has been demonstrated by famous non-injuring amputations, in which the tying off of a body part with a hair until it becomes detached allows for amputation without severing tissue (Guder et al., 2006; Newman, 1974). Such studies showed that without an injury stimulus regeneration was not induced, which is speculated to be due to the epithelium remaining intact (Tursch et al., 2022).

The proliferative nature of β -catenin signaling in developmental and regenerative growth is also reflected by its role in tumor growth and its function as a proto-oncogene (Semaan et al., 2019; Zhan et al., 2017). cWnt is a major topic in cancer research and there is a wealth of data showing that mutations in cWnt pathway signaling components are found in many

studied cancers (Jackstadt et al., 2020). This makes a better understanding of cWnt function ever more impactful and necessary.

The membrane signaling complex of Wnt, Frizzled and LRP5/6

Wnt

Wnts are secreted lipoglycoproteins which carry numerous cysteines in distinct, highly conserved patterns which form intra- and intermolecular disulfide bonds critical to their folding structure and functional activity as ligands (Logan & Nusse, 2004; MacDonald et al., 2014; Willert et al., 2003; Willert & Nusse, 2012). Their characteristic cysteine-rich composition renders their resemblance to a hand, made up of an "index finger" and "thumb" linked by a "palm" (Fig. 2A) (Janda et al., 2012). Wnts undergo multiple post-translational modifications prior to secretion which further influence their functionality such as the linkage of palmitate to a conserved serine, which is the characteristic lipid extending from the "thumb", and glycosylation (Bänziger et al., 2006; Bartscherer et al., 2006; Coombs et al., 2010; Janda et al., 2012; Kurayoshi et al., 2007; Lu, 2018; Port & Basler, 2010; Takada et al., 2006; Tang et al., 2012). The palmitoleate of Wnt has been shown to be critical in its processing, transport and eventual signaling through receptor interaction (Galli et al., 2007; Komekado et al., 2007; Nile & Hannoush, 2016). Although Wnts are characteristically well conserved, the linker region between the N-terminal and C-terminal domains is highly variable across Wnts and is postulated to play a role in conferring differential selectivity and specificity to the different receptors they interact with (Hirai et al., 2019; Tsutsumi et al., 2022; Willert & Nusse, 2012).

Although the scheme in Figure 2A shows a highly exposed lipid moiety, *in vivo* it would require some shielding from the aqueous environment for Wnts to move away from the cell they are secreted from to carry out any long range morphogen activity (Mulligan et al., 2012). This protective feature is postulated to be carried out by potential carriers/chaperones or membrane interactions in the extracellular environment (McGough et al., 2020; Mulligan et al., 2012; Willert & Nusse, 2012). The movement in the extracellular environment post-secretion can be regulated by a multitude of mechanisms, differing by organism and tissue (Port & Basler, 2010). Studies have shown that HSPGs (Heparan sulfate proteoglycans), lipoprotein particles, exosomes and cytonemes can carry out the extracellular transport of Wnt (Mehta et al., 2021).

Next to the many "supportive" partners in the extracellular matrix, Wnts also face an array of antagonists. WIF (Wnt inhibitory factor) which binds and sequesters Wnts (Poggi et al., 2018), TIKI, a protease capable of cleaving Wnt N-terminal regions (Zhang et al., 2012) and Notum, a serine hydrolase, which can remove the palmitoleate (Kakugawa et al., 2015) are only some of the extracellular modulators secreted Wnts may encounter.

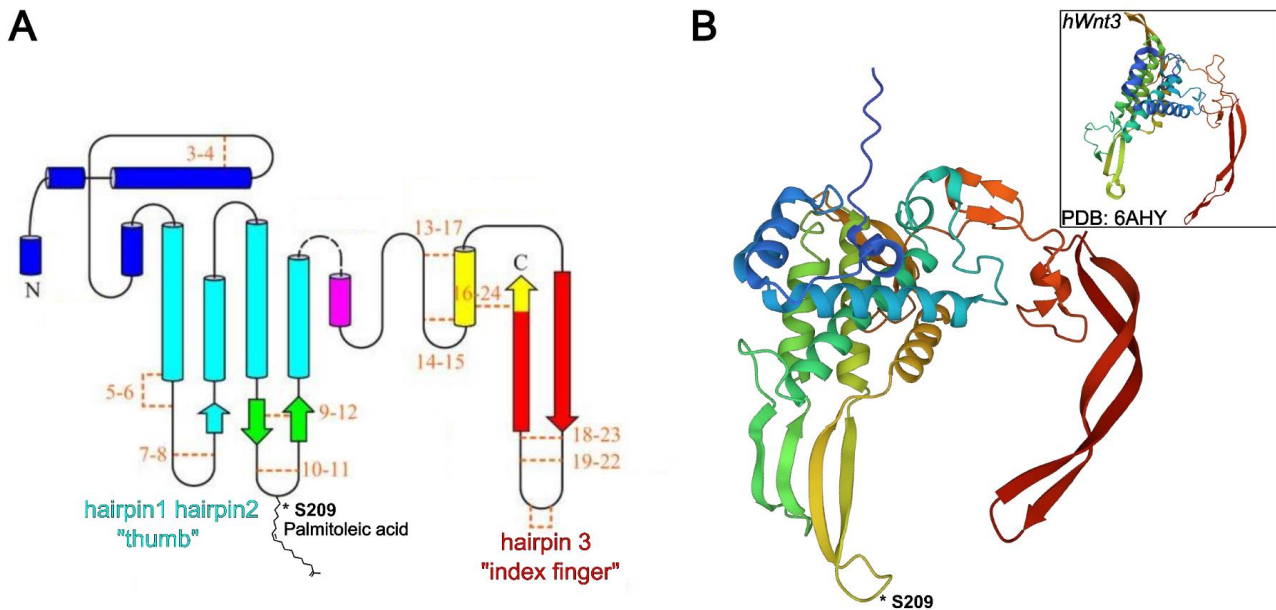


Figure 2. Wnt ligand structure.

(A) The topology of Wnts. Often the analogy of a hand is used when describing the three-dimensional structure of Wnts where two hairpins form a "thumb" from which the palmitoleic acid modification protrudes and a "palm" links it to another hairpin representing an "index-finger" (Janda et al., 2012; MacDonald et al., 2014). The highly conserved cysteines and disulfide bonds are indicated by orange dashed lines. The conserved palmitoleic acid at S209 in hWnt3a and NvWnt3 is indicated by an asterisk. Reproduced from MacDonald et al. (2014). **(B)** The AlphaFold (Jumper et al., 2021) prediction of *Nematostella* Wnt3 using the AlphaFold ColabFold notebook (Mirdita et al., 2022) with the structure of human Wnt3 deposited in the Protein Data Bank (PDB, Berman et al., 2000) (6AHY, Hirai et al., 2019) in the top right corner for comparative visual reference.

Frizzled

Frizzled (Fz) receptors are seven-pass transmembrane receptors of the F-family of GPCRs (Schulte & Bryja, 2007; Schulte & Wright, 2018). Their N-terminal CRD (cysteine rich domain) holds 10 highly conserved cysteines (Pei & Grishin, 2012) and their intracellular loops and tail hold interaction sites for the intracellular master regulator Dishevelled (MacDonald & He, 2012) as well as sites regulating interactions with other signaling co-factors (such as EGFR) (Grainger et al., 2018). The Fz-determining KTxxxW motif (Fig. 3A) is essential for cWnt signal transduction, as any mutation therein abrogates cWnt signaling (Umbhauer et al., 2000). It is required for Dishevelled sequestration and phosphorylation (Umbhauer et al., 2000). Fz structures and sequences are highly conserved, apart from the intrinsically disordered linker region between the membrane and the CRD, which can play a role in conferring specificity and selectivity (Eubelen et al., 2018; Ko et al., 2022).

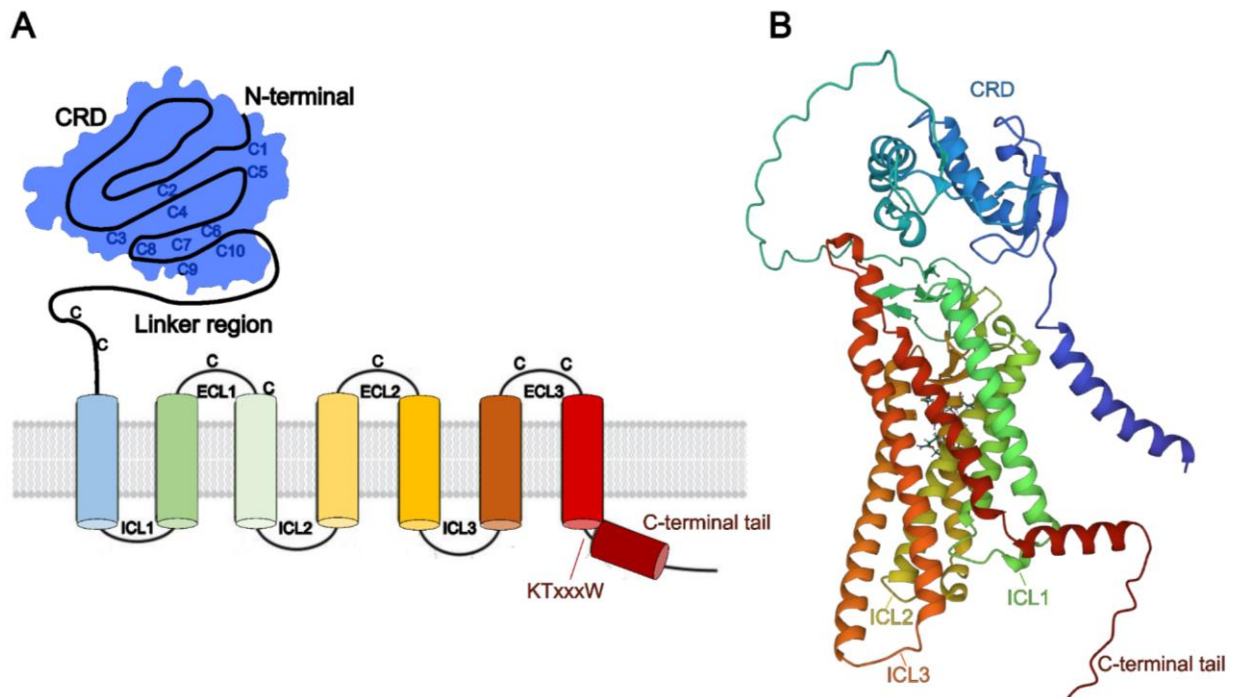


Figure 3. Frizzled receptors.

(A) Domain topology of Fz receptors. The KTxxxW motif in the carboxy-terminal tail is characteristic of Frizzled receptors and necessary for their cWnt signaling function and interaction with Dishevelled. CRD: Cysteine rich domain, ECL: Extracellular loop, ICL: Intracellular loop, C: highly conserved cysteine residues. Reproduced from MacDonald & He (2012). **(B)** AlphaFold prediction of *Nematostella* Fz5 structure using the AlphaFold ColabFold notebook (Mirdita et al., 2022). There is no crystal structure of untagged/unmodified Fz deposited in the PDB, which I could show for comparison.

LRP5/6

The third party in the ternary membrane complex of cWnt signaling is the co-receptor LRP5/6 (low-density lipoprotein receptor-related protein 5 and 6). It is a large receptor with a single transmembrane domain and four characteristic extracellular propellers and an intracellular tail critical for signaling (Fig. 4A) (Brennan et al., 2004; MacDonald et al., 2011; Metcalfe et al., 2010; Mi & Johnson, 2005; Piao et al., 2008). Although all of the propellers are YWTD-type β -propellers formed by six YWTD repeats, the sequence similarity across the four is relatively low, which is presumed to underlie their individual binding specificities to extracellular modulators and Wnts (Bourhis et al., 2010; Cheng et al., 2011; MacDonald & He, 2012; Matoba et al., 2017). In 2022 Tsutsumi et al. demonstrated that differences of binding to either the E1-E2 versus E3-E4 propeller domains of LRP5/6 by distinct Wnts (and Wnt modulators) (Fig. 4A) was due to the interactions of the linker domain and N-terminus of Wnts (Fig. 2A) with the LRP6 propellers (Tsutsumi et al., 2022). These linker regions in Wnts also happen to be less well conserved between different Wnts compared to their otherwise high conservation (Tsutsumi et al., 2022).

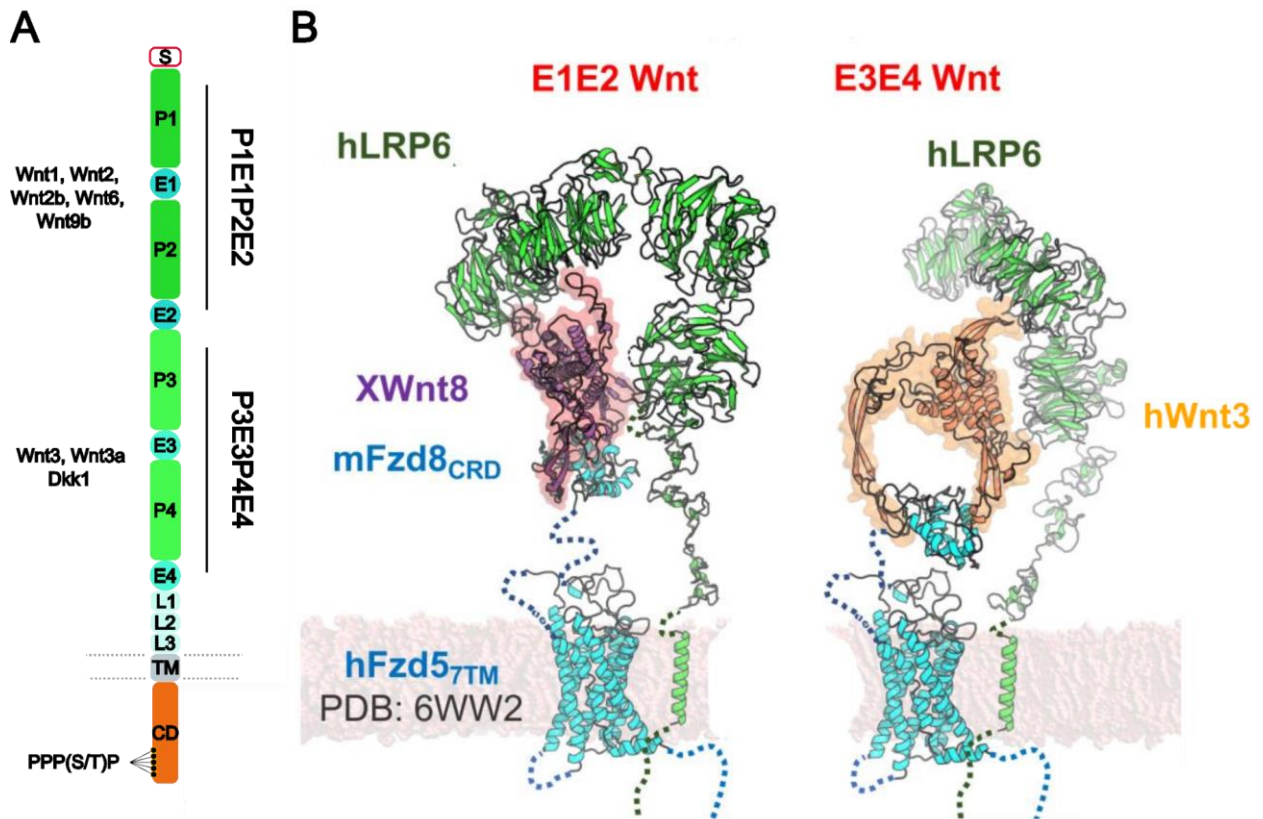


Figure 4. Structure of LRP5/6 receptors and the proposed trimeric membrane complex.

(A) Domain topology of the human LRP6 receptor. Wnt1, Wnt2, Wnt2b, Wnt6, Wnt9b preferentially bind to the P1E1P2E2 region of LRP6 whereas Wnt3, Wnt3a and Dickkopf1 (Dkk1) bind in the P3E3P4E4 region (Raisch et al., 2019). The PPP(S/T)P motif is the characteristic LRP6 phosphorylation site which interacts with GSK3 β and CK1 γ . S: Signal peptide, P: Propeller domain, E: EGF-like domain repeat, L: LDLR type A repeat, TM: Transmembrane domain, CD: Cytoplasmic domain. Reproduced from Raisch et al. (2019).

(B) The membrane complex of bound Wnt-Fz-LRP6, where different Wnts have been shown to bind in two different regions to LRP6. Wnt8 is shown to bind in the region of the first two β -propellers, whereas Wnt3 binds in the region of the last two propellers (Tsutsumi et al., 2022). CRD: Cysteine rich domain. hLRP6: human LRP6, hFzd5: human Fz5, XWnt8: *Xenopus* Wnt8, mFzd8: murine Fz8, PDB: Protein Data Bank, 7TM: 7 Transmembrane. Reproduced from Tsutsumi et al. (2022).

The canonical and the non-canonical Wnt signaling pathways and the promiscuity of the signaling components

In canonical Wnt signaling, the "default" state of the cell is the situation when Wnt ligands are not bound to the receptors. In this case, cytosolic β -catenin is continuously tagged for degradation by the "destruction complex" composed of APC (Adenomatous polyposis coli), GSK3 β (Glycogen synthase kinase-3 beta), CK1 α (Casein kinase 1 alpha) and Axin (Grainger & Willert, 2018). This tagging is followed by β -TrCP (E3 ubiquitin ligase β -transducin repeat-containing protein)-mediated ubiquitination and proteasomal degradation of β -catenin (Aberle et al., 1997). When a membrane complex of the ligand Wnt, the receptor Frizzled and the co-receptor LRP5/6 is formed, a series of phosphorylation events causes the intracellular master regulator Dishevelled to sequester the destruction complex components at the membrane, thus protecting cytosolic β -catenin from degradation (Gammons & Bienz, 2018; Willert et al., 1999). β -catenin accumulates in the cytosol without being ubiquitinated and can be phosphorylated by JNK (c-Jun NH2-terminal kinase) in order to be translocated into the nucleus (Wu et al., 2008). When β -catenin translocates to the nucleus and interacts with UBR5, a HECT E3 ubiquitin ligase, it leads to ubiquitination of the co-repressor Groucho (Flack et al., 2017). This releases TCF (T-cell factor), a nuclear co-factor of β -catenin, from Groucho and allows β -catenin to bind TCF and recruit further proteins constituting the so-called enhanceosome to activate transcription (Flack et al., 2017; Gammons & Bienz, 2018)(Fig. 5).

Wnt and Fz are starting points of multiple signaling pathways aside from the cWnt/ β -catenin pathway; termed "non-canonical" signaling. These include the planar cell polarity pathway (PCP), Wnt-cGMP/Ca⁺ pathway, Wnt-ROR2-JNK, Wnt-YAP/TAZ, Wnt/STOP, Wnt-sPKC, Wnt-PKA, Wnt-RYK, Wnt-mTOR and more (Fig. 5) (Acebron & Niehrs, 2016; Croce & McClay, 2008; García de Herreros & Duñach, 2019; Park et al., 2015; Semenov et al., 2007; Villarroel et al., 2020). Not only are Fz and Wnt involved in multiple pathways, but also their intracellular effectors, such as Dishevelled, are shared among different cascades (Fig. 5)(Acebron & Niehrs, 2016; Croce & McClay, 2008; García de Herreros & Duñach, 2019; Park et al., 2015; Semenov et al., 2007; Villarroel et al., 2020). Cnidarians host a single Dishevelled whereas additional Dishevelled paralogs can be found in later branching groups (Dillman et al., 2013). Another key regulator essential in the cWnt as well as other signaling pathways is GSK3 β , one of the destruction-complex components. Its role in the destruction complex is to phosphorylate β -catenin at T41, S37 and S33 after it has been primed by S45 phosphorylation through CK1 α (Wu & Pan, 2010). In cWnt/ β -catenin signaling GSK3 β 's phosphorylation of LRP5/6's Pro/Ser-rich motifs (PPPSPxS) upon sequestration to the membrane via its bond with Axin in the destruction complex renders the destruction complex inactive (Piao et al., 2008; Stamos et al., 2014). The sharing of key intracellular regulators between the different Wnt signaling pathways is also likely to be important as a means of cross-regulation between them.

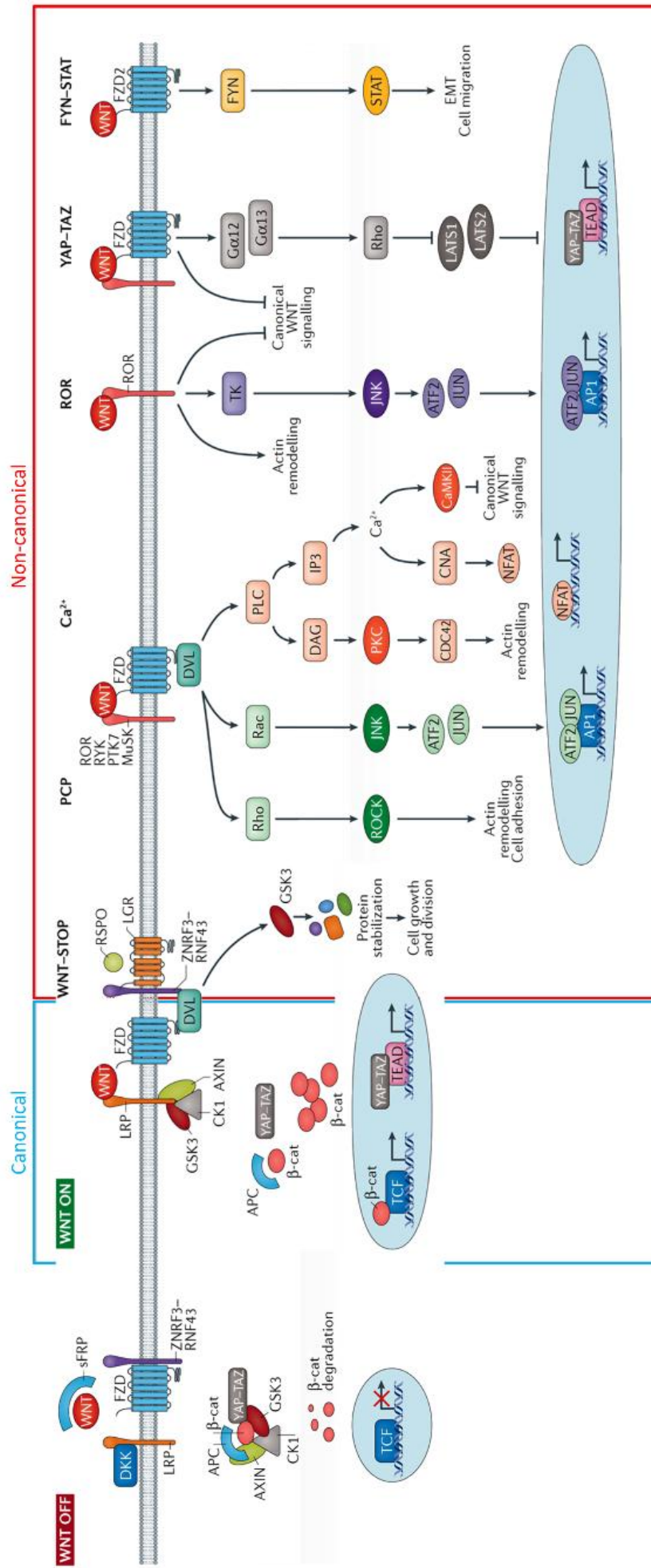


Figure 5. Wnt signaling in the cell.

In the default state ("Wnt-OFF"), cytosolic β-catenin levels are limited through activity of the destruction complex. In the "Wnt-ON" state of cWnt signaling, the activity of the destruction complex is hindered and β-catenin levels accumulate and translocate to the nucleus to modulate transcription. Wnt and Fz are involved in many signaling pathways other than the cWnt/β-catenin pathway (blue outline) which are grouped together as Non-canonical signaling (orange outline). Reproduced from Murillo-Garzón & Kypta (2017).

The hallmark of the canonical Wnt/ β -catenin signaling is the use of the co-receptor LRP5/6. Although the Wnt/LRP6 interaction can lead to events other than the direct influence on β -catenin/TCF activity (Acebron & Niehrs, 2016), LRP5/6 is the key component that sets the most well understood mode of direct cWnt/ β -catenin signaling apart from the other pathways (García de Herreros & Duñach, 2019). In humans, there are two LRP5/6 paralogs that have been shown to have the capacity to transduce cWnt signaling; LRP5 and LRP6 (Hua et al., 2018). In *Nematostella* there is one *LRP5/6*. Previously, there was a keenness to group the different Wnts into canonical vs. non-canonical ligands. This mutual exclusivity however, has been discredited as the same Wnts can elicit signals in different pathways. For example, the classically "canonical" Wnt3a was shown to induce both the cWnt/ β -catenin as well as the Wnt/YAP/TAZ pathway, which could also be stimulated by the classically "non-canonical" Wnt5 (Park et al., 2015). So far, predicting the propensity for one given pathway over the other through sequence or structural characteristics of individual Wnts has remained elusive and is likely far more complex and context variant (Willert & Nusse, 2012). However, bioinformatics approaches at predicting various binding affinities is a promising avenue to aid and guide this future research (Agostino et al., 2017; Agostino & Pohl, 2019). Even "intra-pathway" differences in agonistic and/or antagonistic behavior of the same Wnt in the same context is possible. Taking the same example, Wnt3a induced β -catenin signaling, but it simultaneously stimulated the YAP pathway resulting in antagonistic downstream effects on β -catenin signaling through the expression of Dickkopf (Park et al., 2015), which competes with Wnt3a for a binding site on LRP5/6 (Chen et al., 2011). It is also not feasible to compartmentalize the Fz receptors exclusively to only one of the pathways as they too have been shown to hold the capacity of signaling through more than one pathway (Medina et al., 2000; Rulifson et al., 2000; Y. Wang et al., 2016; Yu et al., 2012). Only Fz3/6, evolutionarily the most recent Fz innovation, which is not found in invertebrates (Schenkelaars et al., 2015), appears to be exclusive to the PCP pathway (Wang et al., 2016).

Although the minimalist scheme of a trimeric complex (Wnt/Fz/LRP5/6) has been the working model for most cWnt studies, there has been evidence that this too is more complex. The stoichiometry of the different components is debated (Hua et al., 2018; Nile et al., 2017). Studies have demonstrated the ability of dimeric receptor complexes to transduce signals (Chen et al., 2014; Hua et al., 2018) as well as shown that binding of receptors and ligands without a co-receptor can take place (Schihada et al., 2021). Moreover, optogenetically-induced oligomerization of LRP6 was shown to be sufficient to activate β -catenin without a ligand in HEK293T (human embryonic kidney cells) (Bugaj et al., 2013), a fact which may be directly relevant to my results below.

Nematostella cWnt/ β -catenin dependent axis formation

Nematostella vectensis as a model organism

Cnidaria are considered the only pre-bilaterian group which has a "full set" of *Wnts* (Isaeva & Kasyanov, 2021). *Nematostella vectensis* is a bilaterally symmetric cnidarian and has emerged as a useful model to study axial patterning (Genikhovich & Technau, 2017). It can follow both an asexual (Fig. 6B-C) as well as a sexual reproduction cycle (Fig. 6A). In the latter, oocytes mature in the female mesenteries before being released into the environment and fertilized by the sperm. After passing through a hollow blastula stage, the embryo develops into an invaginating gastrula within 1 day post fertilization (dpf), followed by a swimming planula stage, which partitions its endodermal cell layer into 8 mesenterial chambers by 4 dpf. Approximately by 7 dpf, the embryo reaches a sessile primary polyp stage with four primary tentacles. Asexually, adult animals can form another sessile polyp through transverse fission ("foot pinching" aka. "physal pinching") (Hand & Uhlinger, 1995) (Fig. 6B) and polarity reversal (Röttinger, 2021) (Fig. 6C).

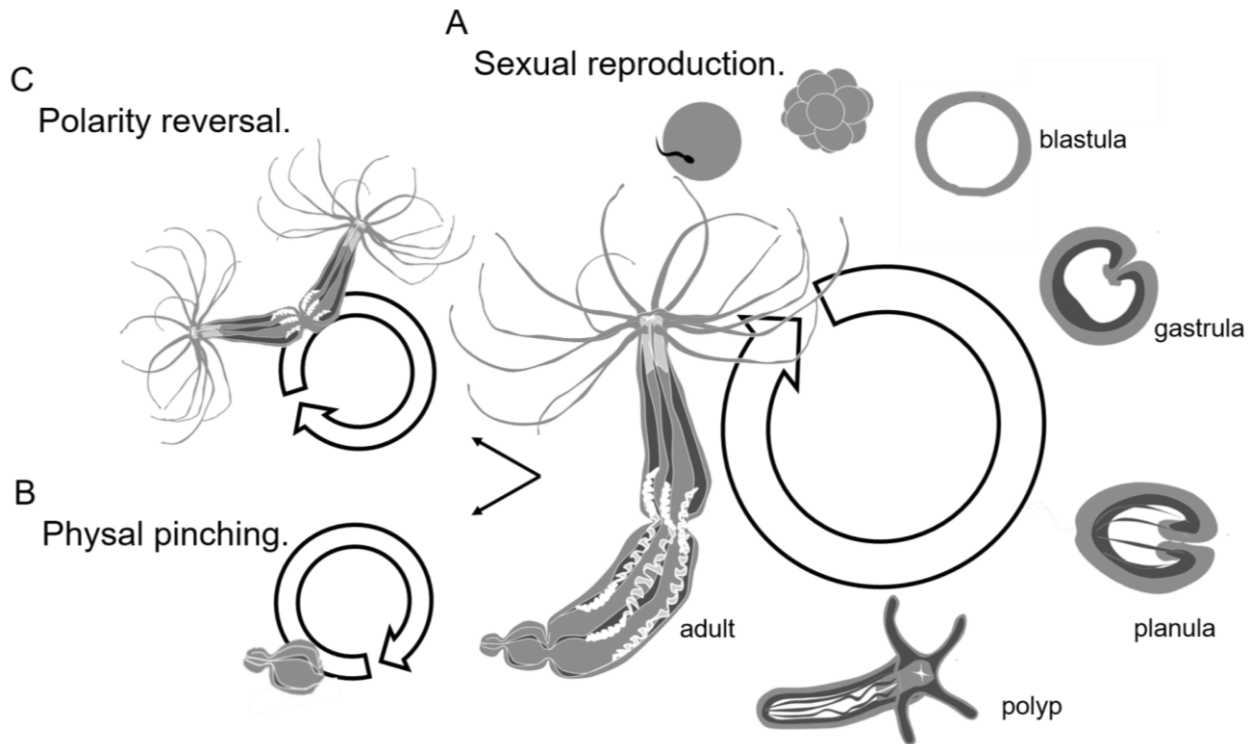


Figure 6. Stages of the *Nematostella vectensis* lifecycle.

(A) The stages of *Nematostella* development starting at external fertilization of the egg, cleavage and formation of the blastula. A gastrula stage is followed by a motile planula and results in a sessile polyp which matures into an adult. The modes of asexual propagation by transverse fission through (B) physal pinching or (C) polarity reversal. Figure by Paul Knabl after Röttinger (2021).

Nematostella vectensis can be cultured in a laboratory setting and the production of eggs and sperm can be induced through light and temperature cycling (Fritzenwanker & Technau, 2002). The trigger for the asexual reproduction is less well understood. A definitive causal

event is still unknown and thus far only the presence of sediment to burrow in has been shown to promote rates of transverse fission in *Nematostella* (Al-Shaer et al., 2023). In *Nematostella*, the primary axis is the oral-aboral axis (O-A) which is patterned by Wnt signaling (Genikhovich & Technau, 2017). As a member of Anthozoa, the cnidarian class encompassing bilaterally symmetric Cnidaria, *Nematostella* possesses a secondary axis, the so-called directive axis, orthogonal to the O-A axis. Its directive axis patterning is regulated by BMP signaling (Genikhovich et al., 2015; Genikhovich & Technau, 2017).

Nematostella vectensis cWnt signaling

Nematostella vectensis has representatives of the main four *Fz* receptor families (Schenkelaars et al., 2015) and an array of 12 of the 13 *Wnt* families found in chordates as well as a *WntA*, a *Wnt* lost in vertebrates (Lee et al., 2006; Somorjai et al., 2018). As is the case in many other organisms, in the early *Nematostella* embryo, the Wnt expression maximum lies at the site of gastrulation (Petersen & Reddien, 2009). The expression domains of the early *Wnts* emanate from the oral pole in a sequential, partially overlapping fashion. The aboral domain is free of *Wnt* expression (Lee et al., 2006). The expression characteristics of *Nematostella Fz*s are also reflective of that in other organisms; *Fz5* is the most anteriorly expressed *Fz*, excluded from the posterior ectoderm and the pole where the maximum of Wnt ligand expression lies (Darras et al., 2018; Leclère et al., 2016). Only *Fz1/2/7* and *Fz5/8* are maternally deposited whereas *Fz4* and *Fz9/10* are zygotic (Darras et al., 2018; Leclère et al., 2016; Röttinger et al., 2012; Warner et al., 2018; Wijesena et al., 2022).

As in many early embryonic stages of Bilaterian models, β -catenin nuclearization at one side of the embryo has been shown in *Nematostella* as well (Kumburegama et al., 2011; Leclère et al., 2016; Wikramanayake et al., 2003). *Nematostella* also shows similarities to bilaterian models concerning the role of β -catenin in organizer function (Kraus et al., 2016). Kraus et al. (2016) demonstrated a role of *Nematostella Wnt1* and *Wnt3* in conferring axial organizer potential when injected or transplanted. The work by Kraus et al. (2016) also revealed a dose-dependent behavior of axis marker genes upon β -catenin signaling manipulation which laid the groundwork for the research of the following thesis papers. Even earlier in *Nematostella Wnt* research, Rigo-Watermeier et al. (2012) found that *Nematostella Wnt5a* and *Wnt11* followed the concept of "non-canonical" PCP Wnts, and most strikingly, demonstrated that *Nematostella Wnt11* was able to rescue *Xenopus Wnt5a* morphants and *Nematostella Wnt5* was able to rescue *Xenopus Wnt11* morphants, both in a dose-dependent manner. Further functional research of *NvWnt11* carried out by Ritthaler and colleagues (2012), however, found no significant axis perturbation in *NvWnt11* Morpholino (MO) injected samples (Ritthaler, 2012).

Although the structure and sequence of Wnts is highly conserved, their functionality and expression context can vary quite a lot (Hensel et al., 2014). Even within the group of Cnidaria, spatial and tissue contexts of Wnt expression across body plans can differ substantially (Momose et al., 2008). Moreover, it remains unclear, what the specific roles of such an extensive complement of Wnt ligands and Frizzled receptors is in animals morphologically as "simple" as cnidarians, and what can it tell us about the evolution of this signaling pathway. This question led us to formulate the aims of my PhD project.

Aims of the PhD project

Like in Bilateria, the primary body axis of the anthozoan cnidarian model *Nematostella vectensis* is patterned by Wnt signaling. However, the regulatory logic of this patterning remained unknown by the time I started my project. Moreover, in spite of its very simple morphology, *Nematostella* possesses multiple Wnt ligands and Fz receptors, whose signaling preference and the role in axial patterning was to a very large extent unknown. In my project I aimed to elucidate the role of the individual cWnt signaling components on the early development of *Nematostella vectensis* utilizing *in vitro* and *in vivo* approaches. I addressed the following research questions:

1. Which Fz receptors and Wnt ligands of *Nematostella vectensis* can signal through the canonical Wnt/ β -catenin pathway?

Different Wnt and Fz proteins are known to be involved in multiple different signaling pathways. In my project, I utilized an *in vitro* reporter system to test all possible ligand-receptor combinations and analyze their ability to drive TCF-mediated expression. This question is addressed in Chapter I.

2. What is the molecular logic of the O-A patterning in *Nematostella*, which of the Wnt ligands and Fz receptors play a role in it, and what is their function?

I used loss-of-function studies to determine the roles of LRP5/6, individual Wnt and Fz proteins, and of their combinations in regulating O-A axis patterning. I also contributed to the analysis of the regulatory logic of the O-A patterning downstream of β -catenin. These questions are addressed in Paper I, published in *Development*, and Paper II, published in *Nature Communications*.

3. Does Wnt/Fz/LRP5/6-mediated β -catenin signaling regulate endomesoderm specification in *Nematostella*, or is its function limited to axial patterning?

It has been presumed that sequential involvement of β -catenin signaling in the specification of the endomesoderm and axial patterning is shared between Cnidaria and Bilateria. We tested this both by addressing the function of Wnt, Fz and LRP5/6 (see Paper I) and by direct analysis of the fluorescently tagged endogenous β -catenin described in Paper III, a preprint published on bioRxiv.

Results

Chapter I: Analysis of the *Nematostella* Wnt-Fz signaling preferences in cell-culture

The wide array of evolutionarily conserved Wnt ligands and Fz receptors suggests that preferential binding may exist between some specific ligand-receptor pairs. The hunt for matching pairs has however not resulted in a clear list of binary binding partners. Some Fz receptors can bind many of the Wnt ligands, however, with different affinities and varying efficiency in different cell types, with presence or absence of other cofactors and at different developmental time points (Dijksterhuis et al., 2014, 2015; Eubelen et al., 2018; Grainger & Willert, 2018; van Amerongen, 2012). Yet, other Frizzleds are capable of Wnt/ β -catenin signaling only with distinct partners (Voloshanenko et al., 2017).

In an effort to elucidate potential signaling partner selectivity or specificity among *Nematostella* Wnt and Frizzled (NvWnt and NvFz) proteins, I emulated previous studies investigating these relationships in other models. Transfection with the TOPFlash::Luciferase β -catenin/TCF reporter (Veeman et al., 2003) is one of the most commonly used cell signaling assays when studying the canonical Wnt/ β -catenin pathway and has been described extensively (Bourhis et al., 2010; Dijksterhuis et al., 2015; Ettenberg et al., 2010; Eubelen et al., 2018; Gong et al., 2010; Lai et al., 2017; Voloshanenko et al., 2017; Xu et al., 2004; Yu et al., 2012). This reporter uses the firefly luciferase gene expression driven by 7 TCF binding sites. Since TCF is the nuclear cofactor of β -catenin in canonical Wnt/ β -catenin target gene expression, the luminescence readout, normalized to a co-transfected GFP (green fluorescent protein) signal, can be used as a measure of active β -catenin nuclearization and target gene transcription.

Results of the cell culture experiments

Prof. Dr. Vanhollebeke's lab from the Laboratory of Neurovascular Signaling at the Université Libre de Bruxelles has kindly shared their *Fz* knockout HEK293T (hFz-KO) cell line with us (Eubelen et al., 2018) allowing us to apply the TOPFlash assays in a HEK293T-cell context without the confounding signals of endogenous human Fz receptors. I transfected all possible combinations of the *Nematostella* Fz receptors, Wnt ligands and LRP5/6 using concentrations previously used for a similar study with human Wnt and Fz molecules (Voloshanenko et al., 2017). The expected clear-cut results, however, were not obtained due to a low signal-to-noise ratio (data not shown). Upon detailed analyses, which I do not present here, I could conclude that:

1. None of the *Nematostella* Wnt ligands were capable of inducing notable luciferase activity when co-transfected with the TOPFlash reporter alone in a Fz-KO background.
2. None of the *Nematostella* Fz receptors were capable of inducing notable luciferase activity when co-transfected with the TOPFlash reporter alone.
3. Overexpression of *Nematostella* LRP5/6 was sufficient to induce TOPFlash activity and did not require additional Wnt or Fz expression.

Thus, the component generating the confounding background noise was NvLRP5/6. The ability of LRP5/6 to generate a β -catenin nuclearizing signal through its intracellular tail, independent of binding to Fz or Wnt extracellularly is a known phenomenon (Mao et al., 2001; Mi & Johnson, 2005). Thus, the main difficulty was finding and titrating the relative and appropriate concentrations of the various transfected constructs to obtain interpretable results. Extensive troubleshooting eventually allowed for useful data collection.

Proof of concept

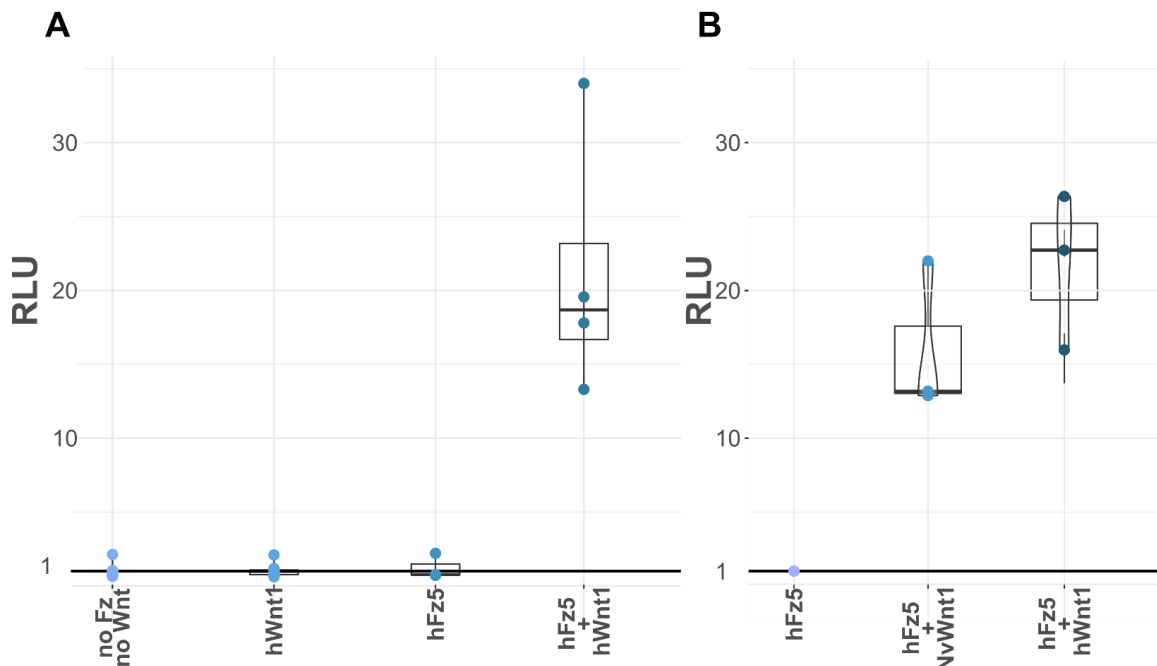


Figure 7. Proof of concept experiments show that the TOPFlash reporter assay works as expected.

(A) Strong TOPFlash reporter activity in hFz-KO cells is observed only upon co-transfection with human Fz5 and Wnt1 (hFz5+hWnt1) but not in untransfected controls (no Fz, no Wnt), and not upon individual transfection with either hWnt1 or hFz5. **(B)** Co-transfection of hFz5 with *Nematostella* Wnt1 produces a level of TOPFlash reporter activity comparable to the one caused by co-transfection of hFz5+hWnt1. On (A), the luciferase signal is relative to the signal produced by the TOPFlash reporter construct transfected alone as baseline set to 1. On (B), the luciferase signal is relative to the signal produced by the TOPFlash reporter construct co-transfected with hFz5 as baseline set to 1. RLU: Relative Luciferase Units.

As the initial experiments generated only meaningless data, I used human components to replicate established TOPFlash signaling readout. As expected, I could show that the basic principle of the TOPFlash reporter assay worked in my hands when human Wnt1 and human Fz5 were used (Fig. 7). Since the hFz-KO cells I was using did not produce any endogenous Fz, the addition of Wnt did not generate a detectable signal, and transfection of human Fz5 also showed that background endogenous Wnt did not generate a signal close to that of overexpression through the transfection. Only when both Fz and Wnt were transfected there was meaningful signal generated (Fig. 7A). Importantly, substituting human Wnt1 with *Nematostella* Wnt1 in the transfections resulted in comparable levels of reporter activity (Fig.

7B). This suggests that the lack of signal in the original experiments with *Nematostella* Wnt signaling components was not likely due to a defect in the expression and/or secretion of the *Nematostella* Wnts by the human expression and secretion machinery (at least in the case of NvWnt1).

The next important control was to show that *Nematostella* Fz receptors were capable of transducing a Wnt signal in the human cell. To test that, I co-transfected human Wnt1 with each of the four *Nematostella* Fz receptors (Fig. 8). Although the reporter activity was much lower than in the hFz5-hWnt1 combination, some reporter activity was observed. The ability of hWnt1 to signal via the *Nematostella* Fz showed that the noisy, low intensity signal I observed in the initial experiments with the *Nematostella* Wnt, Fz and LRP5/6 was likely not due to the inability of the human Dishevelled to interact with the intracellular domain of the *Nematostella* Fz (Fig. 8).

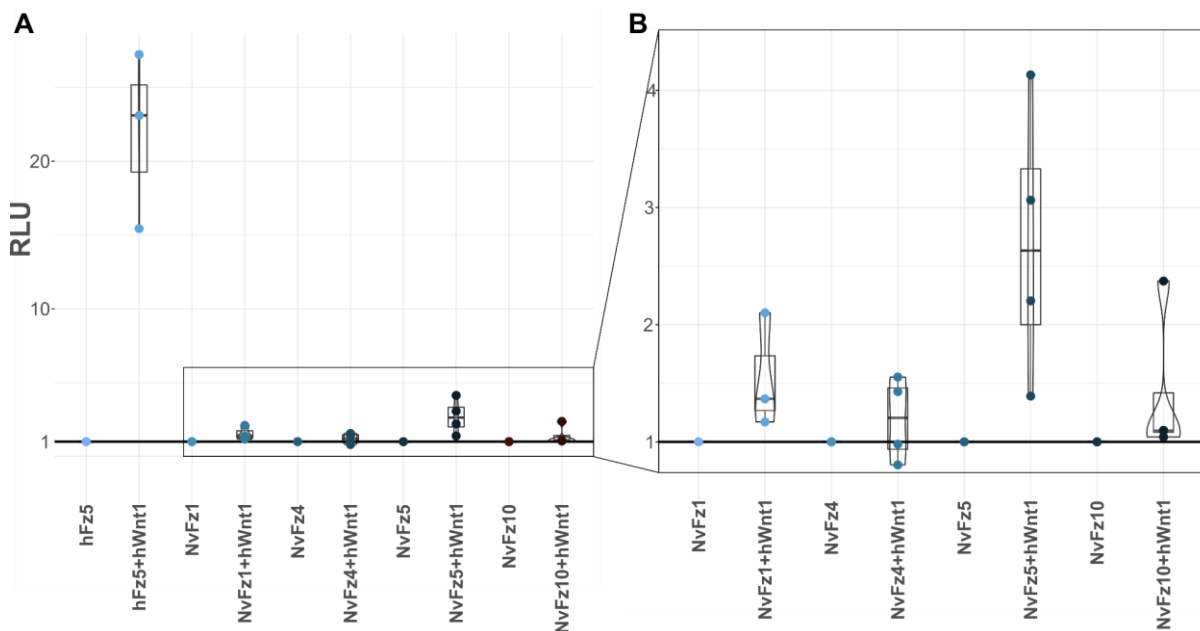


Figure 8. human Wnt1 can generate some TOPFlash signal in a NvFz-only background.

(A) Human Wnt1 is able to act through some of the NvFz, even though the signaling efficiency is much lower in comparison to human Fz5-mediated signal induction. **(B)** shows the zoomed in region boxed on (A). The signal of each Fz-hWnt1 combination is relative to the signal generated by the respective Fz transfected without hWnt1 as baseline set to 1. RLU: Relative Luciferase Units.

Since my earlier results showed that *Nematostella* LRP5/6 was capable of strongly signaling alone, the only way to use NvLRP5/6 in all further experiments was to treat the NvLRP5/6 transfection as the baseline. Hence, next, we tested whether an increase in the reporter activity could be detected once Wnt and Fz were co-transfected with NvLRP5/6 (Fig. 9). The assays showed that in the NvLRP5/6 background, without Fz co-transfection, Wnt co-transfection did not generate a discernible signal. Co-transfection of human Fz5 generated some signal, potentially due to the presence of some endogenous human Wnt or due to the

properties of Fz+LRP5/6 interactions being able to transduce the signal independent of Wnt, as has been shown previously (Hua et al., 2018; Mao et al., 2001; Mi & Johnson, 2005). Finally, co-transfection of hFz5 and human or *Nematostella* Wnt1 in the NvLRP5/6 background resulted in an even stronger signal (Fig. 9). However, since both human and *Nematostella* Wnt1 are capable of signaling via hFz5 in the absence of the co-transfected NvLRP5/6 (Fig. 7B), it is unclear whether NvLRP5/6 was involved in the signaling in this case.

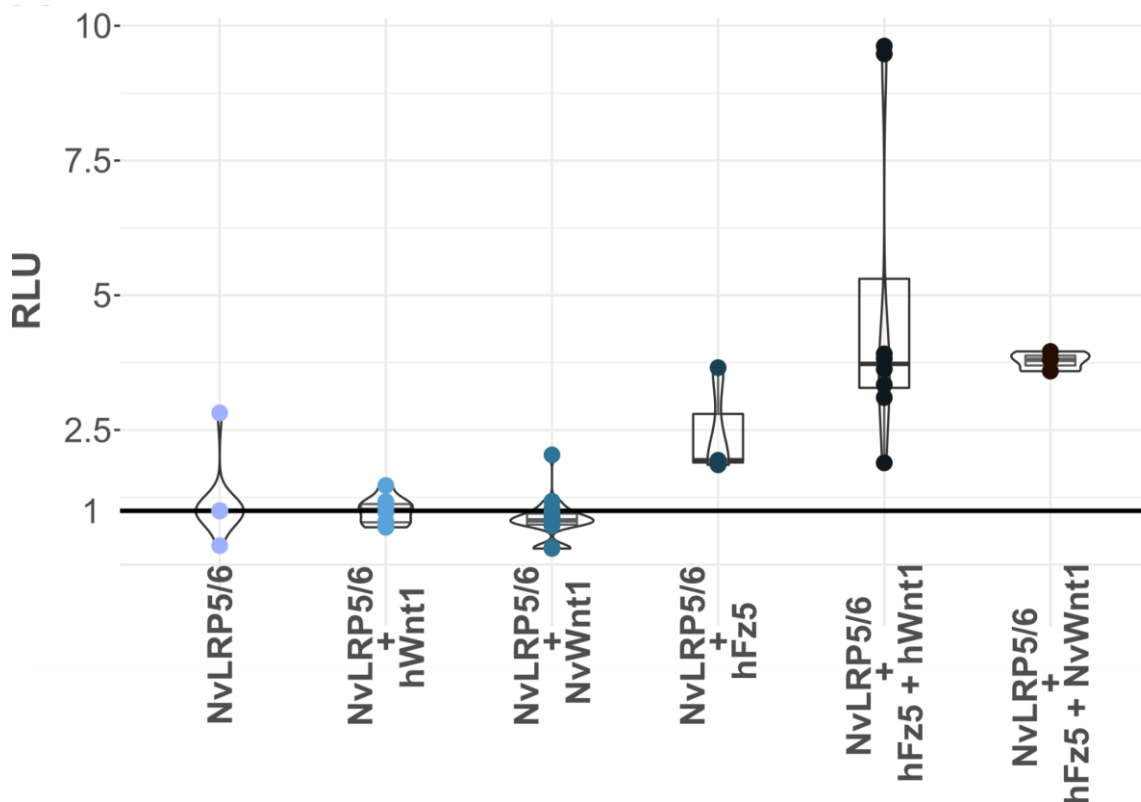


Figure 9. Co-transfection of Fz and Wnt with *Nematostella* LRP5/6 increases reporter activity. The signal of combined transfections is shown relative to the signal of NvLRP5/6 transfected alone as baseline set to 1. RLU: Relative Luciferase Units.

Nematostella Fz+Wnt assays

Once all the controls described above had been performed and extensive titration of the relative amounts of the different components to transfect was determined, I was able to start identifying the ligand-receptor preferences among *Nematostella* Wnt ligands and Fz receptors for cWnt signaling. Unfortunately, the experiments had to be interrupted due to the Sars-CoV2 lockdown, and then finally abandoned due to time constraints. The ligand and receptor concentrations I used probably required some more adjustment, and the amount of utilizable data was not extensive enough to apply rigorous statistical testing. However, I have identified several preferential ligand-receptor pairs, which were later discovered as likely interaction partners also in the *in vivo* LOF analyses (see Paper I). The baseline used as control which all conditions are compared to is the combined NvFz+NvLRP5/6 expression without NvWnt coexpression. This analysis showed that significant (** $p < 0.01$) luciferase signal increase was observed for NvFz5+NvWnt4, NvFz10+NvWnt3, and NvFz10+NvWnt4 combinations (Fig. 10). If the significance threshold is set to $p < 0.05$, the NvFz1+NvWnt4 and

NvFz5+NvWnt1 combinations also showed some significance ($*p < 0.05$) in the Dunnett test (Fig. 10).

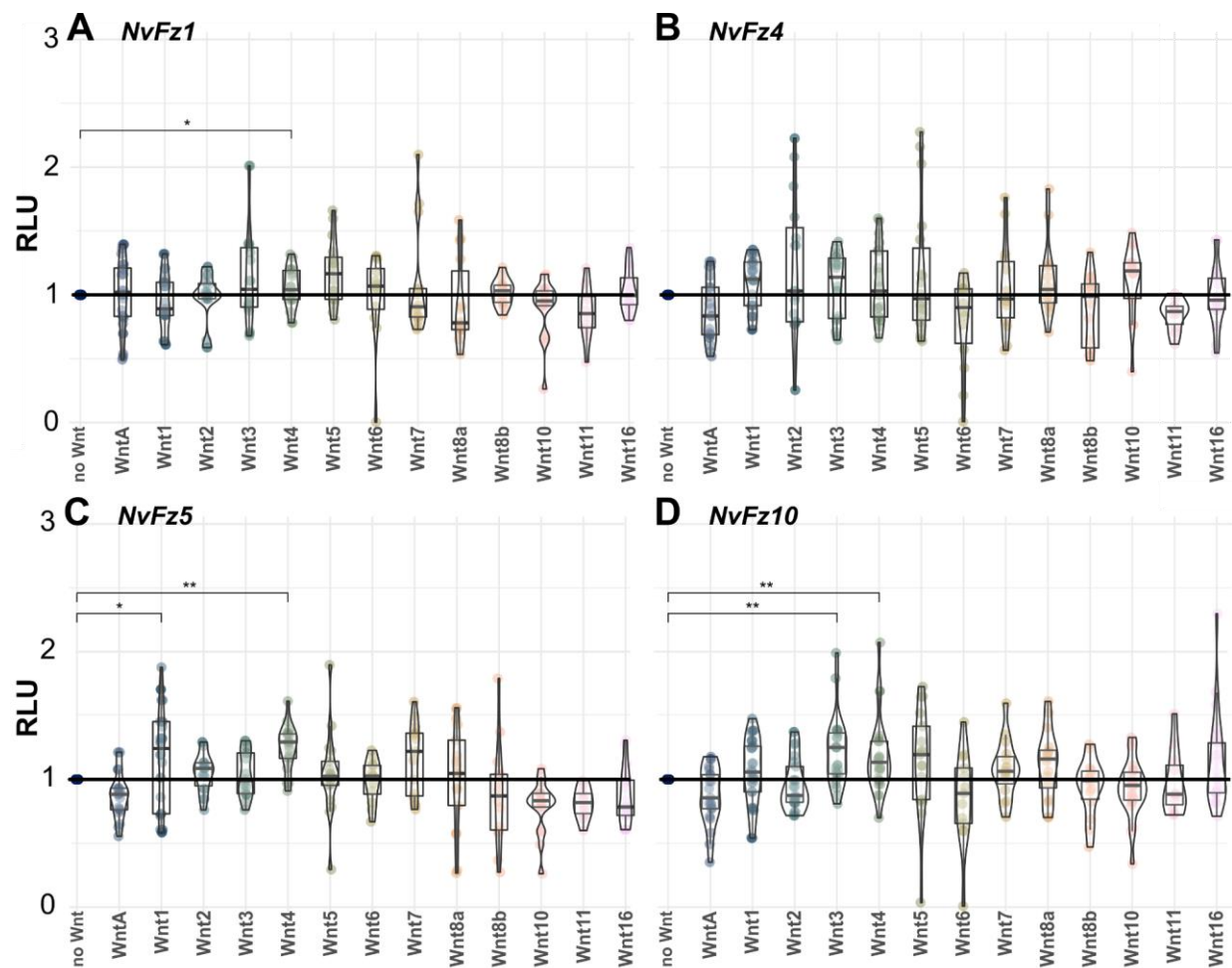


Fig.10. Signaling abilities of the different *Nematostella* ligand - receptor combinations.

To compare many treatment groups to a single control condition, ANOVA followed by a Dunnett's test was used (Lee & Lee, 2018). All possible NvFz+NvWnt combinations were tested under the same conditions. Statistically significant signaling ($**p < 0.01$) was shown for the NvFz5+NvWnt4 combination (C) and the NvFz10+NvWnt3 and NvFz10+NvWnt4 combinations (D). The NvFz1+NvWnt4 (A) and NvFz5+NvWnt1 (C) combinations showed some significance in the Dunnett test ($*p < 0.05$). NvFz4 did not display any significant signaling power (B). The RLU signal is shown relative to the respective NvFz+NvLRP5/6 signal as baseline set to 1. RLU: Relative Luciferase Units.

Discussion

The major issue faced in this assay was found to be the capacity of *Nematostella* LRP5/6 to signal alone when overexpressed. It has been shown previously that LRP5/6 has the capacity to elicit Wnt/ β -catenin signaling even without a binding ligand or other receptors (Mao et al., 2001). The extensive troubleshooting it took to reach the expression levels and Wnt/Fz/LRP5/6 ratios that allowed to elevate "real signaling" above the background signal hampered the progress of this project.

In order to further investigate whether the low signaling efficiency was due to inefficient interaction between the intracellular domains of the *Nematostella* Fz and LRP5/6 proteins and human Dishevelled, I generated hybrid constructs for Fz5 and LRP5/6. For LRP5/6, the extracellular region was that of NvLRP5/6 whereas the transmembrane domain and intracellular tail was that of human LRP6. In the Fz5 hybrid, the CRD and extracellular linker domain were that of NvFz5 whereas, starting from the first intracellular loop onward, the human Fz5 sequence was used. Due to the Sars-CoV2 lockdown, however, further systematic testing of these was not possible and this part of the project was abandoned. It would have been intriguing to research which domains or structural components that differed between human Fz and *Nematostella* Fz were responsible for the strong differences in signal initiation. It would also be interesting to find out, which sequences differing between the four *Nematostella* Fzs conferred the respective signal initiation differences by performing further domain swap experiments. Unfortunately, this was not possible.

Conclusion

My attempt at using the cell culture system and the TOPFlash reporter assay to decipher Wnt/Fz signaling partners emulating previous studies allows only limited conclusions since it had to be abandoned exactly at the time I started obtaining the first interpretable results. A significant level of TOPFlash signal was only elicited by NvFz5+NvWnt4, NvFz10+NvWnt4 and NvFz10+NvWnt3 combinations. The biological relevance of the NvFz5+NvWnt4 and NvFz10+NvWnt3 combinations, however, was independently reflected in our *in vivo* findings discussed in the following papers.

Materials and Methods

Constructs

In order to allow optimal efficacy of the *Nematostella* protein translation in the HEK293T context, we ordered codon-optimized versions of NvLRP5/6, all NvWnt and all NvFz at GeneArt (ThermoFisher) and had them cloned in a pcDNA3.1+ expression vector (Invitrogen™, Cat.# V79020). Human Wnt1 (GenBank accession number: NP_005421.1) and human Fz5 (GenBank accession number: NP_003459.2) were amplified from HEK293T cDNA and cloned into the same pcDNA3.1+ vector. For the Luciferase reporter assay, the reporter M50 Super 7x TOPFlash (Addgene plasmid # 12456) was used. To normalize the transfection efficiency, pEGFP-N1 plasmid was used (GenBank Accession: U55762; Clontech).

Transfections

All transfections were carried out using Lipofectamine™ 3000 (Invitrogen™, Cat.# L3000001). Fz-KO HEK293T cells (Eubelen et al., 2018) were seeded in 96-well plates at approximately 30k cells/well in 100 µl DMEM (Dulbecco's Modified Eagle Medium) without phenol red and 4.5 g/L-glucose, supplemented with 2 mM L-glutamine, 100 U/ml benzylpenicillin, 100 µg/ml streptomycin and 10% heat-inactivated FBS (fetal bovine serum) and incubated at 37°C and 5% CO₂ on the day prior to transfections in order to have approximately 70-90% confluency at the time of the transfection the following day. Prior to transfection, the medium was exchanged for serum-free-DMEM (SF-DMEM: as above but without FBS). Transfections were conducted as described in the Lipofectamine™ 3000 protocol with the exception that SF-DMEM was used instead of Opti-MEM™. The volumes

which led to optimal transfection were 0.1 µl P3000 reagent™ and 0.1 µl Lipofectamine™ 3000 per 35 ng DNA constructs per well. Five hours post-transfection, another media exchange, this time for standard DMEM (containing 10% FBS) was performed and the cells were placed back into the incubator for approximately 40 hours. After aspiration of the supernatant, the cell plates were frozen at -80° for 2 hours. Cells were then thawed at room temperature and the Luciferase Reporter Assay (Promega, Cat.# E4030) was performed. The lysis buffer master mix was composed of 4.8 ml ddH₂O, 1.2 ml Promega 5x Reporter Lysis Buffer (Promega, Cat.# E3971), 6 µl CoenzymeA and 6 µl DTT. 50 µl of lysis master mix was added per well and the plate was placed on a plate shaker for 10 minutes. 40 µl of the cell lysate was transferred to the black 96 well measurement plate and placed on the plate shaker again for 5 minutes to remove any bubbles prior to placing the plate into the Tecan Infinite M200Pro plate reader using Luciferin and ATP solutions according to the plate reader's protocol.

The optimal concentrations of the different constructs per 96-well plate well were as follows: LRP5/6: 1 ng, Fz: 5 ng, Wnt: 1 ng, M50 Super 7x TOPFlash reporter: 20 ng, eGFP: 4 ng. To reach the same amount of total DNA constructs per well empty pcDNA3.1+ vector was used.

Data analysis

Plotting and analyses were conducted using the R Statistical language (version 3.6.1; R Core Team, 2019) on Windows 10 x64 (build 19044), in the RStudio environment (v1.2.1335, RStudio Team, 2018) using the following packages:

Andri et mult. al. S (2021). DescTools: Tools for Descriptive Statistics. R package version 0.99.41, <https://cran.rproject.org/package=DescTools>.

Galili T (2021). installr: Using R to Install Stuff on Windows OS (Such As: R, 'Rtools', 'RStudio', 'Git', and More!). R package version 0.23.2, <https://CRAN.Rproject.org/package=installr>.

Henry L, Wickham H (2020). purrr: Functional Programming Tools. R package version 0.3.4, <https://CRAN.Rproject.org/package=purrr>.

Højsgaard S, Halekoh U (2021). doBy: Groupwise Statistics, LSmeans, Linear Contrasts, Utilities. R package version 4.6.11, <https://CRAN.Rproject.org/package=doBy>.

Hvitfeldt E (2021). paletteer: Comprehensive Collection of Color Palettes. R package version 1.3.0, <https://github.com/EmilHvitfeldt/paletteer>.

Kassambara A (2020). ggpubr: 'ggplot2' Based Publication Ready Plots. R package version 0.4.0, <https://CRAN.Rproject.org/package=ggpubr>.

Kassambara A (2021). rstatix: PipeFriendly Framework for Basic Statistical Tests. R package version 0.7.0, <https://CRAN.Rproject.org/package=rstatix>.

Makowski D, Lüdecke D, Patil I, Thériault R, BenShachar M, Wiernik B (2023). "Automated Results Reporting as a Practical Tool to Improve Reproducibility and Methodological Best Practices Adoption." CRAN. <https://easystats.github.io/report/>.

Patil I (2021). "Visualizations with statistical details: The 'ggstatsplot' approach." Journal of Open Source Software, *6*(61), 3167. doi: 10.21105/joss.03167, <https://doi.org/10.21105/joss.03167>.

Pedersen T (2021). ggforce: Accelerating 'ggplot2'. R package version 0.3.3, <https://CRAN.Rproject.org/package=ggforce>.

Pedersen T (2022). patchwork: The Composer of Plots. R package version 1.1.2, <https://CRAN.Rproject.org/package=patchwork>.

R Core Team (2019). R: A Language and Environment for Statistical Computing. R

Foundation for Statistical Computing, Vienna, Austria. <https://www.Rproject.org/>.

Rinker TW, Kurkiewicz D (2018). pacman: Package Management for R. version 0.5.0, <http://github.com/trinker/pacman>.

Robinson D, Hayes A, Couch S (2022). broom: Convert Statistical Objects into Tidy Tibbles. R package version 1.0.1, <https://CRAN.Rproject.org/package=broom>.

Silge J, Robinson D (2016). "tidytext: Text Mining and Analysis Using Tidy Data Principles in R." JOSS, *1*(3). doi: 10.21105/joss.00037, <http://dx.doi.org/10.21105/joss.00037>.

Wickham H (2011). "The SplitApplyCombine Strategy for Data Analysis." Journal of Statistical Software, *40*(1), 129. <http://www.jstatsoft.org/v40/i01/>.

Wickham H (2016). ggplot2: Elegant Graphics for Data Analysis. SpringerVerlag New York. ISBN 9783319242774, <https://ggplot2.tidyverse.org>.

Wickham H (2019). stringr: Simple, Consistent Wrappers for Common String Operations. R package version 1.4.0, <https://CRAN.Rproject.org/package=stringr>.

Wickham H, Averick M, Bryan J, Chang W, McGowan LD, François R, Golemund G, Hayes A, Henry L, Hester J, Kuhn M, Pedersen TL, Miller E, Bache SM, Müller K, Ooms J, Robinson D, Seidel DP, Spinu V, Takahashi K, Vaughan D, Wilke C, Woo K, Yutani H (2019). "Welcome to the tidyverse." Journal of Open Source Software, *4*(43), 1686. <https://doi.org/10.21105/joss.01686>.

Wickham H, François R, Henry L, Müller K (2021). dplyr: A Grammar of Data Manipulation. R package version 1.0.6, <https://CRAN.Rproject.org/package=dplyr>.

Wickham H, Hester J (2020). readr: Read Rectangular Text Data. R package version 1.4.0, <https://CRAN.Rproject.org/package=readr>.

Xie Y (2021). knitr: A GeneralPurpose Package for Dynamic Report Generation in R. R package version 1.34, <https://yihui.org/knitr/>.

Paper I

"Sea anemone Frizzled receptors play partially redundant roles in oral-aboral axis patterning."

Authors:

Isabell Niedermoser¹, Tatiana Lebedeva¹ & Grigory Genikhovich¹

¹Department of Neurosciences and Developmental Biology, Faculty of Life Sciences, University of Vienna, Djerassiplatz 1, Vienna, Austria

Status:

Published in *Development*, 2022, 149 (19): dev200785.

<https://doi.org/10.1242/dev.200785>

Contributions:

Conceptualization: G.G.; Methodology: G.G.; Validation: I.N., T.L.; Investigation: I.N., T.L., G.G.; Writing - original draft: I.N., G.G.; Writing - review & editing: I.N., T.L., G.G.; Visualization: I.N., T.L., G.G.; Supervision: G.G.; Project administration: G.G.; Funding acquisition: G.G.

RESEARCH ARTICLE

Sea anemone Frizzled receptors play partially redundant roles in oral-aboral axis patterning

Isabell Niedermoser^{1,2}, Tatiana Lebedeva^{1,2} and Grigory Genikhovich^{1,*}

ABSTRACT

Canonical Wnt (cWnt) signalling is involved in a plethora of basic developmental processes such as endomesoderm specification, gastrulation and patterning the main body axis. To activate the signal, Wnt ligands form complexes with LRP5/6 and Frizzled receptors, which leads to nuclear translocation of β -catenin and a transcriptional response. In Bilateria, the expression of different Frizzled genes is often partially overlapping, and their functions are known to be redundant in several developmental contexts. Here, we demonstrate that all four Frizzled receptors take part in the cWnt-mediated oral-aboral axis patterning in the cnidarian *Nematostella vectensis* but show partially redundant functions. However, we do not see evidence for their involvement in the specification of the endoderm – an earlier event likely relying on maternal intracellular β -catenin signalling components. Finally, we demonstrate that the main Wnt ligands crucial for the early oral-aboral patterning are Wnt1, Wnt3 and Wnt4. Comparison of our data with knowledge from other models suggests that distinct but overlapping expression domains and partial functional redundancy of cnidarian and bilaterian Frizzled genes may represent a shared ancestral trait.

KEY WORDS: Cnidaria, *Nematostella*, Axial patterning, Gastrulation

INTRODUCTION


Wnt ligands and their Frizzled (Fz) receptors are involved in multiple cellular signalling pathways, one of which leads to the nuclear accumulation of β -catenin and is termed the ‘canonical’ Wnt/ β -catenin pathway or the cWnt pathway (MacDonald and He, 2012; van Amerongen and Nusse, 2009). In the ‘cWnt-off’ state, cytosolic β -catenin is continuously tagged for degradation by the ‘destruction complex’ containing APC, Axin, CK1 α and GSK3 β (Grainger and Willert, 2018), ubiquitinated by β -TrCP and degraded by the proteasome (Aberle et al., 1997). In the ‘Wnt-on’ state, a complex of Wnt, Fz and the co-receptor LRP5/6 forms at the membrane, which results in the sequestering of the destruction complex by Dishevelled, which, in turn, prevents tagging β -catenin for degradation (Gammons and Bienz, 2018; Willert et al., 1999).

Non-tagged β -catenin accumulates in the cytosol and becomes translocated into the nucleus, where it displaces the transcriptional co-repressor Groucho and interacts with TCF to activate target genes (Flack et al., 2017). In addition to their role in cWnt signalling, which is characterized by the involvement of LRP5/6 and the nuclear translocation of β -catenin, Wnt ligands and Fz receptors are the starting points of multiple ‘non-canonical’ signalling pathways (Acebron and Niehrs, 2016; Croce and McClay, 2008; Garcia de Herreros and Duñach, 2019; Park et al., 2015; Semenov et al., 2007; Villarreal et al., 2020). In mammals, ten different Fz receptors that make up five families may demonstrate partially overlapping functions, and the effects of their individual or combined knockouts are usually attributed to a mixed action of the abnormal cWnt and non-canonical signalling (Fischer et al., 2007; Wang et al., 2016). Among the mammalian Fz receptors, only Fz4 appears to act exclusively in the cWnt pathway, while Fz3 and Fz6 seem to be exclusively involved in the Wnt/PCP pathway (Wang et al., 2016).

One of the ancestral roles of the β -catenin signaling is to define the gastrulation site, as well as to pattern the main body axis in animals – a feature that appears to be conserved across Metazoa. Localized expression of the Wnt signalling components along the main body axis has been documented in the earliest branching animal lineages such as ctenophores (Pang et al., 2010) and sponges (Adamska et al., 2010; Leininger et al., 2014). In Cnidaria, the bilaterian sister group, the role of the cWnt pathway in gastrulation and oral-aboral (OA) axis patterning has been confirmed by functional analyses (Kraus et al., 2016; Lebedeva et al., 2021; Leclère et al., 2016; Marlow et al., 2013; Momose et al., 2008; Momose and Houliston, 2007; Röttinger et al., 2012; Wikramanayake et al., 2003). Recently, we demonstrated that the regulatory logic of the β -catenin-dependent OA patterning in the sea anemone *Nematostella vectensis* and the posterior-anterior (PA) patterning of deuterostome Bilateria is highly similar, suggesting a common evolutionary origin of the OA and the PA axes (Darras et al., 2018, 2011; Kiecker and Niehrs, 2001; Lebedeva et al., 2021; Nordström et al., 2002). Although the way *Nematostella* interprets different intensities of β -catenin signal is largely understood (Kraus et al., 2016; Lebedeva et al., 2021), we still have very little idea about which Wnt ligands and which Fz receptors are involved in the cWnt-dependent axial patterning in this morphologically simple model organism. The complement of Wnt and Fz molecules in *Nematostella* is surprisingly large. It has representatives of 12 out of the 13 conserved bilaterian Wnt gene families, only lacking *Wnt9*, which has been lost in Cnidaria but is present in the earlier branching Ctenophora (Kusserow et al., 2005; Lee et al., 2006; Pang et al., 2010). *Nematostella* Wnt genes are expressed in staggered domains along the OA axis, with different Wnt sets transcribed in the ectoderm and in the endoderm (Kusserow et al., 2005; Lee et al., 2006). The *Nematostella* genome also harbours representatives of four out of five vertebrate Frizzled receptor families, Fz1/2/7 (Fz1 in

¹Department of Neurosciences and Developmental Biology, Faculty of Life Sciences, University of Vienna, Djerassiplatz 1, Vienna A-1030, Austria. ²Vienna Doctoral School of Ecology and Evolution, University of Vienna, Vienna A-1030, Austria.

*Author for correspondence (grigory.genikhovich@univie.ac.at)

 I.N., 0000-0002-5301-3361; T.L., 0000-0003-2182-1492; G.G., 0000-0003-4864-7770

This is an Open Access article distributed under the terms of the Creative Commons Attribution License (<https://creativecommons.org/licenses/by/4.0>), which permits unrestricted use, distribution and reproduction in any medium provided that the original work is properly attributed.

Handling Editor: Cassandra Extavour
Received 22 March 2022; Accepted 12 September 2022

the text below), *Fz4*, *Fz5/8* (*Fz5* in the text below) and *Fz9/10* (*Fz10* in the text below), and lacks only *Fz3/6*, which appears to be chordate specific (Bastin et al., 2015; Schenkelaars et al., 2015).

In this study, we asked which of the four Fz receptors and the many Wnt ligands are involved in the cWnt-dependent patterning of the oral-aboral axis in the *Nematostella* embryo. As the involvement of LRP5/6 is the hallmark of the cWnt signalling, we reasoned that analysing its loss-of-function phenotypes would tell us which parts of the OA patterning process are under cWnt control, thus facilitating the interpretation of the Fz loss-of-function data. We show that the knockdown of LRP5/6 suppresses the expression of the β -catenin-dependent oral and midbody genes, and expands aboral molecular identity without affecting endoderm specification. This results in a loss of the oral structures after gastrulation and a global expansion of the aboral/anterior molecular identity – a typical β -catenin loss-of-function phenotype. Individual knockdowns of the three orally expressed Fz genes do not affect oral marker gene expression. In contrast, dual- and triple-knockdowns of all possible Fz gene combinations partially phenocopy the LRP5/6 knockdown, while quadruple Fz gene knockdown replicates it at the molecular and morphological levels. These data suggest partial redundancy of the Fz receptors and involvement of all the *Nematostella* Fz receptors in cWnt-dependent OA patterning. We also demonstrate that Wnt1, Wnt3 and Wnt4 are the key Wnt ligands mediating OA patterning during early development.

RESULTS

Normal expression of the Fz and LRP5/6 genes in *Nematostella*

We analysed temporal and spatial expression dynamics of Fz, LRP5/6 and LRP4/5/6-like in *Nematostella* embryos and larvae by interrogating the NvERTx RNA-Seq database (Warner et al., 2018) and by performing whole-mount *in situ* hybridization. Transcriptomics data show that two out of four Fz genes, *Fz1* and *Fz5*, and LRP5/6 are abundant in the unfertilized egg, and their expression is maintained at an approximately constant level. In contrast, the other two Fz genes, *Fz4* and *Fz10*, are zygotic and become activated around 8 h post-fertilization (hpf) (Fig. S1A). LRP4/5/6-like (Fig. S1B) is a weakly expressed gene that starts to be upregulated around 48 hpf; its expression becomes confined to the forming apical organ (Fig. S1C). Thus, we reasoned that LRP4/5/6-like is unlikely to be involved in cWnt signalling (at least not before 48 hpf) and did not consider it further.

In situ hybridization analysis of the *Fz1*, *Fz5* and LRP5/6 (Fig. 1) show the initially ubiquitous distribution of the mRNA before 10 hpf, which then appears to be followed by the formation of a clearing in the expression that likely corresponds to the future pre-endodermal plate. At the same time, *Fz4* and *Fz10* expression starts to be detectable. As the development progresses, a second clearing in the *Fz10* expression domain appears on the putative aboral end, while *Fz5* expression becomes most prominent aborally (see also Lebedeva et al., 2021; Leclère et al., 2016; Röttinger et al., 2012; Wijesena et al., 2022). At the onset of gastrulation, *Fz1*, *Fz4* and LRP5/6 are expressed ubiquitously; additionally, LRP5/6 is becoming ever more prominent in the aboral ectodermal domain. *Fz10* is expressed in the oral and midbody ectoderm, but it also starts to be strongly expressed in the invaginating endodermal plate. At late gastrula, a narrow clearing in *Fz1* expression starts to appear between the midbody ectoderm and the aboral ectoderm, and *Fz5* acquires an additional expression domain in the aboral endoderm. During planula development, *Fz1* expression forms an oral-to-aboral gradient with the maximum in the oral ectoderm and oral

endoderm; however, *Fz1* transcript is also detectable in the apical organ. *Fz4* transcription forms a shallow oral-to-aboral gradient in both germ layers; however, in contrast to *Fz1*, *Fz4* is not expressed in the apical organ. *Fz5* is expressed in an aboral-to-oral gradient in both cell layers with the ectodermal expression fading out at the aboral/midbody boundary. Apical organ cells express *Fz5* particularly strongly, and there it is co-expressed with *Fz1*. Strong *Fz10* expression is detectable in the pharyngeal, oral and midbody ectoderm. Additionally, *Fz10* forms an oral-to-aboral gradient of expression in the endoderm. Finally, LRP5/6 is expressed ubiquitously; however, apical organ cells appear to produce much more LRP5/6, and a shallow aboral-to-oral gradient appears to exist in the endoderm (Fig. 1).

LRP5/6 knockdown

To assess the role of LRP5/6, we performed shRNA-mediated knockdowns (KDs, Fig. S2A-C) and characterized their effect on marker gene expression. We used *Brachyury* (*Bra*), *Wnt2* and *Six3/6* as markers of the oral, midbody and aboral domains, respectively (Lebedeva et al., 2021; Sinigaglia et al., 2013), *Axin* as a β -catenin signalling target gene with broader expression (Kraus et al., 2016; Lebedeva et al., 2021), as well as several additional markers for specific areas in the embryo. Notably, the midbody marker *Wnt2* is also positively regulated by β -catenin signalling but it is suppressed orally by *Bra* (Lebedeva et al., 2021). At the late gastrula stage (30 hpf), LRP5/6 RNAi resulted in a strong suppression of the oral markers *Bra*, *FoxA* and *FoxB*, as well as *Axin* (Fig. 2, Fig. S3). *Wnt2* was reduced and only detectable in the oral domain, while *Six3/6* strongly expanded orally and acquired an additional area of expression in the pharyngeal ectoderm (Fig. 2). The suppression of the oral ectodermal and the expansion of the aboral ectodermal domain signature into the oral ectodermal territory persisted into later developmental stages, even though LRP5/6 expression was re-established by 3 days post fertilization (dpf) (Fig. S4). Despite normal gastrulation, oral and pharyngeal structures were later lost, and by 4 dpf all LRP5/6 RNAi embryos resembled diploblastic spheres (Fig. 3A). In summary, LRP5/6 RNAi phenocopied the outcome of dominant-negative *Tcf* (*dnTcf*) mRNA overexpression (Röttinger et al., 2012), and was strikingly similar to the effect of the combined KD of *Bra*, *Lmx*, *FoxA* and *FoxB* – the four β -catenin-dependent transcription factors determining the oral molecular identity of the embryo (Lebedeva et al., 2021). Thus, LRP5/6 RNAi resulted in a typical β -catenin loss-of-function phenotype (Leclère et al., 2016), apart from the obvious fact that the embryos gastrulated normally, which was also the case in *dnTcf* mRNA-injected embryos (Röttinger et al., 2012) but, curiously, not in β -catenin morphants (Leclère et al., 2016) or in embryos subjected to shRNA-mediated β -catenin RNAi (Karabulut et al., 2019). Unlike LRP5/6 RNAi and *dnTcf* overexpression, β -catenin morpholino injection resulted in a complete suppression of the oral, midbody and aboral ectoderm markers, and in a ubiquitous upregulation of the endodermal marker *SnailA* (Leclère et al., 2016). In contrast, pharmacological activation of β -catenin signalling with azakenpaullone (AZK) starting at fertilization also blocked gastrulation; however, in this case, *SnailA* expression was abolished, and oral ectoderm markers were expressed ubiquitously instead (Leclère et al., 2016, see also Fig. 4A). Curiously, endodermal marker expression, as well as the gastrulation process, was not affected by AZK treatment if the treatment started after 6 hpf (Fig. 4A), which corresponds to the reported time of the activation of the zygotic genome (Helm et al., 2013). This suggests that endoderm specification probably relies on maternally deposited

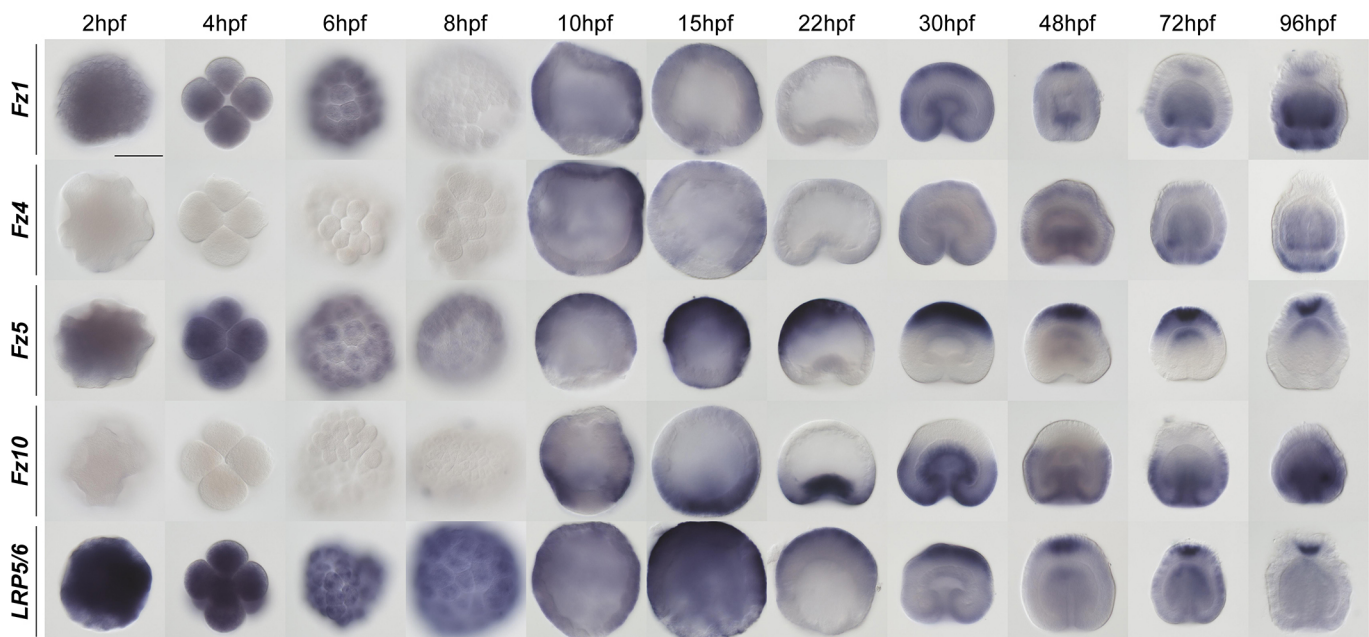


Fig. 1. Normal developmental expression of the Fz genes and LRP5/6. From 10 hpf onwards, the animal/oral pole of the embryo is pointing downwards. *In situ* hybridization with digoxigenin-labelled RNA probes followed by anti-Dig-AP staining and NBT/BCIP detection. Scale bar: 100 μ m.

mRNA and proteins, and occurs before 6 hpf, and that, once specified, the endoderm becomes insensitive to modulations in β -catenin signalling at least until late gastrula stage. Moreover, normal gastrulation and endodermal marker gene expression in shLRP5/6 embryos (Fig. 4B) raises the possibility that endoderm specification and the gastrulation movements, although obviously β -catenin dependent, may not require Wnt/Fz/LRP5/6-mediated signalling. To address this in more detail, we first asked how soon the effect of LRP5/6 knockdown started to manifest itself after the RNAi. Despite clear LRP5/6 suppression as early as 6 hpf, the effect of LRP5/6 RNAi on the sensitive β -catenin signalling target *Bra* was not apparent at 10 hpf, and only became observable at late blastula (18 hpf) stage (Fig. S5). As this comparatively late manifestation of the LRP5/6 RNAi effect, rather than endoderm specification and invagination being Wnt/Fz/LRP5/6-independent, may be the reason for the difference between the morpholino-mediated β -catenin KD and the RNAi-mediated LRP5/6 KD, we repeated LRP5/6 KD using a translation-blocking morpholino (MO, Fig. S2C). By 30 hpf (late gastrula stage in controls), LRP5/6 MO injection resulted in a phenotype similar to that of LRP5/6 RNAi, although more pronounced: not only *Bra*, but also *Wnt2* expression was abolished, and *Six3/6* was expanded throughout the whole ectoderm. In contrast to LRP5/6 RNAi, gastrulation was delayed in the morphants; nevertheless, as for RNAi, the specification of the *SnailA*-positive, *Six3/6*-negative pre-endodermal plate took place normally (Fig. 5A). By 48 hpf, the LRP5/6 MO-injected embryos remained arrested in gastrulation, demonstrating a miniature blastopore lip and a slightly submerged endoderm (Fig. 5B). By 4 dpf, LRP5/6 morphants displayed the same ‘bi-layered aboralized sphere’ phenotypes as the LRP5/6 RNAi embryos (Figs 3A and 5B). Both RNAi- and MO-mediated knockdown clearly show that LRP5/6 is required for the cWnt-mediated patterning of the ectoderm in *Nematostella*. The conspicuous lack of endodermal mesenteries in the 4 dpf LRP5/6 RNAi and morphant embryos is a clear sign of the disrupted BMP signalling resulting in the loss of the second, ‘directive’ body axis (Genikhovich et al., 2015; Leclère and

Rentzsch, 2014). Previously, we have demonstrated that β -catenin is required for the onset of the expression of *BMP2/4* and *Chordin* – the core components of the BMP signalling network in *Nematostella* (Genikhovich et al., 2015; Kirillova et al., 2018; Saina et al., 2009). Surprisingly, upon LRP5/6 RNAi, the directive axis is formed, but later lost, as evidenced by *Chordin* expression, which is initially normal and bilaterally symmetric at the gastrula stage, but disappears by 3 dpf (Fig. S6). In summary, we conclude that LRP5/6 is required for the β -catenin-dependent patterning of the ectoderm along the OA axis, and for the maintenance of the directive axis, but we do not find evidence of its involvement in the specification of the endoderm.

Knockdown of Fz receptors

In contrast to *Fz5* RNAi, which reproduced the *Fz5* morpholino knockdown phenotype published earlier (Leclère et al., 2016; this paper), individual RNAi of *Fz1*, *Fz4* and *Fz10* did not result in changes in the *Bra*, *Wnt2*, *Six3/6* and *Axin* expression (Fig. S7). The *Fz5* RNAi phenotype was similar to that of LRP5/6 RNAi, with the aboral, *Six3/6*-expressing domain expanded, and the midbody *Wnt2*-expressing domain constricted towards the oral pole (Fig. 2). However, in contrast to LRP5/6 RNAi, oral markers *Bra*, *FoxA* and *FoxB* were not affected by *Fz5* RNAi, and only the midbody expression of *Axin* was suppressed, while oral expression was retained (Fig. 2, Fig. S3). Endodermal expression of *SnailA*, *ERG* and *Fz10* was also not affected by any of the Fz RNAi knockdowns, except for *Fz10* expression, which, naturally, was abolished upon *Fz10* RNAi (Fig. 4B). Individual Fz gene RNAi did not lead to significant morphological defects apart from a slight gastrulation delay in *Fz1* and *Fz10* RNAi, and a previously reported slight shortening of the OA axis in *Fz5* RNAi (Leclère et al., 2016). By 4 dpf, the KD embryos developed eight normal mesenteries (Fig. 3B).

Surprisingly, these results contradicted the recently published *Fz1* and *Fz10* KD phenotypes (Wijesena et al., 2022). In this paper, the authors stated that overexpression of the dominant-negative

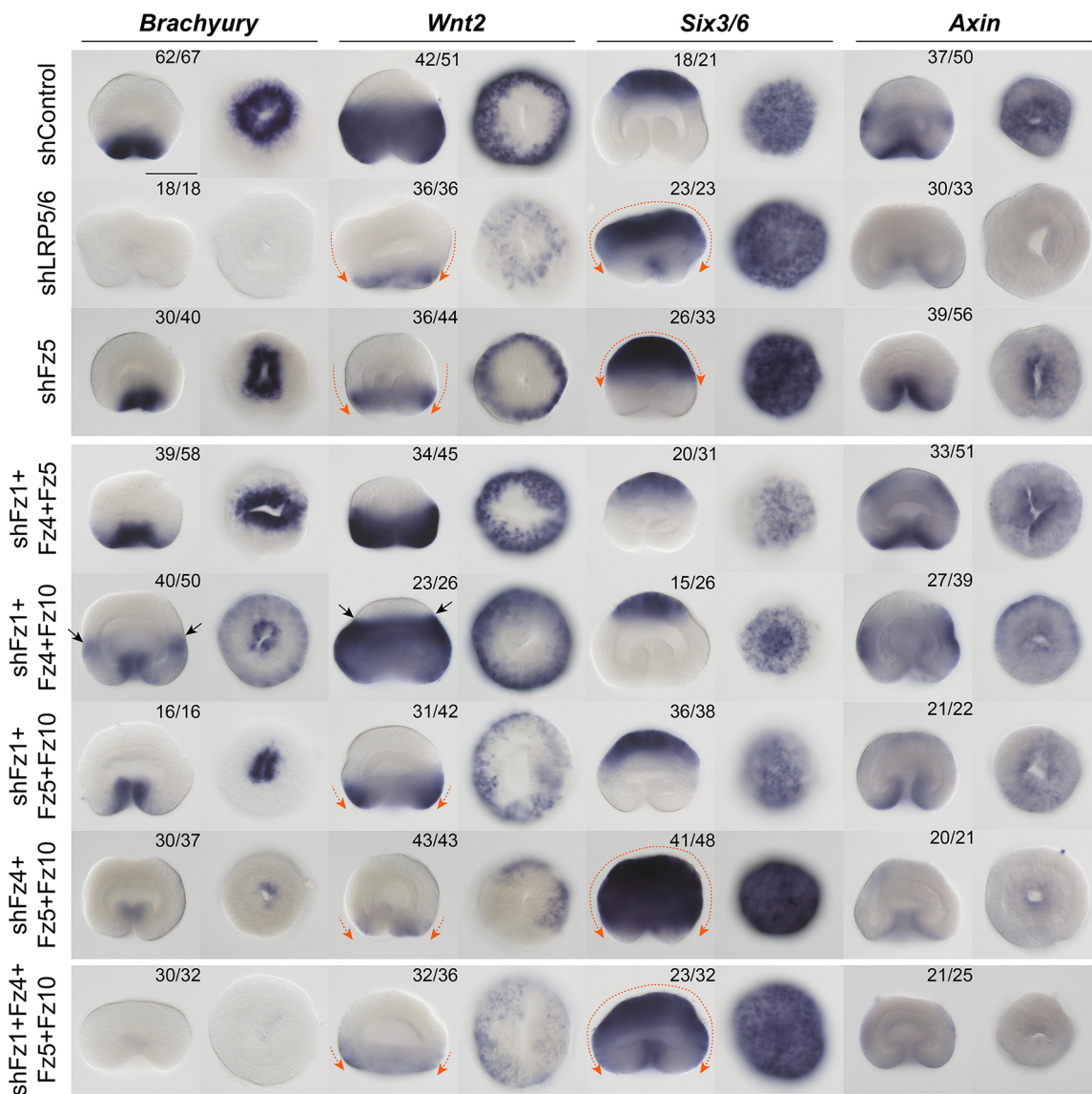


Fig. 2. Effects of RNAi-mediated KD of *LRP5/6* and *Fz5*, as well as triple and quadruple *Fz* gene KD combinations on the expression of the β -catenin-dependent markers of different axial domains in the 30 hpf late gastrula. To keep the row labels readable, simultaneous RNAi of, for example, *Fz1*, *Fz5* and *Fz10* is marked as shFz4+Fz5+Fz10 rather than shFz4+shFz5+shFz10. The same labelling convention applies to all the other figures showing simultaneous KDs. Orange arrows indicate the direction of the drastic expression shifts. There is curious asymmetric expression of *Bra* and *Wnt2* upon *Fz4+Fz5+Fz10* RNAi, indicating possible abnormal feedback from the directive axis patterning mechanism. Black arrows indicate the ring of stronger *Bra* expression in the midbody and the aboral expansion of *Wnt2* domain, suggesting an ectopic enhancement of the β -catenin signalling. The numbers in the top right corners show the fraction of embryos demonstrating this phenotype. Scale bar: 100 μ m. For each gene, lateral views (oral end down) are on the left and oral (or aboral in the case of *Six3/6*) views are on the right. *In situ* hybridization with digoxigenin-labelled RNA probes followed by anti-Dig-AP staining and NBT/BCIP detection.

form of *Fz1* (*dnFz1*) caused oral expansion of *Fz5*, suppression of *FoxA* in the blastopore lip, and the loss of the endodermal expression of *SnailA* and *Fz10* without interfering with the gastrulation process. In contrast, their *Fz10* morpholino injection suppressed endoderm invagination without affecting *SnailA*. This latter result was somewhat surprising, as the disappearance of *Fz10* expression Wijesena et al. observed upon *Fz1* KD did not lead to a gastrulation failure. These results led the authors to conclude that *Fz1* was controlling the cWnt-dependent specification of the endoderm, while *Fz10* was regulating the non-canonical Wnt-dependent endoderm invagination (Wijesena et al., 2022).

Remembering the more pronounced effect of morpholino-mediated *LRP5/6* KD in comparison with RNAi, we repeated individual *Fz1*, *Fz4* and *Fz10* KD using the *Fz1MO*, *Fz4MO* and

Fz10MO (Fig. 5, Fig. S2D). Similar to the RNAi result, *Fz1MO* and *Fz4MO* injection did not lead to changes in the expression of the oral, midbody, aboral and endodermal markers (Fig. 5A). In our hands, the overexpression of *dnFz1-mCherry* mRNA also did not cause any change in *Bra*, *Wnt2*, *Six3/6* and *SnailA* expression (Fig. S8), similar to the *Fz1* RNAi and *Fz1MO* KD. In contrast, *Fz10* morpholino injection led to a delay in gastrulation without affecting *Bra*, *Wnt2*, *Six3/6* and *SnailA* expression (Fig. 5A). By 48 hpf, *Fz10MO* morphants completed invagination, although their endoderm still looked irregular and they had open blastopores (Fig. 5B). Their morphology mostly normalized by 96 hpf, with the only deviation being the lower number of mesenteries suggesting developmental delay or, potentially, problems with integrating the oral-aboral and the directive axis patterning (Fig. 5B). Thus, it is

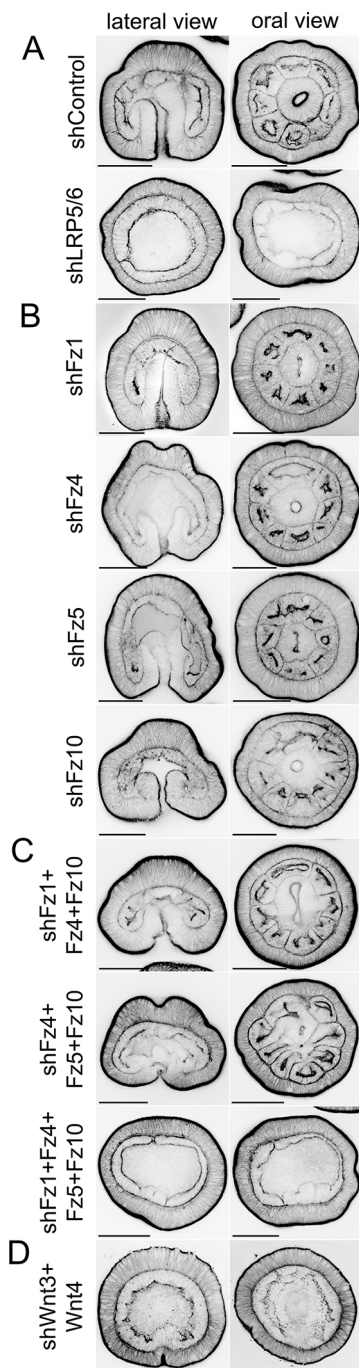


Fig. 3. Effects of the RNAi-mediated KD of *LRP5/6*, Fz genes and the *Wnt3/Wnt4* combination on the later development of the embryo. (A–D) Effects of the KD of *LRP5/6* (A), of individual Fz genes (B), of triple and quadruple Fz gene KDs (C), and of the double KD of *Wnt3* and *Wnt4* (D). 4 dpf embryos are stained using phalloidin-AlexaFluor488 to visualize actin filaments. Scale bars: 100 μ m. In the lateral views, the oral end points downwards.

likely that *Fz10* plays a role in regulating gastrulation; however, the similarity of the effect of *Fz10* and *LRP5/6* morpholino KD on the overall morphology of the gastrula raises the possibility that the gastrulation delay may be caused by the cWnt signalling-related defect. The proposed role of *Fz10* in mediating non-canonical Wnt signalling cannot be excluded and has to be directly assessed in the future; however, we do not find clear support for the ‘*Fz1* for cWnt and endoderm specification versus *Fz10* for non-canonical

Wnt signalling and endoderm invagination’ distinction proposed previously (Wijesena et al., 2022).

As individual RNAi of the orally expressed Fz genes did not elicit an effect, we presumed that they might be partially or completely redundant at the gastrula stage, and performed simultaneous RNAi of all possible combinations of two, three or four Frizzleds. Double Fz gene knockdowns showed effects on marker genes only if shFz5 was in the mix, and recapitulated the individual *Fz5* KD (Fig. S7). In triple RNAi, a β -catenin loss-of-function phenotype similar to the *LRP5/6* RNAi started to emerge in some cases, most notably in the *Fz4+Fz5+Fz10* combination (Fig. 2). Simultaneous RNAi of *Fz1+Fz4+Fz10* resulted in a curious phenotype, which we are currently unable to explain: expression of *Bra* and *Axin* at the oral end of the gastrula became weaker, and a narrow ring of relatively strong *Bra* expression and a wider ring of strong *Axin* expression appeared in the midbody of the gastrula, suggesting stronger than usual β -catenin signalling in this area. This occurred concomitantly with the aboral expansion of the *Wnt2* domain and reduction of the *Six3/6* domain. *Wnt2* expression in this case was strongest in an area located between the *Bra*-expressing ring in the midbody and the diminished *Six3/6* expression domain (Fig. 2). In spite of the prominent effects at the gastrula stage, triple Fz gene RNAi embryos formed eight mesenteries by 4 dpf, although the mesenteries in the *shFz4+Fz5+Fz10* combination always looked somewhat irregular (Fig. 3C). Finally, quadruple RNAi of all four Fz receptors phenocopied *LRP5/6* RNAi at the molecular as well as at the morphological level (Figs 2 and 3A,C). Taken together, we show that three orally expressed Fz receptors play a partially redundant function in the OA axis patterning of the *Nematostella* gastrula. The fact that only combined RNAi of all four Fz receptors phenocopies the *LRP5/6* knockdown at the molecular and morphological level hints towards the involvement of all *Nematostella* Fz proteins in the *LRP5/6*-mediated cWnt signalling. We do not find evidence that endoderm specification depends on *LRP5/6*/Fz-mediated β -catenin signalling.

Knockdown of Wnt ligands

Wnt genes of *Nematostella* are expressed in staggered domains along the OA axis (Kusserow et al., 2005; Lee et al., 2006); however, their individual roles in OA patterning are still unclear. We have shown previously that co-expression of two Wnt genes, *Wnt1* and *Wnt3*, was sufficient to convey axial organizer capacity to any area of the *Nematostella* gastrula ectoderm, while other early Wnt ligands failed to elicit this effect (Kirillova et al., 2018; Kraus et al., 2016). However, even for *Wnt1* and *Wnt3*, the possible role in axial patterning was not analysed. In order to achieve some indication of which Wnt ligands might be involved in transmitting the signals patterning the *Nematostella* ectoderm along the OA axis, we analysed the loss-of-function phenotypes of all the Wnt genes expressed in the early embryo of *Nematostella*. The following Wnt genes are active in the embryo at or before gastrula stage: *Wnt1*, *Wnt2*, *Wnt3*, *Wnt4*, *Wnt5*, *Wnt8a* and *WntA* (Fig. S9). RNAi of *Wnt5*, which was not very efficient with both shRNAs we used, and *WntA* did not elicit any noticeable effect on the expression of *Bra*, *Wnt2* and *Six3/6* in the gastrula. RNAi of the orally expressed *Wnt1* and, even more prominently, of *Wnt3* resulted in a reduction of the expression of the oral marker *Bra* and its expansion to the bottom of the pharynx (Fig. 6A, Fig. S10) – a phenotype similar to the KD effect of one of the four key regulators of the oral molecular identity: *FoxB* (Lebedeva et al., 2021). RNAi of *Wnt2* and *Wnt8a*, which are normally expressed in the midbody domain, resulted in the moderate oral expansion of the aboral marker *Six3/6*, while the KD of the

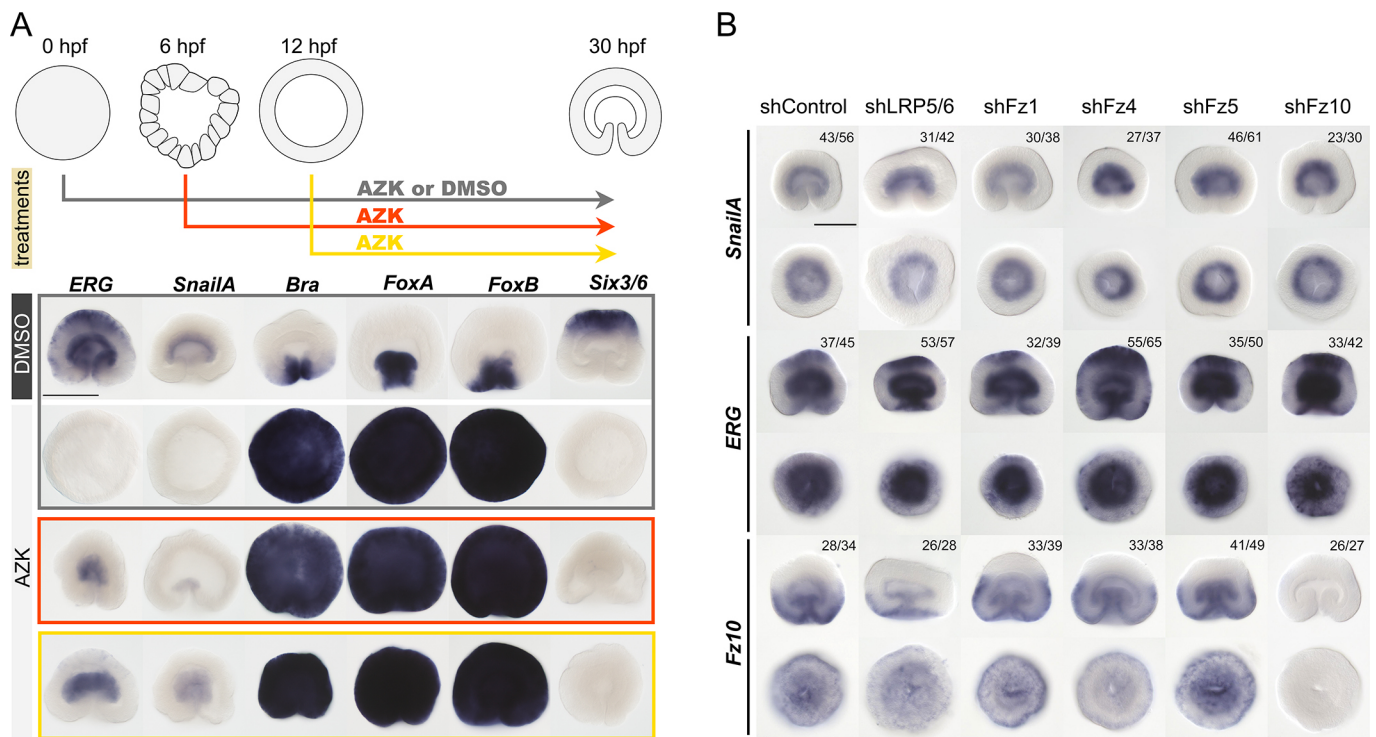


Fig. 4. Endoderm specification is an early event that does not seem to depend on Fz and LRP5/6. (A) Identification of the time of endoderm specification. Lateral views of 30 hpf embryos, oral end downwards. (B) Endodermal marker expression is not affected by the KD of *LRP5/6* or by knockdown of individual Fz genes. The numbers in the top right corners show the fraction of embryos showing this phenotype. For each gene, lateral views (oral end down) are at the top and oral (or aboral in the case of *Six3/6*) views are at the bottom. All embryos are late gastrulae at 30 hpf. Scale bars: 100 μ m. *In situ* hybridization with digoxigenin-labelled RNA probes followed by anti-Dig-AP staining and NBT/BCIP detection.

orally expressed *Wnt4* led to a strong aboralization of the embryo comparable with the effect of *Fz5* KD (Fig. 6A). None of the RNAi-mediated *Wnt* KDs affected *SnailA* expression (data not shown) or gastrulation. In spite of the oral-aboral marker expression changes we observed at 30 hpf in several individual *Wnt* KDs, the embryos appeared to have regulated their development by 4 dpf, building normal pharynges and mesenteries (Fig. S11).

Next, we tested whether concomitant knockdowns of the individual Fz receptors would lead to a synergistic effect with any of the *Wnt* genes, which showed an oral-aboral phenotype at 30 hpf upon individual KDs (Fig. 6B, Fig. S12). Simultaneous KD of *Wnt3* with individual Fz receptor genes showed a more prominent reduction in the expression of the oral marker *Bra* than *Wnt3* KD alone in all combinations. However, this effect was strongest in the shWnt3+Fz10 and the shWnt3+Fz5 combinations. A similar, although slightly weaker, effect was observed in the shWnt1+Fz combinations (Fig. S12). When shWnt4+Fz combinations were tested, the effects were even more noticeable. Oral expression of *Bra* was reduced in all shWnt4+Fz combinations in comparison with *Wnt4* RNAi alone. The aboralization of the embryo characteristic for the *Wnt4* KD was observed in all combinations; however, simultaneous KD of *Wnt4* and *Fz5* resulted in a more extensive aboralization than that observed upon individual KDs of *Wnt4* or *Fz5*, suggesting *Fz5* as a highly probable interaction partner for *Wnt4* – a hypothesis that can be tested by biochemical analyses in the future. Other shWnt+Fz double KDs did not lead to a noticeable synergistic effect (Fig. S12). Finally, we tested the result of the double KD of different *Wnt* genes. The strongest synergistic effect was observed in the shWnt3+Wnt4 and (to a slightly lesser degree) in the shWnt1+Wnt4 combination. Similar to the *LRP5/6* KD and

the combined KD of all Fz receptors, shWnt3+Wnt4, as well as shWnt1+Wnt4, resulted in a strong aboralization of the gastrula, and loss of the oral structures and mesenteries by 4 dpf (Figs 3D and 6C, Figs S13, S14). Thus, we conclude that *Wnt1*, *Wnt3* and *Wnt4* are required for the *LRP5/6*/Fz-dependent OA patterning, and for the maintenance of the directive axis in *Nematostella*.

DISCUSSION

The role of Wnt/Fz-mediated signalling in development and disease is difficult to overestimate; however, the variety of signalling pathways that may be activated by a Wnt-Fz interaction makes such investigation highly challenging. The initial hope that a multitude of vertebrate Fz receptors and a corresponding multitude of Wnt ligands would fall into an orderly system of signalling partnerships was not supported by the data. Phylogenetic analyses showed that the large diversity of the conserved Wnt gene families in Planulozoa (Cnidaria+Bilateria) is much more ancient than the Fz gene diversity found in vertebrates (Kusserow et al., 2005). Instead, non-vertebrate planulozoans normally have four Fz genes: *Fz1/2/7*, *Fz4*, *Fz5/8* and *Fz9/10*, which have to cope with all the various Wnt ligands (Bastin et al., 2015; Janssen et al., 2015; Qian et al., 2013; Robert et al., 2014; Wijesena et al., 2022). Work on bilaterian – mostly vertebrate – models demonstrated partial redundancy of Fz receptors, as well as the involvement of the same receptors in both the cWnt and the non-canonical Wnt signalling (Bhat, 1998; Dong et al., 2018; Fischer et al., 2007; Voloshanenko et al., 2017; Wang et al., 2016; Yu et al., 2012).

One of the Wnt-mediated signalling pathways, the cWnt or Wnt/ β -catenin pathway, appears to be the oldest axial patterning system present in animals. cWnt pathway involvement in the patterning of

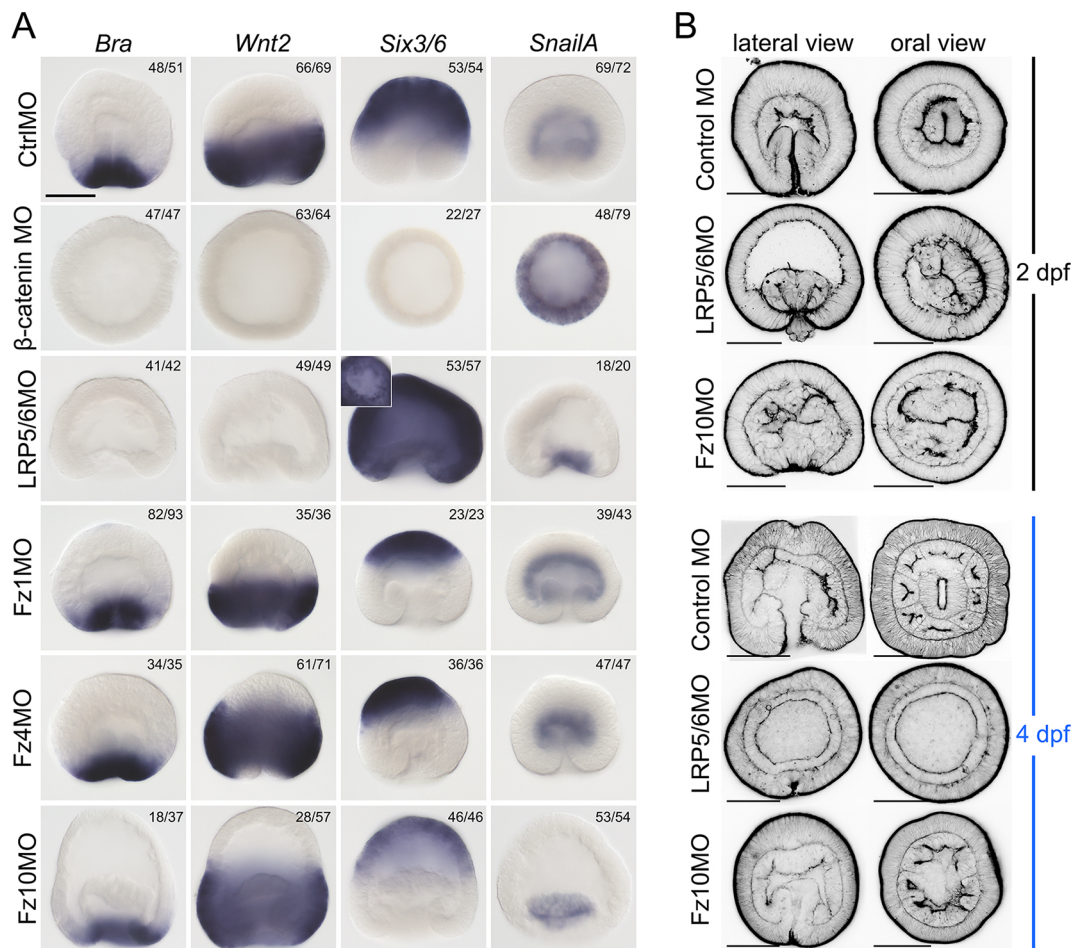


Fig. 5. Effect of the morpholino-mediated KD of *LRP5/6* and orally expressed *Fz* genes on the early development of *Nematostella*. (A) Effect of the knockdowns on the expression of the markers of the distinct axial domains in the ectoderm and on the expression of the endodermal marker *SnailA*. *In situ* hybridization with digoxigenin-labelled RNA probes followed by anti-Dig-AP staining and NBT/BCIP detection. All embryos are fixed at 30 hpf. The numbers in the top right corners show the fractions of embryos demonstrating this phenotype. Scale bar: 100 μ m. Lateral views, oral end downwards. The inset image of an oral view of the LRP5/6 morphant stained for *Six3/6* shows that the pre-endodermal plate does not express *Six3/6*. (B) Effects of the LRP5/6 and Fz10 morpholino KDs on the later development of the embryos. Phalloidin staining of the 2 dpf and 4 dpf planulae. Scale bars: 100 μ m.

the PA axis of Bilateria and the OA axis of Cnidaria has been convincingly demonstrated functionally during the past 30 years (Darras et al., 2018, 2011; Fu et al., 2012; Kiecker and Niehrs, 2001; Kraus et al., 2016; Lebedeva et al., 2021; Marlow et al., 2013; McCauley et al., 2015; Nordström et al., 2002; Prühs et al., 2017; Range et al., 2013), and expression data suggest that cWnt may also be responsible for axial patterning in the earlier branching ctenophores and sponges (Leininger et al., 2014; Pang et al., 2010). Another ancestral developmental function of β -catenin appears to be the definition of the endomesodermal and, subsequently, the endodermal domain during germ layer specification in Bilateria and Cnidaria (Henry et al., 2008; Leclère et al., 2016; Lhomond et al., 2012; Logan et al., 1999; Martín-Durán et al., 2016; Momose et al., 2008; Momose and Houlston, 2007; Wikramanayake et al., 2003). Among cnidarians, the role of Fz-mediated signalling in gastrulation and OA patterning has been addressed in a hydroid *Clytia hemisphaerica*. There, two Fz mRNAs, *CheFz1* (*Fz1/2/7* ortholog) and *ChFz3* (*Fz9/10* ortholog), are maternally localized to the animal and the vegetal hemispheres of the egg, respectively, and appear to have opposing functions. *CheFz1* KD results in a delayed endoderm formation and suppression of the animal/oral marker gene expression, while

CheFz3 KD leads to the oralization of the embryo, abolishes vegetal/aboral marker genes and accelerates the ingress of the endodermal cells (Momose and Houlston, 2007). *CheFz1* is also reported to be involved in the Strabismus/Dishevelled-mediated embryo elongation in *Clytia*, suggesting that *CheFz1* is active in the cWnt as well as in the Wnt/PCP pathways (Momose et al., 2012). *CheWnt3* (*Wnt3* ortholog), the mRNA of which is maternally localized to the animal pole, appears to be the key ligand responsible for the oralization, likely by signalling via *CheFz1* (Momose et al., 2008). This mode of regulation, however, does not recapitulate the situation we observed in the anthozoan cnidarian model *Nematostella vectensis*. In *Nematostella*, *Fz1*, *Fz5* and *LRP5/6* mRNAs are maternally deposited; however, these mRNAs are evenly distributed throughout the egg. Fz gene expression during early development is in partially overlapping domains, and it roughly recapitulates the expression of Fz genes in sea urchin embryos of comparable stages (Robert et al., 2014). With the possible expression of *Wnt5*, which shows some maternal transcript (Fig. S9), *Nematostella* Wnt genes, *Fz4* and *Fz10* are zygotically expressed. Proteomics data indicate that, among the four Fz receptors, LRP5/6 and all Wnt ligands, only Fz5 protein is detectable in the *Nematostella* egg, early cleavage and blastula

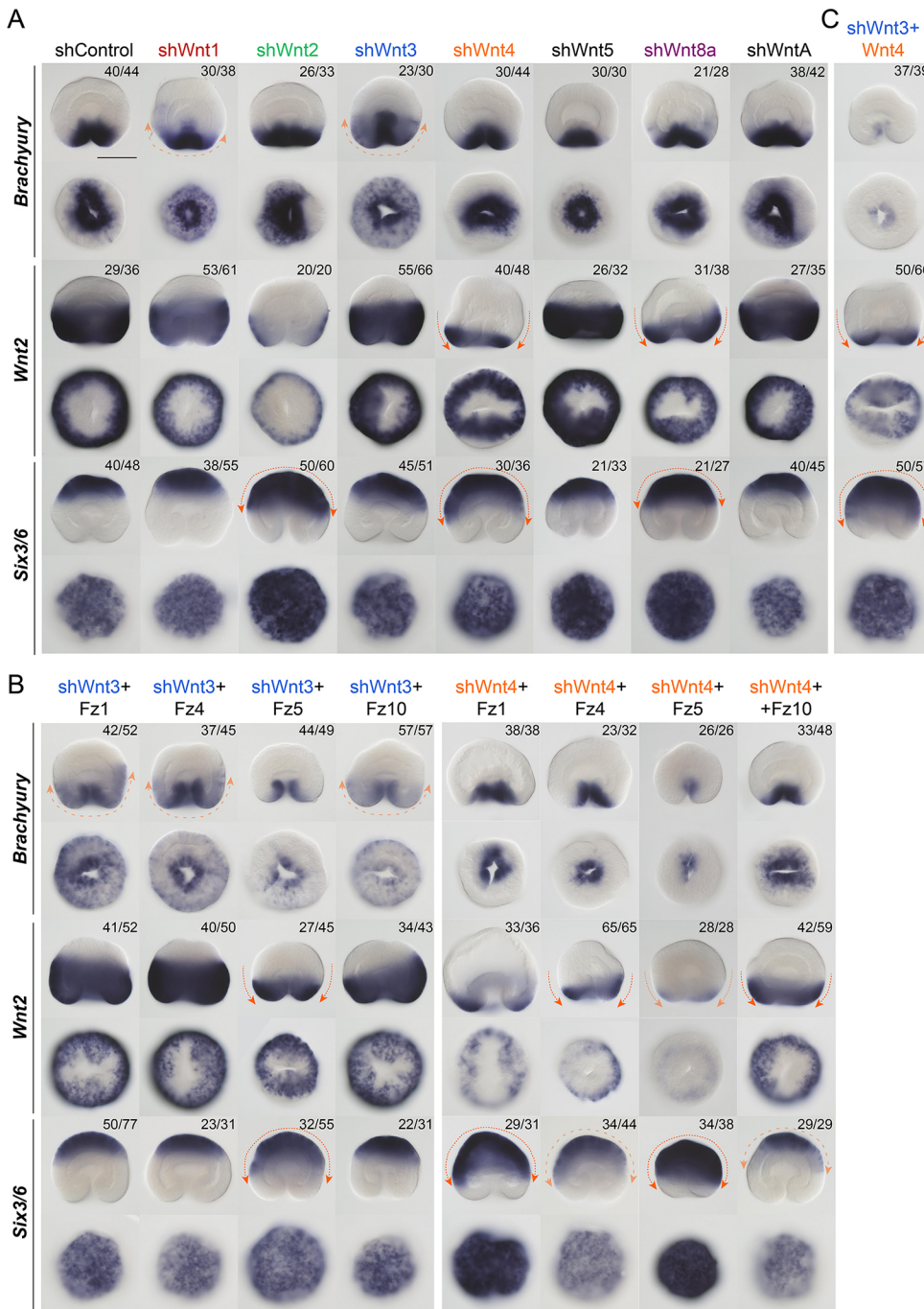


Fig. 6. Effect of the KD of Wnt genes on the expression of the oral, midbody and aboral ectoderm markers in the 30 hpf gastrulae. (A) KDs of individual Wnt genes. (B) Simultaneous KDs of *Wnt3* or *Wnt4* with the individual Fz receptor genes. (C) Simultaneous KDs of *Wnt3* and *Wnt4*. Orange arrows indicate the direction of the particularly drastic expression shifts. The numbers in the top right corners show the fractions of embryos demonstrating this phenotype. Scale bar: 100 μm . For each gene, lateral views (oral end downwards) are at the top and oral (or aboral in the case of *Six3/6*) views are at the bottom. *In situ* hybridization with digoxigenin-labelled RNA probes followed by anti-Dig-AP staining and NBT/BCIP detection.

stage embryos (Levitan et al., 2015). Our AZK treatment experiments suggest that β -catenin-dependent specification of the future pre-endodermal plate is an early event that occurs before the onset of the zygotic transcription around 6 hpf, and is thus likely to rely on maternally deposited molecules. We observed normal endoderm invagination, normal expression of the endodermal markers *SnailA* and *ERG* (Fig. 4B), which are negatively controlled by β -catenin, and the lack of the expression of the β -catenin signalling targets such as *Bra* in the endoderm of the embryos treated with AZK after 6 hpf (Lebedeva et al., 2021). This indicates that, after being specified, the future endoderm becomes insensitive to the modulation of the β -catenin signalling intensity. Moreover, normal endoderm specification upon RNAi and morpholino knockdowns of the maternally deposited *LRP5/6*, *Fz1* and *Fz5*

suggest that this process may not require Fz/LRP5/6-mediated signalling but relies on the cytoplasmic components of the β -catenin signalling pathway. Because currently we cannot fully exclude the possibility that some LRP5/6 and Wnt protein remained undetected in all the proteomic datasets (Levitan et al., 2015) or that their translation from maternal mRNA was not sufficiently suppressed in our KDs, additional genetic work will be required. In the future, generation and incrossing of the β -catenin^{w^t-} and LRP5/6^{w^t-} knockout lines will allow us to definitively answer the question of whether or not endoderm specification relies on maternal β -catenin and is LRP5/6 independent, as our data currently seem to suggest. The gastrulation delay in LRP5/6 morphants also indicates the likely involvement of LRP5/6-mediated β -catenin signalling in the process of gastrulation.

In echinoderms, the early β -catenin-dependent specification of the endomesodermal domain is followed by the segregation of the endoderm from the mesoderm, and the subsequent Wnt-dependent PA patterning. In the endoderm, β -catenin signalling remains strong, while in the mesoderm β -catenin signalling becomes suppressed (Lhomond et al., 2012; Logan et al., 1999; McCauley et al., 2015; McClay et al., 2021; Range et al., 2013; Sun et al., 2021; Wikramanayake et al., 1998, 2004). A similar sequence of events – the early β -catenin-dependent definition of the future endodermal domain, the formation of the boundary between the β -catenin-sensitive future oral ectoderm and the β -catenin-insensitive future endoderm – and the subsequent Wnt-dependent OA patterning of the ectoderm also occurs in *Nematostella*, and these events seem to follow the same regulatory logic as described for the sea urchin. Recently, we described the regulatory principle underlying β -catenin-dependent OA patterning of the ectoderm in *Nematostella*, which leads to the subdivision of the ectoderm into oral, midbody and aboral domains (Lebedeva et al., 2021). This subdivision happens as follows. A number of transcription factor-coding genes, the expression of which is positively regulated by β -catenin signalling, start to be expressed in the oral hemisphere of the *Nematostella* embryo. Their expression resolves into specific domains along the oral-aboral axis because some of these genes, which are expressed more orally, encode transcriptional repressors acting on the genes, which are expressed more aborally. This creates the two main molecular boundaries of the early embryo of *Nematostella* – the oral/midbody boundary and the midbody/aboral boundary. We showed that the oral/midbody boundary is established by the module of four transcription factors: Brachyury, Lmx, FoxA and FoxB. The midbody/aboral boundary is created due to the activity of the transcription factor Sp6-9 (Lebedeva et al., 2021). The whole regulatory principle and the genes involved in the OA patterning of the *Nematostella* embryo showed striking resemblance to the logic and the components of the PA patterning in deuterostome Bilateria (Darras et al., 2018, 2011; Kiecker and Niehrs, 2001; Lebedeva et al., 2021; Nordström et al., 2002; Range, 2018; Range et al., 2013). In contrast to endoderm specification, axial patterning is strongly affected by the knockdowns of LRP5/6 or combined knockdowns of Fz receptors, which demonstrate partial functional redundancy. The fact that LRP5/6 phenotype is phenocopied only by the simultaneous knockdown of all four Fz receptors suggests that all of them are involved in β -catenin signalling. The similarity of the combined *Wnt3+Wnt4* KD phenotype, as well as of the combined *Wnt1+Wnt4* KD phenotype, to the *LRP5/6* KD and the quadruple Fz gene KD indicates that these three orally expressed Wnt ligands play the main role in the Fz/LRP5/6-mediated OA patterning during early *Nematostella* development. KD phenotype similarity also suggests that, among these three Wnt ligands, Wnt4 appears to be the one predominantly signalling via the aborally expressed Fz5.

Taken together, our data suggest the crucial role of the Wnt/LRP5/6/Fz-mediated signalling in the OA patterning of the sea anemone *Nematostella vectensis*, in which different Fz receptors play partially redundant roles. In contrast, we do not find evidence for the involvement of Fz/LRP5/6-mediated signalling in the specification of the pre-endodermal plate. With this work, we lay the foundation for the future research, which will show whether Fz functions become more distinct at later developmental stages, identify the possible signalling preferences of the different Wnt ligands towards different Fz receptors, and address the role of the non-canonical Wnt pathways in *Nematostella* development. Ultimately, it will be important to understand not only the

difference between the functions of the different Fz molecules but also the role of their redundancy and the selective pressures maintaining what appears to be an ancestral Fz redundancy conserved in Cnidaria and Bilateria.

MATERIALS AND METHODS

Animals, microinjection and electroporation

Adult *Nematostella vectensis* polyps were kept separated by sex in 16‰ artificial sea water (*Nematostella* medium=NM) at 18°C in the dark. Spawning was induced by placing the polyps into an illuminated incubator set to 25°C for 10 h. The eggs were de-jellied with 3% L-cystein/NM as described previously (Genikhovich and Technau, 2009). Microinjection of the shRNAs and morpholinos and electroporation of shRNAs against maternally expressed transcripts was performed prior to fertilization. For zygotic transcripts, electroporation and microinjection was performed after fertilization. The embryos were raised at 21°C.

Gene knockdown, mRNA overexpression and inhibitor treatments

shRNA-mediated gene knockdown was performed as described previously (Karabulut et al., 2019). Two independent, non-overlapping shRNAs were used for each gene to make sure that the KD result was specific. Regardless of whether one or more genes was being knocked down, the concentration of the shRNA against each transcript was 500 ng/ μ l. shRNA against *mOrange* was used as a control (shControl). In cases of simultaneous knockdowns, shControl was used at a concentration corresponding to the maximum combined shRNA concentration used against the genes of interest, i.e. in case of a quadruple knockdown, we used 2000 ng/ μ l shControl. RNAi efficiency was tested by *in situ* hybridization and quantitative PCR (Fig. S2A–C). For morpholino KDs, all MOs were used at a concentration of 250 μ M. The activity of the morpholinos was confirmed by co-injecting each of them with 20 ng/ μ l *mCherry* mRNA containing the recognition sequence for the respective morpholino oligonucleotide and testing whether *mCherry* translation was suppressed in comparison with the situation, when the same mRNA was co-injected with a control MO (Fig. S2D), which we have tested previously (Kraus et al., 2016; Lebedeva et al., 2021). To generate the *dnFz1-mCherry* construct, the fragment of *Fz1* cDNA encoding the C-terminal domain (27 amino acids of the protein following the seventh transmembrane domain) was replaced with *mCherry*-coding sequence. *In vitro* transcribed *dnFz1-mCherry* mRNA was microinjected at a concentration of 250 ng/ μ l. Control *mCherry* mRNA was injected at a concentration of 75 ng/ μ l since *mCherry* is \sim 3.2 times shorter than *dnFz1-mCherry*. mRNA was synthesized with mMessage mMachine kit (Life Technologies) and purified with the Monarch RNA clean-up kit (NEB). 5 μ M 1-azakenpaulone (Sigma) used for the treatments was prepared by diluting 5 mM AZK dissolved in DMSO with NM. An equal volume of DMSO was used to treat the control embryos. The duration of the treatment is described on Fig. 4A. The recognition sequences for the shRNAs, as well as the morpholino sequences are shown in Tables S1 and S2. Accession numbers for the genes used in the study are presented in Table S3.

In situ hybridization and phalloidin staining

In situ hybridization was performed as described previously (Kraus et al., 2016) with a single change: the embryos were fixed for 1 h at room temperature in 4%PFA/PBS, washed several times in PTw (1 \times PBS and 0.1% Tween 20), then in 100% methanol and finally stored in 100% methanol at –20°C. Digoxigenin-labelled RNA probes were detected with anti-digoxigenin-AP Fab fragments (Roche) diluted 1:4000 in 0.5% blocking reagent (Roche) in 1 \times MAB. After unbound antibody was removed by a series of ten PTw washes of 10 min each, the embryos were stained with a mixture of NBT/BCIP, embedded in 86% glycerol and imaged using a Nikon 80i compound microscope equipped with the Nikon DS-Fi1 camera. For phalloidin staining, the embryos were fixed in 4%PFA/PTwTx (1 \times PBS, 0.1% Tween 20 and 0.2% Triton X-100) for 1 h at room temperature, washed five times with PTwTx, incubated in 100% acetone pre-cooled to –20°C for 7 min on ice and washed three more times with PTwTx. 2 μ l of phalloidin-AlexaFluor488 (ThermoFisher) was added per

100 µl PTwTx, and the embryos were stained overnight at 4°C. After eight 10-min washes with PTwTx, the embryos were gradually embedded in Vectashield (Vector labs) and imaged with the Leica SP8 CLSM.

Acknowledgements

We are grateful to the Core Facility for Cell Imaging and Ultrastructure Research of the University of Vienna for the access to the confocal microscope. We thank David Mörsdorf for his valuable comments on the manuscript, and Leonie Drakos for help with the generation of the constructs and mRNAs for testing morpholino efficiency.

Competing interests

The authors declare no competing or financial interests.

Author contributions

Conceptualization: G.G.; Methodology: G.G.; Validation: I.N., T.L.; Investigation: I.N., T.L., G.G.; Writing - original draft: I.N., G.G.; Writing - review & editing: I.N., T.L., G.G.; Visualization: I.N., T.L., G.G.; Supervision: G.G.; Project administration: G.G.; Funding acquisition: G.G.

Funding

This work was funded by the Austrian Science Foundation (FWF) (P30404-B29 to G.G.). Open Access funding provided by Universität Wien. Deposited in PMC for immediate release.

Peer review history

The peer review history is available online at <https://journals.biologists.com/dev/lookup/doi/10.1242/dev.200785.reviewer-comments.pdf>

References

- Aberle, H., Bauer, A., Stappert, J., Kispert, A. and Kemler, R. (1997). β -catenin is a target for the ubiquitin-proteasome pathway. *EMBO J.* **16**, 3797-3804. doi:10.1093/emboj/16.13.3797
- Acebron, S. P. and Niehrs, C. (2016). β -catenin-independent roles of Wnt/LRP6 signaling. *Trends Cell Biol.* **26**, 956-967. doi:10.1016/j.tcb.2016.07.009
- Adamska, M., Larroux, C., Adamski, M., Green, K., Lovas, E., Koop, D., Richards, G. S., Zwafink, C. and Degnan, B. M. (2010). Structure and expression of conserved Wnt pathway components in the demosponge *Amphimedon queenslandica*. *Evol. Dev.* **12**, 494-518. doi:10.1111/j.1525-142X.2010.00435.x
- Bastin, B. R., Chou, H.-C., Pruitt, M. M. and Schneider, S. Q. (2015). Structure, phylogeny, and expression of the frizzled-related gene family in the lophotrochozoan annelid *Platynereis dumerilii*. *Evodevo* **6**, 37. doi:10.1186/s13227-015-0032-4
- Bhat, K. M. (1998). frizzled and frizzled 2 play a partially redundant role in wingless signaling and have similar requirements to wingless in neurogenesis. *Cell* **95**, 1027-1036. doi:10.1016/S0092-8674(00)81726-2
- Croce, J. C. and McClay, D. R. (2008). Evolution of the Wnt pathways. *Methods Mol. Biol.* **469**, 3-18. doi:10.1007/978-1-60327-469-2_1
- Darras, S., Gerhart, J., Terasaki, M., Kirschner, M. and Lowe, C. J. (2011). β -catenin specifies the endomesoderm and defines the posterior organizer of the hemichordate *Saccoglossus kowalevskii*. *Development* **138**, 959-970. doi:10.1242/dev.059493
- Darras, S., Fritzenwanker, J. H., Uhlinger, K. R., Farrelly, E., Pani, A. M., Hurley, I. A., Norris, R. P., Osowitz, M., Terasaki, M., Wu, M. et al. (2018). Anteroposterior axis patterning by early canonical Wnt signaling during hemichordate development. *PLoS Biol.* **16**, e2003698. doi:10.1371/journal.pbio.2003698
- Dong, B., Vold, S., Olvera-Jaramillo, C. and Chang, H. (2018). Functional redundancy of frizzled 3 and frizzled 6 in planar cell polarity control of mouse hair follicles. *Development* **145**, dev168468. doi:10.1242/dev.168468
- Fischer, T., Guimera, J., Wurst, W. and Prakash, N. (2007). Distinct but redundant expression of the Frizzled Wnt receptor genes at signaling centers of the developing mouse brain. *Neuroscience* **147**, 693-711. doi:10.1016/j.neuroscience.2007.04.060
- Flack, J. E., Mieszczynek, J., Novcic, N. and Bienz, M. (2017). Wnt-Dependent Inactivation of the Groucho/TLE Co-repressor by the HECT E3 Ubiquitin Ligase Hyd/UBR5. *Mol. Cell* **67**, 181-193.e185. doi:10.1016/j.molcel.2017.06.009
- Fu, J., Posnien, N., Bolognesi, R., Fischer, T. D., Rayl, P., Oberhofer, G., Kitzmann, P., Brown, S. J. and Bucher, G. (2012). Asymmetrically expressed axin required for anterior development in *Tribolium*. *Proc. Natl. Acad. Sci. USA* **109**, 7782-7786. doi:10.1073/pnas.1116641109
- Gammons, M. and Bienz, M. (2018). Multiprotein complexes governing Wnt signal transduction. *Curr. Opin. Cell Biol.* **51**, 42-49. doi:10.1016/j.cob.2017.10.008
- García de Herreros, A. and Duñach, M. (2019). Intracellular signals activated by canonical Wnt ligands independent of GSK3 inhibition and beta-catenin stabilization. *Cells* **8**, 1148. doi:10.3390/cells8101148
- Genikhovich, G. and Technau, U. (2009). Induction of spawning in the starlet sea anemone *Nematostella vectensis*, in vitro fertilization of gametes, and dejellying of zygotes. *CSH Protoc.* **2009**, pdb prot5281. doi:10.1101/pdb.prot5281
- Genikhovich, G., Fried, P., Prünster, M. M., Schinko, J. B., Gilles, A. F., Meier, K., Iber, D. and Technau, U. (2015). Axis patterning by BMPs: cnidarian network reveals evolutionary constraints. *Cell Rep.* **10**, 1646-1654. doi:10.1016/j.celrep.2015.02.035
- Grainger, S. and Willert, K. (2018). Mechanisms of Wnt signaling and control. *Wiley Interdiscip. Rev. Syst. Biol. Med.* **10**, e1422. doi:10.1002/wsbm.1422
- Helm, R. R., Siebert, S., Tulin, S., Smith, J. and Dunn, C. W. (2013). Characterization of differential transcript abundance through time during *Nematostella vectensis* development. *BMC Genomics* **14**, 266. doi:10.1186/1471-2164-14-266
- Henry, J. Q., Perry, K. J., Wever, J., Seaver, E. and Martindale, M. Q. (2008). β -catenin is required for the establishment of vegetal embryonic fates in the nemertean, *Cerebratulus lacteus*. *Dev. Biol.* **317**, 368-379. doi:10.1016/j.ydbio.2008.02.042
- Janssen, R., Schönauer, A., Weber, M., Turetzek, N., Hogvall, M., Goss, G. E., Patel, N. H., McGregor, A. P. and Hilbrant, M. (2015). The evolution and expression of panarthropod frizzled genes. *Frontiers Ecol. Evol.* **3**, 96. doi:10.3389/fevo.2015.00096
- Karabulut, A., He, S., Chen, C.-Y., McKinney, S. A. and Gibson, M. C. (2019). Electroporation of short hairpin RNAs for rapid and efficient gene knockdown in the starlet sea anemone, *Nematostella vectensis*. *Dev. Biol.* **448**, 7-15. doi:10.1016/j.ydbio.2019.01.005
- Kiecker, C. and Niehrs, C. (2001). A morphogen gradient of Wnt/ β -catenin signalling regulates anteroposterior neural patterning in *Xenopus*. *Development* **128**, 4189-4201. doi:10.1242/dev.128.21.4189
- Kirililova, A., Genikhovich, G., Pukhlyakova, E., Demilly, A., Kraus, Y. and Technau, U. (2018). Germ-layer commitment and axis formation in sea anemone embryonic cell aggregates. *Proc. Natl. Acad. Sci. USA* **115**, 1813-1818. doi:10.1073/pnas.1711516115
- Kraus, Y., Aman, A., Technau, U. and Genikhovich, G. (2016). Pre-bilaterian origin of the blastoporal axial organizer. *Nat. Commun.* **7**, 11694. doi:10.1038/ncomms11694
- Kusserow, A., Pang, K., Sturm, C., Hroudá, M., Lentfer, J., Schmidt, H. A., Technau, U., von Haeseler, A., Hobmayer, B., Martindale, M. Q. et al. (2005). Unexpected complexity of the Wnt gene family in a sea anemone. *Nature* **433**, 156-160. doi:10.1038/nature03158
- Lebedeva, T., Aman, A. J., Graf, T., Niedermoser, I., Zimmermann, B., Kraus, Y., Schatka, M., Demilly, A., Technau, U. and Genikhovich, G. (2021). Cnidarian-bilaterian comparison reveals the ancestral regulatory logic of the β -catenin dependent axial patterning. *Nat. Commun.* **12**, 4032. doi:10.1038/s41467-021-24364-8
- Leclère, L. and Rentzsch, F. (2014). RGM regulates BMP-mediated secondary axis formation in the sea anemone *Nematostella vectensis*. *Cell Rep.* **9**, 1-10. doi:10.1016/j.celrep.2014.11.009
- Leclère, L., Bause, M., Sinigaglia, C., Steger, J. and Rentzsch, F. (2016). Development of the aboral domain in *Nematostella* requires β -catenin and the opposing activities of Six3/6 and Frizzled5/8. *Development* **143**, 1766-1777. doi:10.1242/dev.120931
- Lee, P. N., Pang, K., Matus, D. Q. and Martindale, M. Q. (2006). A WNT of things to come: evolution of Wnt signaling and polarity in cnidarians. *Semin. Cell Dev. Biol.* **17**, 157-167. doi:10.1016/j.semcdb.2006.05.002
- Leininger, S., Adamski, M., Bergum, B., Guder, C., Liu, J., Laplante, M., Bråte, J., Hoffmann, F., Fortunato, S., Jordal, S. et al. (2014). Developmental gene expression provides clues to relationships between sponge and eumetazoan body plans. *Nat. Commun.* **5**, 3905. doi:10.1038/ncomms4905
- Levitan, S., Sher, N., Brekhman, V., Ziv, T., Lubzens, E. and Lotan, T. (2015). The making of an embryo in a basal metazoan: proteomic analysis in the sea anemone *Nematostella vectensis*. *Proteomics* **15**, 4096-4104. doi:10.1002/pmic.201500255
- Lhomond, G., McClay, D. R., Gache, C. and Croce, J. C. (2012). Frizzled1/2/7 signaling directs β -catenin nuclearisation and initiates endoderm specification in macromeres during sea urchin embryogenesis. *Development* **139**, 816-825. doi:10.1242/dev.072215
- Logan, C. Y., Miller, J. R., Ferkowicz, M. J. and McClay, D. R. (1999). Nuclear beta-catenin is required to specify vegetal cell fates in the sea urchin embryo. *Development* **126**, 345-357. doi:10.1242/dev.126.2.345
- MacDonald, B. T. and He, X. (2012). Frizzled and LRP5/6 receptors for Wnt/ β -catenin signaling. *Cold Spring Harb. Perspect. Biol.* **4**, a007880. doi:10.1101/cshperspect.a007880
- Marlow, H., Matus, D. Q. and Martindale, M. Q. (2013). Ectopic activation of the canonical wnt signaling pathway affects ectodermal patterning along the primary axis during larval development in the anthozoan *Nematostella vectensis*. *Dev. Biol.* **380**, 324-334. doi:10.1016/j.ydbio.2013.05.022
- Martín-Durán, J. M., Passamaneck, Y. J., Martindale, M. Q. and Hejnol, A. (2016). The developmental basis for the recurrent evolution of deuterostomy and protostomy. *Nat. Ecol. Evol.* **1**, 5. doi:10.1038/s41559-016-0005

- McCauley, B. S., Akyar, E., Saad, H. R. and Hinman, V. F.** (2015). Dose-dependent nuclear β -catenin response segregates endomesoderm along the sea star primary axis. *Development* **142**, 207–217. doi:10.1242/dev.113043
- McClay, D. R., Croce, J. C. and Warner, J. F.** (2021). Conditional specification of endomesoderm. *Cells Dev.* **167**, 203716. doi:10.1016/j.cdev.2021.203716
- Momose, T. and Houliston, E.** (2007). Two oppositely localised frizzled RNAs as axis determinants in a cnidarian embryo. *PLoS Biol.* **5**, e70. doi:10.1371/journal.pbio.0050070
- Momose, T., Derelle, R. and Houliston, E.** (2008). A maternally localised Wnt ligand required for axial patterning in the cnidarian *Clytia hemisphaerica*. *Development* **135**, 2105–2113. doi:10.1242/dev.021543
- Momose, T., Kraus, Y. and Houliston, E.** (2012). A conserved function for Strabismus in establishing planar cell polarity in the ciliated ectoderm during cnidarian larval development. *Development* **139**, 4374–4382. doi:10.1242/dev.084251
- Nordström, U., Jessell, T. M. and Edlund, T.** (2002). Progressive induction of caudal neural character by graded Wnt signaling. *Nat. Neurosci.* **5**, 525–532. doi:10.1038/nn0602-854
- Pang, K., Ryan, J. F., Mullikin, J. C., Baxeavanis, A. D. and Martindale, M. Q.** (2010). Genomic insights into Wnt signaling in an early diverging metazoan, the ctenophore *Mnemiopsis leidyi*. *Evodevo* **1**, 10. doi:10.1186/2041-9139-1-10
- Park, H. W., Kim, Y. C., Yu, B., Morioishi, T., Mo, J.-S., Plouffe, S. W., Meng, Z., Lin, K. C., Yu, F.-X., Alexander, C. M. et al.** (2015). Alternative Wnt signaling activates YAP/TAZ. *Cell* **162**, 780–794. doi:10.1016/j.cell.2015.07.013
- Prühs, R., Beermann, A. and Schröder, R.** (2017). The roles of the Wnt-antagonists Axin and Lrp4 during embryogenesis of the red flour beetle *Tribolium castaneum*. *J. Dev. Biol.* **5**, 10. doi:10.3390/jdb5040010
- Qian, G., Li, G., Chen, X. and Wang, Y.** (2013). Characterization and embryonic expression of four amphioxus Frizzled genes with important functions during early embryogenesis. *Gene Expr. Patterns* **13**, 445–453. doi:10.1016/j.gep.2013.08.003
- Range, R. C.** (2018). Canonical and non-canonical Wnt signaling pathways define the expression domains of Frizzled 5/8 and Frizzled 1/2/7 along the early anterior-posterior axis in sea urchin embryos. *Dev. Biol.* **444**, 83–92. doi:10.1016/j.ydbio.2018.10.003
- Range, R. C., Angerer, R. C. and Angerer, L. M.** (2013). Integration of canonical and noncanonical wnt signaling pathways patterns the neuroectoderm along the anterior–posterior axis of sea urchin embryos. *PLoS Biol.* **11**, e1001467. doi:10.1371/journal.pbio.1001467
- Robert, N., Lhomond, G., Schubert, M. and Croce, J. C.** (2014). A comprehensive survey of wnt and frizzled expression in the sea urchin *Paracentrotus lividus*. *Genesis* **52**, 235–250. doi:10.1002/dvg.22754
- Röttinger, E., Dahlin, P. and Martindale, M. Q.** (2012). A framework for the establishment of a cnidarian gene regulatory network for “Endomesoderm” specification: the inputs of β -catenin/TCF signaling. *PLoS Gen.* **8**, e1003164. doi:10.1371/journal.pgen.1003164
- Saina, M., Genikhovich, G., Renfer, E. and Technau, U.** (2009). BMPs and chordin regulate patterning of the directive axis in a sea anemone. *Proc. Natl. Acad. Sci. USA* **106**, 18592–18597. doi:10.1073/pnas.0900151106
- Schenkelaars, Q., Fierro-Constain, L., Renard, E., Hill, A. L. and Borchiellini, C.** (2015). Insights into Frizzled evolution and new perspectives. *Evol. Dev.* **17**, 160–169. doi:10.1111/ede.12115
- Semenov, M. V., Habas, R., Macdonald, B. T. and He, X.** (2007). SnapShot: noncanonical Wnt signaling pathways. *Cell* **131**, 1378. doi:10.1016/j.cell.2007.12.011
- Sinigaglia, C., Busengdal, H., Leclère, L., Technau, U. and Rentsch, F.** (2013). The bilaterian head patterning gene *six3/6* controls aboral domain development in a cnidarian. *PLoS Biol.* **11**, e1001488. doi:10.1371/journal.pbio.1001488
- Sun, H., Peng, C.-J., Wang, L., Feng, H. and Wikramanayake, A. H.** (2021). An early global role for Axin is required for correct patterning of the anterior-posterior axis in the sea urchin embryo. *Development* **148**, dev191197. doi:10.1242/dev.191197
- van Amerongen, R. and Nusse, R.** (2009). Towards an integrated view of Wnt signaling in development. *Development* **136**, 3205–3214. doi:10.1242/dev.033910
- Villarroel, A., del Valle-Pérez, B., Fuertes, G., Curto, J., Ontiveros, N., Garcia de Herberos, A. and Duñach, M.** (2020). Src and Fyn define a new signaling cascade activated by canonical and non-canonical Wnt ligands and required for gene transcription and cell invasion. *Cell. Mol. Life Sci.* **77**, 919–935. doi:10.1007/s00018-019-03221-2
- Voloshanenko, O., Gmach, P., Winter, J., Kranz, D. and Boutros, M.** (2017). Mapping of Wnt-Frizzled interactions by multiplex CRISPR targeting of receptor gene families. *FASEB J.* **31**, 4832–4844. doi:10.1096/fj.201700144R
- Wang, Y., Chang, H., Rattner, A. and Nathans, J.** (2016). Frizzled receptors in development and disease. *Curr. Top. Dev. Biol.* **117**, 113–139. doi:10.1016/bs.ctdb.2015.11.028
- Warner, J. F., Guerlais, V., Amiel, A. R., Johnston, H., Nedoncelle, K. and Röttinger, E.** (2018). NvERTx: a gene expression database to compare embryogenesis and regeneration in the sea anemone *Nematostella vectensis*. *Development* **145**, dev162867. doi:10.1242/dev.162867
- Wijesena, N., Sun, H., Kumburegama, S. and Wikramanayake, A. H.** (2022). Distinct Frizzled receptors independently mediate endomesoderm specification and primary archenteron invagination during gastrulation in *Nematostella*. *Dev. Biol.* **481**, 215–225. doi:10.1016/j.ydbio.2021.11.002
- Wikramanayake, A. H., Huang, L. and Klein, W. H.** (1998). β -Catenin is essential for patterning the maternally specified animal-vegetal axis in the sea urchin embryo. *Proc. Natl. Acad. Sci. USA* **95**, 9343–9348. doi:10.1073/pnas.95.16.9343
- Wikramanayake, A. H., Hong, M., Lee, P. N., Pang, K., Byrum, C. A., Bince, J. M., Xu, R. and Martindale, M. Q.** (2003). An ancient role for nuclear β -catenin in the evolution of axial polarity and germ layer segregation. *Nature* **426**, 446–450. doi:10.1038/nature02113
- Wikramanayake, A. H., Peterson, R., Chen, J., Huang, L., Bince, J. M., McClay, D. R. and Klein, W. H.** (2004). Nuclear β -catenin-dependent Wnt8 signaling in vegetal cells of the early sea urchin embryo regulates gastrulation and differentiation of endoderm and mesodermal cell lineages. *Genesis* **39**, 194–205. doi:10.1002/gene.20045
- Willert, K., Shibamoto, S. and Nusse, R.** (1999). Wnt-induced dephosphorylation of axin releases beta-catenin from the axin complex. *Genes Dev.* **13**, 1768–1773. doi:10.1101/gad.13.14.1768
- Yu, H., Ye, X., Guo, N. and Nathans, J.** (2012). Frizzled 2 and frizzled 7 function redundantly in convergent extension and closure of the ventricular septum and palate: evidence for a network of interacting genes. *Development* **139**, 4383–4394. doi:10.1242/dev.083352

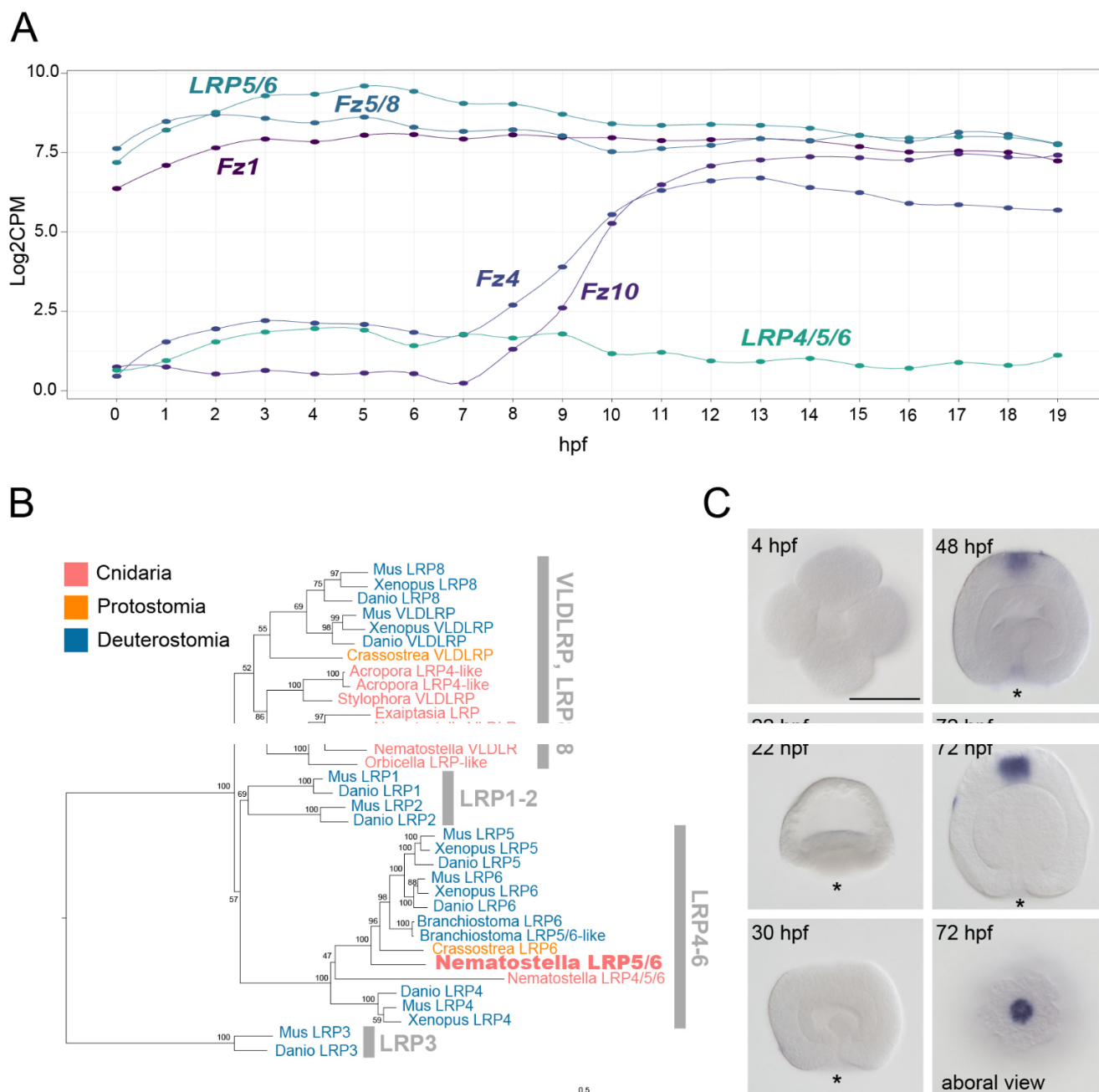


Fig. S1. (A) Expression dynamics of the *LRP5/6*, *LRP4/5/6*-like and *Fz* genes in the first 19 hours of *Nematostella* development according to the NvERTx database (Helm et al., 2013; Warner et al., 2018). (B) Maximum likelihood phylogeny of the LRP proteins (WAG+G4, bootstrap 100). (C) *LRP4/5/6*-like is expressed in the apical organ of the planula. Scale bar 100 μ m.

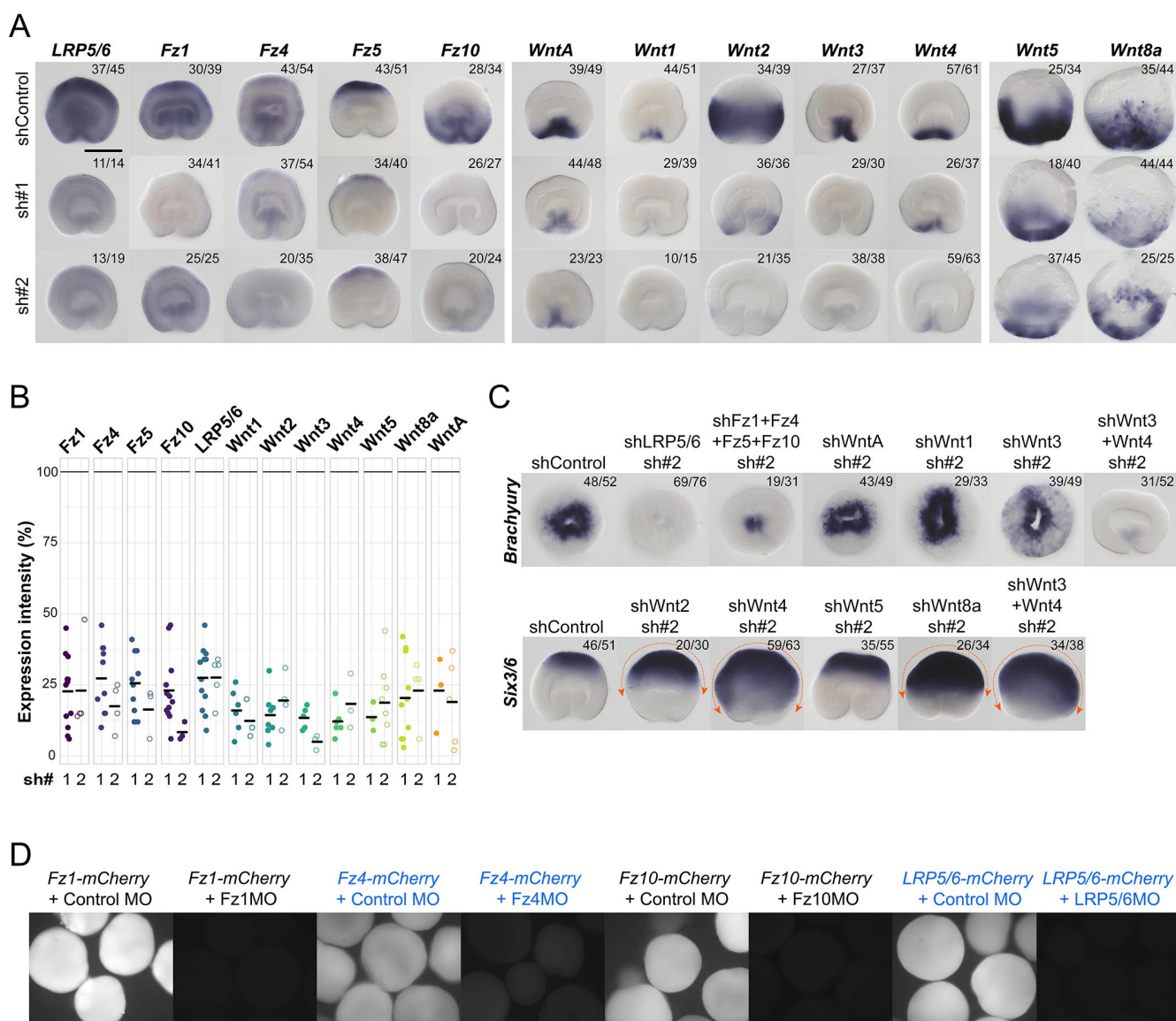


Fig. S2. Controls of the efficiency of the shRNAs and morpholino oligonucleotides. (A) Efficiency of the first (sh#1) and the second (sh#2) shRNA for each gene analyzed by in situ hybridization. *Wnt5* and *Wnt8a* expression has been assessed at mid-blastula stage because unlike all the other genes shown on the figure, *Wnt5* and *Wnt8a* are nearly not expressed at late gastrula stage. All other transcripts are stained in 30 hpf gastrulae. (B) qPCR analysis of the knockdown efficiency of the sh#1 and sh#2 for each gene in relation to shControl (100% expression) at 30 hpf. (C) The phenotypes obtained with the sh#1 (shown on all other figures) are reproduced with minimal differences using the sh#2 in 30 hpf embryos. Oral view is shown for *Bra*, lateral view is shown for *Six3/6*. On (A) and (C), the numbers in the top right corner show the fraction of the embryo demonstrating this phenotype. Scale bar 100 μ m.

(D) In vivo fluorescence shows that *mCherry* mRNA carrying the morpholino recognition sequence for the Fz1MO, Fz4MO, Fz10MO or LRP5/6MO is efficiently translated when co-injected into zygotes together with the control morpholino, but not when co-injected with the morpholinos against Fz1, Fz4, Fz10 or LRP5/6MO, respectively.

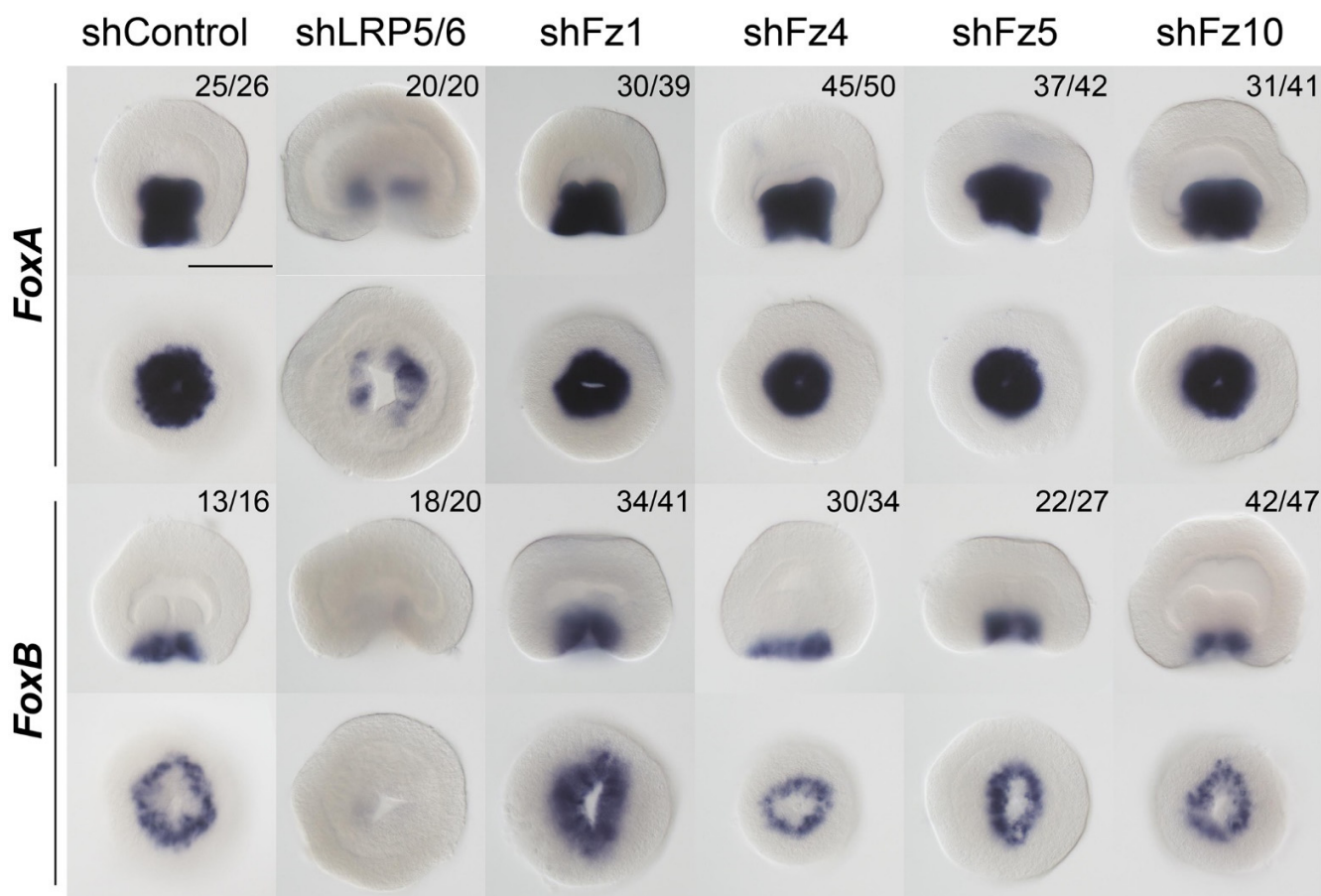


Fig. S3. Expression of the oral markers *FoxA* and *FoxB* upon KDs of *LRP5/6* and individual *Fz* in the 30 hpf gastrula. The numbers in the top right corner show the fraction of the embryo demonstrating this phenotype. For each gene, lateral views (oral end down) on the top, oral views on the bottom. Scale bar 100 μ m.

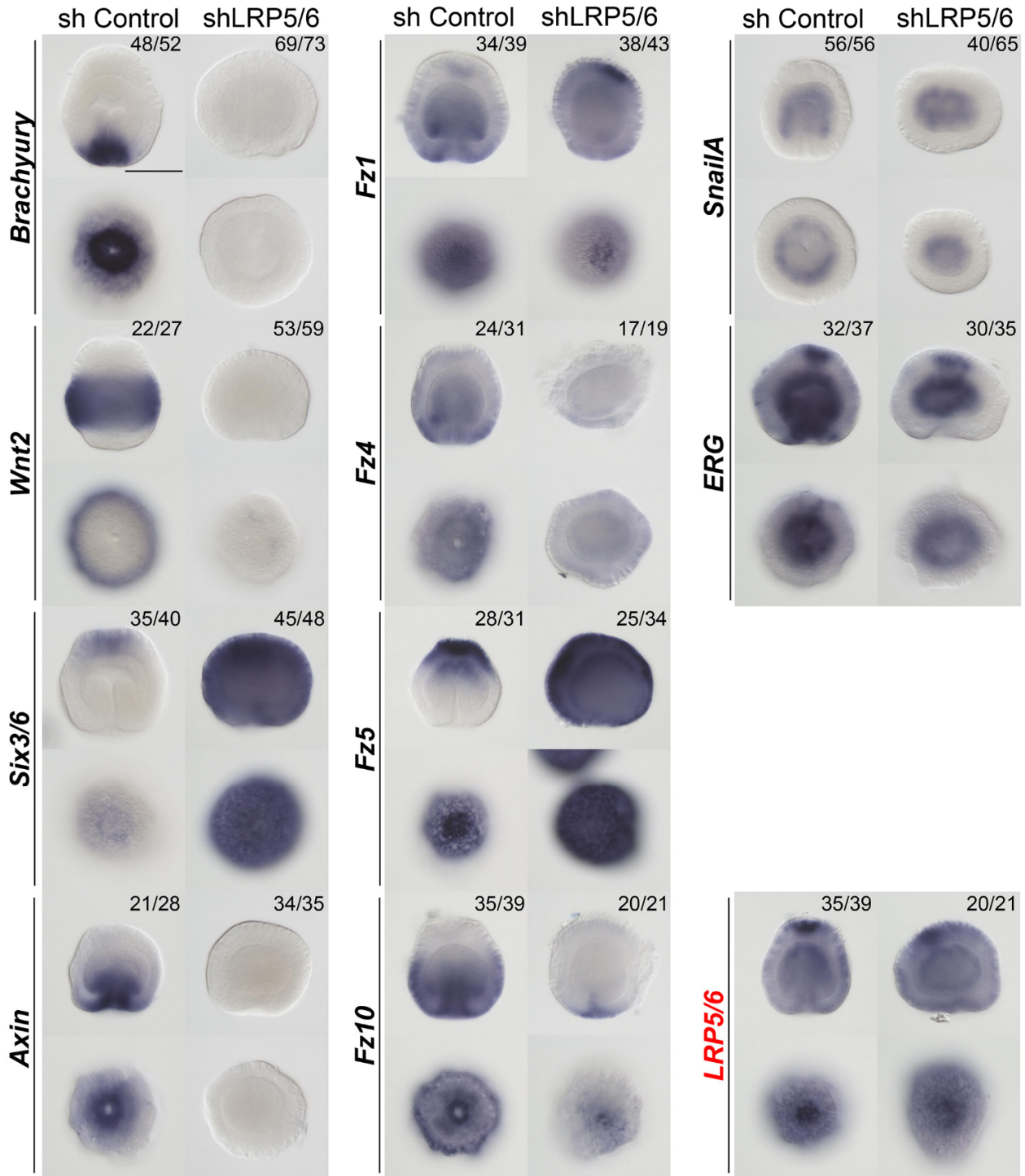


Fig. S4. Marker gene expression in 3 dpf planulae upon *LRP5/6* RNAi. The numbers in the top right corner show the fraction of the embryo demonstrating this phenotype. Scale bar 100 μ m. For each gene, lateral views (oral end down) on the top, oral views on the bottom.

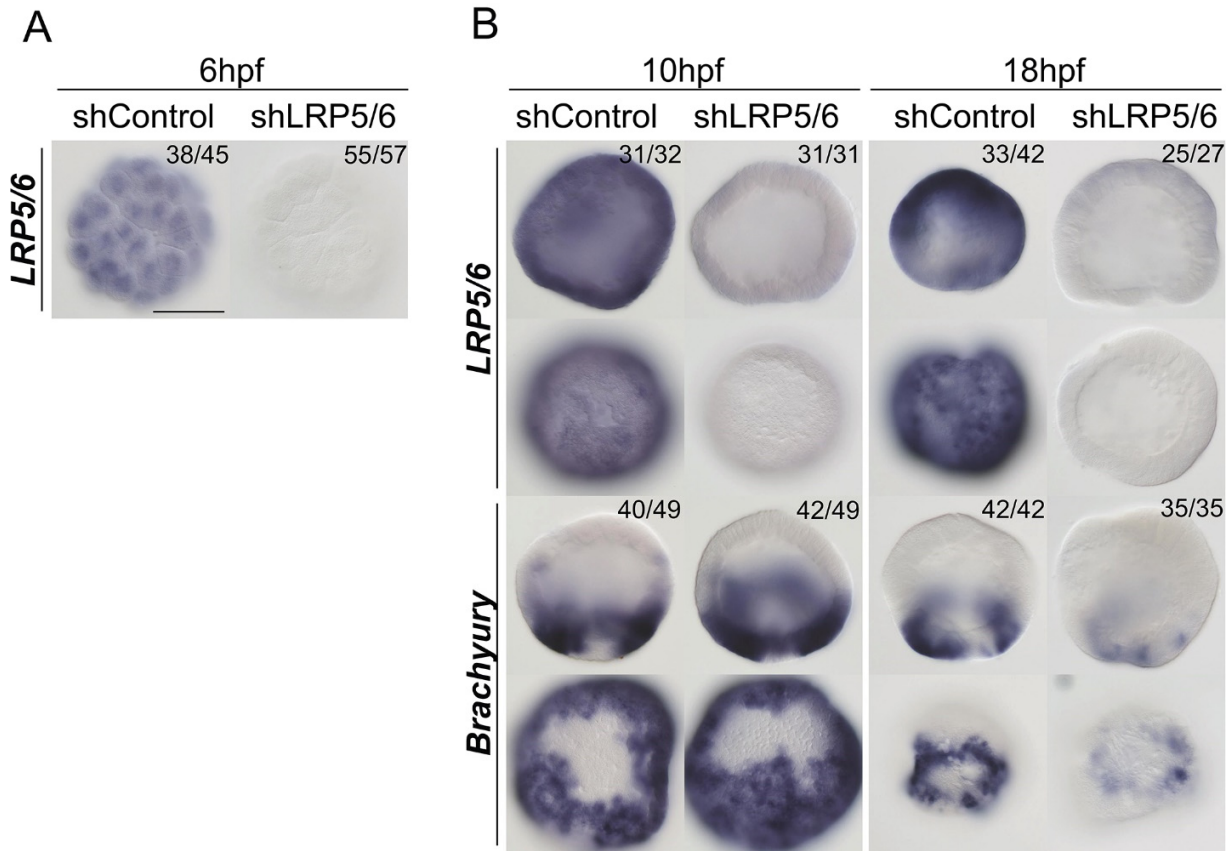


Fig. S5. The onset of the effect of the *LRP5/6* RNAi. (A) *LRP5/6* expression is abolished at 6 hpf. (B) *Bra* expression is not affected at 10 hpf, but starts to be suppressed by 18 hpf. The numbers in the top right corner show the fraction of the embryo demonstrating this phenotype. Scale bar 100 μ m. For each gene, lateral views (oral end down) on the top, oral views on the bottom.

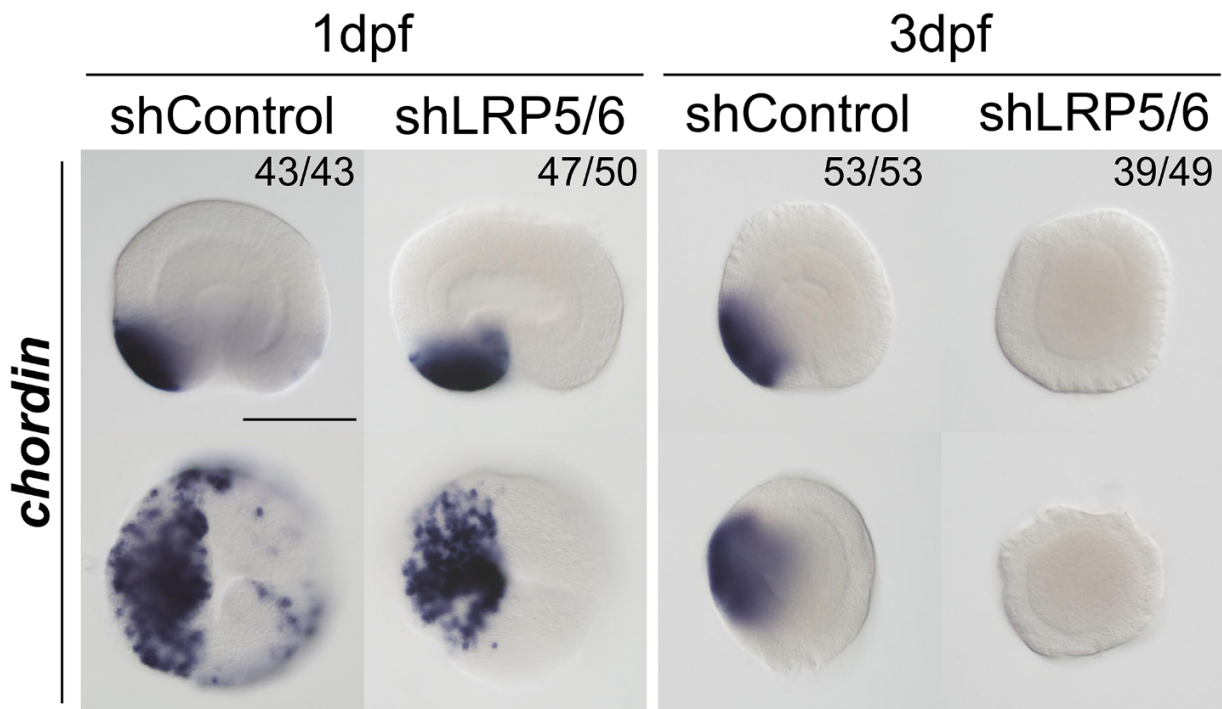


Fig. S6. At late gastrula (1 dpf), asymmetric *Chordin* expression indicates the establishment of the directive axis, which disappears by mid-planula (3 dpf). The numbers in the top right corner show the fraction of the embryo demonstrating this phenotype. Scale bar 100 μ m. Lateral views (oral end down) on the top, oral views on the bottom.

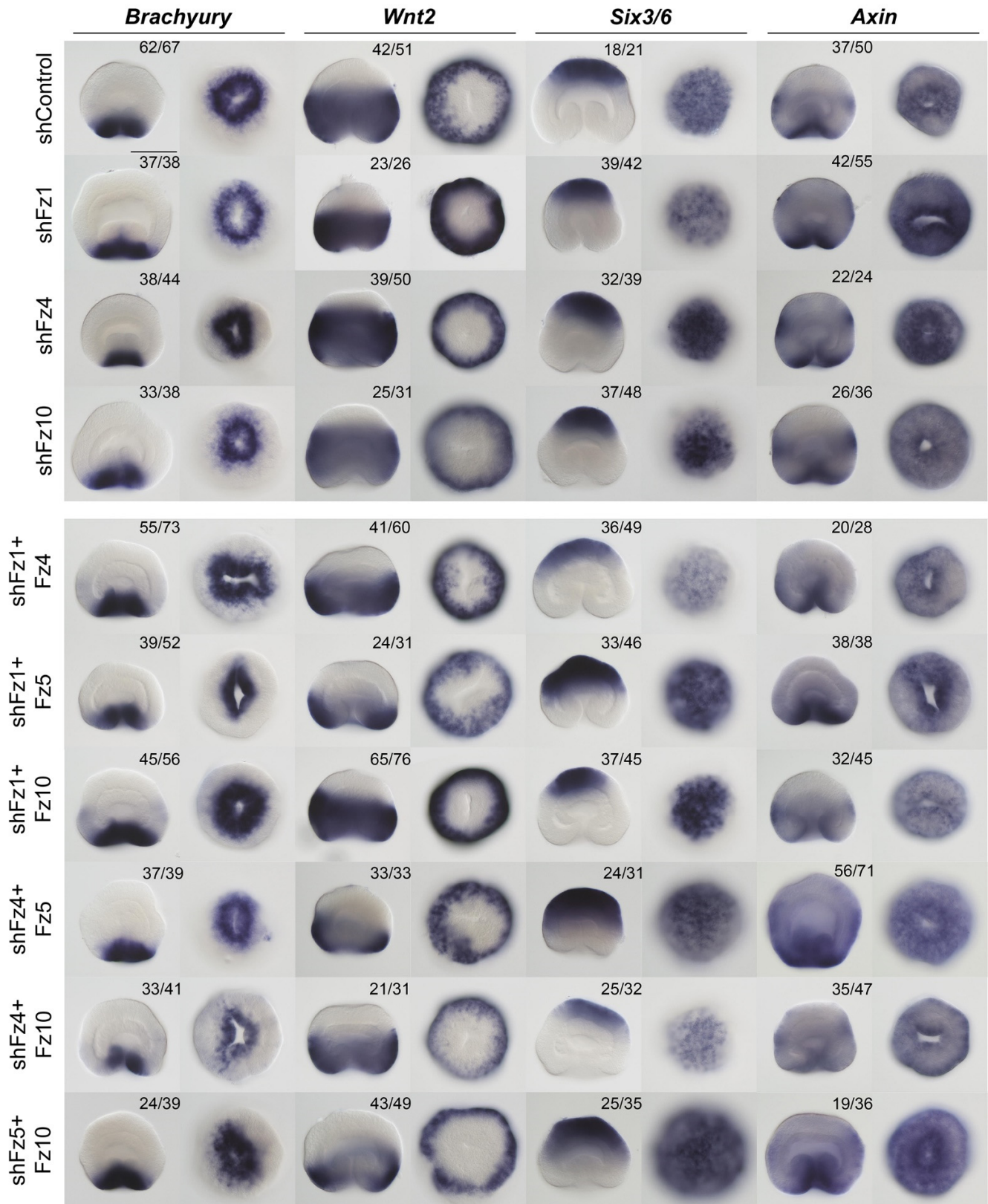


Fig. S7. Effects of the individual RNAi of the orally expressed Fz genes and effects of the simultaneous RNAi of all possible combinations of two Fz genes on the expression of the β -catenin-dependent markers of different axial domains in the 30 hpf gastrula. The numbers in the top right corner show the fraction of the embryo demonstrating this phenotype. Scale bar 100 μ m. For each gene, lateral views (oral end down) on the left, oral (aboral in case of *Six3/6*) views on the right.

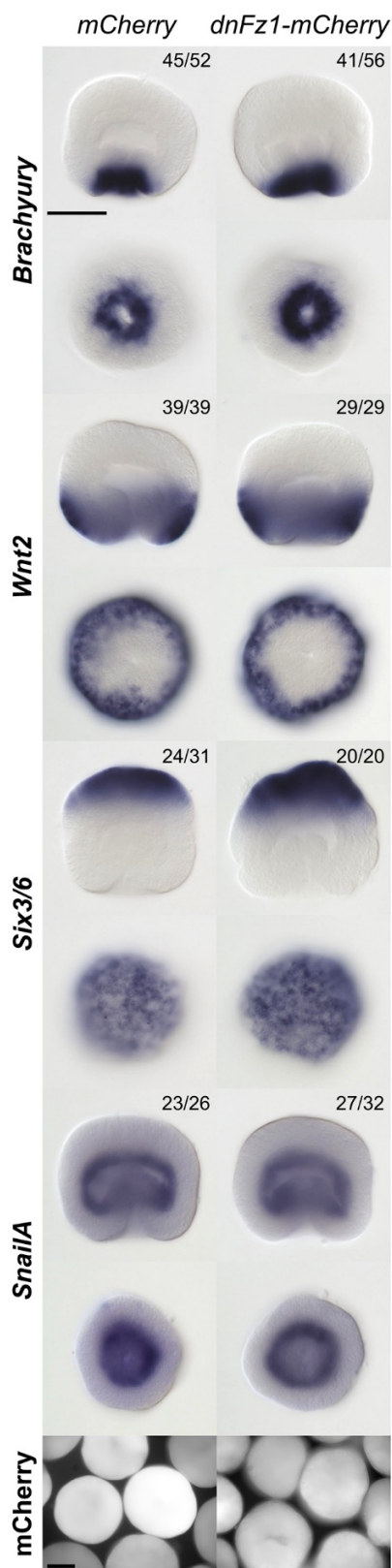


Fig. S8. Microinjection of the *mCherry* mRNA and *dnFz1-mCherry* mRNA show no effect on the expression of the markers of the distinct axial domains in the ectoderm, and on the endodermal marker *SnailA* in the 30 hpf gastrula. The numbers in the top right corner show the fraction of the embryo demonstrating this phenotype. For each gene, lateral views (oral end down) on the top, oral (aboral in case of *Six3/6*) views on the bottom. Lower panel – *mCherry* fluorescence of the microinjected embryos at 24 hpf. Scale bars 100 μ m.

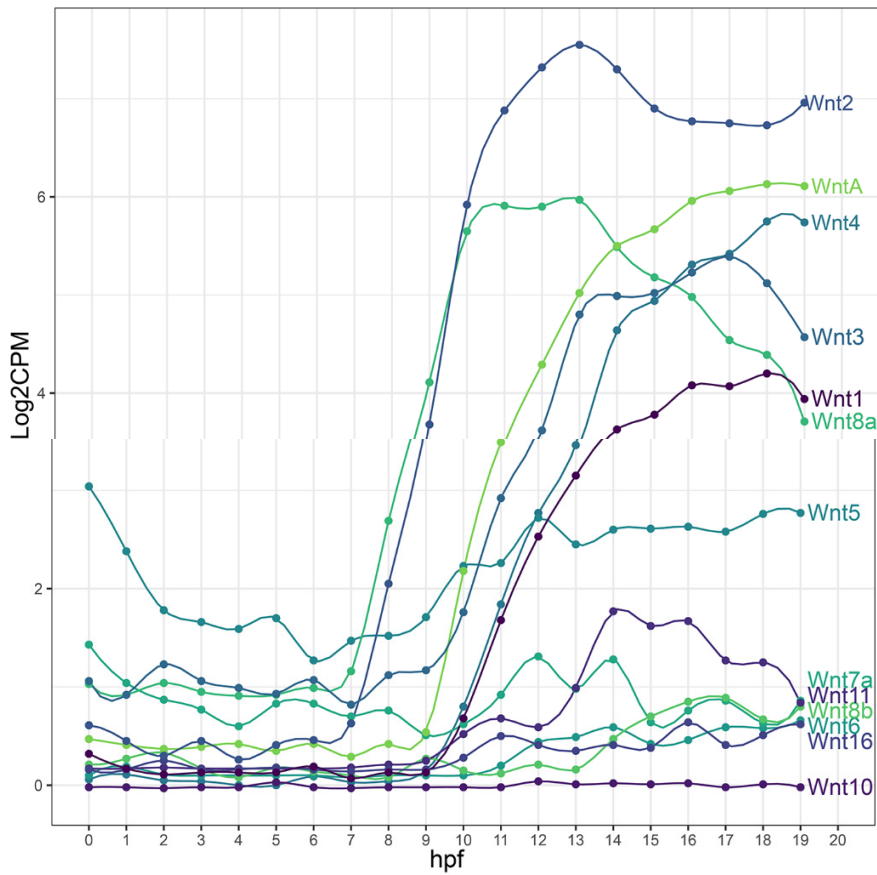


Fig. S9. The dynamics of the *Wnt* gene expression in the first 19 hours of *Nematostella* development according to the NvERTx database (Helm et al., 2013; Warner et al., 2018).

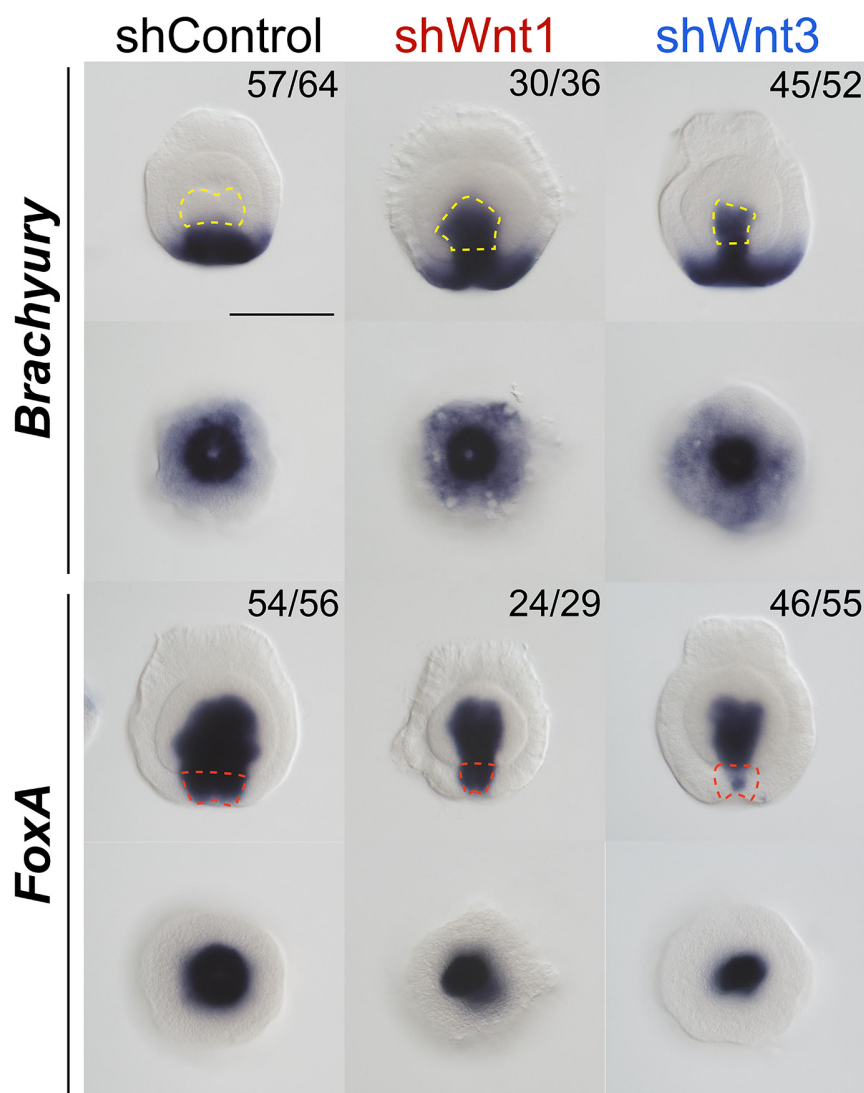


Fig. S10. Analysis of the oral marker expression in the 3 dpf planulae. Similar to the effect seen at the 30 hpf, *Wnt1* and *Wnt3* RNAi result in the expansion of the *Bra* expression to the bottom of the pharynx (yellow dashed line). A similar phenotype was seen in 30 hpf gastrulae upon *FoxB* RNAi (Lebedeva et al., 2021). *Wnt3* RNAi, but not *Wnt1* RNAi results in the suppression of the *FoxA* expression in the outer pharynx (red dashed line). A similar phenotype was seen in 30 hpf gastrulae upon *Bra*, *FoxB*, and *Bra+FoxB* RNAi (Lebedeva et al., 2021). For each gene, lateral views (oral end down) on the top, oral views on the bottom. The numbers in the top right corner show the fraction of the embryo demonstrating this phenotype. Scale bar 100 μ m.

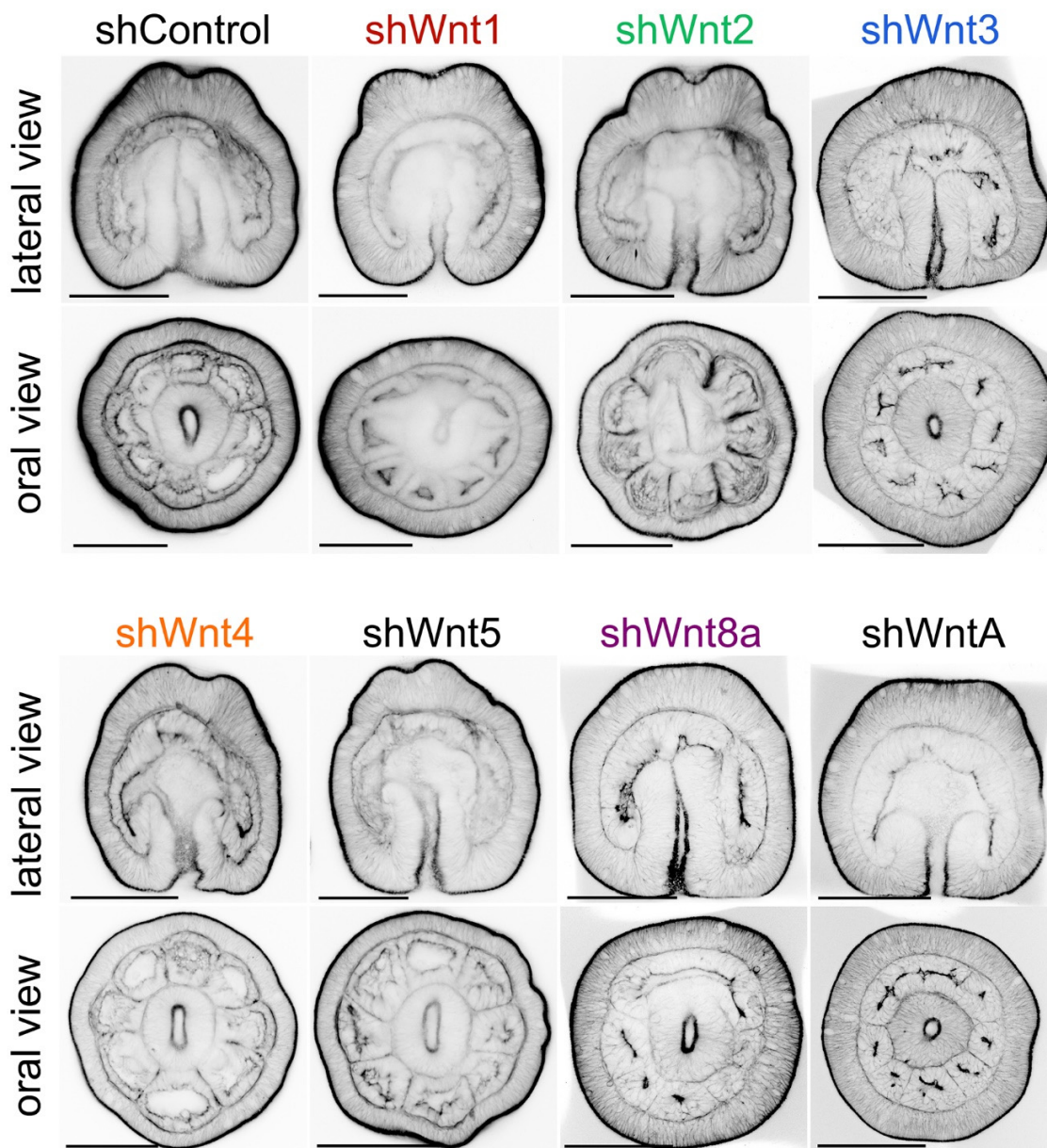


Fig. S11. Phalloidin staining of the 4 dpf planulae upon individual Wnt RNAi. Scale bar 100 μ m. shWnt8a and shWntA embryos appear slightly delayed (the last pair of mesenteries has not yet formed), but their general morphology is entirely normal.

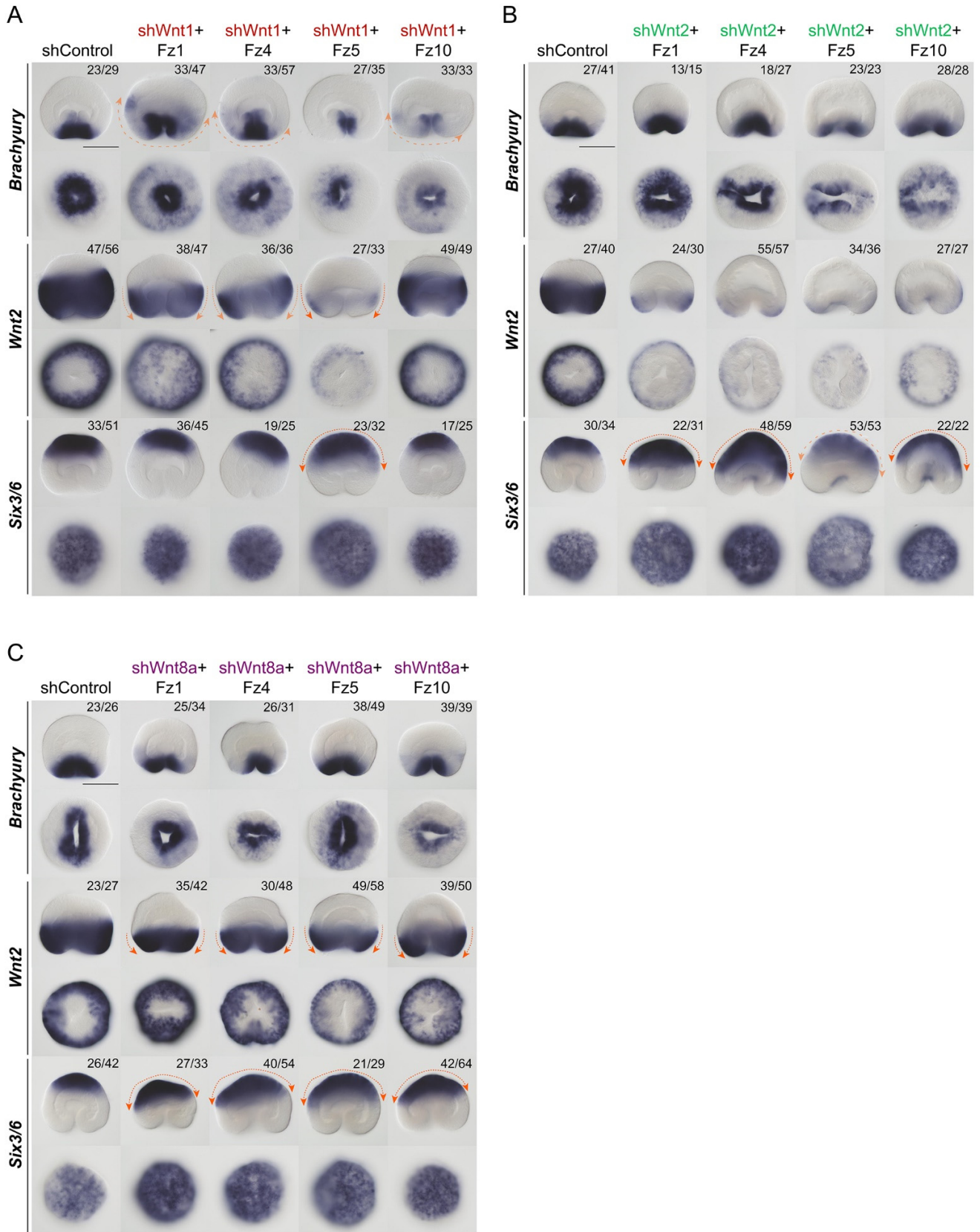


Fig. S12. Results of the simultaneous KD of *Wnt1* (A), *Wnt2* (B), and *Wnt8a* (C) with different *Fz* genes on the expression of the oral, midbody, and aboral markers at 30 hpf. For each gene, lateral views (oral end down) on the top, oral (aboral in case of *Six3/6*) views on the bottom. The numbers in the top right corner show the fraction of the embryo demonstrating this phenotype. Scale bars 100 μ m. The effect of the combined KD of *Wnt1*+*Fz5* and *Wnt1*+*Fz10* on the expression of *Bra*, *Wnt2* and *Six3/6* is very similar to that of the *Wnt3*+*Fz5* and *Wnt3*+*Fz10* RNAi, however, *Wnt2* expression appears weaker in the *Wnt1*+*Fz5* KD than in the *Wnt3*+*Fz5* KD. *Wnt2*-*Fz* and *Wnt8a*-*Fz* combinations do not seem to show any noticeable synergistic effects.

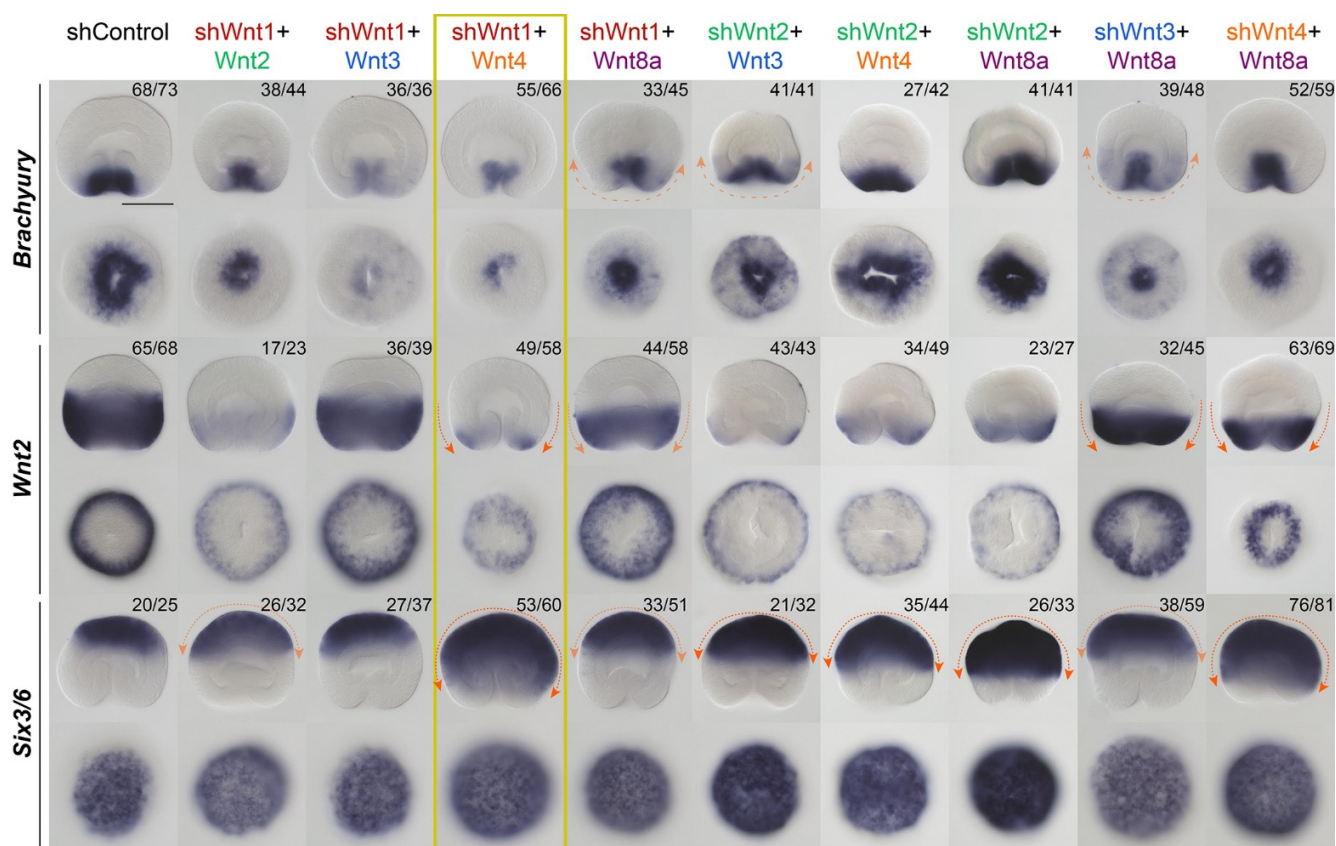


Fig. S13. Results of the double KD of all *Wnt* genes producing oral-aboral phenotype at 30 hpf upon individual KDs (see Fig. 6A in the main text). Expression of the same oral, midbody, and aboral markers at 30 hpf is shown. For each gene, lateral views (oral end down) on the top, oral (aboral in case of *Six3/6*) views on the bottom. The numbers in the top right corner show the fraction of the embryo demonstrating this phenotype. Scale bar 100 μ m. shWnt1+shWnt4 combination (yellow box) produces a phenotype similar to the double KD of *Wnt3* and *Wnt4* (see Fig. 6C in the main text). The expansion of the aboral marker *Six3/6* upon double KD of *Wnt4* and *Wnt8a* appears more pronounced than upon individual KDs of these two *Wnt* genes. Other shWnt combinations did not seem to elicit a synergistic effect on the expression of *Bra*, *Wnt2*, and *Six3/6* in comparison to their individual KDs.

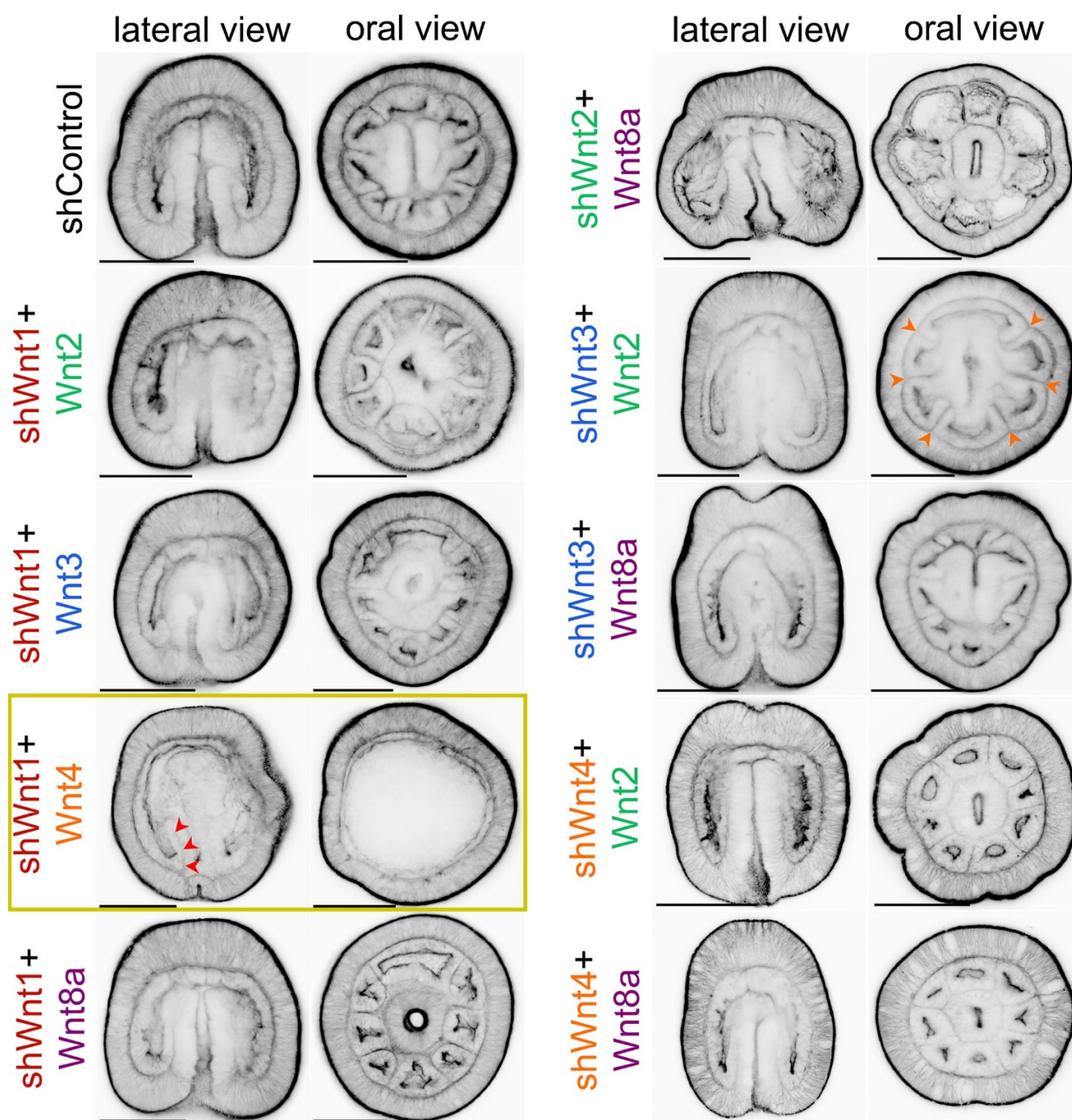


Fig. S14. Phalloidin staining of the 4 dpf planulae upon double KDs of all *Wnt* genes producing and oral-aboral phenotype at 30 hpf. Scale bar 100 μ m. Similar to the shWnt3+Wnt4 combination (see Fig. 3D in the main text for comparison), shWnt1+Wnt4 (yellow box) results in a loss of the mouth, pharynx and mesenteries. However, 1-2 residual mesenteries may still be visible (red arrowheads). shWnt3+Wnt2 combination regularly resulted in embryos having 6 rather than 8 regularly spaced mesenteries (orange arrowheads). Other double knockdowns did not lead to any obvious phenotypes at the 4 dpf stage.

Table S1. Target sequences of the shRNAs

shControl	GCGAGTTCTTCTACAAGGTGA
shLRP5/6 sh#1	GAGAGCCTTCCACTTGTA
shLRP5/6 sh#2	GAGGAATCGTCGCATCTAT
shFz1 sh#1	GAAGGCTGCACGGTTATTT
shFz1sh#2	GCTTGCAATGAGCCTATCA
shFz4 sh#1	GTTCAAAGCACCGAGTCTT
shFz4sh#2	GCCTGAGAAACCTAGACCA
shFz5 sh#1	GCGGAATAGGCTACAATTT
shFz5 sh#2	GCCGGAATGAAATGGTCAA
shFz10 sh#1	GGATGAACTGACAGGTCTT
shFz10 sh#2	GGACAGTACCAGCAATACA
shWntA sh#1	GGATAACATGGGCAAGACA
shWntA sh#2	GGCGTACTATGCCAACTT
shWnt1 sh#1	GGAGGATGCAGTGATAACA
shWnt1 sh#2	GGGATTTCCGTGCTCAGAT
shWnt2 sh#1	GAGGGCGTTGATGAACTTA
shWnt2 sh#2	GAGGATTCGCCAATTACT
shWnt3 sh#1	GGAAGACAGTGCAACTACA
shWnt3 sh#2	GAGACCTCACCAACTACT
shWnt4 sh#1	GCTTCGCTAGTGTACTCAA
shWnt4 sh#2	GAAATTCGATGGAGCTACT
shWnt5 sh#1	GGTGCCGATGCAAGTTTCA
shWnt5 sh#2	GCTCGGACTCTTATGAACT
shWnt8a sh#1	GGCGCAAAGCTGTTAAGAA
shWnt8a sh#2	GCAGCCTGGTCTTCCTAAA

Table S2. Morpholino sequences

Name	Sequence	Reference
Control MO	GATGTGCCTAGGGTACAACAACAAT	(Kraus et al., 2016; Lebedeva et al., 2021)
Fz1MO	GCATAATCCCGGCGATTAACTACG	This paper
Fz4MO	GTGACATTTTGCACGAATGGAGAAC	This paper
Fz10MO	AAGCTAAACGCTTAGCCCCCATATC	(Wijesena et al., 2022)
LRP5/6MO	ACAAAACAACCTTTGGCGAACATCCT	This paper

Table S3. Accession numbers

Gene name	Accession	NvERTx	NVE
<i>Wnt4</i>	XP_001623100	NvERTx.4.48250	NVE17746
<i>Wnt5</i>	XP_001630693	NvERTx.4.146133	NVE1780
<i>Wnt8a</i>	XP_001630032	NvERTx.4.106136	NVE2847
<i>WntA</i>	XP_001637670	NvERTx.4.132141	NVE12095
<i>Wnt1</i>	XP_001641494	NvERTx.4.56072	NVE12960
<i>Wnt2</i>	XP_032238966	NvERTx.4.114443	NVE21992
<i>Wnt3</i>	XP_032241388	NvERTx.4.107815	NVE17595
<i>Fzd1</i>	XP_001647540	NvERTx.4.186145	NVE7119
<i>Fzd5</i>	XP_001634995	NvERTx.4.67323	NVE19736
<i>Fzd10</i>	XP_032235151	NvERTx.4.80873	NVE1835
<i>Fzd4</i>	XP_001622965	NvERTx.4.95377	NVE18184
<i>LRP5/6</i>	XP_032222612	NvERTx.4.111182	NVE16348
<i>FoxA</i>	XP_001634555	NvERTx.4.73097	NVE20630
<i>ERG</i>	XP_032236866	NvERTx.4.84016	NVE25536
<i>SnailA</i>	XP_032243077	NvERTx.4.57438	NVE13986
<i>Axin</i>	XP_001640692	NvERTx.4.66791	NVE22529 (no good NVE model)
<i>FoxB</i>	XP_001631625	NvERTx.4.229455	NVE26195
<i>Chordin</i>	XP_001633548	NvERTx.4.87650	NVE22735
<i>Brachyury</i>	XP_032233913	NvERTx.4.100809	NVE770
<i>Six3/6</i>	XP_032228424	NvERTx.4.97387	NVE12346

NVE gene models can be accessed at

https://figshare.com/articles/Nematostella_vectensis_transcriptome_and_gene_models_v2_0/807696

NvERTx transcripts can be accessed at

http://nvvertx.irca.nyu.edu/ER/ER_plotter/home

References

- Helm, R. R., Siebert, S., Tulin, S., Smith, J. and Dunn, C. W. (2013). Characterization of differential transcript abundance through time during *Nematostella vectensis* development. *BMC genomics* **14**, 266.
- Kraus, Y., Aman, A., Technau, U. and Genikhovich, G. (2016). Pre-bilaterian origin of the blastoporal axial organizer. *Nat Commun* **7**, 11694.
- Lebedeva, T., Aman, A. J., Graf, T., Niedermoser, I., Zimmermann, B., Kraus, Y., Schatka, M., Demilly, A., Technau, U. and Genikhovich, G. (2021). Cnidarian-bilaterian comparison reveals the ancestral regulatory logic of the β -catenin dependent axial patterning. *Nat Commun* **12**, 4032.

- Warner, J. F., Guerlais, V., Amiel, A. R., Johnston, H., Nedoncelle, K. and Rottinger, E.** (2018). NVERTx: a gene expression database to compare embryogenesis and regeneration in the sea anemone *Nematostella vectensis*. *Development (Cambridge, England)* **145**.
- Wijesena, N., Sun, H., Kumburegama, S. and Wikramanayake, A. H.** (2022). Distinct Frizzled receptors independently mediate endomesoderm specification and primary archenteron invagination during gastrulation in *Nematostella*. *Developmental biology* **481**, 215-225.

Paper II

"Cnidarian-bilaterian comparison reveals the ancestral regulatory logic of the β -catenin dependent axial patterning."

Authors:

Tatiana Lebedeva¹, Andrew J. Aman¹, Thomas Graf¹, Isabell Niedermoser¹, Bob Zimmermann¹, Yulia Kraus², Magdalena Schatka¹, Adrien Demilly¹, Ulrich Technau¹ & Grigory Genikhovich^{1*}

¹Department of Neurosciences and Developmental Biology, Faculty of Life Sciences, University of Vienna, Djerassiplatz 1, Vienna, Austria

²Department of Evolutionary Biology, Faculty of Biology, Lomonosov Moscow State University, Leninskiye gory 1/12, Moscow, Russia






Status:

Published in *Nature Communications*, 2021, **12**, 4032. <https://doi.org/10.1038/s41467-021-24346-8>

Contributions:

T.L. performed the majority of the experiments, planned experiments and analyzed data; A.J.A and U.T. conceived the generation of the APC mutant line; A.J.A. generated the APC mutant line, and started its characterization together with A.D.; T.G. and I.N. performed treatments, and prepared RNA for sequencing; B.Z. supervised the bioinformatic analysis; Y.K. performed transplantations on Bra morphants; M.S. generated mosaic EF1 α :: β -cat_{stab} polyps; G.G. conceived the study, planned experiments, performed experiments, analyzed data and wrote the paper. All authors edited the paper.

Cnidarian-bilaterian comparison reveals the ancestral regulatory logic of the β -catenin dependent axial patterning

Tatiana Lebedeva ¹, Andrew J. Aman¹, Thomas Graf¹, Isabell Niedermoser ¹, Bob Zimmermann ¹, Yulia Kraus^{1,2}, Magdalena Schatka¹, Adrien Demilly¹, Ulrich Technau ¹ & Grigory Genikhovich ¹✉

In animals, body axis patterning is based on the concentration-dependent interpretation of graded morphogen signals, which enables correct positioning of the anatomical structures. The most ancient axis patterning system acting across animal phyla relies on β -catenin signaling, which directs gastrulation, and patterns the main body axis. However, within Bilateria, the patterning logic varies significantly between protostomes and deuterostomes. To deduce the ancestral principles of β -catenin-dependent axial patterning, we investigate the oral-aboral axis patterning in the sea anemone *Nematostella*—a member of the bilaterian sister group Cnidaria. Here we elucidate the regulatory logic by which more orally expressed β -catenin targets repress more aborally expressed β -catenin targets, and progressively restrict the initially global, maternally provided aboral identity. Similar regulatory logic of β -catenin-dependent patterning in *Nematostella* and deuterostomes suggests a common evolutionary origin of these processes and the equivalence of the cnidarian oral-aboral and the bilaterian posterior-anterior body axes.

¹Department of Neurosciences and Developmental Biology, Faculty of Life Sciences, University of Vienna, Djerassiplatz 1, Vienna, Austria. ²Department of Evolutionary Biology, Faculty of Biology, Lomonosov Moscow State University, Leninskiye gory 1/12, Moscow, Russia. ✉email: grigory.genikhovich@univie.ac.at

Graded morphogen signals comprise the top tier of the axial patterning cascades in Bilateria and their phylogenetic sister group Cnidaria (corals, sea anemones, jellyfish, hydroids)^{1–3}. Just like the posterior–anterior (P–A) body axis of Bilateria, the oral–aboral (O–A) body axis of Cnidaria is patterned by Wnt/ β -catenin signaling^{4,5} (Fig. 1a). Although it is likely that β -catenin signaling is also involved in the axial patterning of earlier branching ctenophores and sponges^{6,7}, cnidarians are the earliest branching animal phylum for which experimental gene function analyses are available. A cnidarian–bilaterian comparison can inform us about the ancestral logic of the β -catenin-dependent axial patterning and mechanisms of molecular boundary formation. In this paper, we focus on deciphering the mechanism of the O–A axis patterning in the ectoderm of the early embryo of the sea anemone *Nematostella vectensis*.

Morphologically, the O–A axis in *Nematostella* becomes apparent at the onset of gastrulation, when future endoderm starts to invaginate, eventually forming the inner layer of this diploblastic organism. The establishment of the O–A axis in *Nematostella* depends on β -catenin⁸. Its knockdown abolishes the O–A axis both morphologically and molecularly: the embryos fail to gastrulate and do not express oral ectoderm markers⁹. In contrast, mosaic stabilization of β -catenin results in the formation of numerous ectopic oral structures or even complete ectopic axes⁴ (Supplementary Fig. 1a–c). By late gastrula stage, the ectoderm of *Nematostella* can be roughly subdivided into three axial domains: the oral domain characterized by *Brachyury* (*Bra*) expression, the midbody domain where *Wnt2* is expressed, and the aboral domain expressing *Six3/6* (Fig. 1b), whereas endodermal O–A patterning begins later in development¹⁰. Pharmacological experiments, in which β -catenin signaling was upregulated by a range of concentrations of the GSK3 β inhibitor 1-azakenpaulone (AZK) (Fig. 1a), showed that ectodermally expressed β -catenin-dependent genes react to different levels of upregulation of β -catenin signaling dose-dependently and in two distinct ways⁴ (Fig. 1c). Some genes, whose expression is normally restricted to the oral ectodermal domain, increase their expression to saturation upon upregulation of β -catenin signaling and start to be expressed in the ectoderm along the whole O–A axis at high AZK concentrations. We call them “saturating” genes below. Other ectodermally expressed genes, whose normal expression can be observed either in the oral domain or further aborally, require permissive “windows” of β -catenin signaling intensities. Upon weak pharmacological upregulation of β -catenin signaling, “window” gene expression shifts aborally, i.e. into the area where endogenous β -catenin signaling intensity is expected to be lower, while upon strong upregulation of β -catenin signaling their expression ceases altogether⁴ (Fig. 1c). A similar dose-dependent response to “windows” of β -catenin signaling intensity was previously demonstrated in axial patterning of bilaterians. Particularly striking is the resemblance to the P–A patterning in deuterostomes: the neurectoderm in vertebrates^{11,12}, body ectoderm in hemichordates^{13,14} and sea urchins¹⁵, and endomesoderm in sea stars^{15,16}. In protostomes, the P–A axis patterning mechanisms are very diverse, however, the posteriorizing effect of β -catenin signaling can also be observed. Different levels of knockdown of the β -catenin signaling antagonist *Axin* resulted in different extent of posteriorization of the embryo and loss of anterior structures in the short-germ insect *Tribolium castaneum*^{17,18}. Conversely, different levels of *Wnt8* knockdown led to the expansion of the anterior and loss of the posterior segments in the spider *Achaearanea tepidariorum*¹⁹. Within Spiralia, AZK-dependent disappearance of the anterior and expansion of the posterior marker gene expression was observed in the embryos of brachiopods *Novocrania anomala* and *Terebratalia transversa*²⁰, while experimental up- and downregulation of β -catenin signaling

resulted, respectively, in vegetalization and animalization of the embryo of the nemertean *Cerebratulus lacteus*²¹, reminiscent of the effect in deuterostomes^{14,22,23}.

Thus, the regulatory principle behind the “window” behavior may represent the ancestral logic of β -catenin-dependent axial patterning, however, its mechanism is not clear. Since this regulatory behavior is likely to be at the core of the O–A patterning in *Nematostella*, and possibly represents a general mechanism shared by all animals, we attempted to explain it. Since not only oral, but also several midbody and aboral markers were shown to be abolished upon β -catenin knockdown⁹, we hypothesized that both “saturating” and “window” genes are positively regulated by β -catenin (Fig. 1a). However, in order to account for the repression of the “window” genes upon upregulation of β -catenin, we postulated that there exists a “transcriptional repressor X”, which, being a “saturating” gene, becomes upregulated upon increased β -catenin signaling and inhibits the expression of the “window” genes in ever more aboral positions and, eventually, throughout the embryo (Fig. 1a, c). In this study, we set out to test our assumption and search for this hypothetical repressor. We demonstrate that a unit of four transcription factors, *Bra*, *FoxA*, *FoxB* and *Lmx*, rather than a single transcriptional repressor X, is responsible for controlling the “window” gene behavior in the oral domain of the *Nematostella* embryo. We also show that the regulatory logic based on repression of the more aborally expressed β -catenin signaling target genes by the more orally expressed β -catenin signaling target genes is responsible for setting up gene expression domain boundaries along the entire O–A axis and identify *Sp6-9* as a “transcriptional repressor Y” setting up the midbody/aboral boundary. We argue that this represents the ancestral regulatory logic of β -catenin-dependent axial patterning conserved since before the cnidarian–bilaterian split and discuss the implications of this on our understanding of the correspondence of the cnidarian and bilaterian body axes.

Results

Identification of the transcriptional repressor X candidates.

Our hypothesis predicted that: (i) the transcriptional repressor X is to be found among the “saturating” genes upregulated upon increased β -catenin signaling, (ii) it has to be expressed in a contiguous domain along the O–A axis rather than in a salt-and-pepper manner to be able to act cell-autonomously, and that (iii) the loss of function of the transcriptional repressor X will abrogate the β -catenin-dependent repression of “window” genes converting them into “saturating” genes upon pharmacological upregulation of the β -catenin signaling (Fig. 1c). To test these predictions, we devised an RNA-Seq-based strategy for finding all transcription factors fulfilling these criteria (Fig. 1d). In order to obtain an off-target free list of transcription factors upregulated by β -catenin, we used two independent means of upregulating β -catenin signaling by suppressing the activity of two different members of the β -catenin destruction complex, which we further refer to as “treatments”. First, we used AZK treatment spanning different time windows to suppress GSK3 β . Second, we used a line of *Nematostella* carrying a frameshift mutation in the *APC* gene²⁴ (Fig. 1a, e). At 3 days post fertilization (3 dpf), all *APC*^{−/−} embryos display a phenotype similar to that of embryos incubated from early blastula on in AZK (Supplementary Fig. 1d–h). Visual detection of the homozygous *APC* mutants at 1 dpf is impossible, since the phenotype only becomes apparent at 2–3 dpf. However, an earlier study showed that “window” behavior of *Wnt2* persisted until at least 3 dpf⁵, which suggested that the putative repressor X was expressed both at 1 dpf and at 3 dpf. Therefore, we compared the transcriptomes of 1 dpf embryos and 3 dpf embryos incubated in AZK with the transcriptomes of the 3

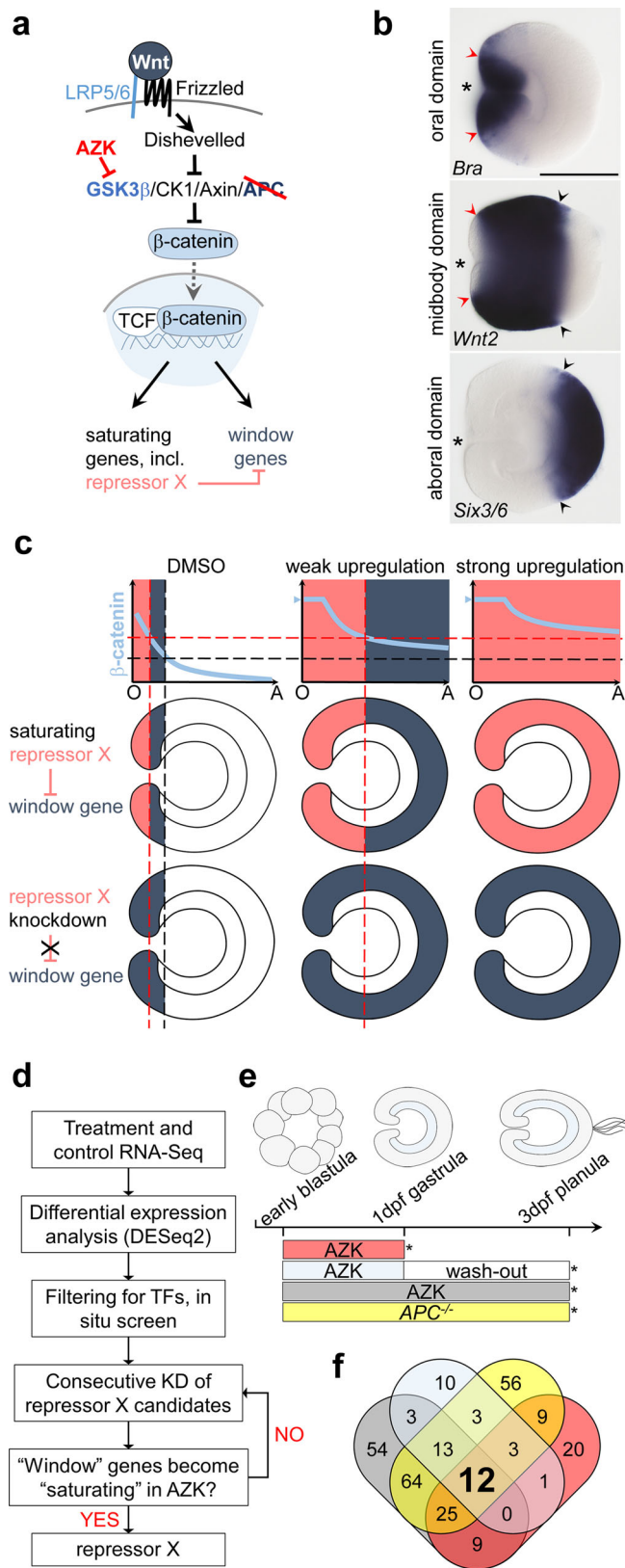


Fig. 1 The “repressor X” concept and the search strategy. **a** Scheme of the Wnt/β-catenin signaling pathway indicating the members manipulated in this study in order to artificially upregulate it. We use two types of treatments (red) to upregulate β-catenin signaling: pharmacological inhibition of GSK3β by AZK and mutation of APC. **b** Oral, midbody, and aboral domains of the 1 day post fertilization (1 dpf) gastrula visualized by molecular markers. Lateral views, oral to the left. Asterisk denotes the blastopore. Arrowheads demarcate corresponding positions. Scale bar 100 μm. **c** Hypothetical mechanism of the response of the “saturating” and “window” genes to different intensities of the β-catenin signaling and the putative role of the transcriptional repressor X in regulating the “window” expression behavior. Hypothetical oral-to-aboral gradient of β-catenin signaling is shown in light blue on the upper panels. Repressor X is a saturating gene expressed above a certain β-catenin signaling intensity indicated by the red dashed line, i.e., orally (pink expression domain on graphs and middle panels). The window gene (blue expression domain) is activated above the β-catenin signaling intensity indicated by the black dashed line, however, it becomes repressed in the area of repressor X expression. Upon AZK treatment, the β-catenin signaling intensity increases eventually reaching saturation (blue arrowhead on the Y-axis). In increasing AZK concentrations, the minimal β-catenin signaling intensity sufficient for repressor X activation shifts aborally, displacing the area available for the window gene expression until it becomes impossible for the window gene to be expressed anywhere in the embryo. Upon repressor X knockdown (bottom panel), the window gene starts to behave as a saturating gene. O and A on graphs indicate the oral and the aboral end. **d** Search strategy used to identify transcriptional repressor X. **e** Scheme of treatments. At 1 dpf, AZK treatments were stopped at 30 h post fertilization (hpf), and either RNA was extracted immediately, or the embryos were washed out and incubated in *Nematostella* medium until 3 dpf (72 hpf). Asterisks indicate time points of RNA extraction. **f** Venn diagram with the numbers of the putative transcription factor coding genes upregulated by different treatments. The color code corresponds to that on **e**.

Supplementary Table 1) of which we excluded five: two as metabolic enzymes falsely annotated by INTERPROSCAN²⁵ as transcription factors (*NVE21786* and *NVE12602*), one, *MsxC*, since it was not expressed in the wild type gastrula, and two, *Unc4* and *Ashc*, because they were expressed in single cells rather than in contiguous domains (Supplementary Fig. 2g). The remaining seven candidates, *Brachyury (Bra)*, *FoxA*, *FoxB*, *LIM homeobox (Lmx)*, *Shavenbaby (Svb)*, *Dachshund (Dac)* and a putative Zn finger transcription factor *NVE11868*, were expressed in distinct continuous domains and displayed a typical “saturating” phenotype (Supplementary Fig. 2h). In order to find out whether any of these transcription factors were capable of repressing window genes, we individually knocked them down (Supplementary Fig. 3a–c), incubated the knockdown embryos either in AZK or in DMSO and compared the expression of two well-characterized “window” genes *Wnt1* and *Wnt2*⁴ in the knockdowns at late gastrula stage. Knockdowns of *Svb*, *Dac* and *NVE11868* led to no significant change in the expression of *Wnt1* and *Wnt2* in comparison to control shRNA (Supplementary Fig. 3d). Therefore, these genes were also excluded from further analyses, and we focused on the remaining four candidates, *Bra*, *FoxA*, *FoxB*, and *Lmx*, and characterized their mutual expression domains and the effect of their knockdowns upon normal and pharmacologically enhanced β-catenin signaling (See also Supplementary Results and Discussion 1).

Repressor X is not a single gene but a unit of four genes. The area of strong *Bra* expression overlaps with the *Wnt1* expression domain and abuts the *Wnt2* expression domain (Fig. 2). Upon

1 dpf *APC*^{-/-} embryos (Fig. 1e; Supplementary Fig. 2a–f), and controls. We then identified all putative transcription factor-coding genes upregulated by elevated β-catenin in all treatments by comparing our lists of differentially expressed genes with the list of gene models with a predicted DNA binding domain. We found twelve such putative transcription factors (Fig. 1f,

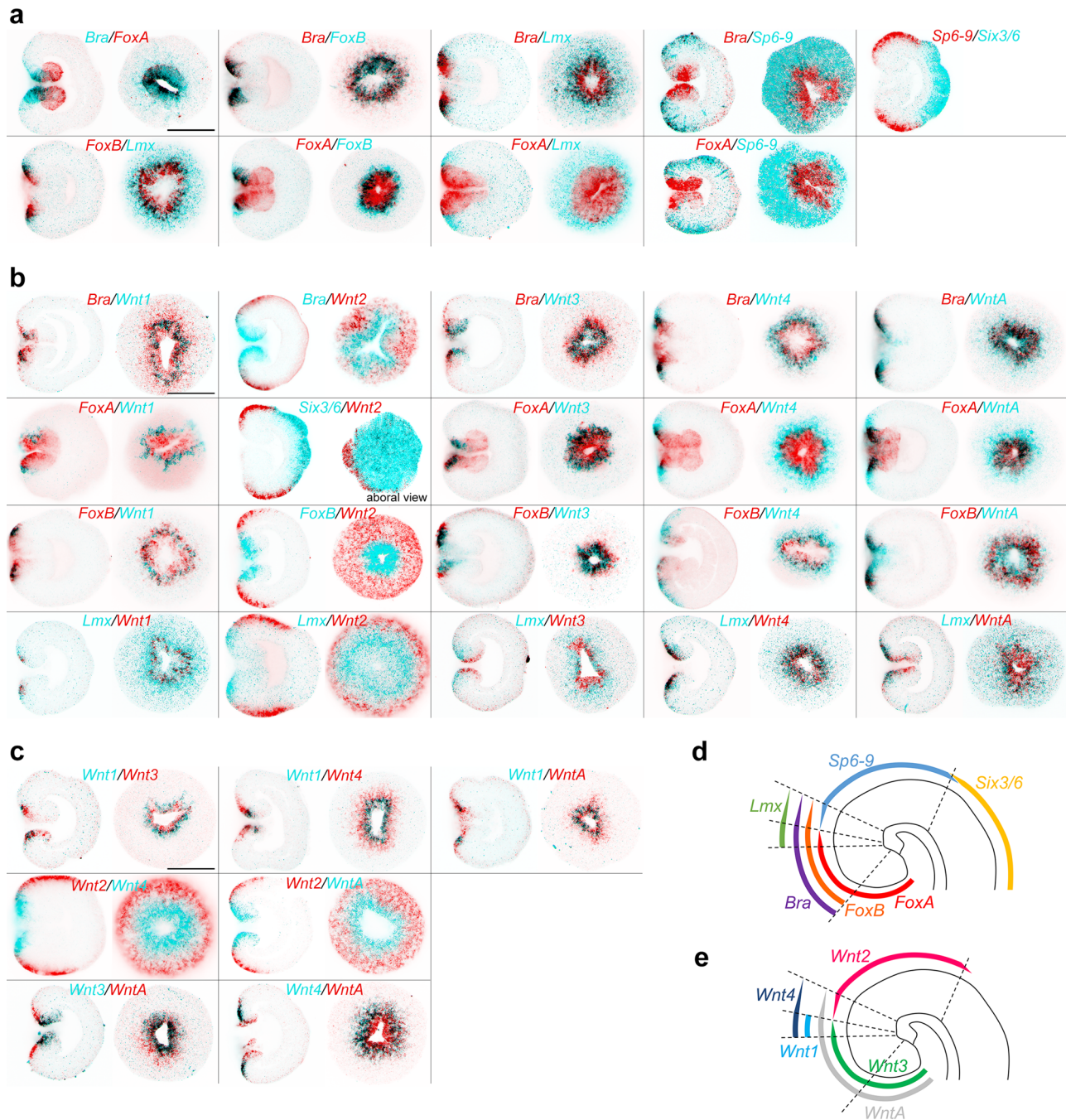


Fig. 2 Double FISH analysis of the expression domains of the four main repressor X candidates, oral *Wnt* genes, midbody markers *Wnt2* and *Sp6-9*, and aboral marker *Six3/6*. **a** FISH analysis of the expression domains of the transcription factor genes *Bra*, *FoxA*, *FoxB*, *Lmx*, *Sp6-9* and *Six3/6* in relation to each other. **b** FISH analysis of the expression domains of the abovementioned transcription factor genes in relation to the expression domains of the ectodermally expressed *Wnt* genes. **c** FISH analysis of the expression domains of the ectodermally expressed *Wnt* genes in relation to each other. **d** Schematic representation of the expression boundaries of the transcription factors in the *Nematostella* gastrula. **e** Schematic representation of the expression boundaries of the *Wnt* genes in the *Nematostella* gastrula. On **a–c**, lateral views (oral to the left) and oral views (unless specified otherwise) of representative embryos from two independent experiments with $n > 30$ for each combination of in situ hybridization probes are shown. Scale bars 100 μm . Dashed lines on **d** and **e** represent the same molecular boundaries.

Bra knockdown, *Wnt1* expression was abolished not only in the AZK treatment but also in the DMSO treated controls, suggesting that *Wnt1* is positively regulated by *Bra* (Fig. 3, Supplementary Fig. 4). In contrast, *Wnt2* expression domain expanded orally in the DMSO controls and became ubiquitous upon the AZK treatment (Fig. 3, Supplementary Fig. 4). This suggests that Brachyury acts as the hypothetical transcriptional repressor X for *Wnt2*, but not for *Wnt1*. *FoxA* is expressed in the future pharynx

of the embryo and in the domain immediately around the blastopore inside the ring of *Wnt1* expressing cells (Fig. 2). *FoxA* knockdown did not affect *Wnt2* expression, but *Wnt1* expression became stronger and expanded further orally in DMSO and globally in the AZK treatment (Fig. 3, Supplementary Fig. 4a). Thus, *FoxA* appears to act as the hypothetical repressor X for *Wnt1*, but not for *Wnt2*. *FoxB* is co-expressed with *Bra* in the domain where *Bra* expression is strong, i.e. abutting the *Wnt2*

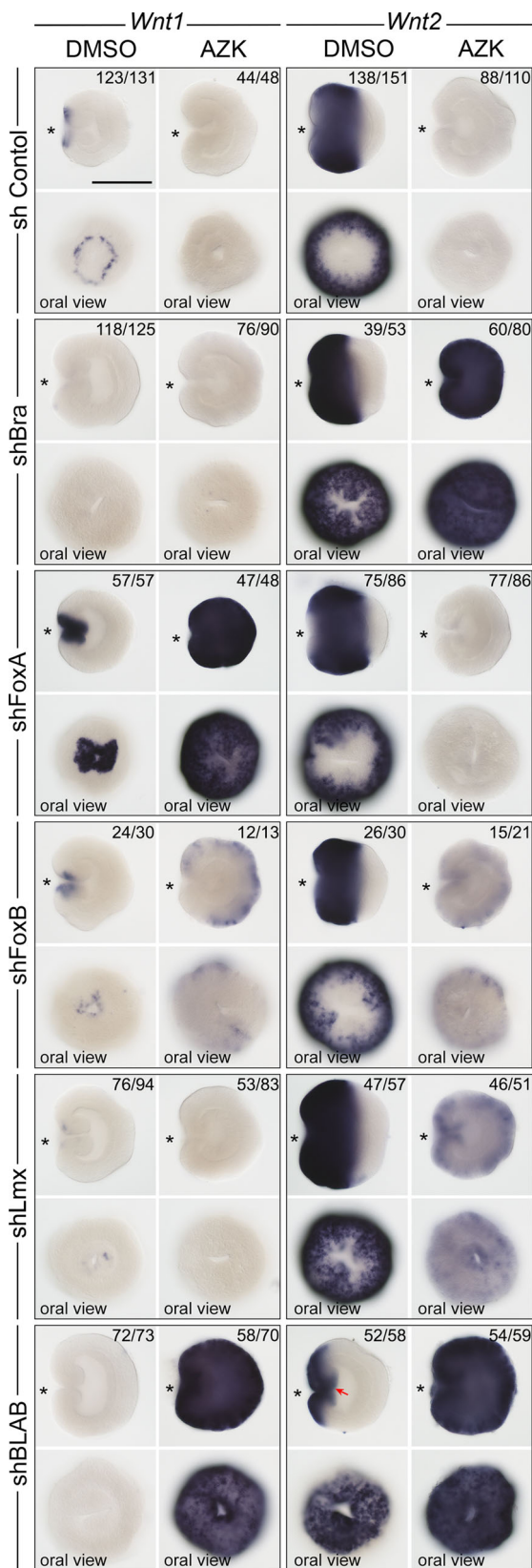


Fig. 3 The effect of the repressor X candidates knockdown on the expression of the “window” genes *Wnt1* and *Wnt2*. *Bra* and *Lmx* knockdowns convert *Wnt2* into a “saturating” gene, while *FoxA* knockdown does the same with *Wnt1*. The effect of *Lmx* knockdown appears to be similar but weaker than that of *Bra*. *FoxB* knockdown results in a “weak AZK effect” on both *Wnt1* and *Wnt2* suggesting that *FoxB* mildly represses both. The effects of the knockdowns of *Bra*, *Lmx*, and *FoxB* on *Wnt2* expression are non-redundant, but similar and additive (see Supplementary Figs. 6 and 7). Quadruple knockdown with shRNA against *Bra*, *Lmx*, *FoxA* and *FoxB* (=shBLAB) removes oral molecular identity of the embryo completely. Red arrow indicates the bottom of the pharynx expressing the midbody marker *Wnt2*. On lateral views, asterisk denotes the blastopore. The numbers in the top right corner show the ratio of embryos displaying the phenotype shown on the image to the total number of embryos treated and stained as indicated on the figure. Scale bar 100 μ m.

(Fig. 3, Supplementary Fig. 4a). Single, double and triple knockdown experiments suggest that the role of these two transcription factors appears to be in supporting the activity of *Bra* and *FoxA* in the areas, where they are co-expressed (Supplementary Results and Discussion 1, Supplementary Figs. 5–7). Simultaneous knockdown of *Bra*, *Lmx*, *FoxA* and *FoxB* with a mixture of shRNAs (shBLAB) completely abolishes the oral identity of the embryo at the molecular level: the midbody marker *Wnt2* shifts orally, expanding all the way to the bottom of the pharynx in DMSO, while the *Wnt2*-free aboral domain expands (Fig. 3, Supplementary Fig. 5). A much more pronounced expansion of the aboral domain and the confinement of the midbody marker *Wnt2* to the oralmost part of the embryo upon the combined knockdown of *Bra* together with either *Lmx* or *FoxB* or both in comparison to the individual *Bra* knockdown shows that the functions of these genes are non-redundant (Fig. 3; Supplementary Results and Discussion 1, Supplementary Figs. 5–7). We conclude that oral “window” genes are activated by β -catenin signaling (either directly or indirectly), and repressed by β -catenin-dependent “saturating” transcription factors. No single transcriptional repressor X exists, but rather *Bra*, *Lmx*, *FoxA* and *FoxB* appear to be the unit defining oral identity in the *Nematostella* embryo. Strikingly, the knockdown of any of these four transcription factors did not prevent normal gastrulation, and all the effects at this developmental stage remained purely molecular, pointing at the potential role of maternal factors in the gastrulation process (see Suppl. Results and Discussion 2–3, Supplementary Figs. 8, 9).

Repressor X regulatory logic applies to the whole O–A axis.

Previous work demonstrated that the aboral markers *FoxQ2a* and *Six3/6*, which are downregulated upon elevated β -catenin signaling, still require some β -catenin signaling in order to be expressed⁹, i.e. they may also be window genes. Therefore, it is conceivable that the patterning logic we discovered for the oral domain may be applicable to the whole of the O–A patterning, with more orally expressed β -catenin-dependent genes acting as transcriptional repressors for the more aborally expressed β -catenin-dependent genes. To test that, we investigated the mechanism of the maintenance of the other clear molecular boundary present in late gastrula ectoderm: the one between the *Wnt2*-positive midbody domain and the *Six3/6*-positive aboral domain (Fig. 1b). If the proposed regulatory logic were correct, there would have to exist at least one “transcriptional repressor Y”, which: (i) has to be expressed in the midbody domain, (ii) has to counteract the oral expansion of the aboral domain, and (iii) has to be positively regulated by β -catenin and repressed by the oral, “saturating” transcription factors (i.e. it has to be encoded by a “window” gene). Since “window” genes are downregulated upon

expression domain, and *Lmx* is a weakly expressed gene active in a domain starting from the *Wnt1* expressing cells and quickly fading out further aborally (Fig. 2). *FoxB* knockdown resulted in the expansion of both *Wnt1* and *Wnt2* expression in AZK, but the staining appeared weak, and *Lmx* RNAi effect on *Wnt1* and *Wnt2* largely recapitulated the effect of *Bra* RNAi, albeit milder

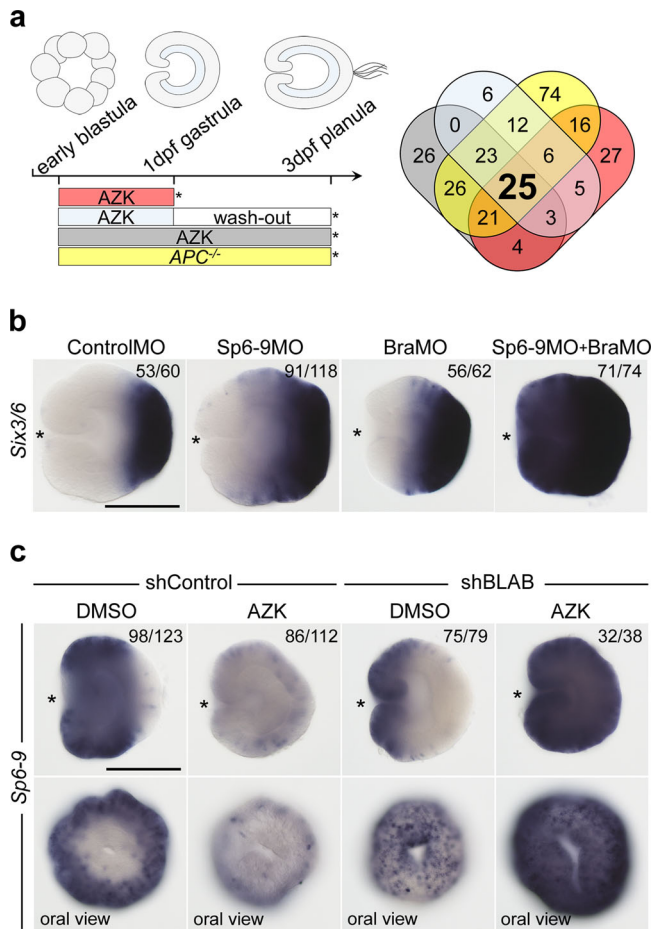


Fig. 4 Midbody domain prevents oral expansion of the aboral domain.

a Scheme of the treatments and Venn diagram showing the number of putative transcription factors downregulated by various treatments. **b** Sp6-9 prevents oral expansion of the aboral marker *Six3/6*. In BraMO, *Six3/6* expression is also expanded orally, likely due to the oral shift of the Sp6-9 expression upon *Bra* knockdown (see Supplementary Fig. 5). Oral expansion of *Six3/6* is enhanced upon double knockdown of Sp6-9 and *Bra*. Lateral views, oral to the left; asterisk denotes the blastopore. **c** Sp6-9 is a “window” gene shifting orally upon simultaneous knockdown of *Bra*, *Lmx*, *FoxA* and *FoxB* (=shBLAB) and expanding globally upon shBLAB knockdown followed by AZK treatment. Sp6-9-free area disappears in shBLAB. Lateral views, oral to the left; asterisk denotes the blastopore. The numbers in the top right corner on **b**, **c** show the ratio of embryos displaying the phenotype shown on the image to the total number of embryos treated and stained as indicated on the figure. Scale bars 100 μ m.

elevated β -catenin signaling, we looked at the transcription factor coding genes downregulated by all treatments in our RNA-Seq experiment, and found 25 such genes (Fig. 4a). We performed in situ hybridization with probes against all of them and excluded 18 genes expressed either in single ectodermal cells, endodermally, or whose expression domain included the aboral pole (Supplementary Fig. 10, Supplementary Table 2). Thus, we were left with seven transcriptional repressor Y candidates expressed in the midbody but not in the aboral domain: *Sp6-9*, *Nkl*, *Dlx*, *MxA*, *FoxG1*, *Rx*, and *HES-like* (Supplementary Fig. 10, Supplementary Table 2). In order to test whether they were capable of counteracting the oral expansion of the aboral domain, we performed individual knockdowns of all of them followed by in situ hybridization against the aboral marker *Six3/6* (Supplementary Fig. 11). Out of all candidates, only the knockdown of the gene encoding the Krüppel-like transcription factor Sp6-9 resulted in

the oral expansion of the *Six3/6* expression domain. (Fig. 4b, Supplementary Fig. 12a, b, Suppl. Results and Discussion 1 and 3). Predictably, since *Bra* knockdown results in the oral shift of the midbody domain (Fig. 3, Supplementary Fig. 5) and expansion of the aboral domain (Fig. 4b), *Six3/6* expansion was much more pronounced upon the combined knockdown of Sp6-9 and *Bra* (Fig. 4b). Finally, we tested whether Sp6-9 fulfilled the remaining transcriptional repressor Y criterion set above, namely whether it was a “window” gene. We could show that the knockdown of the four oral transcription factors *Bra*, *FoxA*, *FoxB* and *Lmx* expanded the expression of Sp6-9 orally in DMSO and globally in AZK (Fig. 4c), i.e. Sp6-9 behaved as a “window” gene. Curiously, in addition to the broad expression in the midbody domain (bordering the *Bra* domain orally and the *Six3/6* domain aborally; Fig. 2), Sp6-9 is also strongly expressed in individual cells scattered all over the embryo. This single-cell expression was not affected by the modulation of the β -catenin signaling (Fig. 4c). Taken together, Sp6-9 appears to act as hypothetical repressor Y at least for *Six3/6*, which suggests that the regulatory logic we proposed is applicable not just to the oral domain but to the whole β -catenin-dependent O–A axis patterning in the *Nematostella* ectoderm.

Aboral identity represents the default state. We demonstrated that the logic of the β -catenin-dependent O–A patterning relied on more orally expressed β -catenin targets displacing the expression domains of the more aborally expressed β -catenin targets further aborally. Therefore, we decided to test whether aboral fate represented the default state of the whole *Nematostella* embryo, which then became progressively restricted to the aboral domain by the orally expressed β -catenin-dependent factors, as it is described for the anterior ectodermal domain in deuterostomes^{13–15,26}. The fact that the major aboral determinant *Six3/6* requires an initial β -catenin signal in order to be expressed⁹ may be used as evidence against this hypothesis. However, *Six3/6* is a zygotic gene, whose expression becomes detectable at 12 h post fertilization (hpf), which is 4 h later than the onset of expression of the oral marker *Bra* (Fig. 5a). Notably, even the earliest expression of *Six3/6* is not ubiquitous, but localized to the future aboral side of the O–A axis. However, we do find aboral markers, whose expression is initially maternal and ubiquitous and subsequently becomes restricted to the aboral end in a β -catenin-dependent manner. One of them is *Frizzled 5/8* (Fig. 5a, b), which was shown to be a negative regulator of *Six3/6* and *FoxQ2a* in *Nematostella* and sea urchin^{9,15,27}. The other one is *SoxB1* (Fig. 5a, b), whose initially ubiquitous expression is cleared β -catenin-dependently out of the organizer and endomesodermal area in deuterostomes^{28,29}. Individual or simultaneous knockdowns of the oral and midbody factors *Bra* and Sp6-9 in *Nematostella* significantly expand the expression domain of *SoxB1* (Fig. 5c). Although qPCR data suggest that sea urchin *SoxB1* is a positive maternal upstream regulator of *FoxQ2*³⁰, the negative effect of *SoxB1* knockdown on *Six3/6* and *FoxQ2a* expression in *Nematostella* is not pronounced (Supplementary Fig. 13), and it is still unclear what kind of positive regulatory input maintains the aboral expression of *Six3/6* and hence other aboral markers. Nevertheless, our data clearly support the aboral-by-default model.

Endoderm is not a prerequisite for the ectodermal patterning.

In many investigated bilaterians, the earliest function of β -catenin signaling is to define the endomesodermal territory, and its role in the P–A patterning appears to kick in later^{13–15,23}. We were interested to see whether this was also the case in *Nematostella*. Previous work showed that *Nematostella* embryos failed to form

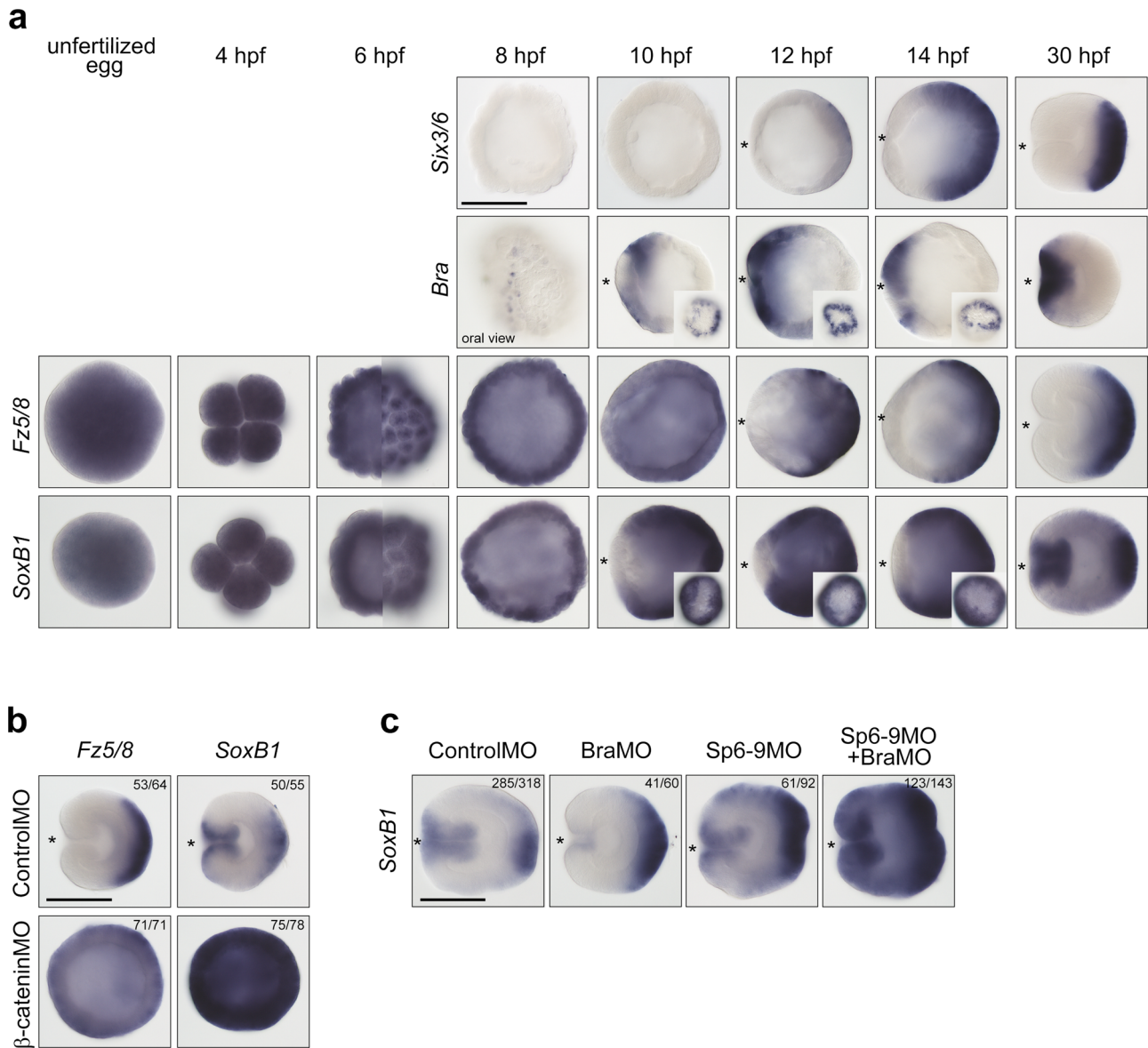


Fig. 5 *Nematostella* embryo initially has aboral identity, which later becomes restricted to the aboral domain. **a** *Six3/6* is detectable in the aboral portion of the embryo from 12 h post fertilization (hpf) on. *Bra* becomes detectable in a group of cells on the future oral side of the embryo as early as 8 hpf, and by 10 hpf it forms a ring around the future preendodermal plate. *Fz5/8* is a maternally deposited transcript. *Fz5/8* expression shifts to the future aboral side by 12 hpf. *SoxB1* is also a maternally deposited transcript. The loss of *SoxB1* staining in the future endodermal territory occurs simultaneously with the formation of the *Bra* ring, and is likely regulated by the same mechanism. By gastrula stage, *SoxB1* is expressed in the blastopore lip and aborally. On all lateral views, on which the O–A axis is discernible, the oral end is marked with an asterisk. Inset images of 10, 12 and 14 hpf embryos stained for *Bra* and *SoxB1* show the lack of expression in the putative preendodermal plate on embryos orientated with their oral ends facing the viewer. 6 hpf images of *Fz5/8* and *SoxB1* expression show the optical midsection (left) and the surface view (right) of the same embryos. **b** *Fz5/8* and *SoxB1* expression remains ubiquitous in the β -catenin morphants. Lateral views of the 30 hpf gastrulae, oral ends are marked with an asterisk. **c** *SoxB1* expression upon *Bra* knockdown appears weaker in the oral domain and expanded in the aboral domain, which is likely due to the oral shift of the *Sp6-9* expression. *Sp6-9* knockdown significantly expands *SoxB1* expression fusing the oral and aboral expression domains. Simultaneous knockdown of *Bra* and *Sp6-9* makes this effect even more pronounced consistent with the general aboralization of the embryo. The numbers in the top right corner on **b**, **c** show the ratio of embryos displaying the phenotype shown on the image to the total number of embryos treated and stained as indicated on the figure. Scale bars 100 μ m.

preendodermal plates and gastrulate when β -catenin signaling was suppressed by *cadherin* mRNA overexpression⁸ or β -catenin morpholino injection⁹. The lack of gastrulation clearly suggested that the role of β -catenin signaling in the determination of the endomesoderm was conserved since before the cnidarian–bilaterian split^{8,31}. In β -catenin morphants, not only the formation of the preendodermal plate, but also the expression of the “saturating” genes responsible for patterning the oral

ectoderm such as *Bra*, *FoxA* and *FoxB* is abolished⁹. Strikingly, the embryos placed in 5 μ M AZK shortly after fertilization (2 hpf) also fail to form preendodermal plates and remain spherical. However, these embryos, unlike β -catenin morphants, express *FoxA* and *FoxB* ubiquitously⁹. In contrast, in our 5 μ M AZK incubation experiments starting at 10 hpf, gastrulation process was not affected, and “saturating” oral ectodermal markers were ubiquitously expressed in the ectoderm but never extended into

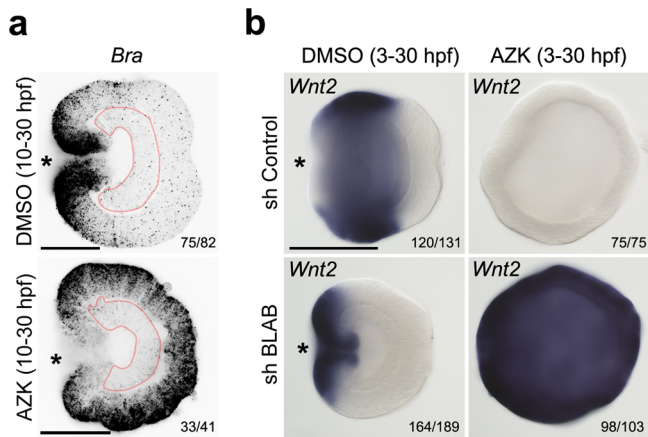


Fig. 6 Endoderm has no influence on O-A patterning of the ectoderm.

a Fluorescence in situ hybridization shows that *Bra* expression does not extend into the endoderm of the embryos (pink outline), which were placed in 5 μ M AZK after the time of the specification of the endodermal domain. **b** 5 μ M AZK incubation starting before the time of the specification of the endodermal domain prevents endoderm formation but still leads to the abolishment of *Wnt2* expression in shControl and to the conversion of *Wnt2* into a “saturating” gene upon shBLAB knockdown (compare with Fig. 3). The numbers in the bottom right corner show the ratio of embryos displaying the phenotype shown on the image to the total number of embryos treated and stained as indicated on the figure. Scale bars 100 μ m.

the endoderm (Fig. 6a) suggesting that the definition of the endodermal territory was complete prior to the onset of the treatment. Since the “saturating” expression behavior of the oral ectoderm markers was observed independent of the presence or absence of the endoderm, we asked whether the same was true for a “window” gene *Wnt2*. We showed that AZK treatment of the shBLAB-injected and control embryos starting at 3 hpf suppressed endoderm formation and that simultaneous knockdown of *Bra*, *FoxA*, *FoxB* and *Lmx* (shBLAB) followed by AZK treatment resulted in ubiquitous expression of *Wnt2*. Thus, the knockdown of the four “saturating” genes controlling the development of the oral domain resulted in the “saturating” expression of the “window” gene *Wnt2* both in the absence (Fig. 6b) and in the presence (Fig. 3) of the endoderm. This suggests that, similar to Bilateria, the roles of β -catenin signaling in defining the endodermal territory and ectodermal patterning in *Nematostella* are separable in time, and that the presence or absence of the endoderm does not influence ectodermal patterning at least until 30 hpf when the embryos were fixed and assayed.

Discussion

As a bilaterian sister group, cnidarians provide us with a key reference point regarding the evolution of body axes patterning and germ layer formation. Like in ambulacrarian deuterostomes, the definition of the future endoderm in *Nematostella* appears to be the earliest patterning event and relies on β -catenin signaling. Since both, morpholino knockdown of β -catenin and AZK-mediated stabilization of β -catenin at 2–3 hpf lead to the failure of the preendodermal plate formation⁹, it appears plausible that a certain precise dose of β -catenin signaling is required for the specification of the endodermal territory. Successful gastrulation of the embryos treated with AZK after 10 hpf suggests that the prospective endoderm is already specified by this time and that, once defined, the endoderm becomes insensitive to β -catenin signaling modulation at least until late gastrula stage. The expression of the genes patterning *Nematostella* ectoderm begins

after the specification of the endodermal territory, and their “window” or “saturating” behavior in response to AZK is not dependent on the presence or absence of the endoderm. In several investigated bilaterians, the early β -catenin signal defining the endomesoderm appears to rely on maternal components^{21,32–34}. In the future, it will be important to test how the switch from the β -catenin signaling-dependent specification of the endodermal domain to the β -catenin signaling-dependent ectodermal patterning in *Nematostella* relates to the activation of the zygotic transcription, which has been reported to occur at some point between 2 and 7 hpf³⁵. Curiously, the canonical β -catenin-dependent deuterostome endomesodermal markers *Bra* and *FoxA*^{13,14,22,36–41} are never expressed in the preendodermal plate of *Nematostella*. Instead, they are markers of the blastopore lip, i.e., of the oral ectoderm, which gives rise to the pharynx of the animal. In contrast, the expression signature and the response of the preendodermal plate to β -catenin signaling is reminiscent of the mesodermal domain in the echinoderm embryos^{9,22,32,42}. This provides some additional support to the hypothesis that the anthozoan endoderm and pharyngeal ectoderm may be homologous to the bilaterian mesoderm and endoderm, respectively⁴³.

Our data also allow re-evaluating the possible correspondence of the cnidarian and bilaterian body axes. In addition to the main, O–A body axis patterned by β -catenin signaling, anthozoans have a second, so-called “directive” axis patterned by BMP signaling^{44–46}, which is strikingly similar to the situation in Bilateria, where the P–A axis is patterned by Wnt/ β -catenin signaling, and the dorsal–ventral axis is patterned by BMP signaling. The similarity can have two possible explanations: either the last common ancestor of Cnidaria and Bilateria was bilaterally symmetric, in which case bilaterality must have been lost in radially symmetric medusozoan cnidarians, or anthozoan Cnidaria and Bilateria evolved bilaterally symmetric body plans independently but used the same signaling pathways for symmetry breaking and patterning². If bilaterality indeed evolved prior to the cnidarian–bilaterian split, the direct correspondence of the anthozoan and bilaterian body axes can be explained by three alternative, extensively debated scenarios. In the first scenario (O–A = A–P, Fig. 7a), the O–A axis is proposed to correspond to the anterior–posterior axis of Bilateria. The proponents of this scenario stress the importance of the direct correspondence of the animal–vegetal axis of the egg to the O–A axis in cnidarians, and the conservation of the origin of the mouth from the animal hemisphere material in Cnidaria, most Protostomia and Deuterostomia. They argue that once the gastrulation site switched from the animal to the vegetal pole at the base of Bilateria, the change in the position of the blastopore did not affect the location of the mouth and other structures. Therefore, it was suggested that cnidarian and bilaterian apical plates—the neurogenic territories developing at the vegetal pole in Cnidaria and at the animal pole in Bilateria—are non-homologous³¹. Finally, the role of the “anterior” *Hox* gene *Anthox6/HoxA* in the development of the oral end and the “non-anterior” *Hox* gene *Anthox1/HoxF* in the development of the aboral end of the *Nematostella* embryo^{45,47} has been seen as a supporting argument for the O–A = A–P scenario. However, *HoxA* and *HoxF* are expressed in non-adjacent domains in the embryo in different germ layers⁴⁷, and are located on different chromosomes in the genome⁴⁸, in contrast to the genomically linked *Hox* genes, which are expressed in staggered domains and generate a Hox code patterning the second, directive axis under BMP control^{46,48,49}. Another piece of evidence against the O–A = A–P scenario is that the apical ectodermal domains opposing the gastrulation sites both in Cnidaria and Bilateria have a strikingly similar expression signature making the homology of the cnidarian and bilaterian

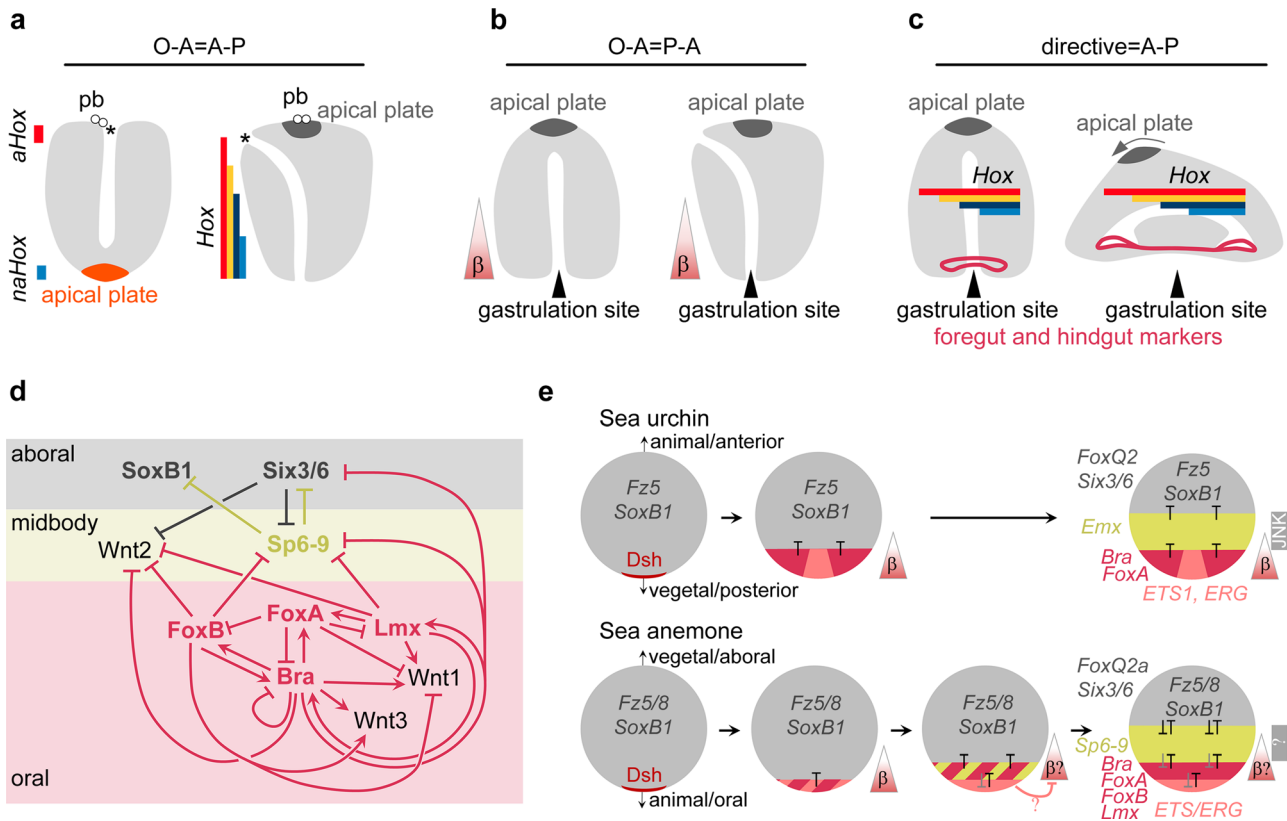


Fig. 7 Oral-aboral patterning regulation in *Nematostella* and P-A patterning in sea urchin are comparable. **a–c** Scenarios of the direct correspondence of the cnidarian and bilaterian body axes. pb – polar bodies, aHox – anterior *Hox* gene, naHox – non-anterior *Hox* gene, asterisk denotes the mouth. Triangles with a β denote the direction of the β -catenin signaling gradient. **d** Putative topology of the gene regulatory network of the β -catenin-dependent O–A patterning in *Nematostella*. The GRN explains why the midbody domain does not expand into the oral and into the aboral domains, and why the aboral domain does not expand into the midbody. It does not explain, however, why the oral domain does not expand aborally. **e** Comparison of the early β -catenin-dependent patterning in sea urchin and *Nematostella* shows clear similarities. Unfertilized egg with maternal *Fz5/8* and *SoxB1* mRNA (future anterior/aboral markers) and maternal Dsh protein localized at the gastrulation pole^{65,66}. Upon activation of β -catenin signaling in the embryo, first in the endomesodermal domain and then in the posterior/oral ectoderm the expression of *Fz5/8* and *SoxB1* is suppressed, and the anterior/aboral markers (including the zygotic genes *Six3/6* and *FoxQ2*) become progressively confined to one side of the axis. The axis becomes patterned by mutually repressive transcription factors (T). Gray “T” in *Nematostella* indicate repressive interactions, for which candidate transcription factors are not known. Triangles with a β denote the direction of the β -catenin signaling gradient. $\beta?$ indicates that in *Nematostella*, nuclear β -catenin could only be experimentally detected until midblastula stage⁹, after which the presence of nuclear β -catenin gradient is deduced based on target gene response. After preendodermal plate is specified in *Nematostella*, β -catenin signaling becomes repressed there by an unknown mechanism⁹, possibly involving ERG⁴².

apical plates highly plausible^{50–52}. Also, the oral end of cnidarians is characterized by a β -catenin signaling maximum, which also appears to be a conserved feature of the posterior rather than the anterior end both in protostome and in deuterostome Bilateria. Thus, the second scenario (O–A = P–A, Fig. 7b) suggests that the O–A axis of Cnidaria corresponds to the posterior–anterior axis of Bilateria. The O–A = P–A scenario, however, does not consider the importance of the *Hox*-dependent axial patterning in Anthozoa. The third scenario (directive = A–P, Fig. 7c) proposes that the directive axis of anthozoans may correspond to the anterior–posterior axis of the ancestral bilaterian, whose blastopore closed in an amphistomic, slit-like fashion generating a mouth and an anus at opposing ends connected by a through gut. This scenario is supported by the circumblastoporal expression of several bilaterian foregut and hindgut markers in Cnidaria and by the role of the staggered expression of *Hox* genes in patterning the directive axis in *Nematostella* and the A–P axis in Bilateria^{49,51,52}. The directive=A–P hypothesis is somewhat hampered by the unclear orthology of the cnidarian and bilaterian *Hox* genes, their likely independent diversification in Cnidaria and Bilateria, and their expression along the body axis patterned by BMP signaling

and under BMP control in *Nematostella*^{2,46}, which is highly unusual for Bilateria.

Although none of the three scenarios above explains the correspondence of the two anthozoan and two bilaterian body axes without contradiction, we can assess whether any of them is supported by our new data on the mechanism of the β -catenin-dependent patterning of the main cnidarian body axis better than the others. Here we showed that *Bra*, *FoxA*, *Lmx* and *FoxB* define the oral molecular identity of the *Nematostella* embryo and prevent oral expansion of the more aborally expressed β -catenin targets (Fig. 7d). We also identified *Sp6-9*, a “window” gene expressed in the midbody domain, as the agent preventing the oral expansion of the aboral domain (Fig. 7d). The whole *Nematostella* embryo initially represents an aboral ectodermal territory, which is established maternally (Fig. 7e). During the first day of development, this territory becomes restricted to the aboral end of the O–A axis in a β -catenin-dependent manner by “saturating” and “window” transcriptional repressors, which form mutually repressive pairs capable of generating sharp domain boundaries (Fig. 7e). This is highly similar to the situation demonstrated in non-chordate deuterostomes like echinoderms and hemichordates^{13–15,28,32}.

Comparison with sea urchin reveals remarkable conservation of the components of the axial patterning gene regulatory network downstream of β -catenin. In sea urchin, *Bra* and *FoxA* are central in the β -catenin-dependent axial patterning of the blastoporal domain^{40,53}. The midbody domain of the sea urchin embryo appears to be defined by an Antennapedia class transcription factor *Emx*^{54,55}, rather than by a Krüppel-like factor *Sp6-9*. However, the patterning of the apical ectoderm is again accomplished by the same components in the sea anemone and sea urchin embryos^{15,50}. Importantly, not only the genes involved, but also the regulatory logic of gradual restriction of the apical ectodermal territory by β -catenin-dependent transcription factors appears to be highly similar in the β -catenin-dependent O–A patterning of the ectoderm in the anthozoan *Nematostella* and in the posterior–anterior patterning in sea urchin and other investigated deuterostomes, including vertebrates^{11,13–16,40,53} (Fig. 7e), while the situation in protostomes appears to be more derived. Based on this remarkable similarity we conclude that the processes of ectodermal patterning of the cnidarian O–A axis and the deuterostome P–A patterning share a common evolutionary origin predating the cnidarian–bilaterian split. Thus, independent of whether the second, BMP-dependent body axes of anthozoans and bilaterians evolved independently or not, we propose that the cnidarian O–A and the deuterostome P–A body axes are likely homologous (O–A = P–A).

Methods

Animals, microinjection, APC mutants, and transplantations. *Nematostella* polyps were kept in *Nematostella* medium (16‰ artificial seawater, NM) at 18 °C in the dark and induced to spawn by placing them into a 25 °C, illuminated incubator for 10 h. The eggs were fertilized for 30 min and dejellied in 3% L-cysteine/NM and washed 6 times in NM. Microinjection was performed under the Nikon TS100F microscope using Eppendorf Femtojet and Narishige micromanipulators. The APC mutant line was generated by injecting *Nematostella* zygotes with 500 ng/ μ l single gRNAs (protospacer 5' CACAGCTATGAGGGCCAC) and 500 ng/ μ l nls-Cas9 (PNA Bio, Thousand Oaks, CA, USA). Mosaic F0 animals were crossed to produce APC^{+/–} F1 carrying a single T insertion after the position 331 of the coding sequence of *Nematostella* APC (Genbank KT381584). Heterozygous F1 were crossed to obtain F2. In situ hybridization analysis showed that 27% of the F2 embryos expressed *Bra* throughout the ectoderm of the gastrula, while 73% had normal *Bra* expression ($N = 221$). At 3 dpf, 10 out of 10 randomly selected F2 embryos demonstrating the typical bagel phenotype similar to that of the AZK treated embryos proved to be APC^{–/–} when genotyped by Sanger sequencing of the mutated locus (Supplementary Fig. 1d). For genotyping live polyps, individual primary polyps or tentacle clips were fixed by 3 washes in 100% methanol, aspirated, and dried for 20 min at 50 °C with the tube lids open. Then, samples were digested in 30 μ l of extraction buffer (10 mM Tris-HCl pH8, 1 mM EDTA pH8, 25 mM NaCl, 200 μ g/ml proteinase K) for 2 h at 50 °C, and proteinase K was inactivated by heating the samples to 95 °C for 5 min. After proteinase K inactivation, 3 μ l of the digest was used as template for the PCR with the primers flanking the locus recognized by the gRNA (APCspF 5'AGAATCCTGCA GAAGATGAACA, APCspR 5'CTCGCATACAAAGGTGACA). The PCR product was purified and directly sequenced with the APCspF primer. For genotyping embryos after in situ hybridization, the embryos were dehydrated in ethanol series, washed twice with 100% ethanol, embedded into Murray's clear solution (benzyl benzoate:benzyl alcohol = 2:1), imaged, washed several times in 100% methanol and then processed as described above. During experiments, the embryos were kept in the 21 °C incubator. Blastopore lip transplantations were performed as described⁴. The significance of the difference in the transplantation outcomes was assessed by performing the Z score test for two population proportions (<https://www.socscistatistics.com/tests/ztest/default.aspx>).

Pharmacological treatments, gene knockdown, overexpression. 1-azakenpauillon (Sigma) used for the treatments was prepared by diluting 5 mM AZK dissolved in DMSO with NM. Equal volume of DMSO was used to treat the control embryos. 5 μ M AZK was used for treating the embryos used for the RNA-Seq experiments as well as for the transcriptional repressor X and Y search. The time windows of the treatments are presented in Fig. 1e; briefly, unless specified otherwise, the embryos were incubated in AZK or DMSO from 10 hpf (early blastula) until either 30 hpf (late gastrula) or 72 hpf (3 dpf planula larva). For the embryos incubated from 10 until 30 hpf, RNA was extracted either immediately at 30 hpf or after a wash-out and a 42 h long incubation in NM (i.e., at 72 hpf). Gene knockdowns were performed by electroporation with shRNA as specified^{49,56}. Two non-overlapping shRNAs were used for each of the genes to confirm the specificity of the observed phenotypes except for the cases of *Brachyury*, *Sp6-9*, *Nkl*, and *Dlx*, where two or one shRNAs and one translation-blocking morpholino (MO) were used (Supplementary

Tables 3–4). shRNA against *mOrange* was used as a control for all other shRNA, and a control MO we described previously⁴ (Supplementary Table 4) was used to control for the BraMO, NklMO, DlxMO, and Sp6-9MO phenotypes. The RNAi efficiency was estimated by in situ hybridization and Q-PCR (Supplementary Fig. 3a, b, Supplementary Fig. 11a, b, Supplementary Table 5), and the activity of the morpholinos was assayed by co-injecting them with the wild type and 5-mismatch mRNA containing the morpholino recognition sequences fused to mCherry (Supplementary Fig. 3c, Supplementary Fig. 11c). Capped mRNA was synthesized using mMessage mMachine kit (Life Technologies) and purified with the Monarch RNA clean-up kit (NEB). *Bra* and *FoxB* mRNA for overexpression was also produced as described above. A stabilized form of β -catenin was generated by removing the first 240 bp of the β -catenin coding sequence as described in⁵⁷. An ATG was added, and the fragment, which we called β -cat_{stab}, was cloned into an expression vector downstream of the ubiquitously active *EF1 α* promoter⁴³. Mosaic expression of the *EF1 α : β -cat_{stab}* was achieved by meganuclease-assisted transgenesis, as described⁵⁸. Primers against GAPDH were used as normalization control in QPCR.

Transcriptome sequencing and analysis. Total RNA was extracted with TRIZOL (Life Technologies) or with GeneElute Mammalian Total RNA Miniprep Kit (Sigma) according to the manufacturer's protocol; poly-A enriched mRNA library preparation (Lexogen), quality control, and multiplexed Illumina HiSeq2500 sequencing (50 bp, single-end) were performed at the Vienna BioCenter Core Facilities. The number of the sequenced biological replicates of different treatments is shown in the Supplementary Fig. 2. SAMtools 1.11⁵⁹ was used for format conversion. The reads were aligned with STAR⁶⁰ to the *Nematostella vectensis* genome⁶¹ using the ENCODE standard options, with the exception that alignIntronMax was set to 100 kb. Hits to the gene models v2.0 (https://figshare.com/articles/Nematostella_vectensis_transcriptome_and_gene_models_v2_0/807696) were tallied with featureCounts⁶², and differential expression analysis was performed with DESeq2⁶³. Expression changes in genes with Benjamini-Hochberg adjusted p-value < 0.05 were considered significant. No additional expression fold change cutoff was imposed. Transcription factor candidates were determined by analyzing the transcriptome with INTERPROSCAN²⁵ and filtering for genes containing the domains described in⁶⁴. The intersection between the latter set and our differentially expressed genes comprised the models of putative transcription factors.

In situ hybridization, SEM. In situ hybridization was performed exactly as described in⁴ with a minor change in the fixation protocol: here, we fixed the embryos for 1 h in 4% PFA/PBS at room temperature and washed the embryos several times first in PTw (1 \times PBS, 0.1% Tween 20) and then in 100% methanol prior to storing them at –20 °C. For the single chromogenic in situ hybridization, the RNA probes were detected with anti-Digoxigenin-AP Fab fragments (Roche) diluted 1:4000 in 0.5% blocking reagent (Roche) in 1 \times MAB followed by a substrate reaction with a mixture of NBT/BCIP as in⁴. Imaging was performed with a Nikon 80i compound microscope equipped with the Nikon DS-Fi1 camera. For the fluorescent double in situ hybridization, the hybridization protocol was similar to the single chromogenic in situ protocol except for the changes outlined below. FITC- and Dig-labeled RNA probes were simultaneously added to the sample. After stringent post-hybridization washes, the embryos were blocked in the 0.5% TSA Blocking Reagent (Perkin-Elmer) in TNT buffer for 1 h, and stained overnight at 4 °C with anti-Digoxigenin-POD Fab fragments (Roche) diluted 1:100 in blocking buffer. The unbound antibody was then removed by 10 \times 10 min TNT washes, and the fluorescent signal was developed using the TSA Plus Cyanine 3 System (Perkin-Elmer) according to the manufacturer's protocol. The staining was stopped by multiple TNT washes, and peroxidase was inactivated by a 20 min wash in 1% H₂O₂/TNT in the dark. After that, the embryos were washed several times with TNT, blocked as described above and stained with the anti-Fluorescein-POD Fab fragments (Roche) diluted 1:50 in blocking buffer. Fluorescent signal was then developed as described above using the TSA Plus Fluorescein System (Perkin-Elmer). After stopping the staining with multiple TNT washes the embryos were embedded in Vectashield (Vectorlabs) and imaged with the Leica SP8 CLSM. Preparation of the samples for the SEM was performed as described in⁴. Imaging was done using the JEOL IT 300 scanning electron microscope.

Phalloidin and antibody staining. For phalloidin staining of fibrillar actin and anti-acetylated tubulin staining of cilia, the embryos were fixed in 4% PFA/PTwTx (1 \times PBS, 0.1% Tween 20, 0.2% Triton X100) for 1 h at room temperature, washed 5 times with PTwTx, incubated in 100% acetone pre-cooled to –20 °C for 7 min on ice, and washed 3 more times with PTwTx. Then, the embryos were incubated for 2 h in blocking solution (95% v/v of 1% BSA/PTwTx and 5% v/v of heat-inactivated sheep serum). Blocked embryos were stained overnight at 4 °C in 0.4U of Alexa Fluor 488 Phalloidin (ThermoFisher) and 0.1 μ l of mouse monoclonal anti-acetylated tubulin (Sigma) dissolved in 100 μ l blocking solution. Unbound primary antibody and phalloidin were washed away by five 10 min PTwTx washes, and the embryos were stained for 2 h at room temperature in the dark in 0.4U of Alexa Fluor 488 Phalloidin and 0.1 μ l of Alexa Fluor 568 rabbit anti-mouse IgG (Molecular Probes) dissolved in 100 μ l blocking solution. After five more 10 min PTwTx washes, the embryos were gradually embedded in Vectashield (Vectorlabs) and imaged with the Leica SP8 CLSM.

Reporting summary. Further information on research design is available in the Nature Research Reporting Summary linked to this article.

Data availability

All data needed to evaluate the conclusions in the paper are present in the paper or the supplementary materials. Raw RNA-seq reads have been deposited in the NCBI BioProject database under the accession code: [PRJNA661731](https://www.ncbi.nlm.nih.gov/bioproject/PRJNA661731).

Received: 22 October 2020; Accepted: 30 May 2021;

Published online: 29 June 2021

References

- Niehrs, C. On growth and form: a Cartesian coordinate system of Wnt and BMP signaling specifies bilaterian body axes. *Development* **137**, 845–857 (2010).
- Genikhovich, G. & Technau, U. On the evolution of bilaterality. *Development* **144**, 3392–3404 (2017).
- Simion, P. et al. A large and consistent phylogenomic dataset supports sponges as the sister group to all other animals. *Curr. Biol.* **27**, 958–967 (2017).
- Kraus, Y., Aman, A., Technau, U. & Genikhovich, G. Pre-bilaterian origin of the blastoporal axial organizer. *Nat. Commun.* **7**, 11694 (2016).
- Marlow, H., Matus, D. Q. & Martindale, M. Q. Ectopic activation of the canonical wnt signaling pathway affects ectodermal patterning along the primary axis during larval development in the anthozoan *Nematostella vectensis*. *Dev. Biol.* **380**, 324–334 (2013).
- Pang, K., Ryan, J. F., Mullikin, J. C., Baxeveanis, A. D. & Martindale, M. Q. Genomic insights into Wnt signaling in an early diverging metazoan, the ctenophore *Mnemiopsis leidyi*. *EvoDevo* **1**, 10 (2010).
- Leininger, S. et al. Developmental gene expression provides clues to relationships between sponge and eumetazoan body plans. *Nat. Commun.* **5**, 3905 (2014).
- Wikramanayake, A. H. et al. An ancient role for nuclear β -catenin in the evolution of axial polarity and germ layer segregation. *Nature* **426**, 446–450 (2003).
- Leclère, L., Bause, M., Sinigaglia, C., Steger, J. & Rentzsch, F. Development of the aboral domain in *Nematostella* requires β -catenin and the opposing activities of Six3/6 and Frizzled5/8. *Development* **143**, 1766–1777 (2016).
- Kusserow, A. et al. Unexpected complexity of the Wnt gene family in a sea anemone. *Nature* **433**, 156–160 (2005).
- Kiecker, C. & Niehrs, C. A morphogen gradient of Wnt/ β -catenin signalling regulates anteroposterior neural patterning in *Xenopus*. *Development* **128**, 4189–4201 (2001).
- Nordström, U., Jessell, T. M. & Edlund, T. Progressive induction of caudal neural character by graded Wnt signaling. *Nat. Neurosci.* **5**, 525–532 (2002).
- Darras, S. et al. Anteroposterior axis patterning by early canonical Wnt signaling during hemichordate development. *PLoS Biol.* **16**, e2003698 (2018).
- Darras, S., Gerhart, J., Terasaki, M., Kirschner, M. & Lowe, C. J. β -catenin specifies the endomesoderm and defines the posterior organizer of the hemichordate *Saccoglossus kowalevskii*. *Development* **138**, 959–970 (2011).
- Range, R. C., Angerer, R. C. & Angerer, L. M. Integration of canonical and noncanonical Wnt signaling pathways patterns the neuroectoderm along the anterior–posterior axis of sea urchin embryos. *PLoS Biol.* **11**, e1001467 (2013).
- McCauley, B. S., Akyar, E., Saad, H. R. & Hinman, V. F. Dose-dependent nuclear β -catenin response segregates endomesoderm along the sea star primary axis. *Development* **142**, 207–217 (2015).
- Fu, J. et al. Asymmetrically expressed axin required for anterior development in *Tribolium*. *Proc. Natl Acad. Sci. USA* **109**, 7782–7786 (2012).
- Prühs, R., Beermann, A. & Schröder, R. The roles of the Wnt-antagonists Axin and Lrp4 during embryogenesis of the red flour beetle *Tribolium castaneum*. *J. Dev. Biol.* **5**, 10 (2017).
- McGregor, A. P. et al. Wnt8 is required for growth-zone establishment and development of opisthosomal segments in a spider. *Curr. Biol.* **18**, 1619–1623 (2008).
- Martín-Durán, J. M., Passamaneck, Y. J., Martindale, M. Q. & Hejnol, A. The developmental basis for the recurrent evolution of deuterostomy and protostomy. *Nat. Ecol. Evol.* **1**, 5 (2016).
- Henry, J. Q., Perry, K. J., Wever, J., Seaver, E. & Martindale, M. Q. Beta-catenin is required for the establishment of vegetal embryonic fates in the nemertean, *Cerebratulus lacteus*. *Dev. Biol.* **317**, 368–379 (2008).
- Logan, C. Y., Miller, J. R., Ferkowicz, M. J. & McClay, D. R. Nuclear β -catenin is required to specify vegetal cell fates in the sea urchin embryo. *Development* **126**, 345–357 (1999).
- Wikramanayake, A. H., Huang, L. & Klein, W. H. β -catenin is essential for patterning the maternally specified animal-vegetal axis in the sea urchin embryo. *Proc. Natl Acad. Sci. USA* **95**, 9343–9348 (1998).
- Pukhlyakova, E., Aman, A. J., Elsayad, K. & Technau, U. β -Catenin-dependent mechanotransduction dates back to the common ancestor of Cnidaria and Bilateria. *Proc. Natl Acad. Sci. USA* **115**, 6231–6236 (2018).
- Madeira, F. et al. The EMBL-EBI search and sequence analysis tools APIs in 2019. *Nucleic Acids Res.* **47**, W636–W641 (2019).
- Khadka, A., Martínez-Bartolomé, M., Burr, S. D. & Range, R. C. A novel gene's role in an ancient mechanism: secreted Frizzled-related protein 1 is a critical component in the anterior-posterior Wnt signaling network that governs the establishment of the anterior neuroectoderm in sea urchin embryos. *EvoDevo* **9**, 1 (2018).
- Croce, J., Duloquin, L., Lhomond, G., McClay, D. R. & Gache, C. Frizzled5/8 is required in secondary mesenchyme cells to initiate archenteron invagination during sea urchin development. *Development* **133**, 547–557 (2006).
- Angerer, L. M., Newman, L. A. & Angerer, R. C. SoxB1 downregulation in vegetal lineages of sea urchin embryos is achieved by both transcriptional repression and selective protein turnover. *Development* **132**, 999–1008 (2005).
- Shih, Y.-H. et al. SoxB1 transcription factors restrict organizer gene expression by repressing multiple events downstream of Wnt signalling. *Development* **137**, 2671–2681 (2010).
- Li, E., Cui, M., Peter, I. S. & Davidson, E. H. Encoding regulatory state boundaries in the pregastrular oral ectoderm of the sea urchin embryo. *Proc. Natl Acad. Sci. USA* **111**, E906–E913 (2014).
- Martindale, M. Q. & Hejnol, A. A developmental perspective: changes in the position of the blastopore during bilaterian evolution. *Dev. Cell* **17**, 162–174 (2009).
- Davidson, E. H. et al. A genomic regulatory network for development. *Science* **295**, 1669–1678 (2002).
- Kawai, N., Iida, Y., Kumano, G. & Nishida, H. Nuclear accumulation of β -catenin and transcription of downstream genes are regulated by zygotic Wnt5a and maternal Dsh in ascidian embryos. *Dev. Dyn.* **236**, 1570–1582 (2007).
- Imai, K., Takada, N., Satoh, N. & Satou, Y. (beta)-catenin mediates the specification of endoderm cells in ascidian embryos. *Development* **127**, 3009–3020 (2000).
- Helm, R. R., Siebert, S., Tulin, S., Smith, J. & Dunn, C. W. Characterization of differential transcript abundance through time during *Nematostella vectensis* development. *BMC genomics* **14**, 266 (2013).
- Arnold, S. J. et al. *Brachyury* is a target gene of the Wnt/ β -catenin signaling pathway. *Mech. Dev.* **91**, 249–258 (2000).
- Charney, R. M., Paraiso, K. D., Blitz, I. L. & Cho, K. W. Y. A gene regulatory program controlling early *Xenopus* mesoderm formation: Network conservation and motifs. *Semin Cell Dev. Biol.* **66**, 12–24 (2017).
- Yamaguchi, T. P., Takada, S., Yoshikawa, Y., Wu, N. & McMahon, A. P. T (*Brachyury*) is a direct target of Wnt3a during paraxial mesoderm specification. *Genes Dev.* **13**, 3185–3190 (1999).
- Vonica, A. & Gumbiner, B. M. Zygotic Wnt activity is required for *Brachyury* expression in the early *Xenopus laevis* embryo. *Dev. Biol.* **250**, 112–127 (2002).
- de-Leon, S. B. & Davidson, E. H. Information processing at the *foxa* node of the sea urchin endomesoderm specification network. *Proc. Natl Acad. Sci. USA* **107**, 10103–10108 (2010).
- Gross, J. M. & McClay, D. R. The role of *Brachyury* (T) during gastrulation movements in the sea urchin *Lytechinus variegatus*. *Dev. Biol.* **239**, 132–147 (2001).
- Amiel, A. R. et al. A bipolar role of the transcription factor ERG for cnidarian germ layer formation and apical domain patterning. *Dev. Biol.* **430**, 346–361 (2017).
- Steinmetz, P. R., Aman, A., Kraus, J. E. M. & Technau, U. Gut-like ectodermal tissue in a sea anemone challenges germ layer homology. *Nat. Ecol. Evol.* **1**, 1535–1542 (2017).
- Saina, M., Genikhovich, G., Renfer, E. & Technau, U. BMPs and chordin regulate patterning of the directive axis in a sea anemone. *Proc. Natl Acad. Sci. USA* **106**, 18592–18597 (2009).
- Finnerty, J. R., Pang, K., Burton, P., Paulson, D. & Martindale, M. Q. Origins of bilateral symmetry: *Hox* and *dpp* expression in a sea anemone. *Science* **304**, 1335–1337 (2004).
- Genikhovich, G. et al. Axis patterning by BMPs: cnidarian network reveals evolutionary constraints. *Cell Rep.* **10**, 1646–1654 (2015).
- DuBuc, T. Q., Stephenson, T. B., Rock, A. Q. & Martindale, M. Q. *Hox* and Wnt pattern the primary body axis of an anthozoan cnidarian before gastrulation. *Nat. Commun.* **9**, 2007 (2018).
- Zimmermann, B. et al. Sea anemone genomes reveal ancestral metazoan chromosomal macrosynteny. Preprint at <https://doi.org/10.1101/2020.10.30.359448> (2020).
- He, S. et al. An axial *Hox* code controls tissue segmentation and body patterning in *Nematostella vectensis*. *Science* **361**, 1377–1380 (2018).
- Sinigaglia, C., Busengdal, H., Leclère, L., Technau, U. & Rentzsch, F. The bilaterian head patterning gene *six3/6* controls aboral domain development in a cnidarian. *PLoS Biol.* **11**, e1001488 (2013).

51. Arendt, D., Tosches, M. A. & Marlow, H. From nerve net to nerve ring, nerve cord and brain—evolution of the nervous system. *Nat. Rev. Neurosci.* **17**, 61–72 (2016).
52. Nielsen, C., Brunet, T. & Arendt, D. Evolution of the bilaterian mouth and anus. *Nat. Ecol. Evol.* **2**, 1358–1376 (2018).
53. Peter, I. S. & Davidson, E. H. A gene regulatory network controlling the embryonic specification of endoderm. *Nature* **474**, 635–639 (2011).
54. Li, E., Cui, M., Peter, I. S. & Davidson, E. H. Encoding regulatory state boundaries in the pregastrular oral ectoderm of the sea urchin embryo. *Proc. Natl Acad. Sci. USA* **111**, E906–E913 (2014).
55. Cui, M., Siriwon, N., Li, E., Davidson, E. H. & Peter, I. S. Specific functions of the Wnt signaling system in gene regulatory networks throughout the early sea urchin embryo. *Proc. Natl Acad. Sci. USA* **111**, E5029–E5038 (2014).
56. Karabulut, A., He, S., Chen, C. Y., McKinney, S. A. & Gibson, M. C. Electroporation of short hairpin RNAs for rapid and efficient gene knockdown in the starlet sea anemone, *Nematostella vectensis*. *Dev. Biol.* **448**, 7–15 (2019).
57. Gee, L. et al. β -catenin plays a central role in setting up the head organizer in hydra. *Dev. Biol.* **340**, 116–124 (2010).
58. Renfer, E., Amon-Hassenzahl, A., Steinmetz, P. R. & Technau, U. A muscle-specific transgenic reporter line of the sea anemone, *Nematostella vectensis*. *Proc. Natl Acad. Sci. USA* **107**, 104–108 (2010).
59. Danecek, P. et al. Twelve years of SAMtools and BCFtools. *Gigascience* **10**, <https://doi.org/10.1093/gigascience/giab008> (2021).
60. Dobin, A. et al. STAR: ultrafast universal RNA-seq aligner. *Bioinformatics* **29**, 15–21 (2013).
61. Putnam, N. H. et al. Sea anemone genome reveals ancestral eumetazoan gene repertoire and genomic organization. *Science* **317**, 86–94 (2007).
62. Liao, Y., Smyth, G. K. & Shi, W. featureCounts: an efficient general purpose program for assigning sequence reads to genomic features. *Bioinformatics* **30**, 923–930 (2014).
63. Love, M. I., Huber, W. & Anders, S. Moderated estimation of fold change and dispersion for RNA-seq data with DESeq2. *Genome Biol.* **15**, 550 (2014).
64. de Mendoza, A. et al. Transcription factor evolution in eukaryotes and the assembly of the regulatory toolkit in multicellular lineages. *Proc. Natl Acad. Sci. USA* **110**, E4858–E4866 (2013).
65. Peng, C. J. & Wikramanayake, A. H. Differential regulation of dishevelled in a novel vegetal cortical domain in sea urchin eggs and embryos: implications for the localized activation of canonical Wnt signaling. *PLoS ONE* **8**, e80693 (2013).
66. Lee, P. N., Kumburegama, S., Marlow, H. Q., Martindale, M. Q. & Wikramanayake, A. H. Asymmetric developmental potential along the animal-vegetal axis in the anthozoan cnidarian, *Nematostella vectensis*, is mediated by Dishevelled. *Dev. Biol.* **310**, 169–186 (2007).

Acknowledgements

This work was funded by the Austrian Science Foundation (FWF) grant P30404-B29 to G.G., A.J.A. was supported by an HFSP postdoctoral fellowship (LT000809/2012-L). Y.K. was supported by the Lise Meitner FWF fellowship (M1140-B17). We are grateful to the Core Facility for Cell Imaging and Ultrastructure Research of the University of Vienna

for the access to the confocal and scanning electron microscopes, Patrick Steinmetz for the fluorescent ISH protocol, Patricio Ferrer Murguía for an shRNA against *FoxA*, Saskia Hartmann for the initial genotyping of the *APC* mutants, Rohit Dnyansagar for the help with bioinformatics, Paul Knabl for drawing Fig. 7a, Emmanuel Haillot for discussions, and David Mörsdorf for critically reading the manuscript.

Author contributions

T.L. performed the majority of the experiments, planned experiments and analyzed data; A.J.A. and U.T. conceived the generation of the *APC* mutant line; A.J.A. generated the *APC* mutant line, and started its characterization together with A.D.; T.G. and I.N. performed treatments, and prepared RNA for sequencing; B.Z. supervised the bioinformatic analysis; Y.K. performed transplantations on *Bra* morphants; M.S. generated mosaic *EF1 α :: β -cat \cdot stab* polyps; G.G. conceived the study, planned experiments, performed experiments, analyzed data and wrote the paper. All authors edited the paper.

Competing interests

The authors declare no competing interests.

Additional information

Supplementary information The online version contains supplementary material available at <https://doi.org/10.1038/s41467-021-24346-8>.

Correspondence and requests for materials should be addressed to G.G.

Peer review information *Nature Communications* thanks Christopher Lowe and the other, anonymous, reviewer(s) for their contribution to the peer review of this work. Peer reviewer reports are available.

Reprints and permission information is available at <http://www.nature.com/reprints>

Publisher's note Springer Nature remains neutral with regard to jurisdictional claims in published maps and institutional affiliations.



Open Access This article is licensed under a Creative Commons Attribution 4.0 International License, which permits use, sharing, adaptation, distribution and reproduction in any medium or format, as long as you give appropriate credit to the original author(s) and the source, provide a link to the Creative Commons license, and indicate if changes were made. The images or other third party material in this article are included in the article's Creative Commons license, unless indicated otherwise in a credit line to the material. If material is not included in the article's Creative Commons license and your intended use is not permitted by statutory regulation or exceeds the permitted use, you will need to obtain permission directly from the copyright holder. To view a copy of this license, visit <http://creativecommons.org/licenses/by/4.0/>.

© The Author(s) 2021

Supplementary Information

Cnidarian-bilaterian comparison reveals the ancestral regulatory logic of the β -catenin dependent axial patterning

Tatiana Lebedeva, Andrew J. Aman, Thomas Graf, Isabell Niedermoser, Bob Zimmermann, Yulia Kraus, Magdalena Schatka, Adrien Demilly, Ulrich Technau and Grigory Genikhovich

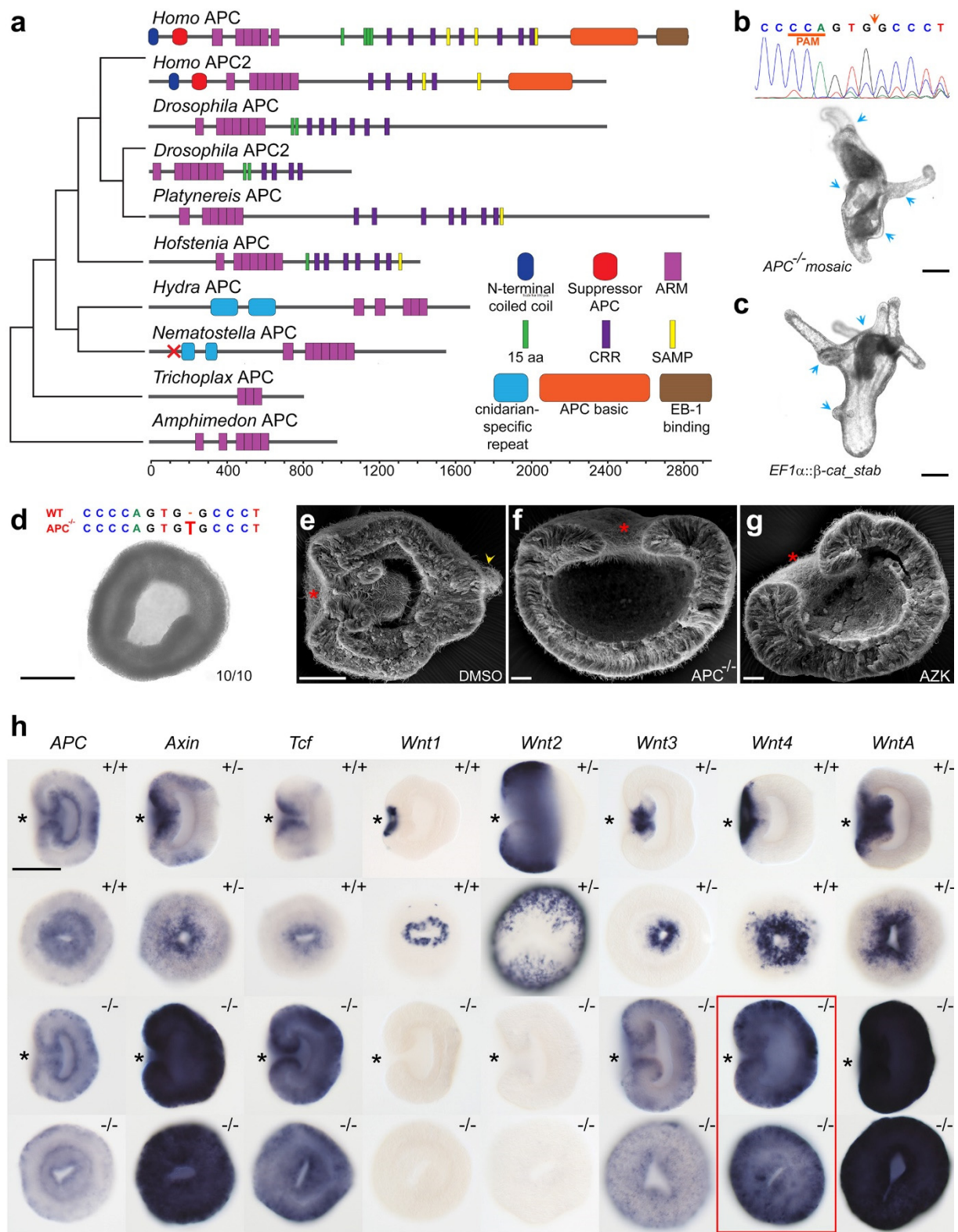
Contents

Supplementary Figures 1-10

Supplementary Results and Discussion 1-3

Supplementary Tables 1-5

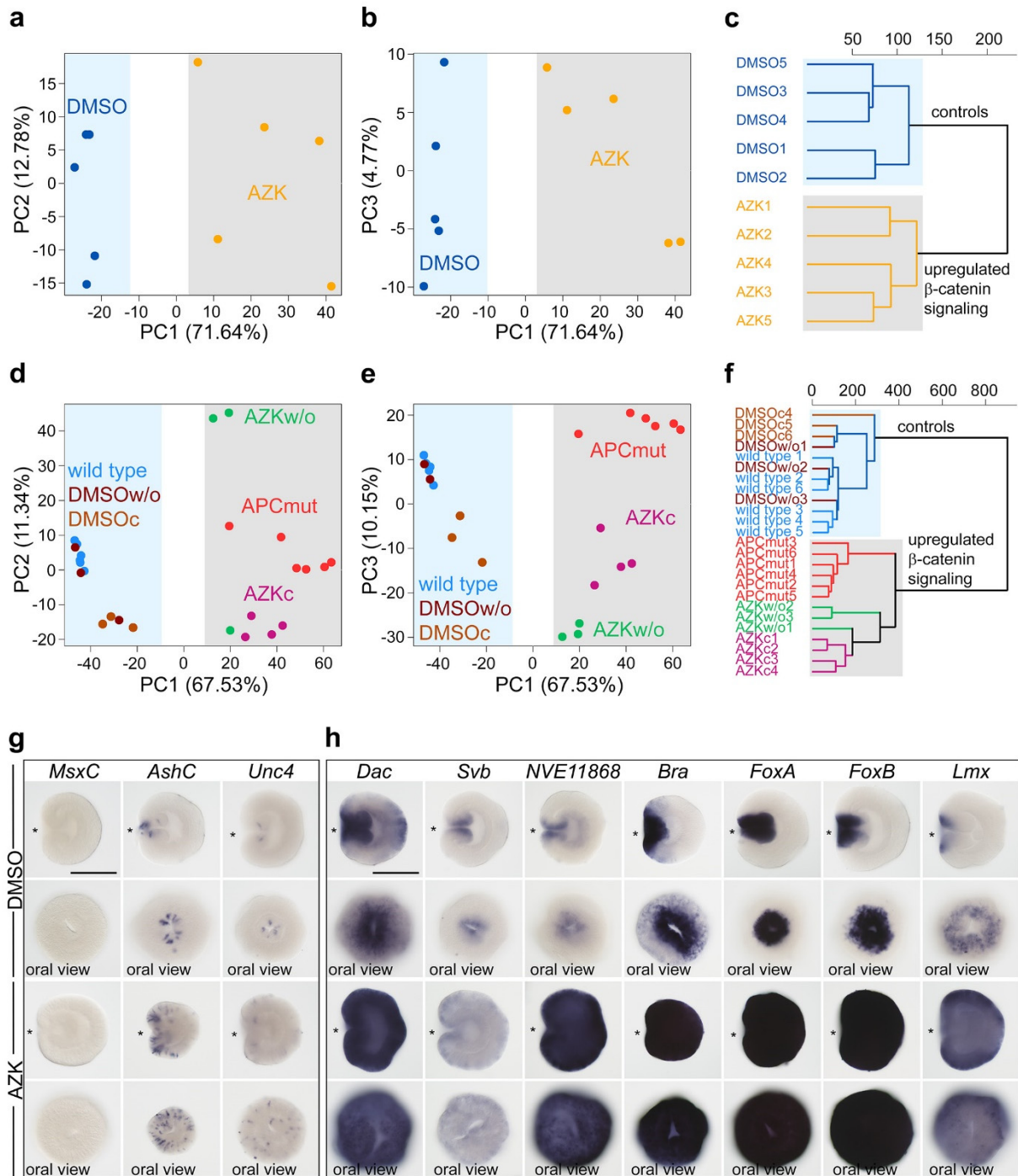
Supplementary References



Supplementary Fig. 1: Characterization of the APC mutants. **a**, SMART annotation¹ of the domain structure of the animal APC proteins. Cnidarian APCs have armadillo repeats (ARM), but appear to be missing the typical 15 and 20 amino acid repeats (15 aa, CRR) present in Bilateria and used for β-catenin binding. SAMP – Axin binding domain. Red cross on the *Nematostella* protein indicates the position of the frameshift mutation. **b**, **c**, Although

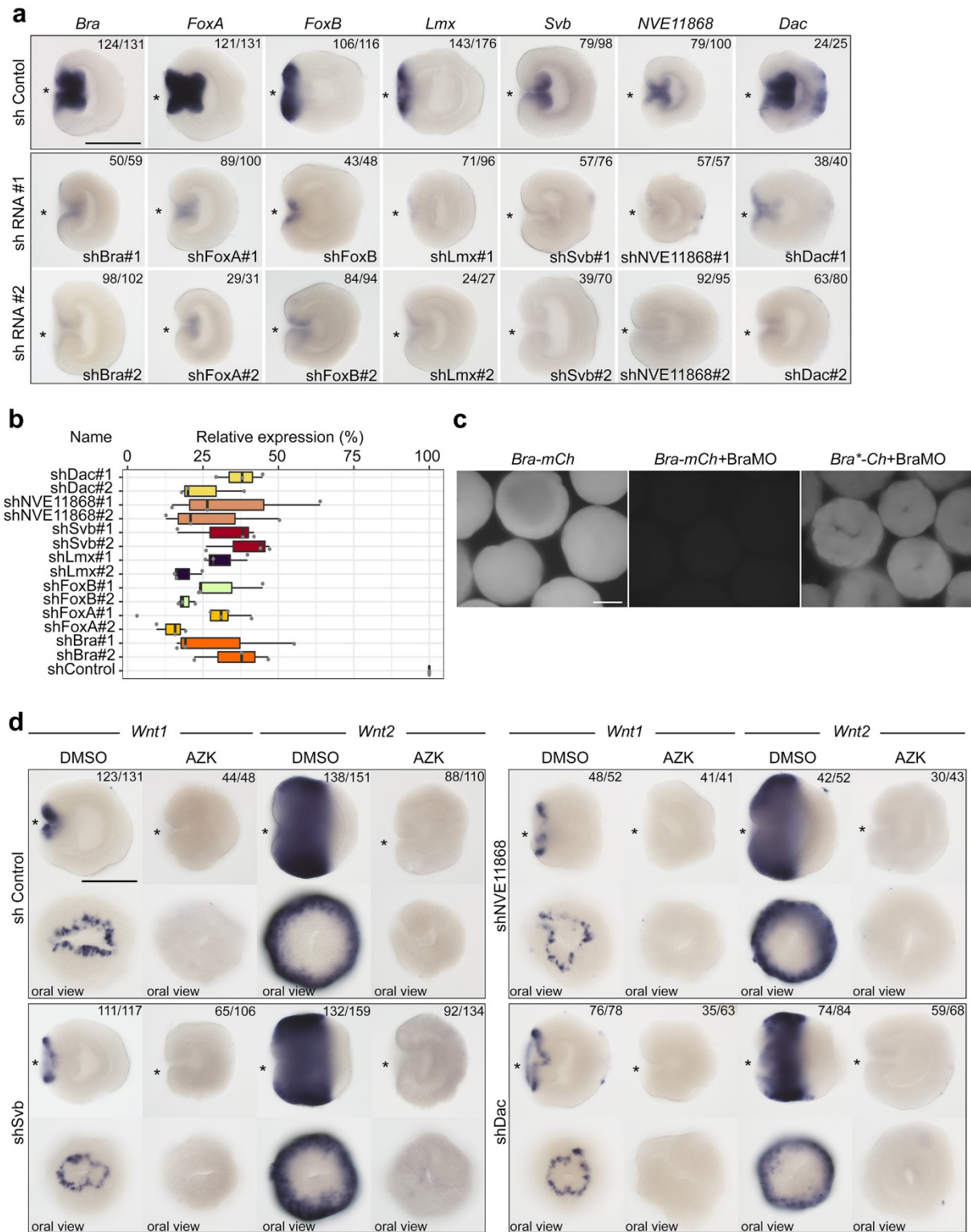
several important domains are missing in the non-bilaterian APC proteins, *Nematostella* APC appears to act via β -catenin. **(b)** Mosaic *APC* mutant develops multiple ectopic oral structures such as mouths and/or tentacles (blue arrows). Upon genotyping of this polyp, the sequencing chromatogram shows the accumulation of extra peaks around the Cas9 cutting site (orange arrow). **(c)** Mosaic expression of the stabilized form of the *Nematostella* β -catenin results in a comparable phenotype. Blue arrows – ectopic oral structures. **d**, Genotyping shows that 10/10 3 dpf F2 embryos demonstrating the oralization phenotype are homozygous *APC* mutants with a T insertion. The image shows a representative *APC* mutant (oral view). **e-g**, SEM image of a control 3 dpf planula **(e)** with an elongated oral-aboral axis, a closed mouth (asterisk), a pharynx, and an apical tuft (arrowhead) compared to a homozygous *APC* mutant **(f)** and an AZK treated embryo **(g)**. The latter two **(f-g)**, show a flattened morphology, no pharynx and a secondarily widely open mouth (asterisk). The representative phenotypes shown on **(e-g)** are observed in all scanned embryos (n>10). **h**, In situ hybridization analysis of *APC* and known “saturating” and “window” genes at the late gastrula stage. Oral views are shown below the corresponding lateral views. The genotype of the embryo is shown in the upper right corner of each photo. +/+ wild type; +/- heterozygous *APC* mutant; -/- homozygous *APC* mutant. *APC* is expressed in the endoderm, the forming pharynx and in a shallow aboral-to-oral gradient in the ectoderm. *Axin* and *Tcf*, in contrast, are expressed in an oral-to-aboral gradient with a second area of stronger expression at the aboral boundary of the midbody domain. *APC* behaves as a saturating gene in the *APC* mutant (just as *Axin*, *Tcf*, *Wnt3* and *WntA* – as previously described for AZK treatments²). *Wnt1* and *Wnt2* behave as window genes in the *APC* mutants and upon AZK treatment². The only discrepancy in the expression behavior was observed in the case of *Wnt4*, which, for a yet unknown reason, behaves as a saturating gene in the *APC* mutant, but as a “window” gene in the AZK² (red frame). Lateral views (oral to the left) and oral views are shown. Asterisks on lateral views indicate the blastopore.

Scale bars: b-d, h – 100 μ m, e – 50 μ m, f-g – 20 μ m.



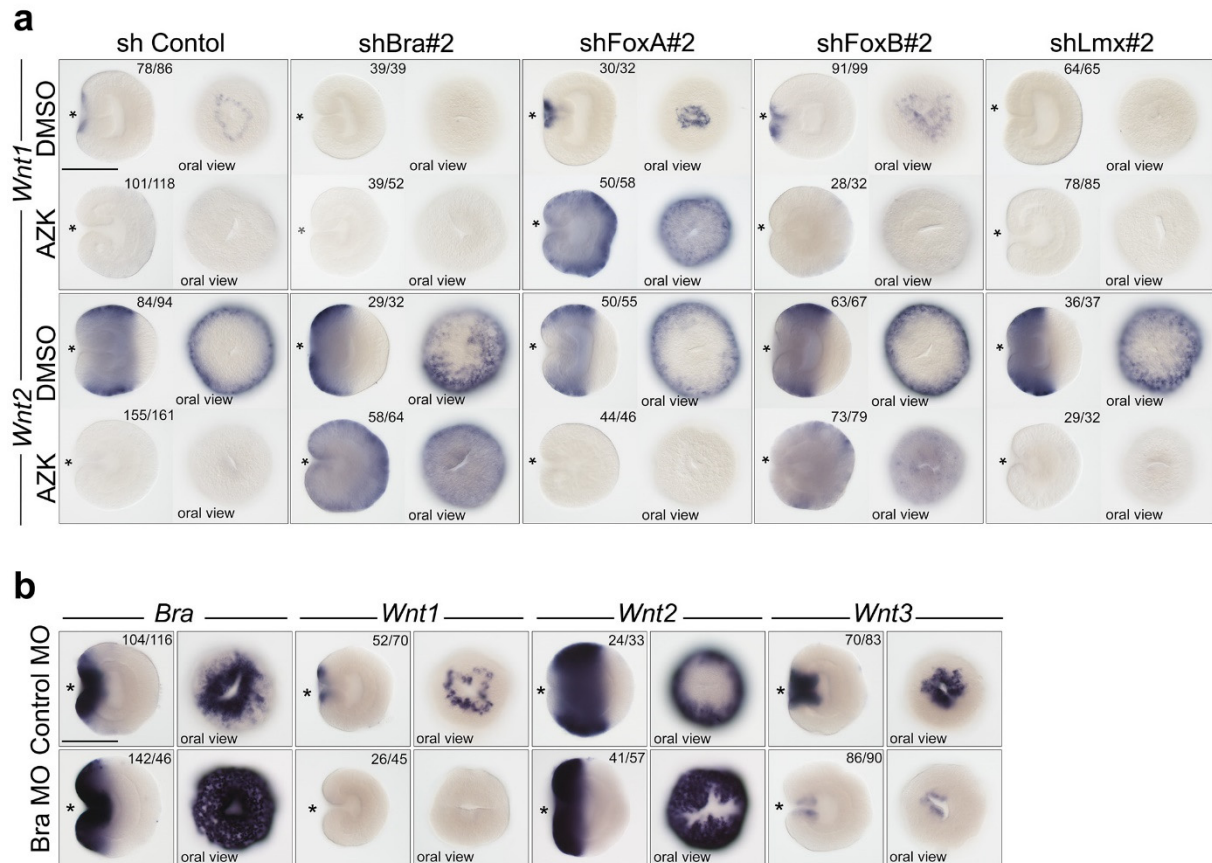
Supplementary Fig. 2: Comparison of transcriptomes after different treatments and expression of the repressor X candidates in DMSO and AZK. a-c, Principle component analysis and a cluster dendrogram clearly separate the transcriptomes of the biological replicates of the AZK treated (grey background) and DMSO treated (blue background) 30 hpf embryos. d-f, Principle component analysis and a cluster dendrogram clearly separate the transcriptomes of the biological replicates of the AZK treated embryos and APC mutants (grey background) versus DMSO treated and untreated wild type (blue background) 3 dpf

embryos. *AZKc* – continuous AZK treatment for 3d, *AZKw/o* – AZK treatment from 10 hpf until 30 hpf followed by a washout for 2 days. **g-h**, Identification of the saturating genes among the ten repressor *X* candidates. *MsxC* is not detectable at 1 dpf, *AshC* and *Unc4* increase their expression in AZK but are expressed in individual cells (**g**). The seven remaining genes display a typical saturating phenotype (**h**). Lateral views (oral to the left) and oral views are shown. Asterisks on lateral views indicate the blastopore. Scale bars 100 μm .

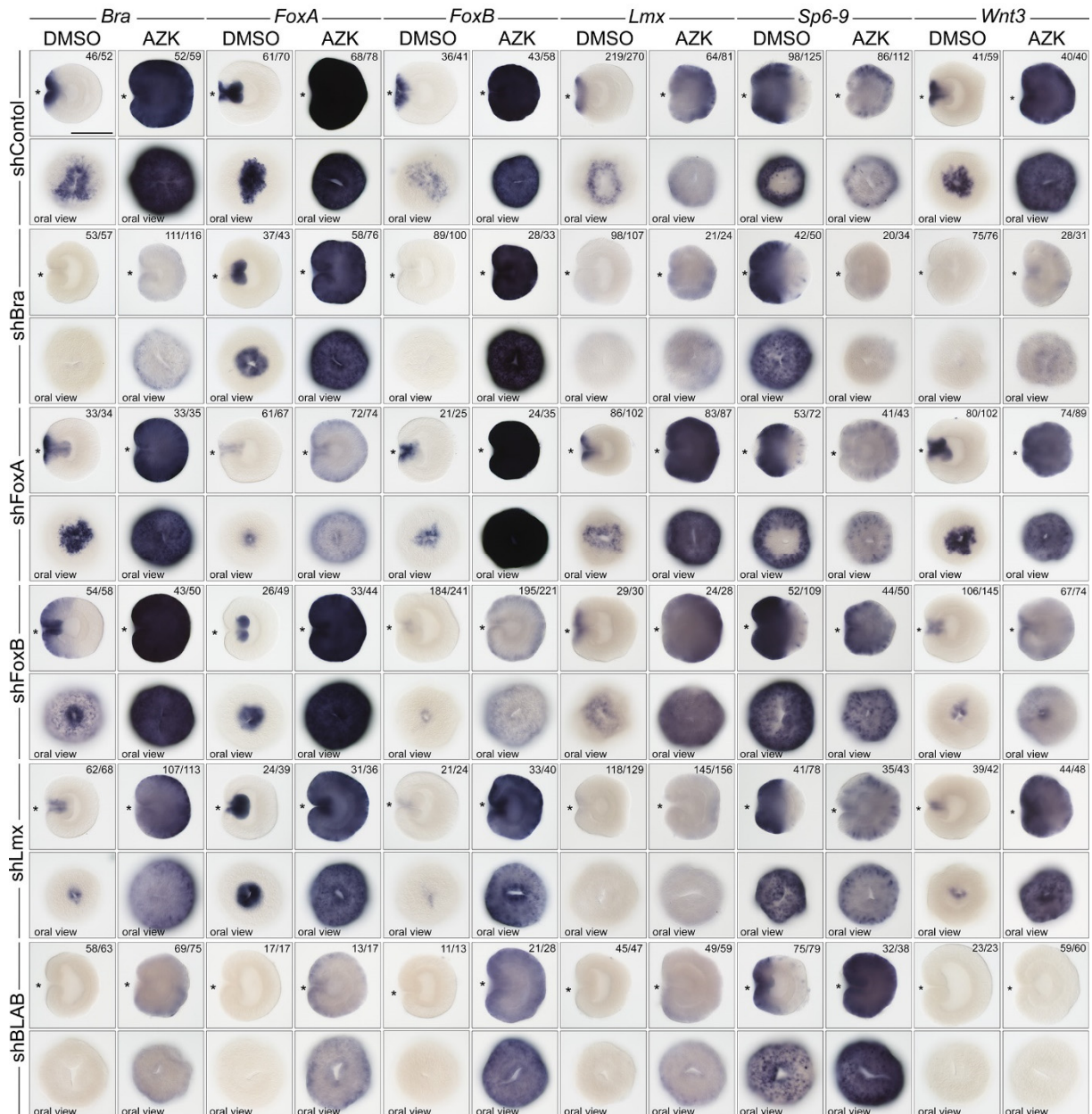


Supplementary Fig. 3: Testing the efficiency of the shRNAs and morpholino, and identification of the three candidates not fulfilling the last repressor X criterion. For each gene, two shRNAs have been selected. For *Bra*, a translation blocking morpholino was used as an alternative means of knockdown (kdn). **a**, In situ hybridization shows reduction in the staining intensity upon shRNA mediated knockdown of the repressor X candidates.

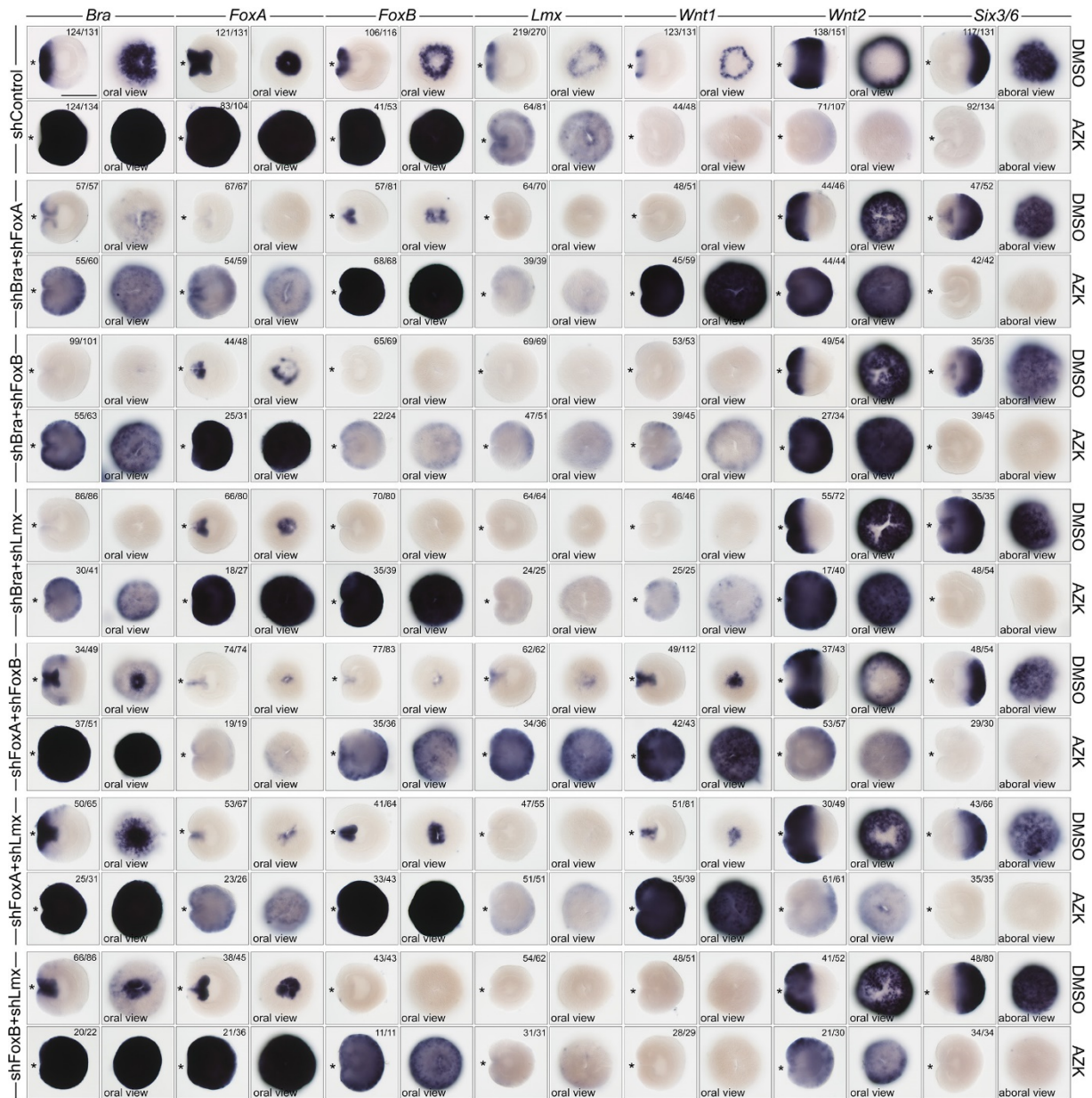
Lateral views (oral to the left) are shown. **b**, qPCR quantification of the knockdown efficiency for shRNAs used on **(a)**. For each shRNA, qPCR was performed on biological triplicates (n=3) except for shFoxA#1 (n=5). The data were normalized to GAPDH expression, and the expression is shown in percent relative to the shControl condition (set to 100%). The box represents the 25-75% interquartile range with the median indicated with the line, the whiskers represent the maximum example within 1.5x the interquartile range. Individual datum point are shown as grey dots. **c**, When co-injected, BraMO binds mRNAs containing BraMO recognition sequence fused to the mCherry coding sequence (*Bra-mCh*) and suppressed its translation. In contrast, no repression of translation is observed when BraMO is coinjected with mRNA containing a 5-mismatch recognition sequence for BraMO fused to the mCherry coding sequence (*Bra*-mCh*), (replicated twice, n>300 in each case). **d**, *Wnt1* and *Wnt2* are expressed normally in DMSO and are not de-repressed in AZK upon *Svb*, *NVE11868* and *Dac* knockdown, which eliminates these transcription factors from the list of the potential repressor X candidates. Lateral views (oral to the left) and oral views are shown. Asterisks on lateral views indicate the blastopore. On **(a)** and **(d)**, the numbers in the top right corner show the ratio of embryos displaying the phenotype shown on the image to the total number of embryos treated and stained as indicated on the figure. Scale bars 100 μ m.



Supplementary Fig. 4: Effects of second shRNAs and of the Bra morpholino. **a**, The effects of the second shRNAs against repressor X candidates on *Wnt1* and *Wnt2* expression are similar to the effects of the first shRNA. Compare to Fig. 3 in the main text. **b**, Injection of BraMO has a similar effect on *Wnt1*, *Wnt2* and *Wnt3* expression as shBra. In contrast, *Bra* expression is clearly upregulated upon BraMO injection suggesting a negative feedback loop. The numbers in the top right corner show the ratio of embryos displaying the phenotype shown on the image to the total number of embryos treated and stained as indicated on the figure. Scale bars 100 μ m.

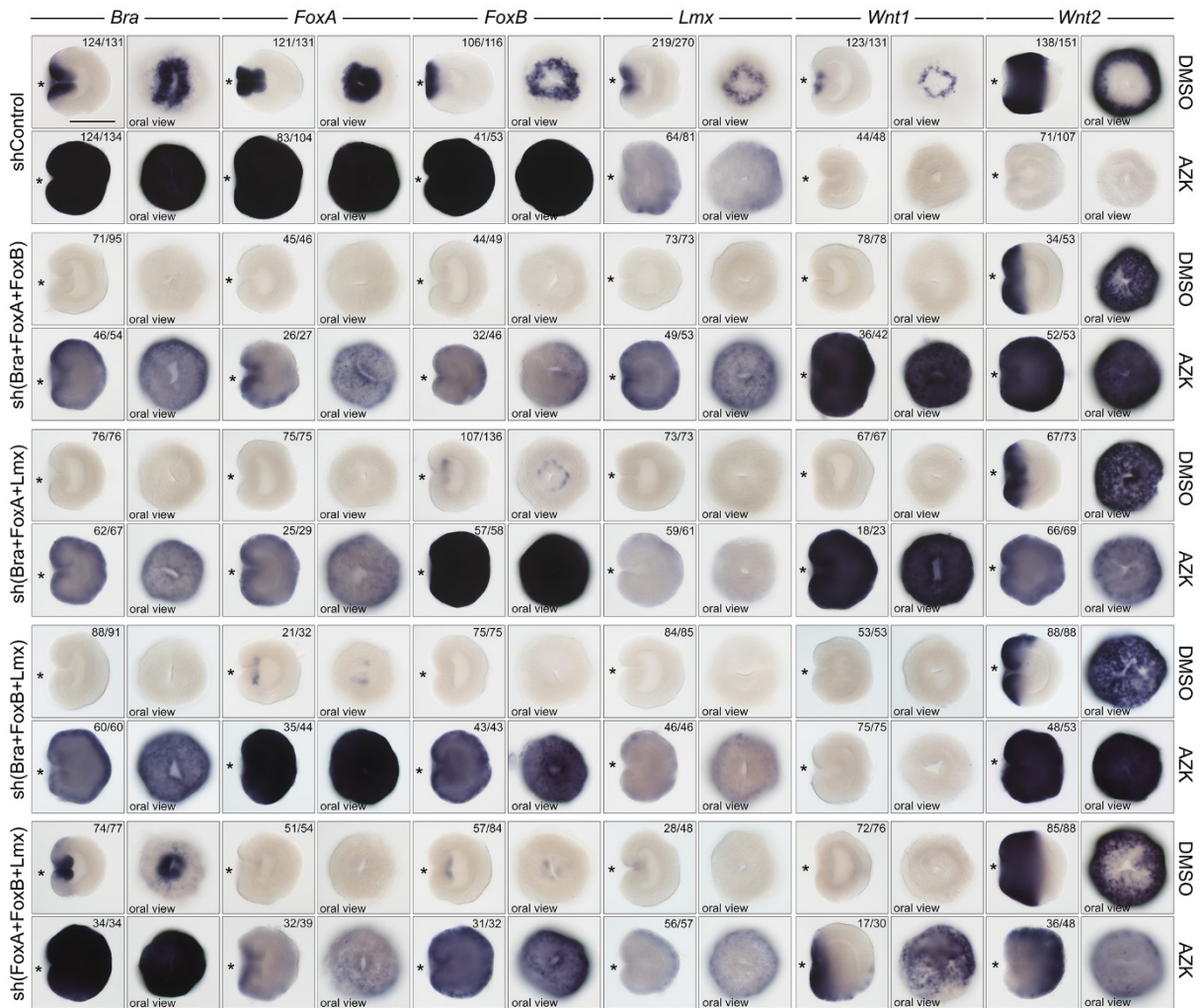


Supplementary Fig. 5: Effects of the individual knockdowns and of the simultaneous knockdown of all four repressor X candidates on their own expression, and on the expression of *Sp6-9* and *Wnt3*. The same shRNAs as on Fig. 3 are used. Lateral views (oral to the left) and oral views are shown. Asterisks on lateral views indicate the blastopore. The numbers in the top right corner show the ratio of embryos displaying the phenotype shown on the image to the total number of embryos treated and stained as indicated on the figure. Scale bar 100 μ m. For interpretation, see main text and Supplementary Results and Discussion 1.

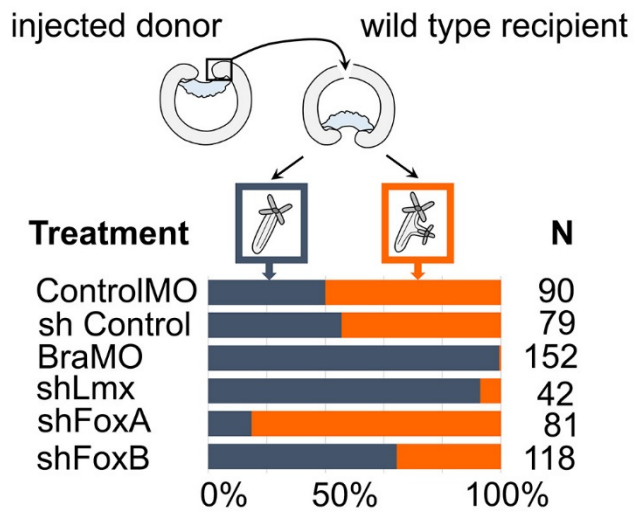


Supplementary Fig. 6: Effects of the double knockdowns of all possible combinations of the four repressor X candidates on their own expression and on the expression of *Wnt1*, *Wnt2*, and of the aboral marker *Six3/6*.

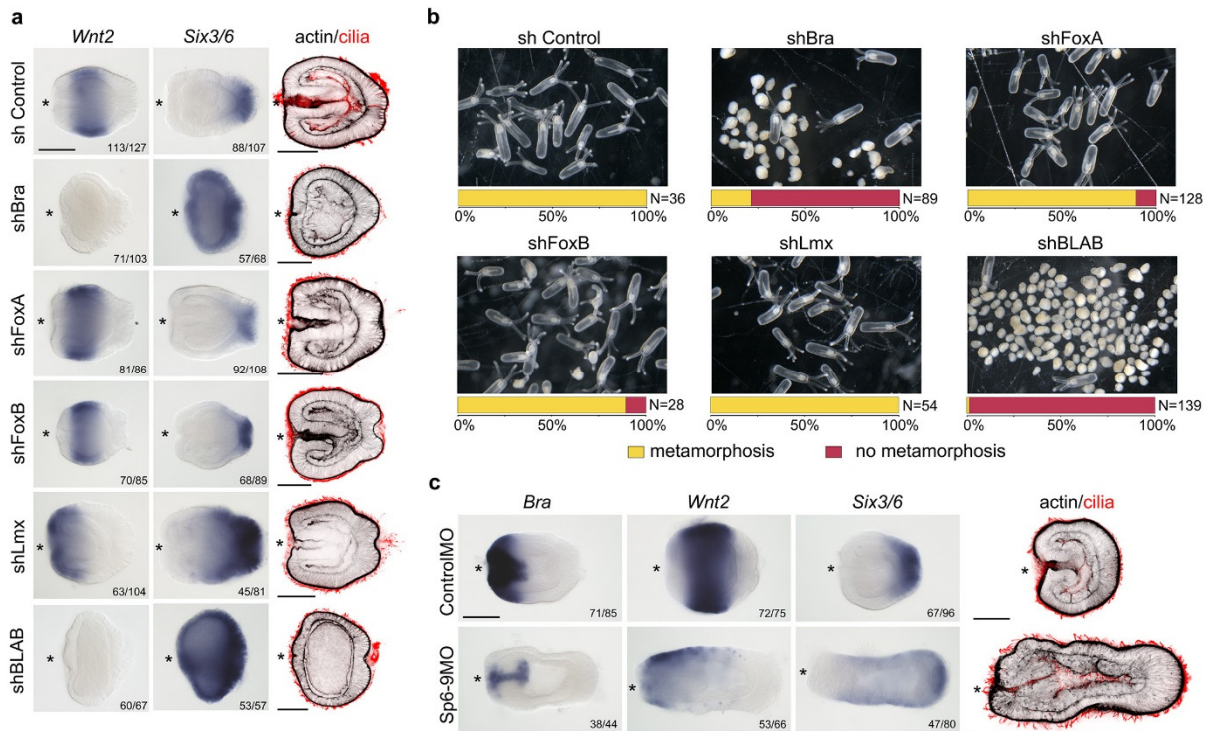
Lateral views (oral to the left) and oral views are shown. For interpretation, see main text and Supplementary Results and Discussion 1. Note oral expansion of *Six3/6* upon knockdowns with shRNA combinations containing *Lmx* and, especially, *Bra*. *Bra* knockdown also leads to the expression of *Six3/6* at the bottom of the pharynx. The numbers in the top right corner show the ratio of embryos displaying the phenotype shown on the image to the total number of embryos treated and stained as indicated on the figure. Scale bar 100 μm .



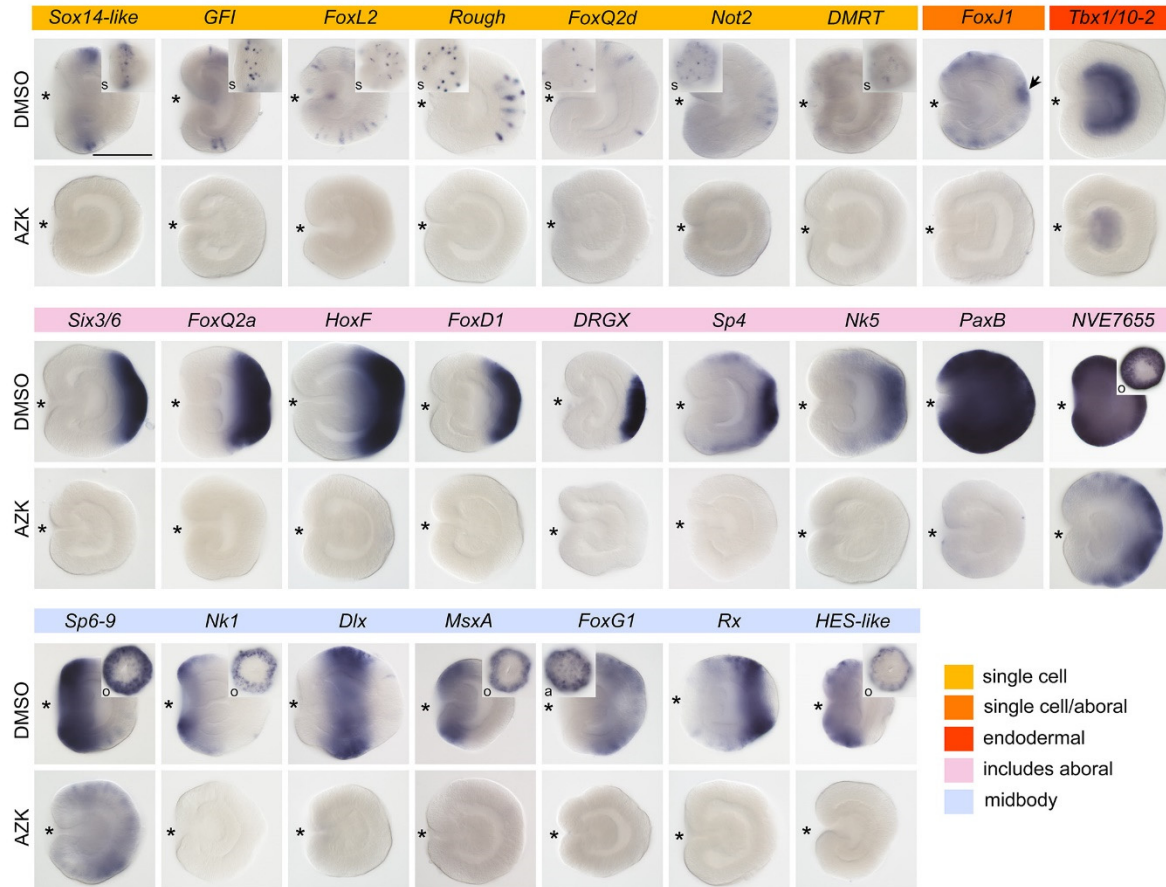
Supplementary Fig. 7: Effects of the tripple knockdowns of all possible combinations of the four repressor X candidates on their own expression and on the expression of *Wnt1* and *Wnt2*, and the results of the blastopore lip transplantation experiments. Effects of the triple knockdowns of all possible combinations of the four repressor X candidates on their own expression and on the expression of *Wnt1*, and *Wnt2*. Lateral views (oral to the left) and oral views are shown. The numbers in the top right corner show the ratio of embryos displaying the phenotype shown on the image to the total number of embryos treated and stained as indicated on the figure. Scale bar 100 μ m. For interpretation, see main text and Supplementary Results and Discussion 1.



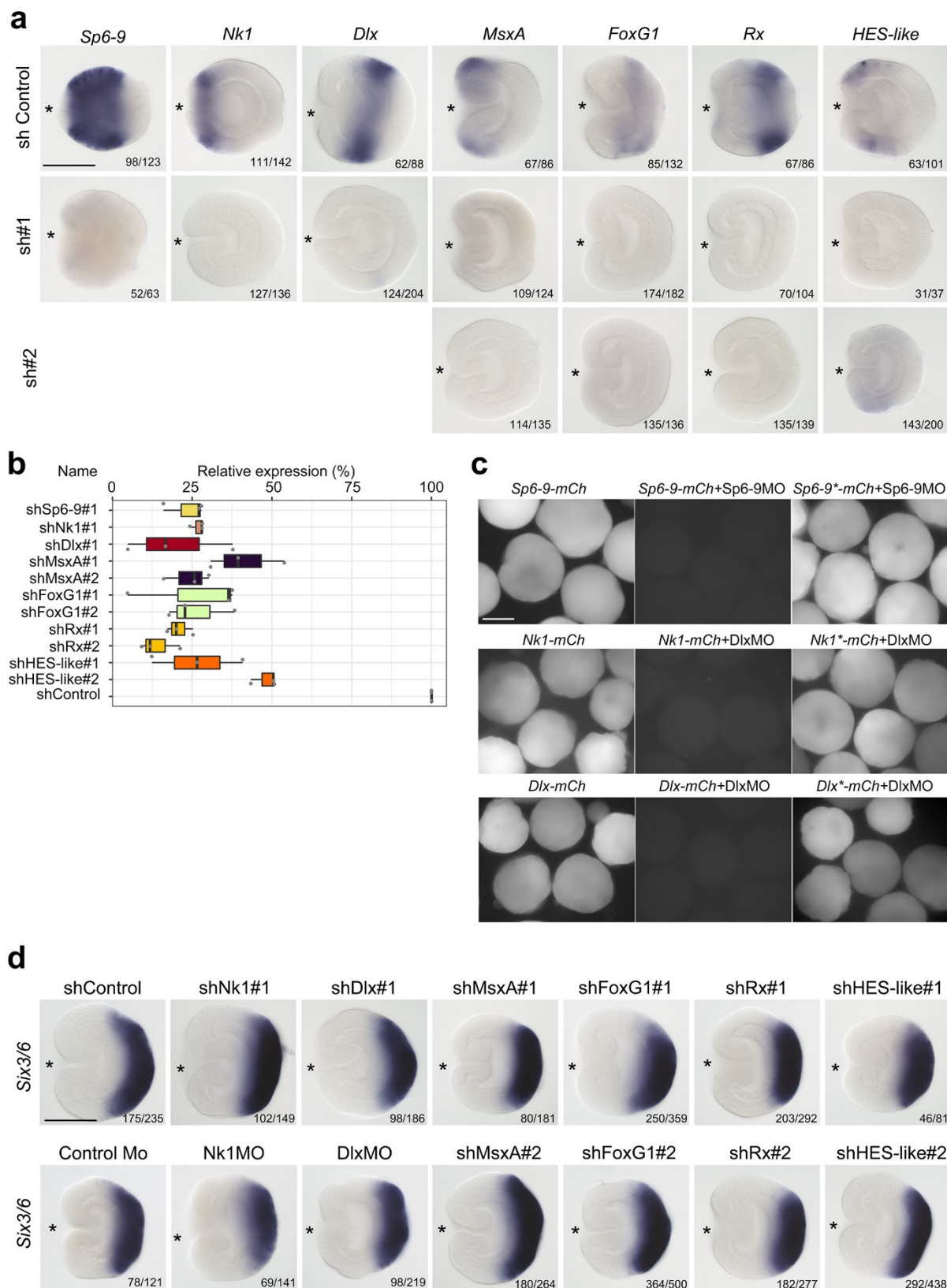
Supplementary Fig. 8: Effect of the knockdown of repressor X candidates on the inductive capacity of the blastopore lip. The ectopic axis induction capacity of the blastopore lip fragment increases drastically if *FoxA* is knocked down in the donor and sinks if *Bra* or *Lmx* expression in the donor is suppressed.



Supplementary Fig. 9: Effect of the Bra, FoxA, FoxB, Lmx and Sp6-9 knockdown on later development. **a**, *Wnt2* and *Six3/6* expression and morphology (F-actin is stained with phalloidin, cilia are stained with anti-acetylated Tubulin antibody) of 4 day old knockdown embryos. shBra and especially shBLAB embryos are strongly aboralized with the oral and the midbody domain as well as mouth and pharynx disappearing. shLmx embryos are mildly aboralized with the *Wnt2* expression shifted orally and *Six3/6* expression domain expanded but with no obvious effect on the morphology. shFoxA and shFoxB embryos appear normal. **b**, The proportion of metamorphosis by 10 days post fertilization. shFoxA, shFoxB and shLmx embryos are able to compensate for the effect of the knockdown and metamorphose normally. In shBra (19/89) and especially in shBLAB (2/139), metamorphosis is impaired. **c**, *Bra*, *Wnt2* and *Six3/6* expression and morphology of the 3 day old Sp6-9 knockdown embryos. The embryos are elongated and severely aboralized. On **(a)** and **(c)**, the numbers in the bottom right corner show the ratio of embryos displaying the phenotype shown on the image to the total number of embryos treated and stained as indicated on the figure. Scale bars 100 μ m.

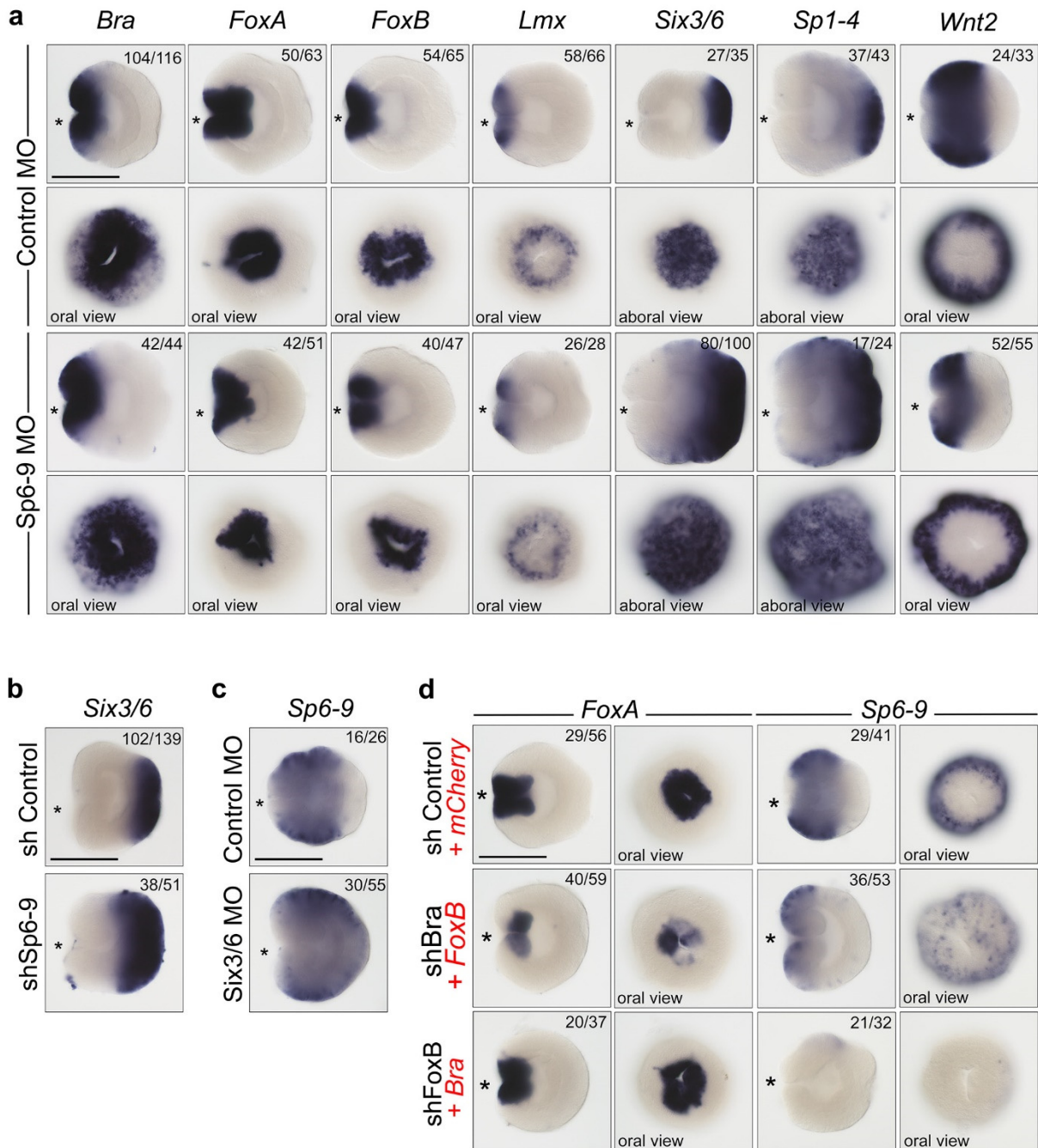


Supplementary Fig. 10: Expression of 25 transcriptional repressor Y candidates. All 25 are downregulated in AZK. Different expression groups are color-coded. Scale bar 100 μ m.



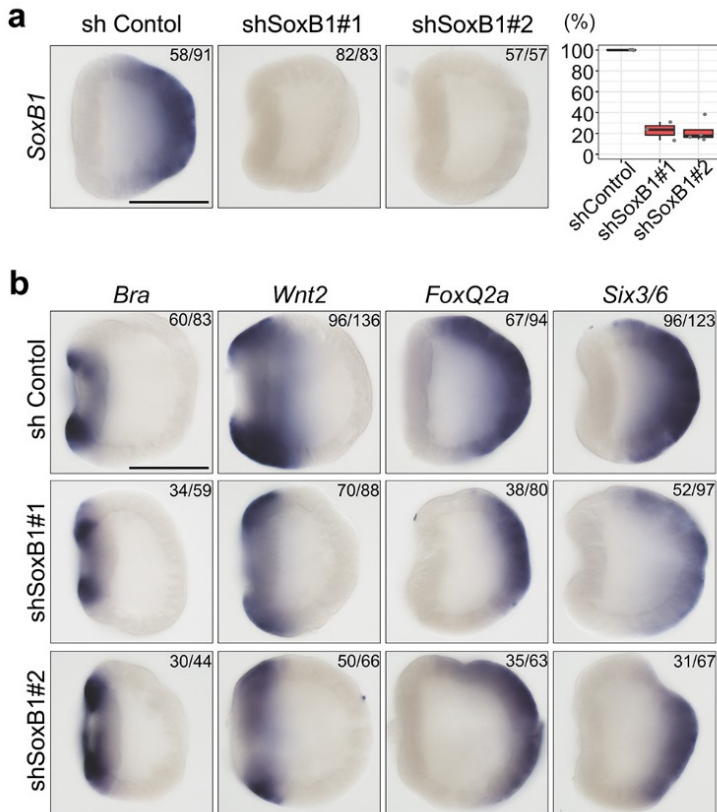
Supplementary Fig. 11: Testing the efficiency of the shRNAs and morpholinos, and identification of the six candidates not fulfilling the last repressor Y criterion. For each gene except for *Sp6-9*, *Nk1* and *Dlx*, two shRNAs have been selected. For *Sp6-9*, *Nk1* and *Dlx*, translation blocking morpholinos were used as an alternative means of knockdown (kdn)

since no second functional shRNA could be found. **a**, In situ hybridization shows reduction in the staining intensity upon shRNA mediated knockdown of the repressor Y candidates. Lateral views (oral to the left) are shown. **b**, qPCR quantification of the knockdown efficiency for shRNAs used on **(a)**. For each shRNA, qPCR was performed on biological triplicates (n=3). The data were normalized to GAPDH expression, and the expression is shown in percent relative to the shControl condition (set to 100%). The box represents the 25-75% interquartile range with the median indicated with the line, the whiskers represent the maximum example within 1.5x the interquartile range. Individual datum point are shown as grey dots. **c**, When co-injected with mRNAs containing their respective recognition sequences fused to the mCherry coding sequence (*Sp6-9-mCh*, *Nk1-mCh*, *Dlx-mCh*), Sp6-9MO, Nk1MO and DlxMO bind and suppress their translation. In contrast, no repression of translation is observed when Sp6-9MO, Nk1MO and DlxMO are coinjected with mRNAs containing their 5-mismatch recognition sequences fused to the mCherry coding sequence (*Sp6-9*-mCh*, *Nk1*-mCh*, *Dlx*-mCh*). Replicated twice, n>300 in each case. **d**, *Six3/6* is expressed normally upon shRNA- or MO-mediated knockdown of six out of seven repressor Y candidates . Lateral views (oral to the left) and oral views are shown. On **(a)** and **(c)**, the numbers in the bottom right corner show the ratio of embryos displaying the phenotype shown on the image to the total number of embryos treated and stained as indicated on the figure. Asterisks on lateral views indicate the blastopore. Scale bars 100 μ m.



Supplementary Fig. 12: Functional analysis of *Sp6-9* and rescue experiments with *Bra* and *FoxB*. **a**, *Sp6-9*MO does not affect *Bra*, *FoxA*, *FoxB* and *Lmx* expression. *Wnt2* ring becomes narrower, while *Six3/6* and *Sp1-4* expression domains expand orally. **b**, sh*Sp6-9* affects *Six3/6* expression in the same way as the *Sp6-9*MO. **c**, *Six3/6*MO injection leads to aboral expansion of *Sp6-9*. **d**, Effects of the co-injection of the indicated shRNA (black letters) and mRNA (red letters). Ubiquitous *Bra* expression compensates for the lack of *FoxB* and rescues *FoxA* in its normal domain without causing ectopic overexpression. In contrast, *FoxB* mRNA does not rescue the sh*Bra* effect on *FoxA* expression. *Bra* overexpression abolishes *Sp6-9* irrespective of the lack of *FoxB*, while *FoxB* overexpression makes the sh*Bra*

effect on *Sp6-9* milder without alleviating it completely (weaker *Sp6-9* expression with a milder oral expansion in comparison to shBra alone). Lateral views (oral to the left) and oral views are shown. See Supplementary Fig. 5 for the shBra and shFoxB knockdown phenotypes. The numbers in the top right corner show the ratio of embryos displaying the phenotype shown on the image to the total number of embryos treated and stained as indicated on the figure. Scale bars 100 μ m.



Supplementary Fig. 13: *SoxB1* is repressed in the midbody domain and does not seem to be the critical regulator of *Six3/6* and *FoxQ2a* expression. a, *SoxB1* is efficiently knocked down by two independent shRNAs, as demonstrated by in situ hybridization and qPCR (n=3; the box represents the 25-75% interquartile range with the median indicated with the line, the whiskers represent the maximum example within 1.5x the interquartile range. Individual datum point are shown as grey dots). b, *SoxB1* knockdown does not affect the expression of oral and midbody markers *Bra* and *Wnt2*, and appears to slightly reduce the expression of the aboral markers *Six3/6* and *FoxQ2a* at the 18 hpf pregastrula stage. The numbers in the top right corner show the ratio of embryos displaying the phenotype shown on the image to the total number of embryos treated and stained as indicated on the figure. Scale bars 100 μ m.

Supplementary Results and Discussion

1. Topology of the gene regulatory network

In order to understand the genetic interactions between the four factor X candidates we analyzed their expression in individual, double, triple and quadruple knockdowns (Supplementary Fig. 5-7). While identification of the exact topology of this network requires stage-by-stage ChIP data for all the transcription factors from the onset of their expression until late gastrula, we can suggest a possible topology based on genetic interactions. Upon shRNA mediated knockdown of *Bra*, *FoxB* and *Lmx* become abolished. *FoxA* expression is confined to the bottom of the forming pharynx, where *Bra* is not expressed, suggesting that Bra activates the expression of these three genes in the area where they are normally co-expressed with *Bra* (Supplementary Fig. 5). The effect of *Bra* knockdown on *Bra* expression is more complex: while shRNA-mediated knockdown reduces the amount of *Bra* mRNA (Supplementary Fig. 5), the translation blocking morpholino-mediated knockdown of *Bra* upregulates the expression of *Bra* gene (Supplementary Fig. 4b). The most likely explanation for this is that Bra protein may act as a transcriptional repressor of the *Bra* gene. In contrast, the effects of the shRNA-mediated and morpholino-mediated knockdown of *Bra* on *Wnt1*, *Wnt2*, and *Wnt3* expression are essentially the same (Fig. 3, Supplementary Figs. 4-5). While *Wnt2* clearly appears to be de-repressed by *Bra* knockdown, the expression *Wnt1* and *Wnt3* becomes abolished in DMSO and in AZK (Fig. 3, Supplementary Fig. 5). Interestingly, *Wnt1* is expressed in AZK in quadruple knockdowns (Fig. 3) and in triple knockdowns, whenever shFoxA is used (Supplementary Fig. 7a). Thus, the regulation of *Wnt1* by β -catenin may still be direct. *Wnt3*, in contrast, is abolished in AZK in quadruple knockdowns (Supplementary Fig. 5b). This suggests that *Wnt3* is either regulated by β -catenin indirectly via Bra and FoxB, or that a yet unidentified “window” transcriptional repressor normally preventing aboral expansion of the *FoxA/Wnt1/Wnt3* boundary (Fig. 2) becomes de-repressed in AZK upon quadruple knockdown and suppresses *Wnt3* (just like *Wnt2* becomes de-repressed in shBLAB and expands orally).

According to double and triple knockdowns followed by AZK treatment, *Bra*, *FoxB*, *Lmx* and *FoxA* are likely to be direct β -catenin targets (Supplementary Fig. 6-7). Upon individual *FoxB* shRNA knockdown, in DMSO, the ring of *Wnt1* concentrates around the blastopore opening and appears weaker, and in AZK, *Wnt1* expression expands aborally but remains weak and absent in blastopore lips (Fig. 3). *Wnt2* expression in *FoxB* knockdown is slightly expanded

orally in DMSO and globally in AZK, but also remains weak (Fig. 3). This is strikingly similar to the effects we documented in wild type embryos treated with lower concentrations of AZK². The effect of its knockdown on the expression of the *Wnt* genes suggests that FoxB might act as an enhancer of Bra and FoxA activity. The role of *Lmx* is also not fully clear, since the effect of its knockdown on *Wnt1* and *Wnt2* seems to be weaker but similar to the effect of the *Bra* knockdown (Fig. 3), suggesting that Bra and Lmx proteins might cooperate in regulating the same targets. The only observable difference is that *Lmx* is not co-expressed with *Wnt3* (Fig. 2), which is localized to the *FoxA/Bra* co-expression domain, and *Lmx* knockdown does not abolish *Wnt3* expression (Supplementary Fig. 5). The role of Lmx and FoxB appears to be in supporting the expression and function of *Bra* in their respective co-expression domains (Fig. 2, Supplementary Fig. 5-7, see also main text), while strong FoxA appears to suppress *Bra* expression in the absence of FoxB (i.e. at the bottom of the pharynx, Supplementary Fig. 5). Similar expression of *Bra* upon single knockdown of *FoxB* (Supplementary Fig. 5), double knockdown of *FoxB+Lmx* or *FoxB+FoxA* (Supplementary Fig. 6), and triple knockdown of *FoxB+FoxA+Lmx* (Supplementary Fig. 7) points towards the critical role of FoxB in maintaining the normal domain of strong *Bra* expression. One yet unclear effect is the nearly normal expression of *Bra* (normal domain plus bottom of the pharynx) and upregulation of *FoxB* upon double knockdown of *Lmx* and *FoxA* (Supplementary Fig. 6), although single knockdowns of these genes reduced *Bra* expression restricting it to the bottom of the pharynx (Supplementary Fig. 5). In spite of the effects of the *FoxB* knockdown and the *Bra* knockdown on *FoxA* expression being highly similar (expression is confined to the bottom of the pharynx, Supplementary Fig. 5), overexpression of *FoxB* in the shBra background does not rescue the *FoxA* phenotype (Supplementary Fig. 12d). In contrast, overexpression of *Bra* mRNA in the shFoxB background completely rescues the shFoxB effect on *FoxA* without inducing *FoxA* expression outside of its normal domain (Supplementary Fig. 12d). The lack of ectopic expression of *FoxA* upon *Bra* overexpression suggests that the genes encoding transcription factors repressing *FoxA* aborally are not under Bra control. Identical effects of *Bra*, *FoxB* and *Lmx* knockdowns on the expression of the midbody marker *Sp6-9* (Supplementary Fig. 5) suggest that these factors might co-operate in preventing the oral expansion of the expression domain of this gene. However, Bra is clearly the key player in this inhibition: co-injection of shBra with *FoxB* mRNA does not fully suppress *Sp6-9* expression, although *Sp6-9* appears to be much weaker than in control, and its oral expansion appears to be less pronounced in comparison to the shBra alone (compare Supplementary Fig. 5 and Supplementary Fig. 12d). In contrast, co-

injection of shFoxB with *Bra* mRNA drastically reduces *Sp6-9* expression (Supplementary Fig. 12d). Notably, *Sp6-9* knockdown does not cause aboral expansion of *Bra*, *FoxA*, *FoxB* and *Lmx* (Supplementary Fig. 12a), suggesting that they may be suppressed by the yet unidentified midbody genes. Similarly, it is unclear what prevents aboral expansion of the other oral markers expressed in concentric rings, e.g. *Wnt1*, *Wnt3*, *Wnt4* and *WntA* (see Fig. 2). In contrast, *Sp6-9* clearly prevents oral expansion of the aborally expressed *Six3/6*, *Sp1-4* and *SoxB1* (Figs. 4c and 5c; Supplementary Fig. 12a-b). Conversely, *Six3/6* knockdown results in the aboral expansion of *Sp6-9* (although the penetrance is not too high at 55%, N=55) (Supplementary Fig. 12c). Since the suppression of *Sp6-9* alone does not result in the aboral expansion of *Bra*, it is clear that some yet unidentified factors are involved in preventing aboral expansion of the oral and midbody genes. The deduced topology of the genetic interactions in this GRN is summarized in the Fig. 6a.

2. Knockdown of the four oral TFs affects de novo axis formation but not the normal gastrulation

Our analysis of the effects of the knockdowns of the four transcription factors defining oral identity in *Nematostella* provided another highly surprising result. Although gastrulation in *Nematostella* is abolished by β -catenin morpholino³, and ectodermal co-expression of *Wnt1* and *Wnt3* is sufficient to induce axis and germ layer formation at any position in the embryo^{2,4}, neither individual knockdowns nor the quadruple knockdown of *Bra*, *Lmx*, *FoxA* and *FoxB*, affected the process of gastrulation in any detectable way. This was unexpected, since *Bra* knockdown abolishes both *Wnt1* and *Wnt3*, and *Lmx* knockdown abolishes *Wnt1* (Fig. 3; Supplementary Fig. 5). In order to address this discrepancy, we tested whether the expression of our four candidate transcription factors affects ectopic axis induction by blastopore lip transplantation (Supplementary Fig. 8). We predicted that if any of these molecules were necessary for axis induction, their loss from the donor blastopore lip tissue would abolish its inductive potential. Indeed, the knockdowns of *Bra* and *Lmx* nearly abolished the inductive capacity of the blastopore lip when compared to the transplantations from Control MO or shControl injected embryos (Z-test, $p < 1e-5$ in both cases), and *FoxB* knockdown significantly reduced it (Z-test, $p < 0.01$). This latter effect might be due to the reduced *Wnt1* and *Wnt3* expression in shFoxB embryos (Fig. 3, Supplementary Fig. 5). In contrast, the knockdown of *FoxA*, which appears to be the transcriptional repressor of *Wnt1*, strongly increased induction efficiency (Z-test, $p < 1e-5$). This suggests that all these factors affect the ectopic axis and germ

layer formation, while normal gastrulation in the embryo relies primarily on maternally deposited determinants.

3. Effects of the *Bra*, *FoxA*, *FoxB*, *Lmx* and *Sp6-9* knockdown on later development

We then asked what the effects of the knockdowns of the four oral TFs were in terms of later development. Since most of the orally expressed marker genes appeared to be controlled by *Bra* at the gastrula stage, we focused on analyzing the expression of the midbody and the aboral ectoderm markers *Wnt2*, and *Six3/6*, general morphology and percentage of metamorphosis. Among the sh*Bra*, sh*FoxA*, sh*FoxB*, sh*Lmx*, and shBLAB, only sh*Bra* and shBLAB showed a strong aboralization phenotype by 4 dpf (late planula larva) (Supplementary Fig. 9a). Marker gene expression upon individual knockdown of other three genes appeared either normal in sh*FoxA* and sh*FoxB* or aboralized in sh*Lmx*, with *Wnt2* and *Six3/6* expression expanding orally in more than 50% of the embryos. However, morphologically, sh*FoxA*, sh*FoxB*, and sh*Lmx* knockdown embryos appeared normal for their developmental stage (Supplementary Fig. 9a). The aboralization of shBLAB embryos was similar but always more pronounced than that of the sh*Bra* embryos. These embryos appeared shorter than controls, they lacked mouths and pharynges, and their endoderm partitioning was missing or heavily disrupted. At the molecular level, the midbody marker *Wnt2* was abolished, which is different from the situation in the gastrula, and may be due to the fact that *Bra* is a positive regulator of the oral Wnt genes (e.g. *Wnt1* and *Wnt3*, see Fig. 3, Supplementary Fig. 5). Consistent with the loss of the oral and the midbody domain, the aboral marker *Six3/6* was ubiquitously expressed (Supplementary Fig. 9a). This is reflected by the percentage of the knockdown embryos capable of undergoing metamorphosis (scored at 10 dpf). In contrast to shControl injected embryos (100% metamorphosis, N=36), sh*FoxA* injected embryos (89% metamorphosis, N=128), sh*FoxB* injected embryos (89% metamorphosis, N = 28) and sh*Lmx* injected embryos (100% metamorphosis, N=54), only 21% (N=89) of the sh*Bra* injected and 1% (N=139) of the shBLAB injected embryos underwent metamorphosis and formed primary polyps (Supplementary Fig. 9b). Normal gastrulation followed by the loss of the pharynx and the disappearance of the *Wnt2* transcript at later developmental stages is consistent with the previously reported results of the CRISPR/Cas9-mediated excision of *Bra* locus by simultaneous use of 5 non-overlapping gRNAs in F0⁵. The fact that sh*Bra* and shBLAB embryos survived until 10 dpf and had an

uncompartmentalized but otherwise more or less normally looking endoderm (Supplementary Fig. 9a) suggests that the death of the embryos by day 4 reported previously⁵ may have been caused by some unaccounted for off-target action of the gRNAs rather than by the lack of pharynges, as it was suggested.

We then tested late developmental effects of the *Sp6-9* knockdown on the morphology and expression of the oral ectoderm marker *Bra*, midbody marker *Wnt2* and aboral marker *Six3/6*. By 3 dpf, the injection of the *Sp6-9* morpholino resulted in the formation of worm-like embryos with a shortened oral and strongly elongated aboral domain and non-compartmentalized endoderm. The expression of the oral marker *Bra* and the midbody marker *Wnt2* was reduced, and *Six3/6* was significantly expanded orally (Supplementary Fig. 9c). *Sp6-9* morphant embryos do not undergo metamorphosis and die at some point between 4 and 7 dpf.

Supplementary Table 1: Transcriptional repressor X candidates

GeneID	Curated ID	Fold change				Expression
		3d APCmut vs. WT	3dAZKc vs. DMSO	3dAZKwo vs. DMSO	1dAZK vs. DMSO	
NVE21786*	<i>EIF3C</i>	1.62	1.92	1.50	1.34	not assayed
NVE12602*	<i>ORC1</i>	1.66	1.83	1.64	1.58	not assayed
NVE12977	<i>MsxC</i>	2.08	5.78	4.35	3.99	not expressed
NVE14550	<i>Unc4</i>	17.79	19.23	5.38	2.87	single cells
NVE20732	<i>AshC</i>	13.35	13.70	4.63	3.92	single cells
NVE3568	<i>Brachyury</i>	8.98	9.52	2.97	3.34	oral ectoderm
NVE20630	<i>FoxA</i>	10.05	12.05	5.85	5.45	oral ectoderm
NVE26195	<i>FoxB</i>	45.00	40.00	5.03	4.84	oral ectoderm
NVE16579	<i>Lmx</i>	5.85	4.67	2.59	3.22	oral ectoderm
NVE13527	<i>Shavenbaby</i>	3.04	3.57	4.15	2.08	oral ectoderm
NVE24711	<i>Dachshund</i>	4.52	4.52	4.93	1.99	oral ectoderm
NVE11868	<i>Zn finger protein</i>	12.55	6.99	5.15	3.27	oral ectoderm

* NVE21786 and NVE12602 are greyed out as metabolic enzymes falsely automatically annotated as transcription factors

Supplementary Table 2: Transcriptional repressor Y candidates

GeneID	Curated ID	Fold change				Expression
		3d APCmut vs. WT	3dAZKc vs. DMSO	3dAZKwo vs. DMSO	1dAZK vs. DMSO	
NVE15777	<i>Sox14-like</i>	0.05	0.04	0.02	0.34	single cells
NVE16639	<i>GFI</i>	0.37	0.46	0.39	0.23	single cells
NVE1324	<i>FoxL2</i>	0.06	0.34	0.41	0.57	single cells
NVE21292	<i>Rough</i>	0.10	0.24	0.15	0.35	single cells
NVE17371	<i>FoxQ2d</i>	0.03	0.02	0.02	0.15	single cells
NVE4967	<i>Not2</i>	0.27	0.25	0.14	0.27	single cells
NVE4006	<i>DMRT</i>	0.29	0.39	0.08	0.57	single cells
NVE14608	<i>FoxJ1</i>	0.12	0.18	0.30	0.30	single cells/aboral
NVE8569	<i>TBX1/10-2</i>	0.29	0.37	0.17	0.26	endodermal
NVE12346	<i>Six3/6</i>	0.06	0.04	0.03	0.14	includes aboral
NVE14268	<i>FoxQ2a</i>	0.04	0.02	0.03	0.12	includes aboral
NVE16373	<i>HoxF/Anthox1</i>	0.04	0.03	0.02	0.15	includes aboral
NVE21434	<i>FoxD1</i>	0.09	0.03	0.03	0.04	includes aboral
NVE14554	<i>DRGX</i>	0.11	0.17	0.08	0.08	includes aboral
NVE21395	<i>Sp1-4</i>	0.26	0.12	0.46	0.28	includes aboral
NVE20898	<i>Nk5</i>	0.08	0.08	0.40	0.23	includes aboral
NVE5430	<i>PaxB</i>	0.17	0.27	0.15	0.54	includes aboral
NVE7655*	<i>unknown</i>	0.11	0.11	0.11	0.44	includes aboral
no model	<i>Sp6-9</i>	0.08	0.31	0.24	0.60	midbody
NVE20899	<i>Nk1</i>	0.07	0.28	0.07	0.35	midbody
NVE8363	<i>Dlx</i>	0.25	0.25	0.15	0.37	midbody
NVE20892	<i>MsxA</i>	0.09	0.19	0.10	0.44	midbody
NVE6876	<i>FoxG1</i>	0.04	0.04	0.03	0.13	midbody
NVE21445	<i>Rx</i>	0.04	0.12	0.25	0.31	midbody
NVE14243	<i>HES-like</i>	0.10	0.20	0.26	0.41	midbody

* NVE7655 encodes a long uncharacterized protein, which is probably falsely automatically annotated as a transcription factor

Supplementary Table 3: Short hairpin RNA targets

Name	Targeted sequence
shControl	GCGAGTTCTTCTACAAGGTGA
shBra#2	GAAGAGATCACGAGTCTAA
shBra	GAATCGCACTCAGCTTACT
shFoxA#2	GCAGGTATGCCCATGAATA
shFoxA	GCTCAAGAAATCCAAGGACAA
shFoxB#2	GAGAAGACGAGGATGAACT
shFoxB	GATTCCCTCTCTTCTACA
shLmx#2	GTGTCACATTCTCCGTACAT
shLmx	GCTTGAGTGTAAGAGTGGT
shSvb#2	GAACCTTAGATCGGAGAGA
shSvb	GCTCCGAGAAGAGAATGTT
shNVE11868#2	GAATGACCTTGAGTGAAGA
shNVE11868	GGAGAGAGAGGTAAGTAT
shDac#2	GCAGAACAGCGAGTAACAA
shDac	GACTCTACTGAGGAACATA
shSp6-9	GCTTGAGGGATCGACTTCA
shSoxB1	GCAGCACAGTCCTTTAATA
shSoxB1#2	GGATCCTACTCGAACATGT
shNk1#1	GCAAGGACTGCTTTCACAT
shDlx#1	GCTTGTCACCGCCTGTATT
shMsxA#1	GCAGTACGACGGAAGATTT
shMsxA#2	GGACTACAAAGCAACTTCT
shFoxG1#1	GAAAGCGCAGAGGAAAGAA
shFoxG1#2	GAGGAGAAGAGATTGACTT
shRx#1	GAGCTCCAACGATGGTAAA
shRx#2	GAACAAGAGCGAAAGACTA
shHES-like#1	GAGTGTGCGCTAGAAGTTA
shHES-like#2	GCTCATCAAACGAGTTCAA

See Supplementary Fig. 3b and 11b for the knockdown efficiency estimation by qPCR and in situ hybridization

Supplementary Table 4: Morpholino sequences

Name	Morpholino sequence	Reference
BraMO	TCGTCCGAGTGCATGTCCGACTATG	new
DlxMO	TCTGGTTTCATGTAATAGGGTACTG	new
Nk1MO	TCAGGCCGCAGCATTGAAGC	new
Sp6-9MO	TCTAGTAGTTCCTGTGAGTAGACAG	new
ControlMO	GATGTGCCTAGGGTACAACAACAAT	²
Six3/6MO	GTAAGTCCGCACTGCAAGACTTGTC	⁶
β -cateninMO	TTCTTCGACTTTAAATCCAACCTCA	³

See Suppl. Fig. 3c and 11c for the confirmation of the sequence-specific activity of the new MOs.

Supplementary Table 5: Primers used for Q-PCR (marked as qF and qR) and for cloning new gene fragments

GeneId	Primer name	Primer 5' ->3'
NVE3568	Bra_qF	CGCACTCAGCTTACTCCCAA
	Bra_qR	AGGTCGATGACTTCGGATGC
NVE20630	FoxA_qF	GCCATGGGTATGGCAGGTAT
	FoxA_qR	TGAAGTGCATGGGGTCGTAG
NVE26195	FoxB_qF	AAACAGTTACGGCAGCGCTAA
	FoxB_qR	GGGAAAATGGTCCATGATGA
NVE16579	Lmx_qF	GACCGAAAGGGACATCAAAGAA
	Lmx_qR	GTAAGGATTGTTTCGCGGTCTT
NVE13527	Shavenbaby_qF	GCGATCATGGAACAAGGAACT
	Shavenbaby_qR	AATCCACTTCCCCCTTTCCT
NVE24711	Dachshund_qF	TCCTCACCATCCACAAACTCC
	Dachshund_qR	GCAATATCAATGCCATTCACG
NVE11868	NVE11868_qF	ATACGACAAGAGGCCACGCA
	NVE11868_qR	TCCTCCTGTTTCCTCGCACTT
NVE20892	MsxA_qF	ACGGAAACACAAAGCGAATC
	MsxA_qR	TGCAGAAAACCTCAGCCCTTT
NVE20899	Nk1_qF	GAACGGAGTGATCGAAGAGC
	Nk1_qR	CTTGTTGGGATCGAGGATGT
NVE8363	Dlx_qF	CGCCTACTTAGGGCTGACAC
	Dlx_qR	GTCGAGGAGCCACTGTTTTC
NVE21445	Rx_qF	CTGAAGCCACAAAACATCCA
	Rx_qR	CTTGGGTTGGAGTCGTTGAT
NVE14243	HES-like_qF	CTTCCACCAGCTGTCAGTCA
	HES-like_qR	TTGAAACTGTGTGGGACCAA
NVE6876	FoxG1_qF	CCAGGCAATAAAGAGGGTGA
	FoxG1_qR	TGATAAGCGCGTTGTACGAG
no NVE model	SP6-9_qF	GCAGCCTCGTATCATCCTCC
	SP6-9_qR	GTGGTTCCTACAGTCACCG
NVE23709	SoxB1_qF	AAGAAATGCCTAGCCCCACA
	SoxB1_qR	CTGCCGGAGGGAGATAAGTG

<i>Supplementary Table 5 (continued)</i>		
NVE12977	MsxC_F	CTGACCCGCTCAAGATCACT
	MsxC_R	AGTAACATCTTCCGCGCTCT
NVE14550	Unc4_F	ATGAGAGTGAGGACGAACTTC
	Unc4_R	CATTCCTCGTGCTCCTTTGC
NVE16579	Lmx_F	GACCGAAAGGGACATCAAAGAA
	Lmx_R	CACATCGAGGCTTGGCTTTC
NVE13527	Shavenbaby_F	GCGATCATGGAACAAGGAACT
	Shavenbaby_R	CGCCAGAGAAACGGTATTGG
NVE24711	Dachshund_F	TCCTCACCATCCACAAACTCC
	Dachshund_R	TCTGAATCTCGCCTCTTGCC
NVE11868	NVE11868_F	ATACGACAAGAGGCCACGCA
	NVE11868_R	TAAATGCTCTCCCGCACTCC
NVE14608	FoxJ1_F	CGTACGCGACGCTTATATGTATGG
	FoxJ1_R	CTGTTAGTCGAAATGAGCTGCTTCAG
NVE4967	Not-like_F	TTACCACCCACAAGCTAACGG
	Not-like_R	TTATCGAACGTTCTGCATCCC
NVE21292	Rough_F	GAAACATGCAAAGTCCCTCCTTC
	Rough_R	CGGTACAGGACTCGCCATAGAT
NVE15777	Sox14-like_F	GAAAAGACGCGCCATGAACA
	Sox14-like_R	CGTTAAGCCAACGGACCTCA
NVE17371	FoxQ2d_F	CGCGATAGATCAAGCTAAGACCG
	FoxQ2d_R	CATAGATTGTTTCGCCAGTGCGT
NVE16639	GFI_F	TCCGAGTGCAAAACTGAGGG
	GFI_R	TCATTAGAAGAGCCCCGCTG
NVE1324	FoxL2_F	TGCCACTACATTGGACACCG
	FoxL2_R	TGCGGAGAAAGATACGAGACAAG
NVE4006	DMRT_F	TGCCTTGTACCATCGCATCC
	DMRT_R	ATTTCTGGCCACATAGGGCG
NVE20898	Nk5_F	TCACAGGCTTAAAACGTCGC
	Nk5_R	ACCTGCTATTTGACCTACACCA
NVE14554	DRGX_F	GCGAGTGTTTCTGCTCAACC
	DRGX_R	ACTGGATGCAAGCTCTTTTGTTT

<i>Supplementary Table 5 (continued)</i>		
NVE21395	Sp1-4_F	GCATGGAAAACTCGTCCACT
	Sp1-4_R	TTCCAGTTCCTCGCCAATGC
NVE5430	PaxB_F	ACGGGCTCCATAAAACCTGG
	PaxB_R	CATTGAGCGGGAACAGCAAA
NVE7655	NVE7655_F	AGTGCGTCAGCAAGAGTGTC
	NVE7655_R	CCATCAACTGCAGCAACGTC
NVE20892	MsxA_F	ATTCACAGCAGGTTAGGCC
	MsxA_R	ACGCTCAAAACGATGGCTCT
NVE20899	Nk1_F	ACACGGAGGGCCAGTAAGTA
	Nk1_R	ACAGCTCTTGACTGTTGGGA
NVE8363	Dlx_F	TGGCGTGTTGATAAGGCCCT
	Dlx_R	GCGTCGAGAATCAGCGATGA
NVE21445	Rx_F	ACGCTGGCCATCATGTATACT
	Rx_R	CACGTATTAGTGCCCGGGAT
NVE14243	HES-like_F	AGCCTCTCTTATGCCTACTCAG
	HES-like_R	TAAGGCTCATGTACGAAAGCA
NVE6876	FoxG1_F	TGGCTTCAAACACACAACAGT
	FoxG1_R	AACGCTGACATACCCTCTTGG
no NVE model	SP6-9_F	ATGCTAGCTGCAACTTGTAGT
	SP6-9_R	TCATGAGTCACTTAGAATGCGCG
NVE16658	APC_F	GAAAGCAGAGCGGAAACAAC
	APC_R	AATTCTCAATCGACGCCATC

Supplementary References

- 1 Letunic, I. & Bork, P. 20 years of the SMART protein domain annotation resource. *Nucleic Acids Res* **46**, D493-D496 (2017).
- 2 Kraus, Y., Aman, A., Technau, U. & Genikhovich, G. Pre-bilaterian origin of the blastoporal axial organizer. *Nat Commun* **7**, 11694 (2016).
- 3 Leclère, L., Bause, M., Sinigaglia, C., Steger, J. & Rentzsch, F. Development of the aboral domain in *Nematostella* requires beta-catenin and the opposing activities of Six3/6 and Frizzled5/8. *Development* **143**, 1766-1777 (2016).
- 4 Kirillova, A. *et al.* Germ-layer commitment and axis formation in sea anemone embryonic cell aggregates. *Proc Natl Acad Sci USA* **115**, 1813-1818 (2018).
- 5 Servetnick, M. D. *et al.* Cas9-mediated excision of *Nematostella brachyury* disrupts endoderm development, pharynx formation and oral-aboral patterning. *Development* **144**, 2951-2960 (2017).
- 6 Sinigaglia, C., Busengdal, H., Leclère, L., Technau, U., Rentzsch, F. The Bilaterian Head Patterning Gene six3/6 Controls Aboral Domain Development in a Cnidarian. *PLoS biology* **11**, e1001488 (2013).

Paper III

" β -catenin-dependent endomesoderm specification appears to be a Bilateria-specific co-option."

Authors:

Tatiana Lebedeva^{1,2}, Johan Boström³, David Mörsdorf¹, Isabell Niedermoser^{1,2}, Evgeny Genikhovich⁴, Igor Adameyko^{3,5}, Grigory Genikhovich^{1*}

¹ Department of Neurosciences and Developmental Biology, Faculty of Life Sciences, University of Vienna, Djerassiplatz 1, Vienna A-1030, Austria.

² Vienna Doctoral School of Ecology and Evolution, University of Vienna, Vienna A-1030, Austria.

³ Department of Neuroimmunology, Center for Brain Research, Medical University Vienna, Vienna, A-1090, Austria.

⁴ Engelsa pr. 40-6, St. Petersburg 194156, Russia.

⁵ Department of Physiology and Pharmacology, Karolinska Institutet, Stockholm SE-171 77, Sweden.

Status:

Preprint published on bioRxiv, 2022, <https://doi.org/10.1101/2022.10.15.512282>

Contributions:

T.L. planned and performed experiments and generated the knock-in line; J.B. performed live imaging; I.N. performed Axin in situ hybridization; D.M. and E.G. measured and analyzed the gradient data; I.A. provided access to the spinning disk confocal microscope; G.G. conceived the project, performed experiments and wrote the paper. All authors edited the paper.

β -catenin-dependent endomesoderm specification appears to be a Bilateria-specific co-option

Tatiana Lebedeva^{1,2}, Johan Boström³, David Mörsdorf¹, Isabell Niedermoser^{1,2}, Evgeny Genikhovich⁴, Igor Adameyko^{3,5}, Grigory Genikhovich^{1,*}

¹ Department of Neurosciences and Developmental Biology, Faculty of Life Sciences, University of Vienna, Djerassiplatz 1, Vienna A-1030, Austria.

² Vienna Doctoral School of Ecology and Evolution, University of Vienna, Vienna A-1030, Austria

³ Department of Neuroimmunology, Center for Brain Research, Medical University Vienna, Vienna A-1090, Austria.

⁴ Engelsa pr. 40-6, St. Petersburg 194156, Russia

⁵ Department of Physiology and Pharmacology, Karolinska Institutet, Stockholm SE-171 77, Sweden

* Author for correspondence: grigory.genikhovich@univie.ac.at

Abstract

Endomesoderm specification based on a maternal β -catenin signal and axial patterning by interpreting a gradient of zygotic Wnt/ β -catenin signalling was suggested to predate the split between Bilateria and their evolutionary sister Cnidaria. However, in Cnidaria, the roles of β -catenin signalling in both these processes have not been proven directly. Here, by tagging the endogenous β -catenin protein in the sea anemone *Nematostella vectensis*, we show that the oral-aboral axis in a cnidarian is indeed patterned by a gradient of β -catenin signalling. Unexpectedly, in a striking contrast to Bilateria, *Nematostella* endoderm specification takes place opposite to the part of the embryo, where β -catenin is translocated into the nuclei. This suggests that β -catenin-dependent endomesoderm specification is a Bilateria-specific co-option, which may have linked endomesoderm specification with the subsequent posterior-anterior patterning.

Main text

During the early development of bilaterian embryos, β -catenin signalling is involved in two fundamental processes occurring sequentially: it specifies the endomesoderm, and it patterns the posterior-anterior (P-A) axis (*1-11*). The central role of the Wnt/ β -catenin (cWnt) signalling in the patterning of the main body axis is not restricted to Bilateria. Expression data indicate that cWnt signalling may regulate axial patterning in the earliest branching metazoan groups Ctenophora and Porifera (*12-14*), and functional analyses of the last 25 years showed the involvement of the graded

cWnt signalling in the patterning of the oral-aboral (O-A) axis in the bilaterian sister group Cnidaria (sea anemones, corals, jellyfish, *Hydra*) (15-21). Moreover, nuclear localization of β -catenin on one side of the sea anemone embryo at the early blastula stage and the failure to gastrulate upon β -catenin loss-of-function suggested that the involvement of β -catenin signalling in the endomesoderm specification was also an ancestral feature conserved at least since before the cnidarian-bilaterian split over 700 Mya (17, 22-24). However, in spite of convincing circumstantial evidence, there was no direct proof for either the presence of the O-A gradient of β -catenin signalling or for the instructive role of β -catenin signalling in the endomesoderm specification in a cnidarian. Here we ventured to obtain such proof and close this knowledge gap by tagging endogenous β -catenin in a model cnidarian – the sea anemone *Nematostella vectensis* – with superfolder GFP (25) and detecting its localization at the time of germ layer specification and in the axial patterning phase.

Previously we showed that genes expressed in distinct ectodermal domains along the O-A axis in *Nematostella* react dose-dependently to different levels of pharmacological upregulation of the β -catenin signalling (17). Downstream, β -catenin signalling activates a set of transcription factors, among which the more orally expressed ones act as transcriptional repressors of the more aborally expressed ones (16). Like this, the initially ubiquitous aboral identity of the embryo is restricted in a β -catenin-dependent manner to the future aboral domain as the oral and the midbody domains appear and become spatially resolved. In this process, JNK signalling appears to act agonistically with β -catenin signalling: JNK inhibitor treatment aboralizes the embryo, and JNK inhibition is also capable of dose-dependently rescuing the oralization caused by pharmacological upregulation of β -catenin signalling with a GSK3 β inhibitor (Supplementary Fig. 1). The regulatory logic of the β -catenin-dependent axial patterning and the complement of the downstream transcription factors is so strikingly similar between the sea anemone and the deuterostome bilaterians that it suggests the homology of the cnidarian O-A and the bilaterian P-A axis (1-3, 16, 26, 27).

To directly verify the presence of the oral-to-aboral β -catenin signalling gradient and the role of β -catenin signalling in the *Nematostella* endoderm specification, we used CRISPR/Cas9-mediated genome editing to generate a knock-in line, in which the nucleotides coding for the first 5 amino acids of β -catenin were replaced by the superfolder GFP (sfGFP) coding sequence. In order to test for the presence of the nuclear β -catenin gradient along the oral-aboral axis of the embryo, we incrossed heterozygous F1 polyps (*wild type/sfGFP- β -catenin*) and allowed the offspring to develop until late gastrula stage. As expected, approximately 3/4 of the embryos were fluorescent, however, fluorescent microscopy of live embryos only revealed strong signal at the cell boundaries – in line with the function of β -catenin in the cell contacts. In order to detect nuclear sfGFP- β -catenin, we fixed the embryos and stained them with an anti-GFP antibody. Antibody staining revealed a comparatively weak but clear nuclear signal forming an oral-to-aboral gradient in the ectoderm (Fig. 1A). Quantification of the signal intensity in all ectodermal nuclei starting from the deepest cell of the

pharyngeal ectoderm (relative position 0.00) and ending with the cell in the centre of the aboral ectoderm (relative position 1.00) showed a peak of nuclear sfGFP- β -catenin in the bend of the blastopore lip (approximately at relative position 0.20), and a second, smaller peak at the border between the midbody and the aboral domain (approximately at relative position 0.60). Both peaks coincide with the peaks of expression of the conserved and highly sensitive β -catenin signalling target *Axin* (15-17) (Fig. 1B-D). Thus, we conclude that the initial assumption that genes expressed in distinct domains along the O-A axis and regulating its patterning react to a graded β -catenin signal is correct.

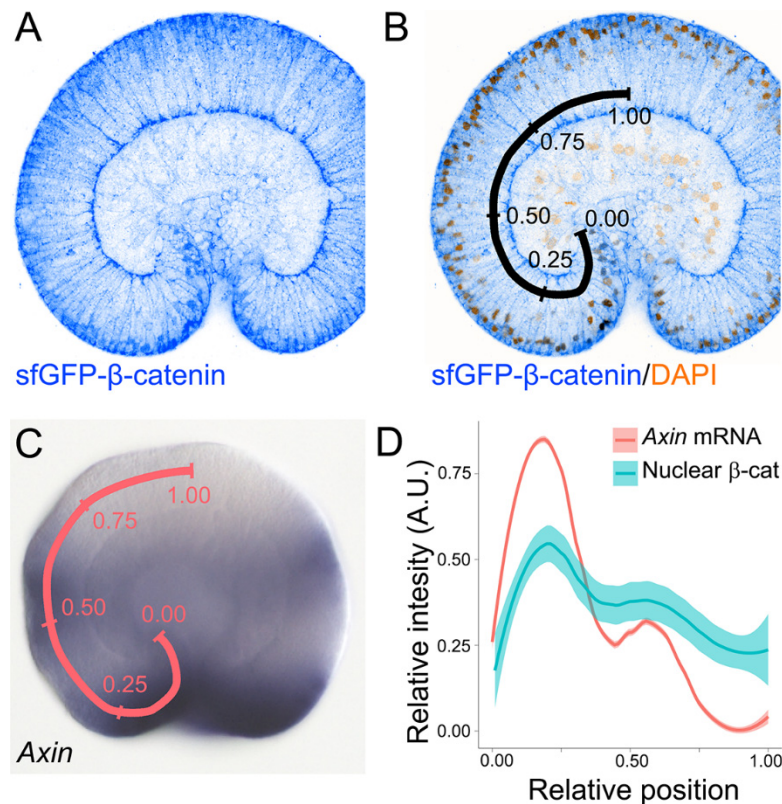


Figure 1. Nuclear sfGFP- β -catenin forms a bimodal oral-to-aboral gradient in late gastrula stage embryos. (A) Anti-GFP antibody staining detects sfGFP- β -catenin at the cell membranes and in the nuclei. (B) Overlay of the anti-GFP signal with the nuclear staining shows the positions, at which anti-GFP staining was quantified. The first nucleus, where anti-GFP staining intensity was measured is located at the relative position 0.00; the last nucleus – at the relative position 1.00. (C) *Axin* in situ hybridization staining intensity was measured along the pink line from the relative position 0.00 to the relative position 1.00. (D) LOESS smoothed curves show that nuclear sfGFP- β -catenin forms an oral-to-aboral gradient with two peaks (n=6). These peaks correspond to the positions where β -catenin target *Axin* expression peaks as well (n=10).

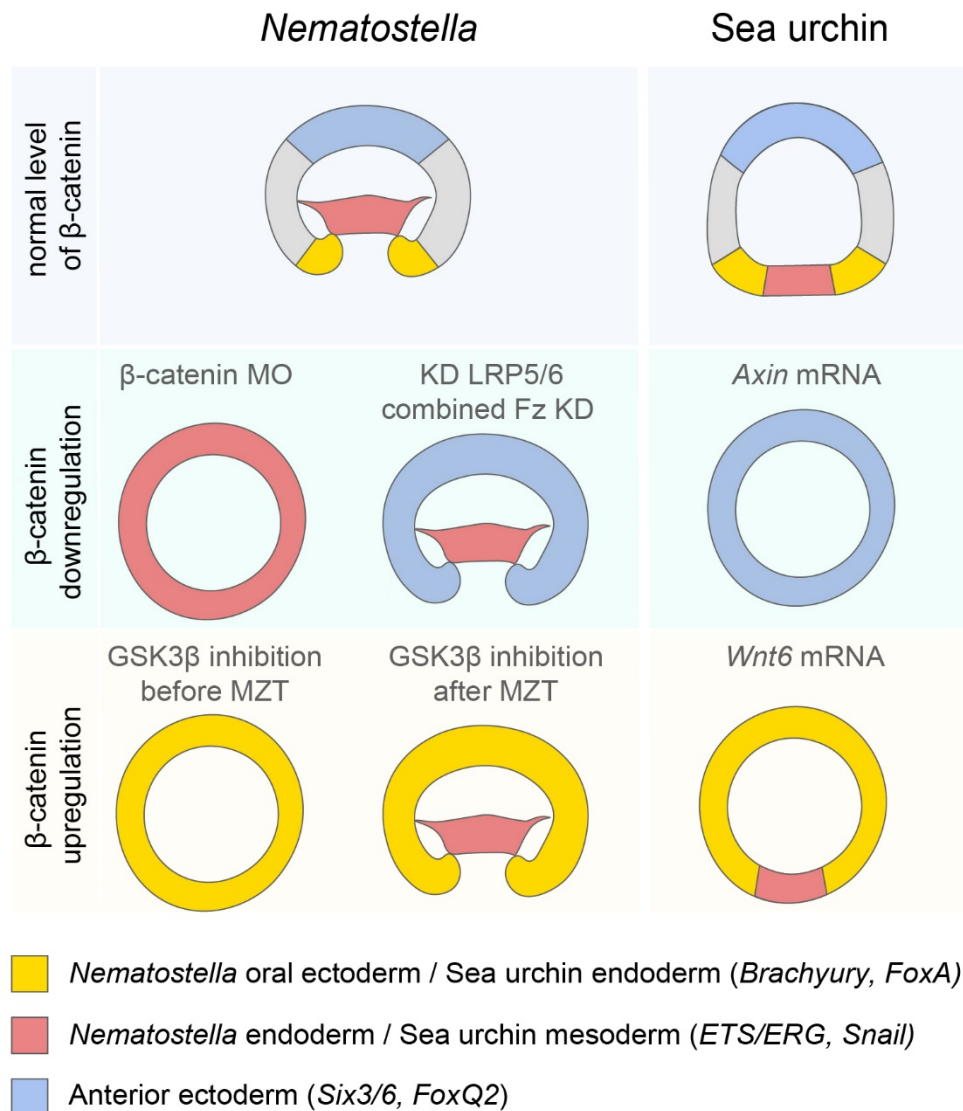


Figure 2. Comparison of the effects of the up- and downregulation of the β -catenin signalling in *Nematostella* and sea urchin. The germ layers are coloured according to the cnidarian-bilaterian germ layer equivalence hypothesis published in (28). The cartoons showing the effects of the up- and downregulation of the β -catenin signalling are based on data from (15, 16, 23, 27, 29). MZT – maternal-to-zygotic transition.

Our next goal was to verify the involvement of β -catenin signalling in the specification of the endoderm in *Nematostella*. Previous analyses of the *β -catenin-GFP* mRNA injected *Nematostella* embryos showed nuclear β -catenin-GFP localization on one side of the early blastula in the untreated embryos and in all blastoderm cells of the embryos upon GSK3 β inhibition (17, 22). Moreover, *Nematostella* embryos with the nuclear localization of β -catenin suppressed either by truncated cadherin mRNA overexpression, injection of the β -catenin translation blocking morpholino or β -

catenin RNAi did not form preendodermal plates, blastopore lips and failed to gastrulate remaining perfect blastula-like spheres (22, 23, 30). Morphologically, this effect perfectly resembled the gastrulation block caused by injection of the mRNA encoding truncated cadherin or the DIX domain of Dishevelled in sea urchin (9) and led to the conclusion that the endoderm in *Nematostella*, just like the endomesoderm in a number of bilaterians, is specified by an early β -catenin signal at the future gastrulation pole of the embryo (22). Although universally accepted in the field (also by us – see for example (17, 31)), this hypothesis was contradicted by several important observations (Fig. 2). First, in spite of lacking preendodermal plates, β -catenin morphants ubiquitously expressed endodermal marker *SnailA*, but not the zygotic aboral/anterior markers *Six3/6* and *FoxQ2a* (16, 23). Second, upon pharmacological activation of β -catenin signalling by GSK3 β inhibitor treatment starting before 6 hours post-fertilization (hpf), the embryos also remained spherical failing to form preendodermal plates, blastopore lips and gastrulate; however, these spheres expressed oral ectoderm markers *Brachyury*, *FoxA* and *FoxB*, while endodermal markers were abolished (15, 23). Third, loss-of-function experiments showed that LRP5/6 and combined Fz knockdowns did not prevent endoderm specification and gastrulation in *Nematostella* in spite of completely aboralizing the ectoderm of embryo i.e. entirely disrupting its oral-aboral patterning (15). Taken together, these data suggest that, unlike the bilaterian endomesoderm, *Nematostella* endoderm specification seems to be repressed by β -catenin signalling rather than activated by it.

Nematostella endoderm specification is an early event happening at or prior to 6 hpf (15, 16), at which time nuclear sfGFP- β -catenin is clearly detectable in the developing embryos by fluorescent microscopy. Hence, in order to verify the involvement of β -catenin signalling in the specification of the endoderm, we immobilized sfGFP- β -catenin expressing embryos in low melting point agarose and performed live imaging from early cleavage until the onset of gastrulation (Fig. 3, Supplementary Movies 1-2). Nuclear sfGFP- β -catenin became detectable as early as during the 32-64 cell stage, and from the very start, nuclear signal was confined to approximately 2/3 of the embryo. Nuclear sfGFP- β -catenin became visible during every cell cycle until shortly after the desynchronization of the mitotic divisions at midblastula (32), after which it became too weak to detect, while the sfGFP- β -catenin signal in the cell contacts remained strong. Strikingly, in all embryos we live-imaged (n=10), the preendodermal plate formed on the side opposite to the side where nuclear sfGFP- β -catenin was detectable at earlier stages, i.e. early nuclear sfGFP- β -catenin was always observed on the aboral side of the embryo. In order to make sure that what we were observing was indeed the nuclear sfGFP- β -catenin dynamics, we also live-imaged sfGFP- β -catenin expressing embryos, which were incubated in the 5 μ M solution of the GSK3 β inhibitor alsterpaullone (ALP) from fertilization on (Supplementary Movies 3-4). In line with the previous publications (17, 22), upon GSK3 β inhibition, fluorescent signal was observed in all nuclei from 16-32 cell stage on, and the embryos failed to gastrulate.

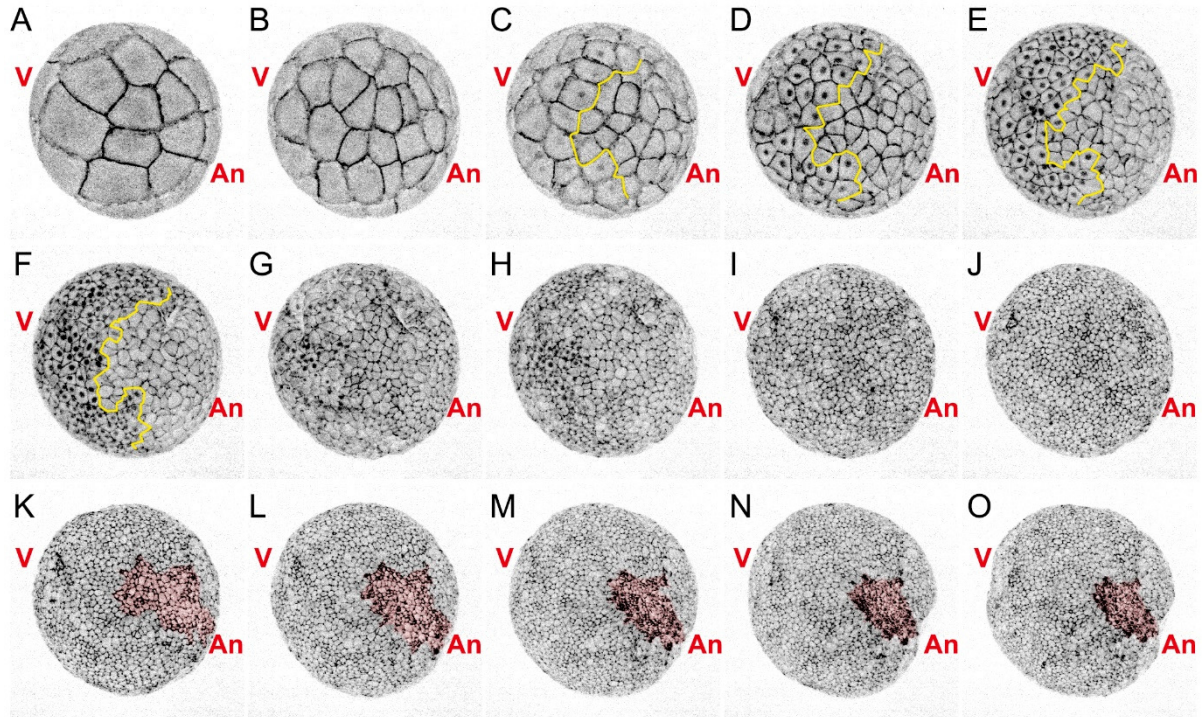


Figure 3. Early sfGFP-β-catenin accumulation is observed at the vegetal pole, opposite to the future gastrulation site. Individual frames from the Supplementary Movie 1 showing the same embryo over the course of development. sfGFP-β-catenin – black signal. An – animal pole, V – vegetal pole, the preendodermal plate is highlighted pink. Note nuclear sfGFP-β-catenin in the vegetal/aboral half of the embryo on (C-H). Yellow line on (C-D) demarcates the sharp boundary between the nuclear sfGFP-β-catenin-positive and nuclear sfGFP-β-catenin-negative cells until the loss of synchronicity in cell division on (G).

The presence of nuclear sfGFP-β-catenin on the aboral rather than oral side in the embryos developing in the absence of ALP (Fig. 3, Supplementary Movies 1-2) suggests that in *Nematostella*, unlike in Bilateria, instead of promoting endoderm specification, β-catenin signalling actually represses it, which resolves all the discrepancies mentioned above. First, it explains why endodermal marker *SnailA* is ubiquitously expressed in the β-catenin morphants but zygotic aboral/anterior ectoderm markers *Six3/6* and *FoxQ2a* are not (23). Second, it explains why upon treatment with a GSK3β inhibitor prior to 6 hpf, the whole embryo acquires the oral ectoderm fate rather than the endoderm fate (15, 23). Third, the lack of β-catenin signalling at the future oral side of the early embryo is in line with our observation that endoderm formation is not controlled by Fz/LRP5/6-mediated signalling (15).

Our finding that an oral-to-aboral gradient of nuclear β-catenin exists in the *Nematostella* gastrula confirms a number of previous assumptions on the mode and logic of the oral-aboral

patterning in this animal and is in line with the idea that the cnidarian O-A axis corresponds to the bilaterian P-A axis (15-17). However, our second observation that *Nematostella* endoderm forms in the β -catenin-negative domain has a much greater import for the understanding of the early evolution of the body axes and germ layers. In Bilateria, unless physically prevented by large amounts of yolk, endomesoderm specification and gastrulation take place at the vegetal pole, i.e. posteriorly. In contrast, in Cnidaria, gastrulation modes are highly variable. Some species gastrulate by

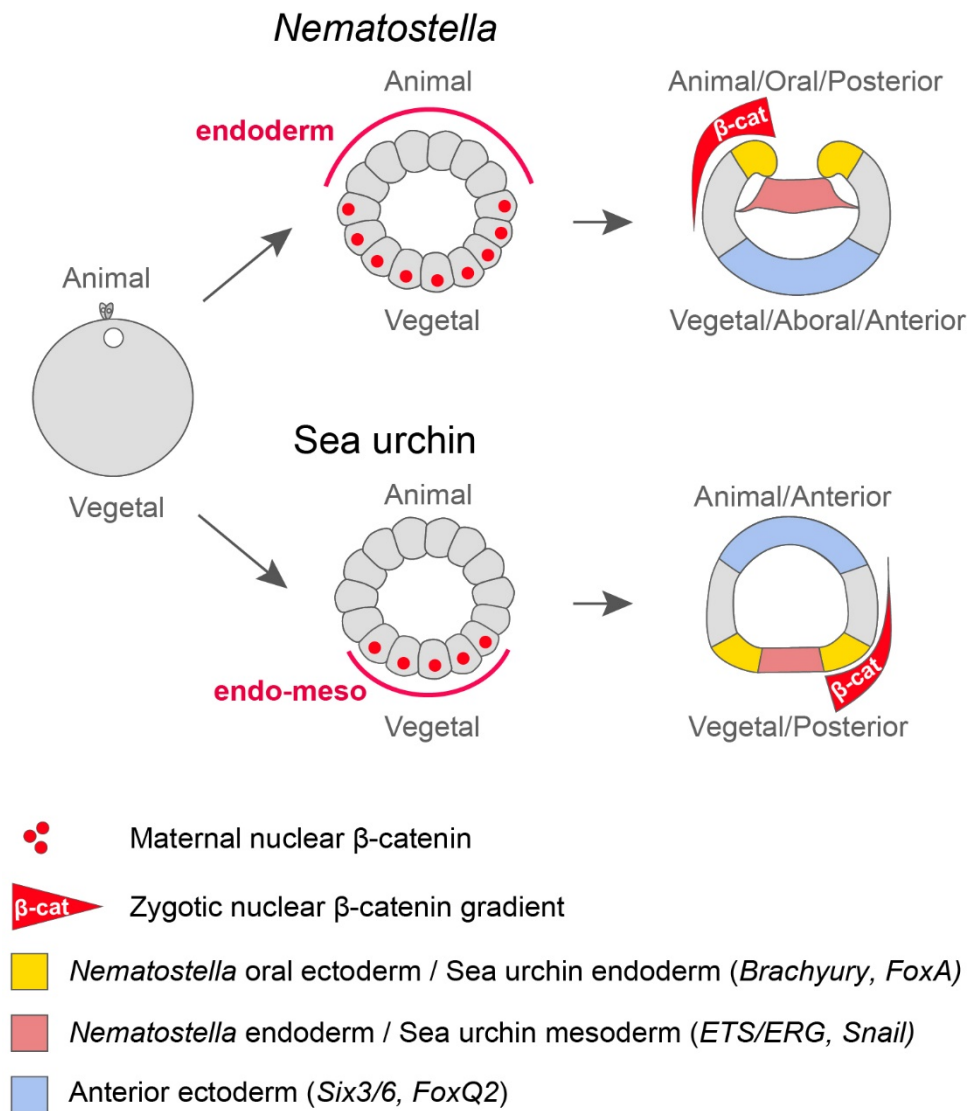


Figure 4. β -catenin signalling may have been co-opted for endomesoderm specification at the base of Bilateria.

invagination, unipolar ingression or epiboly, while others have multipolar modes of gastrulation such as cellular, morular or mixed delamination or multipolar ingression (33). In case of multipolar gastrulation, germ layer specification and gastrulation movements are spatially uncoupled from the universally cWnt-dependent O-A patterning (21, 34-37). Importantly, in cnidarians with a unipolar

mode of gastrulation, endoderm specification and gastrulation always takes place at the animal, rather than at the vegetal pole, and in all cnidarians analysed so far, the animal-vegetal axis exactly corresponds to the O-A axis of the embryo independent of whether they have a multipolar or a unipolar mode of gastrulation (32, 33, 38-40). Previously, it has been proposed that the activation of the β -catenin-dependent endomesoderm specification at the vegetal rather than at the animal pole of a stem bilaterian resulted in the inversion of the position of the gastrulation site in Bilateria (41). Our new data suggest a different scenario (Fig. 4). Both, in *Nematostella* and in Bilateria, maternal β -catenin accumulates in the vegetal pole nuclei, however, the specification of the endomesoderm by this signal appears to be a bilaterian specific co-option, which linked germ layer specification, gastrulation movements and P-A patterning. In contrast, in Cnidaria, endoderm specification appears to be either negatively controlled by β -catenin (as in *Nematostella*) or not to be controlled by β -catenin at all (as in cnidarians with multipolar gastrulation modes), which explains the variety of gastrulation modes observed in this phylum. Many new questions arise with this observation, for example: i) what causes endoderm specification and subsequent gastrulation movements in the β -catenin-negative domain in *Nematostella* and in random positions in cnidarians with multipolar gastrulation modes, or ii) what regulatory changes tethered bilaterian gastrulation to the ancestral site of the nuclear β -catenin accumulation at the vegetal pole? However, our data clearly suggest that the current view on the ancestral mode of endomesoderm specification in animals needs to be re-assessed.

Materials and methods.

Animal culture and generation of the sfGFP- β -catenin knock-in line

The animals were maintained and spawning was induced as described in (42). To generate a *sfGFP- β -catenin* knock-in, a single gRNA 5'-ACCATGGAGACACACGGTAT-3' recognising a sequence starting at the position 134602 on the scaffold_183 of the *Nematostella* genome v.1 (43) was selected using CHOPCHOP (44), and CRISPR/Cas9 genome editing was performed as described in (45). For homologous recombination, we generated a fragment in which the first five triplets of the *Nematostella β -catenin* coding sequence were replaced with the *Superfolder GFP* coding sequence introduced in frame by Gibson assembly. The fragment containing the homology arms and *sfGFP* was amplified using the primers 5'-GTGGAATTCGCAGCATTTCTCA-3' and 5'-TCAAGGATGGCTCAGCAAGC-3', which were modified as described in (46). F0 animals with clear fluorescent patches were raised to sexual maturity and crossed to wild type to generate heterozygous F1. To confirm the knock-in, we clipped single tentacles from individual heterozygous F1 animals, extracted genomic DNA from them and performed PCR using the primers 5'-GGTCGTAGATGGTACCCTAAG-3' and 5'-CAACTCTGGGATAGCACGTGTAG-3' located in

the *β-catenin* genomic locus upstream and downstream of the homology arms. This PCR resulted in two *β-catenin* locus fragments with and without the *sfGFP* insertion, which we confirmed by Sanger sequencing. Genotyped knock-in animals were raised to maturity, sexed and intercrossed. The offspring of these genotyped F1 animals was used in the experiments.

Antibody staining, in situ hybridization and staining intensity measurements

For anti-GFP antibody staining, the embryos were fixed for 1 hr in 4%PFA/PBS-TT (PBS-TT = 1x PBS containing 0.2% Tween20 and 0.2% TritonX100) at 4°C, washed five times for 5 min in PBS-TT, incubated for 2 hours in a blocking solution consisting of 95% BSA/PBS-TT and 5% heat inactivated sheep serum (BSA/PBS-TT = 1% BSA w/v in PBS-TT), and stained overnight at 4°C in rabbit polyclonal anti-GFP (abcam290) diluted 1:500 in the blocking solution. Unbound antibody was removed by five 15 min washes in PBS-TT, then the embryos were blocked again and stained overnight at 4°C with AlexaFluor488 donkey anti-rabbit IgG (Life Technologies) diluted 1:1000 in the blocking solution. The unbound secondary antibody was removed by 5 washes with PBS-TT; DAPI was added to the first wash to counterstain the nuclei, then the embryos were gradually embedded in Vectashield (Vectorlabs). 16 bit images of the DAPI and anti-GFP staining were obtained using the Leica SP8 LSCM equipped with a 63x glycerol immersion objective (n=6). In situ hybridization with an RNA probe against *Nematostella Axin* was performed as described previously (15, 17). The anti-GFP staining intensity was measured over all ectodermal DAPI-positive nuclei starting from the deepest pharyngeal cell (relative position 0) to the cell in the middle of the aboral ectodermal domain (relative position 1) using FIJI (47). Briefly, to identify the ROIs, polygonal selections were drawn to separate the pharynx ectoderm and the outer ectoderm based on DAPI signal. Masks were then generated separately for the outer ectoderm and the pharynx ectoderm parts of the image using the Convert to mask and the Watershed commands. To generate the ROIs for the nuclei, particle analysis with a minimum size of 1 μm^2 was performed. The resulting ROIs were then manually checked and sorted such that they are arranged from the relative position 0 to the relative position 1. The mean intensities in the sfGFP channel were measured for all ROIs. The relative position of each nucleus was determined as a nucleus number divided by the total number of nuclei with measured anti-GFP staining intensity in this particular embryo. *Axin* in situ staining intensity was measured in FIJI (47) on in situ images (n=10) along a line drawn from the deepest pharyngeal cell (relative position 0) to the cell in the middle of the aboral ectodermal domain (relative position 1). The relative position corresponding to each measurement was determined by dividing the measurement number by the total number of measurements. In order to be able to plot the relative staining anti-GFP and *Axin* staining intensities on the same graph, for each embryo, the minimal

measured staining intensity was subtracted from all intensity measurements, and then each measurement was divided by the maximum measurement.

Live imaging

Embryos were embedded in 0.7% low-melting agarose in *Nematostella* medium (*Nematostella* medium = 16‰ artificial sea water, Red Sea Salt) in an optical bottom 35 mm Petri dish (D35-20-1.5-N, Cellvis, US) and imaged with a 20X CFI Plan Apo Lambda Objective (Nikon, Japan) using a Nikon Ti2-E/Yokogawa CSU W1 Spinning Disk Confocal Microscope. A 488 nm laser was used in conjunction with a 525/30 Emission Filter (BrightLine HC, Semrock, US) and a 25 µm pinhole size disk. Images were acquired every 5 minutes using automated imaging, over 25 Z-sections covering 120 µm depth. In the first experiment, the embryos were left to develop in 16‰ artificial sea water. In the second experiment, the embryos were developing in a 5 µM solution of the GSK3β inhibitor alsterpaullone (Sigma) from 1 hpf on. Live imaging was stopped after gastrulation was observed in the sample developing in the absence of alsterpaullone. Since embryos placed into a GSK3β inhibitor do not gastrulate, we continued the imaging of the alsterpaullone-treated embryos for an additional hour in comparison to the normal embryos. During imaging, the medium in the sample dish was continuously pumped through a tube submerged in a room temperature (~23°C) water bath to offset heating from the microscope. This was achieved with a modified sample dish lid with two liquid connectors, and a peristaltic pump (Minipuls 3, Gilson, US). Ten embryos were imaged together in each experiment. After imaging, each Z-stack of images was converted into a maximum intensity projection.

Author contributions

T.L. planned and performed experiments and generated the knock-in line; J.B. performed live imaging; I.N. performed *Axin* in situ hybridization; D.M. and E.G. measured and analysed the gradient data; I.A. provided access to the spinning disk confocal microscope; G.G. conceived the project, performed experiments and wrote the paper. All authors edited the paper.

Acknowledgements

The work in Genikhovich group is funded by the Austrian Science Foundation (FWF) grants P30404 and P32705-B. The work in the Adameyko group is funded by the ERC Synergy grant “KILL-OR-DIFFERENTIATE” 856529. T.L. was a recipient of the PhD completion grant of the Vienna Doctoral School of Ecology and Evolution. D.M. is a recipient of the Lise-Meitner Fellowship M3291-B of the

FWF. We thank the Core Facility for Cell Imaging and Ultrastructure Research of the University of Vienna for the access to the confocal microscope.

References

1. S. Darras *et al.*, Anteroposterior axis patterning by early canonical Wnt signaling during hemichordate development. *PLoS Biol* **16**, e2003698 (2018).
2. S. Darras, J. Gerhart, M. Terasaki, M. Kirschner, C. J. Lowe, beta-catenin specifies the endomesoderm and defines the posterior organizer of the hemichordate *Saccoglossus kowalevskii*. *Development* **138**, 959-970 (2011).
3. B. S. McCauley, E. Akyar, H. R. Saad, V. F. Hinman, Dose-dependent nuclear beta-catenin response segregates endomesoderm along the sea star primary axis. *Development* **142**, 207-217 (2015).
4. U. Nordström, T. M. Jessell, T. Edlund, Progressive induction of caudal neural character by graded Wnt signaling. *Nat Neurosci* **5**, 525-532 (2002).
5. R. Prühs, A. Beermann, R. Schroder, The Roles of the Wnt-Antagonists Axin and Lrp4 during Embryogenesis of the Red Flour Beetle *Tribolium castaneum*. *J Dev Biol* **5**, (2017).
6. C. Kiecker, C. Niehrs, A morphogen gradient of Wnt/beta-catenin signalling regulates anteroposterior neural patterning in *Xenopus*. *Development* **128**, 4189-4201 (2001).
7. H. Sun, C. J. Peng, L. Wang, H. Feng, A. H. Wikramanayake, An early global role for Axin is required for correct patterning of the anterior-posterior axis in the sea urchin embryo. *Development* **148**, dev191197 (2021).
8. J. Q. Henry, K. J. Perry, J. Wever, E. Seaver, M. Q. Martindale, Beta-catenin is required for the establishment of vegetal embryonic fates in the nemertean, *Cerebratulus lacteus*. *Dev Biol* **317**, 368-379 (2008).
9. C. Y. Logan, J. R. Miller, M. J. Ferkowicz, D. R. McClay, Nuclear beta-catenin is required to specify vegetal cell fates in the sea urchin embryo. *Development* **126**, 345-357 (1999).
10. D. R. McClay, J. C. Croce, J. F. Warner, Conditional specification of endomesoderm. *Cells Dev* **167**, 203716 (2021).
11. A. H. Wikramanayake, L. Huang, W. H. Klein, beta-Catenin is essential for patterning the maternally specified animal-vegetal axis in the sea urchin embryo. *Proc Natl Acad Sci USA* **95**, 9343-9348 (1998).
12. K. Pang, J. F. Ryan, J. C. Mullikin, A. D. Baxevanis, M. Q. Martindale, Genomic insights into Wnt signaling in an early diverging metazoan, the ctenophore *Mnemiopsis leidyi*. *EvoDevo* **1**, 10 (2010).
13. M. Adamska *et al.*, Wnt and TGF-beta expression in the sponge *Amphimedon queenslandica* and the origin of metazoan embryonic patterning. *PLoS ONE* **2**, e1031 (2007).
14. S. Leininger *et al.*, Developmental gene expression provides clues to relationships between sponge and eumetazoan body plans. *Nat Commun* **5**, 3905 (2014).
15. I. Niedermoser, T. Lebedeva, G. Genikhovich, Sea anemone Frizzled receptors play partially redundant roles in the oral-aboral axis patterning. *Development* **149**, dev200785 (2022).
16. T. Lebedeva *et al.*, Cnidarian-bilaterian comparison reveals the ancestral regulatory logic of the β -catenin dependent axial patterning. *Nat Commun* **12**, 4032 (2021).
17. Y. Kraus, A. Aman, U. Technau, G. Genikhovich, Pre-bilaterian origin of the blastoporal axial organizer. *Nat Commun* **7**, 11694 (2016).
18. A. Kusserow *et al.*, Unexpected complexity of the Wnt gene family in a sea anemone. *Nature* **433**, 156-160 (2005).
19. H. Marlow, D. Q. Matus, M. Q. Martindale, Ectopic activation of the canonical wnt signaling pathway affects ectodermal patterning along the primary axis during larval development in the anthozoan *Nematostella vectensis*. *Dev Biol* **380**, 324-334 (2013).

20. E. Röttinger, P. Dahlin, M. Q. Martindale, A Framework for the Establishment of a Cnidarian Gene Regulatory Network for "Endomesoderm" Specification: The Inputs of ss-Catenin/TCF Signaling. *PLoS genetics* **8**, e1003164 (2012).
21. G. Plickert, V. Jacoby, U. Frank, W. A. Muller, O. Mokady, Wnt signaling in hydroid development: formation of the primary body axis in embryogenesis and its subsequent patterning. *Dev Biol* **298**, 368-378 (2006).
22. A. H. Wikramanayake *et al.*, An ancient role for nuclear beta-catenin in the evolution of axial polarity and germ layer segregation. *Nature* **426**, 446-450 (2003).
23. L. Leclère, M. Bause, C. Sinigaglia, J. Steger, F. Rentzsch, Development of the aboral domain in *Nematostella* requires beta-catenin and the opposing activities of Six3/6 and Frizzled5/8. *Development* **143**, 1766-1777 (2016).
24. M. Dohrmann, G. Wörheide, Dating early animal evolution using phylogenomic data. *Sci Rep* **7**, 3599 (2017).
25. J. D. Pedelacq, S. Cabantous, T. Tran, T. C. Terwilliger, G. S. Waldo, Engineering and characterization of a superfolder green fluorescent protein. *Nat Biotechnol* **24**, 79-88 (2006).
26. R. C. Range, Canonical and non-canonical Wnt signaling pathways define the expression domains of Frizzled 5/8 and Frizzled 1/2/7 along the early anterior-posterior axis in sea urchin embryos. *Dev Biol* **444**, 83-92 (2018).
27. R. C. Range, R. C. Angerer, L. M. Angerer, Integration of Canonical and Noncanonical Wnt Signaling Pathways Patterns the Neuroectoderm Along the Anterior–Posterior Axis of Sea Urchin Embryos. *PLoS Biol* **11**, e1001467 (2013).
28. P. R. Steinmetz, A. Aman, J. E. M. Kraus, U. Technau, Gut-like ectodermal tissue in a sea anemone challenges germ layer homology. *Nat Ecol Evol* **1**, 1535–1542 (2017).
29. J. Croce *et al.*, Wnt6 activates endoderm in the sea urchin gene regulatory network. *Development* **138**, 3297-3306 (2011).
30. A. Karabulut, S. He, C. Y. Chen, S. A. McKinney, M. C. Gibson, Electroporation of short hairpin RNAs for rapid and efficient gene knockdown in the starlet sea anemone, *Nematostella vectensis*. *Dev Biol* **448**, 7-15 (2019).
31. G. Genikhovich, U. Technau, On the evolution of bilaterality. *Development* **144**, 3392-3404 (2017).
32. J. H. Fritzenwanker, G. Genikhovich, Y. Kraus, U. Technau, Early development and axis specification in the sea anemone *Nematostella vectensis*. *Dev Biol* **310**, 264-279 (2007).
33. Y. Kraus, A. V. Markov, Gastrulation in Cnidaria: The key to an understanding of phylogeny or the chaos of secondary modifications? *Biol Bull Rev* **7**, 7-25 (2017).
34. T. Momose, R. Derelle, E. Houlston, A maternally localised Wnt ligand required for axial patterning in the cnidarian *Clytia hemisphaerica*. *Development* **135**, 2105-2113 (2008).
35. T. Momose, E. Houlston, Two oppositely localised frizzled RNAs as axis determinants in a cnidarian embryo. *PLoS Biol* **5**, e70 (2007).
36. Y. Kraus *et al.*, The embryonic development of the cnidarian *Hydractinia echinata*. *Evol Dev* **16**, 323-338 (2014).
37. A. A. Vetrova *et al.*, From apolar gastrula to polarized larva: Embryonic development of a marine hydroid, *Dynamena pumila*. *Dev Dyn* **251**, 795-825 (2022).
38. P. N. Lee, S. Kumburegama, H. Q. Marlow, M. Q. Martindale, A. H. Wikramanayake, Asymmetric developmental potential along the animal-vegetal axis in the anthozoan cnidarian, *Nematostella vectensis*, is mediated by Dishevelled. *Dev Biol* **310**, 169-186 (2007).
39. G. Freeman, The cleavage initiation site establishes the posterior pole of the hydrozoan embryo. *Roux's Arch Dev Biol* **190**, 123-125 (1981).
40. C. A. Byrum, M. Q. Martindale, in *Gastrulation. From Cells to Embryos.*, C. Stern, Ed. (Cold Spring Harbor Laboratory Press, Cold Spring Harbor, 2004), pp. 33–50.
41. M. Q. Martindale, A. Hejnol, A developmental perspective: changes in the position of the blastopore during bilaterian evolution. *Dev Cell* **17**, 162-174 (2009).
42. G. Genikhovich, U. Technau, Induction of spawning in the starlet sea anemone *Nematostella vectensis*, in vitro fertilization of gametes, and dejellying of zygotes. *CSH protocols* **2009**, pdb prot5281 (2009).

43. N. H. Putnam *et al.*, Sea anemone genome reveals ancestral eumetazoan gene repertoire and genomic organization. *Science* **317**, 86-94 (2007).
44. K. Labun *et al.*, CHOPCHOP v3: expanding the CRISPR web toolbox beyond genome editing. *Nucl Acids Res* **47**, W171-W174 (2019).
45. A. Ikmi, S. A. McKinney, K. M. Delventhal, M. C. Gibson, TALEN and CRISPR/Cas9-mediated genome editing in the early-branching metazoan *Nematostella vectensis*. *Nat Commun* **5**, 5486 (2014).
46. J. A. Gutierrez-Triana *et al.*, Efficient single-copy HDR by 5' modified long dsDNA donors. *eLife* **7**, e39468 (2018).
47. J. Schindelin *et al.*, Fiji: an open-source platform for biological-image analysis. *Nat Methods* **9**, 676-682 (2012).

SUPPLEMENTARY INFORMATION

β -catenin-dependent endomesoderm specification appears to be a Bilateria-specific co-option

Tatiana Lebedeva, Johan Boström, David Mörsdorf, Isabell Niedermoser, Evgeny Genikhovich, Igor Adameyko, Grigory Genikhovich

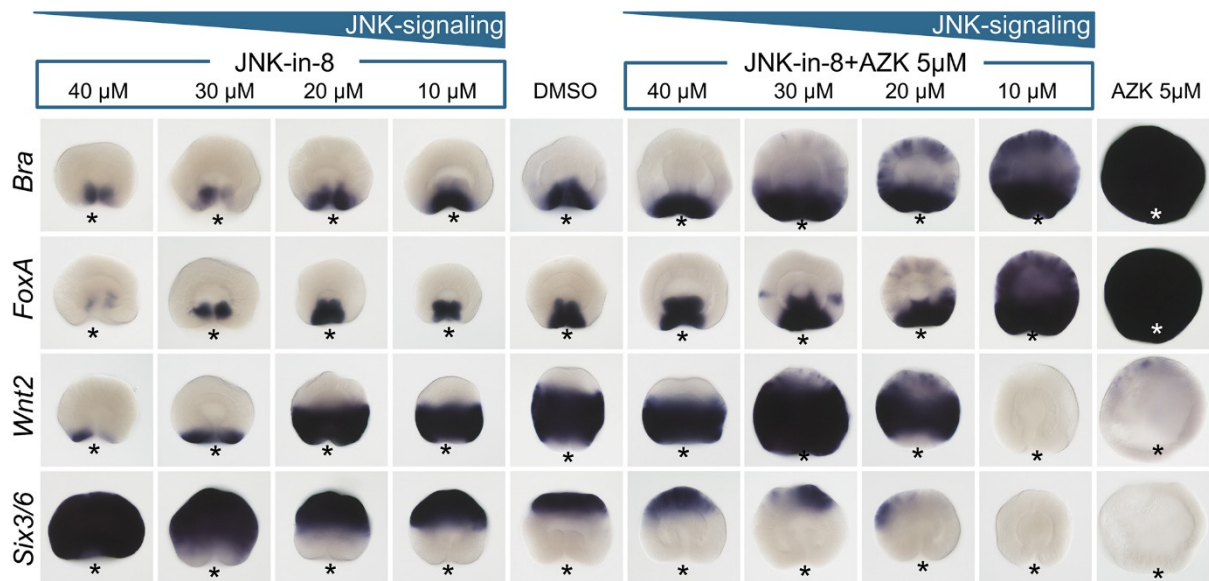
Contents

Supplementary Figure 1

Supplementary Movie legends

Supplementary Movies 1-4

Supplementary Figure



Supplementary Figure 1. JNK-in-8 treatment dose-dependently aboralizes *Nematostella* embryos and rescues oralization caused by β -catenin stabilization with azakenpaullone (AZK).

Asterisks mark the position of the blastopore.

Supplementary movie legends

Supplementary movies 1 and 2. Live imaging of the sfGFP- β -catenin dynamics during development of the *Nematostella* embryo until the onset of gastrulation. Note that nuclear sfGFP- β -catenin is visible in the interphase of every cell cycle until mid-blastula at the side opposite to where the preendodermal plate will form and start to invaginate.

Supplementary movies 3 and 4. Live imaging of the sfGFP- β -catenin dynamics during development of the *Nematostella* embryo upon GSK3 β inhibition with 5 μ M alsterpaullone. Note that nuclear sfGFP- β -catenin is localized in all nuclei throughout the embryo and keeps appearing in every cell cycle until the end of the movie, although the we filmed alsterpaullone-treated embryos for 1 hour longer than the untreated embryos shown in the Supplementary Movies 1 and 2. Also note that, as previously reported (1, 2), in the embryos incubated in GSK3 β inhibitor from fertilization on, preendodermal plates do not form.

1. I. Niedermoser, T. Lebedeva, G. Genikhovich, Sea anemone Frizzled receptors play partially redundant roles in the oral-aboral axis patterning. *Development* **149**, dev200785 (2022).
2. L. Leclère, M. Bause, C. Sinigaglia, J. Steger, F. Rentzsch, Development of the aboral domain in *Nematostella* requires beta-catenin and the opposing activities of Six3/6 and Frizzled5/8. *Development* **143**, 1766-1777 (2016).

Supplementary Movie 1

<https://www.biorxiv.org/content/biorxiv/early/2022/10/16/2022.10.15.512282/DC2/embed/media-2.mp4?download=true>

Supplementary Movie 2

<https://www.biorxiv.org/content/biorxiv/early/2022/10/16/2022.10.15.512282/DC3/embed/media-3.mp4?download=true>

Supplementary Movie 3

<https://www.biorxiv.org/content/biorxiv/early/2022/10/16/2022.10.15.512282/DC4/embed/media-4.mp4?download=true>

Supplementary Movie 4

<https://www.biorxiv.org/content/biorxiv/early/2022/10/16/2022.10.15.512282/DC5/embed/media-5.mp4?download=true>

Discussion

Summary

With my work on studying cWnt/ β -catenin signaling in *Nematostella*, I was able to manipulate the canonical Wnt/ β -catenin signaling, once at the membrane level (see Paper I: "Sea anemone Frizzled receptors play partially redundant roles in oral-aboral axis patterning.") and once at the transcription factor level (see Paper II: "Cnidarian-bilaterian comparison reveals the ancestral regulatory logic of the β -catenin dependent axial patterning."). Both points of investigation resulted in congruent and respectively supportive outcomes. The results from the *in vivo* LOF experiments were further supported by the *in vitro* reporter assay results (see Results Chapter I). Finally, through tagging endogenous β -catenin we found a surprising contradiction to a long-standing dogma concerning β -catenin's early mode of action in *Nematostella*, which significantly changes our understanding of early *Nematostella* developmental programs and their relation to the developmental programs known from the bilaterian models (see Paper III: " β -catenin-dependent endomesoderm specification appears to be a Bilateria-specific co-option.").

In *Nematostella*, zygotic patterning of the O-A axis follows cWnt/ β -catenin cues. The cWnt signaling activity sets into motion the gradual subversion of the aboral environment, restricting it to a degree that allows for the development and patterning of the oral and midbody domains. We showed that, like in Bilateria, *Nematostella* LRP5/6 is also the key co-receptor mediating canonical Wnt signaling. Interfering with specific representatives of the cWnt signaling membrane complex components is sufficient to alter, and in some cases even abolish, oral-aboral axis patterning and domain boundary establishment. This primary axis regulation appears to be a system utilized by the common ancestral organism of Bilateria and Cnidaria whereas endomesoderm development may be divergent.

Gastrulation and axial patterning

We still do not fully understand the role of β -catenin during *Nematostella* gastrulation. We showed that RNAi-mediated suppression of Wnt/ β -catenin signaling either through targeting the membrane signaling complex of Wnt/Fz/LRP5/6 or through knockdown of the key transcription factors downstream of β -catenin (the "oral regulatory module" of Bra, Lmx, FoxA, FoxB) still allowed for gastrulation, while severely affecting axial patterning. Gastrulation, however, does require β -catenin. When injected with β -catenin morpholino or electroporated with β -catenin shRNA, the embryos fail to gastrulate (Karabulut et al., 2018; Leclère et al., 2016) even despite the presence of maternal β -catenin protein clearly detectable via the green fluorescence of the eggs laid by *sfGFP- β -catenin* knock-in females (Lebedeva et al., 2022).

In order to understand the role of β -catenin in the gastrulation process it is also important to consider its likely interactions with other signaling pathways involved in the regulation of gastrulation. For example, inhibition of the PCP pathway, another signaling pathway in which Wnts act, through knockdown of the PCP pathway protein Strabismus is reported to have blocked gastrulation but not endodermal marker expression (Kumburegama et al., 2011). Strabismus morphants in said study appeared to have problems with the apical constriction of the endodermal plate cells and formation of the blastopore lip (Kumburegama et al.,

2011). Blastopore closure through convergent thickening and convergent extension (Shook et al., 2018) is regulated by Wnt11 mediated PCP signaling in *Xenopus*, and XWnt11 knockdown embryos also fail to internalize their endoderm (Shook et al., 2018; Van Itallie et al., 2023). Manipulation of the MAPK signaling pathway was also shown to be able to deregulate the completion of gastrulation in *Nematostella* (Amiel et al., 2017; Layden et al., 2016). Layden and colleagues (2016) showed that embryos treated with U0126, an inhibitor of ERK phosphorylation, initiated gastrulation, yet ultimately failed to complete it. Knockdown of the transcription factor ERG, a conserved upstream activator as well as target of MAPK signaling (Strittmatter et al., 2021), phenocopied the effect of the U0126 treatment (Amiel et al., 2017). ERG morphants segregate the endodermal tissue at the blastopore but fail to fully invaginate and complete gastrulation (Amiel et al., 2017). Curiously, *Brachyury* expression in these embryos is not confined to the blastopore lip but extends into the endodermal plate, while endodermal markers such as *SnailA* are not expressed (Amiel et al., 2017).

Another regulatory mode may also play a role. Differential behavior of invaginating blastopore lip and endodermal cells does not necessarily require a chemical basis; differences in cell shape and movement of identical cells can be driven through mechanical physics of energy minimization in a collective context (Tamulonis et al., 2011). Biological differentiation could result downstream of such mechanical causes changing the trajectories of cells in a manner not driven by biochemical cues (Chan et al., 2019). Endomesoderm triggering through mechanically induced phenomena is postulated by studies showing that mechanosensory dependent release of β -catenin from its E-cadherin bound position frees it to travel into the nucleus in *Drosophila* and Zebrafish (Brunet et al., 2013). Further, 2-cell stage mouse embryos lacking maternally deposited E-cadherin display more β -catenin nuclearization as it is not sequestered to the adhesion complexes (de Vries et al., 2004). Moreover, in *Nematostella*, mechanical compression of the embryo resulted in the upregulation of the expression of β -catenin target genes and rescued their expression in the embryos, where gastrulation movements were suppressed by a myosin light chain kinase inhibitor treatment (Pukhlyakova et al., 2018). It remains to be discovered, however, what signal initiates gastrulation morphogenesis (i.e. bottle cell formation in the endodermal plate & blastopore lip formation) in *Nematostella* development.

Endoderm specification

Our analysis of the embryos treated with AZK at different time points showed that endoderm specification took place very early in development (Niedermoser et al., 2022), and once specified, the endoderm became insensitive to upregulation of β -catenin signaling (Lebedeva et al., 2021). In line with that, in a dissociation-reaggregation experiment of the gastrula stage embryos, aggregates composed solely of endodermal cells converted into mesenchyme and did not develop further, whereas ectoderm-only aggregates, whenever they contained Wnt1- and Wnt3-expressing cells, could re-establish the germ layers, the body axes and develop into polyps (Kirillova et al., 2018). This supports our interpretation that, once specified, the endodermal cells became “uncoupled” from the ectoderm and could not revert to the ectoderm state, while ectodermal cells could become endoderm when provided with the organizer Wnt signals (Kirillova et al., 2018; Kraus et al., 2016).

Based on previous research (Kraus et al., 2016; Lebedeva et al., 2021; Leclère et al., 2016) and the results of the LRP5/6 and combined Fz knockdowns not affecting endodermal marker expression, we initially presumed that endoderm specification relied to some extent on β -catenin, just not on zygotic cWnt/ β -catenin input via the Wnt/Fz/LRP5/6 signaling complex. However, once my fellow PhD student Tatiana Lebedeva succeeded in knocking-in a fluorescent tag into the endogenous *β -catenin* locus, a completely different picture emerged. Contrary to the previous assumptions (Lee et al., 2006; Martindale & Hejnal, 2009; Wikramanayake et al., 2003), these knock-in embryos showed β -catenin nuclearization at the vegetal pole, i.e. they revealed the presence of nuclear β -catenin in all cells except the endodermal cells in the early blastula. This implies that the lack of nuclear β -catenin in the endoderm of the gastrula and, reportedly, in the polyp (Lebedeva et al., 2022; Salinas-Saavedra et al., 2018) is not due to a downregulation of β -catenin at the invaginating plate during gastrulation, but is the continuation of a feature already present in the earliest developmental stages. In the future, it will be important to find out which molecular mechanism is responsible for the endoderm specification in *Nematostella*.

Another prominent signaling mode in metazoan endomesoderm development is the Notch signaling pathway (Favarolo & López, 2018). In zebrafish, upregulation of Notch signaling activity leads to a decrease in endodermal cells, however, the counter-experiment of interfering with Notch signaling does not result in more endoderm (Kikuchi et al., 2004). In sea urchin, overactivation of Notch signaling leads to a shift of the endoderm towards the animal pole, taking over space otherwise held by ectoderm whereas the inhibition of Notch signaling allows the ectoderm to expand towards the vegetal pole restricting the space usually held by endoderm (Sherwood & McClay, 2001). Notch signaling and β -catenin signaling have been shown to interplay in multiple contexts, both synergistically and antagonistically (Andersen et al., 2012). For example, in *Drosophila* wing patterning Notch and Wnt signals rely on each other through mutual feedback loop maintenance; where *Delta* (a Notch ligand) expression activates *Wingless* (the *Drosophila Wnt1* orthologue) expression and vice versa (Hayward et al., 2008). The mode of antagonistic action of Notch signaling on cWnt however, is less well understood and could take place on different levels. For example, Notch's transcriptional targets include co-repressors of Groucho (Favarolo & López, 2018). Groucho is a TCF-repressor which is detached from TCF upon β -catenin nuclearization (Flack et al., 2017). At the protein level, the antagonistic mode of Notch signaling was shown to act on a specific subpopulation of β -catenin (Kwon et al., 2011). Kwon and colleagues (2011) showed that knockdown of Notch led to increased TCF reporter signal. Rather than altering overall β -catenin quantities at the protein or transcriptional level, Notch KD led to an increase of unphosphorylated β -catenin. This "active" form of β -catenin co-precipitated with membrane-tethered Notch, thus implying it regulates behavior of active β -catenin in the cytoplasm (Kwon et al., 2011). The role of Notch signaling during deuterostome gastrulation, however, is primarily focused on the segregation of the β -catenin-positive endoderm and β -catenin-negative mesoderm from the initially common, β -catenin-positive endomesodermal domain (McClay et al., 2021). *Nematostella* β -catenin-negative endoderm displays multiple features characteristic of the bilaterian mesoderm, while *Nematostella* β -catenin-positive oral ectoderm is more similar in cell behavior and gene expression to the bilaterian endoderm (Steinmetz et al., 2017). Therefore, an analysis of Notch signaling during the gastrulation of our model would be very interesting, however, it seems more likely that it may be involved in

the establishment of the boundary between endoderm and the blastopore lip than in the establishment of the endoderm itself.

Many accepted research results may require reevaluation through our finding that characteristics of the two poles during early *Nematostella* development are flipped. The most prominent example is the case of Dishevelled. Research by Lee et al. (2007) showed that Dishevelled protein, the essential cytoplasmic mediator of cWnt signaling, is enriched in the cortical cytoplasm of the animal hemisphere of the oocyte and, subsequently, in the area of the first cleavage furrow (Lee et al., 2007). At the blastula stage it is also confined to a single pole, which is interpreted to be the animal pole, matching the previous stages (Lee et al., 2007). Does Dishevelled relocalize after the first cleavage stages? Is aboral β -catenin nuclearization facilitated by some other forces keeping the destruction complex in check? How can we explain the lack of β -catenin nuclearization at the animal pole of our GFP tagged β -catenin embryos despite the presence of Dishevelled there? Is Dishevelled sequestered somehow at this point, which prevents it from stabilizing cytoplasmic β -catenin until it is time to regulate axial patterning? Or is the stoichiometry in favor of the destruction complex components at this time and space? Previous research in *Drosophila* has shown that significant Axin upregulation could render the destruction complex resistant to being inhibited by endogenous levels of Dishevelled, whereas an increased amount of Dishevelled did not significantly perturb the destruction complex activity (Schaefer et al., 2018; Wang et al., 2016). Schaefer and colleagues (2020) even showed that Dishevelled might even compete with itself for its own Axin binding domains, essentially antagonizing its own capacity of sequestering Axin (Schaefer et al., 2020).

Receptor and ligand redundancy

Through the process of knocking down the Fz receptors in *Nematostella* individually as well as in all possible combinations, a certain redundancy in relation to β -catenin dependent patterning revealed itself. In single Fz gene knockdowns, only Fz5 knockdown elicited the "classic canonical β -catenin inhibition" phenotype, i.e. the aboralization of the embryo, which has already been studied and published several years ago (Leclère et al., 2016). Despite its dominance over the other *Nematostella* Fzs as an individual, the other Fzs clearly also play a role in transducing Wnt signals, as only the quadruple Fz-knockdown, but not any of the triple or double knockdowns, were able to replicate the LRP5/6 LOF phenotype. Despite the noise in the Wnt/ β -catenin reporter assay in cell culture, combined Fz10+ Wnt3 expression elicited a significant level of reporter signal, next to that of Fz5+ Wnt4 and Fz5+ Wnt1 combinations. The phenotypes of the combined Fz+ Wnt knockdowns recapitulate the *in vitro* findings and further support the picture that orally expressed Fz10 may be the next in line in terms of signaling strength and general importance in the cWnt/ β -catenin pathway in *Nematostella*. Further, both Fz1 knockdown, Fz10 knockdown and even more so the Fz10 MO, were often associated with a delay in development at the gastrula stage, which was also sustained to later time points in the case of Fz10 knockdown. This suggests that Fz10-mediated Wnt signaling may be involved in orchestrating the gastrulation movements, which, as discussed previously, require β -catenin. The gastrulation delay phenotype was also a characteristic of Wnt2 knockdowns. In the future, it will be important to address the potential roles of Wnt2 and Fz10 in the blastopore lip formation and its function during the invagination of the endoderm.

Partial redundancies across Fz and Wnt are seen in other systems as well (Bhat, 1998; Dong et al., 2018; Gleason et al., 2006; Matsui et al., 2005; Yu et al., 2012) and have been demonstrated *in vitro* (Voloshanenko et al., 2017).

Unresolved phenotypes

Enhanced β -catenin target gene expression at the midbody/aboral boundary

Early Wnts and many cWnt target genes are expressed orally in *Nematostella* (Lee et al., 2006). Curiously, certain β -catenin target genes highly sensitive to changes in β -catenin signaling levels show an additional or enhanced expression at the boundary between the *Wnt2*-positive midbody domain and the *Wnt*-negative aboral domain. Below, I will refer to this area as the "ring". The presence of the ring suggested enhanced cWnt signaling there. By quantifying the spatial distribution of nuclear β -catenin in the embryos expressing GFP-tagged endogenous β -catenin we revealed a "bump" of β -catenin nuclearization in the ring, reflective of the cWnt target gene expression patterns. The ring of enriched β -catenin target gene expression is evident in wildtype expression of the β -catenin target gene *Axin*. Curiously, this expression is enhanced in the *Fz1+4+10* triple KD, a phenotype already detectable in some of the dual *Fz1+Fz10* and *Fz1+Fz4* knockdowns. Further evidence of the enhanced cWnt/ β -catenin signaling in the ring in the triple *Fz* KD is the upregulated *Brachyury* expression there. This is also reflected in the enhanced signal of *Wnt2* expression in the aboral-most part of the *Wnt2* expression domain as well as a reduction of the expression of the aboral marker *Six3/6* at the oral boundary of its expression. Intriguingly, the *Fz1+4+10* KD, which displays enhanced *Brachyury* expression in the ring, displays weaker oral *Brachyury* expression compared to controls.

One way to explain the ring phenotype is by possible competition between the Fz receptors for the Wnt ligands. Although not strongly expressed at the midbody/aboral boundary, Fz5, being the most potent cWnt/ β -catenin Fz receptor. When left without competition from other Fz proteins, Fz5 likely elicits a stronger than normal β -catenin signaling in this area. The reduction of the *Brachyury* expression in the oral domain upon *Fz1+4+10* KD suggests that even though *Fz5* is expressed in an aboral-to-oral gradient, its quantity on the oral end of the embryo is negligible, and its higher signaling capacity cannot compensate for this.

Addressing the generation of enhanced β -catenin in this ring domain of the gastrula also requires addressing how one could explain a cWnt signaling mode so far away from the oral Wnt expression hub at this stage (with exception of *Wnt2*). In the introduction, I briefly mentioned the studied modes of extracellular Wnt transport and the Wnt characteristics which may complicate its free movement post-secretion. The mechanisms of extracellular Wnt movement in *Nematostella* are still unknown. For example, *Wnt4* KD closely phenocopies *Fz5* KD, which suggests that they are likely signaling partners. However, it is unclear how orally expressed *Wnt4* reaches the aborally expressed Fz5. The potential interactions of Fz5 and Wnt3 would follow the same logic. Interactions of oral Wnts with the other Fz, the expression of which lies in close proximity to the oral Wnt expression domains, would not require such a lengthy travel. Teams around Pani & Goldstein (2018) and

Recouvreux et al. (2023) visualized Wnt movement *in vivo* in *C.elegans*, an organism in which, similar to *Nematostella*, the strongest Fz (MOM-5) expression maximum is not at the site of Wnt maxima but at the opposing side. These teams demonstrated that freely diffusing Wnts could travel from their posterior site of origin all the way to the anterior of the embryo congruous with a model of free diffusion (Recouvreux et al., 2023), seen in axons as well (Pani et al., 2023). Furthermore, it was shown that Wnts could travel half the length of the embryo in under a minute (Recouvreux et al., 2023). These findings would suggest that the long-range interactions of *Nematostella* oral Wnts with the aboral Fz5 through means of diffusion may be less unlikely than previously thought. In the future, it will be interesting to test which Wnt ligands are responsible for the signaling in the "Axin ring" by performing simultaneous KDs of *Fz1+4+10* together with each of the Wnt ligands.

Simultaneous weakening and expansion of *Brachyury* expression

In the *FoxB*, *Wnt1* and *Wnt3* knockdowns (and all the combinations that involve either one of these) the expression domain of *Brachyury* expands both aborally, towards the midbody ("outward expansion"), as well as further orally, invading the bottom of the pharyngeal domain ("inward expansion"). The surface area of expression increases while the expression strength changes differentially concerning the 2 directions of expansion. The *Brachyury* expression of the outward expanding domain appears weaker than the enhanced signal strength detected for the inward expanding domain. Apart from visualizing the weakened-despite-expanding *Brachyury* oral domain through ISH (in situ hybridization), the inductive capacity of the blastopore lip was also shown to be reduced in *FoxB* knockdowns (Lebedeva et al., 2021). ERG-MO embryos also showed weaker *FoxB* expression (although not abolished) and also displayed an expansion of *Brachyury*'s oral expression domain (Amiel et al., 2017). To explain this phenotype further research is necessary.

Outlook

It would be interesting to work out the further implications of the structural differences between different Wnts and Fzs on their binding preferences and signal propagation compatibility in cell culture. For example, investigating if *Nematostella* Wnts reflect to some extent the 2 binding groups for LRP5/6 regions E1E2 vs. E3E4. Especially the domain swapping of cytosolic domains across the different *Nematostella* Fz as well as between *Nematostella* and human Fz is compelling. This could give clues as to which characteristics explain the different signal induction capacities across the different *Nematostella* Fz. It would also be interesting to see if co-expression of *Nematostella* Dishevelled would bring signaling levels up to those seen in the reporter assay results obtained when expressing human Fz. If this were the case, it could suggest that certain intracellular domains of the *Nematostella* membrane complex may not work together with the endogenous human Dishevelled as intended.

Further research is necessary to be able to update our working model of early β -catenin dependent developmental processes and their implications for our understanding of the *Nematostella* MZT (maternal to zygotic transition). Does β -catenin nuclearization happen prior to the MZT, and if yes, does pre-MZT-nuclearization "prime" the zygotic transcriptional response as seen in *Xenopus* (Blythe, 2009; Blythe et al., 2010)? How is this related to the cWnt/ β -catenin chromatin modulation, and subsequent effects on target gene expression,

seen in regenerative processes (Pascual-Carreras et al., 2023)? Previous studies showed that β -catenin/TCF function prior to MZT can suppress β -catenin target activation and dorsal program activation post MZT, whereas blocking β -catenin/TCF function at MZT or post MZT does not prevent the implementation of the dorsal program, showing that the maternal β -catenin activity and zygotic β -catenin activity hold different, sometimes mutually exclusive, functions and capabilities (Blythe, 2009; Hamilton et al., 2001; Heasman et al., 2000; Yang et al., 2002). Is this down to the same or similar mechanisms of pre-transcriptional chromatin modulation?

What keeps our GFP-tagged β -catenin from nuclearization in the pre-endodermal plate? Is it enhanced activity of the destruction complex, the differences of destruction complex component availability or some completely different mechanism? These and many more enticing questions arise from our findings.

Scientific contribution of the PhD project

In my work, I was able to start addressing a long-standing question of the relative relevance and functions of *Nematostella* Wnt and Fz in cWnt/ β -catenin-dependent axis patterning. We showed which components featured most prominently and had the greatest functional impact on cWnt/ β -catenin signaling in early development of *Nematostella*. My functional *in vivo* experiments were supported by my *in vitro* assays and demonstrated the strongest cWnt/ β -catenin signaling roles are taken on by a small number of representatives (i.e. LRP5/6, Fz5, Fz10, Wnt3, Wnt4). The fine-tuning of cWnt/ β -catenin signaling involves a more complex network of nearly all membrane complex representatives taking on more subtle roles in regulating proper embryonic development of *Nematostella vectensis*. I also contributed to the analysis of the roles of β -catenin signaling and transcription factors downstream of β -catenin in the processes of germ layer specification, gastrulation, and axial patterning. Much of the generated data allows for further research into the peculiarities of β -catenin signaling in early *Nematostella* development and how it might place in the evolutionary development of this signaling cascade's functions and mechanisms of action.

References

- Aberle, H., Bauer, A., Kispert, A., & Kemler, R. (1997). β -catenin is a target for the ubiquitin–proteasome pathway. *The EMBO Journal*, 16(13), 3797–3804. <https://doi.org/10.1093/emboj/16.13.3797>
- Acebron, S. P., & Niehrs, C. (2016). β -Catenin-Independent Roles of Wnt/LRP6 Signaling. *Trends in Cell Biology*, 26(12), 956–967. <https://doi.org/10.1016/j.tcb.2016.07.009>
- Agostino, M., & Pohl, S. Ö. G. (2019). Wnt binding affinity prediction for putative frizzled-type cysteine-rich domains. *International Journal of Molecular Sciences*, 20(17). <https://doi.org/10.3390/ijms20174168>
- Agostino, M., Pohl, S. Ö. G., & Dharmarajan, A. (2017). Structure-based prediction of Wnt binding affinities for frizzled-type cysteine-rich domains. *Journal of Biological Chemistry*, 292(27), 11218–11229. <https://doi.org/10.1074/jbc.M117.786269>
- Al-Shaer, L., Leach, W., Baban, N., Yagodich, M., Gibson, M. C., & Layden, M. J. (2023). Environmental and molecular regulation of asexual reproduction in the sea anemone *Nematostella vectensis*. *BioRxiv*, 2023.01.27.525773. <https://doi.org/10.1101/2023.01.27.525773>
- Amiel, A. R., Johnston, H., Chock, T., Dahlin, P., Iglesias, M., Layden, M., Röttinger, E., & Martindale, M. Q. (2017). A bipolar role of the transcription factor ERG for cnidarian germ layer formation and apical domain patterning. *Developmental Biology*, 430(2), 346–361. <https://doi.org/10.1016/j.ydbio.2017.08.015>
- Andersen, P., Uosaki, H., Shenje, L. T., & Kwon, C. (2012). Non-canonical Notch signaling: Emerging role and mechanism. *Trends in Cell Biology*, 22(5), 257–265. <https://doi.org/10.1016/j.tcb.2012.02.003>
- Anlas K, Trivedi V. Studying evolution of the primary body axis in vivo and in vitro. *Elife*. 2021 Aug 31;10:e69066. doi: 10.7554/eLife.69066. PMID: 34463611; PMCID: PMC8456739.
- Bänziger, C., Soldini, D., Schütt, C., Zipperlen, P., Hausmann, G., & Basler, K. (2006). Wntless, a conserved membrane protein dedicated to the secretion of Wnt proteins from signaling cells. *Cell*, 125(3), 509–522. <https://doi.org/10.1016/j.cell.2006.02.049>
- Bartscherer, K., Pelte, N., Ingelfinger, D., & Boutros, M. (2006). Secretion of Wnt ligands requires Evi, a conserved transmembrane protein. *Cell*, 125(3), 523–533. <https://doi.org/10.1016/j.cell.2006.04.009>
- Beddington, R. S. P., & Robertson, E. J. (1999). Axis development and early asymmetry in mammals. *Cell*, 96(2), 195–209. [https://doi.org/10.1016/S0092-8674\(00\)80560-7](https://doi.org/10.1016/S0092-8674(00)80560-7)
- Berman, H. M., Westbrook, J., Feng, Z., Gilliland, G., Bhat, T. N., Weissig, H., Shindyalov, I. N., & Bourne, P. E. (2000). The Protein Data Bank. *Nucleic Acids Research*, 28(1), 235–242. <https://doi.org/10.1093/nar/28.1.235>
- Bhat, K. M. (1998). Frizzled and frizzled 2 Play a Partially Redundant Role in Wingless Signaling and Have Similar Requirements to Wingless in Neurogenesis. *Cell*, 95(7), 1027–1036. [https://doi.org/10.1016/S0092-8674\(00\)81726-2](https://doi.org/10.1016/S0092-8674(00)81726-2)
- Blythe, S. (2009). Transcriptional Poising Prior to the Midblastula Transition Underlies Dorsal Cell Fate Specification by the Wnt/Beta-Catenin Pathway. *Publicly Accessible Penn Dissertations*. <https://repository.upenn.edu/edissertations/242>
- Blythe, S. A., Cha, S.-W., Tadjuidje, E., Heasman, J., & Klein, P. S. (2010). β -catenin Primes Organizer Gene Expression By Recruiting a Histone H3 Arginine 8

- Methyltransferase, Prmt2. *Developmental Cell*, 19(2), 220–231.
<https://doi.org/10.1016/j.devcel.2010.07.007>
- Bourhis, E., Tam, C., Franke, Y., Bazan, J. F., Ernst, J., Hwang, J., Costa, M., Cochran, A. G., & Hannoush, R. N. (2010). Reconstitution of a Frizzled8-Wnt3a-LRP6 signaling complex reveals multiple Wnt and Dkk1 binding sites on LRP6. *Journal of Biological Chemistry*, 285(12), 9172–9179. <https://doi.org/10.1074/jbc.M109.092130>
- Brennan, K., Gonzalez-Sancho, J. M., Castelo-Soccio, L. A., Howe, L. R., & Brown, A. M. C. (2004). Truncated mutants of the putative Wnt receptor LRP6/Arrow can stabilize β -catenin independently of Frizzled proteins. *Oncogene*, 23(28), 4873–4884.
<https://doi.org/10.1038/sj.onc.1207642>
- Brunet, T., Bouclet, A., Ahmadi, P., Mitrossilis, D., Driquez, B., Brunet, A. C., Henry, L., Serman, F., Béalle, G., Ménager, C., Dumas-Bouchiat, F., Givord, D., Yanicostas, C., Le-Roy, D., Dempsey, N. M., Plessis, A., & Farge, E. (2013). Evolutionary conservation of early mesoderm specification by mechanotransduction in Bilateria. *Nature Communications*, 4, 1–15. <https://doi.org/10.1038/ncomms3821>
- Bugaj, L. J., Choksi, A. T., Mesuda, C. K., Kane, R. S., & Schaffer, D. V. (2013). Optogenetic protein clustering and signaling activation in mammalian cells. *Nature Methods*, 10(3), 249–252. <https://doi.org/10.1038/nmeth.2360>
- Cha, S.-W., Tadjuidje, E., White, J., Wells, J., Mayhew, C., Wylie, C., & Heasman, J. (2009). Wnt11/5a complex formation caused by tyrosine sulfation increases canonical signaling activity. *Current Biology: CB*, 19(18), 1573–1580.
<https://doi.org/10.1016/j.cub.2009.07.062>
- Chan, C. J., Costanzo, M., Ruiz-Herrero, T., Mönke, G., Petrie, R. J., Bergert, M., Diz-Muñoz, A., Mahadevan, L., & Hiiragi, T. (2019). Hydraulic control of mammalian embryo size and cell fate. *Nature*, 571(7763), 112–116.
<https://doi.org/10.1038/s41586-019-1309-x>
- Chen, Q., Su, Y., Wesslowski, J., Hagemann, A. I., Ramialison, M., Wittbrodt, J., Scholpp, S., & Davidson, G. (2014). Tyrosine phosphorylation of LRP 6 by Src and Fer inhibits Wnt/ β -catenin signalling. *EMBO Reports*, 15(12), 1254–1267.
<https://doi.org/10.15252/embr.201439644>
- Chen, S., Bubeck, D., MacDonald, B. T., Liang, W. X., Mao, J. H., Malinauskas, T., Llorca, O., Aricescu, A. R., Siebold, C., He, X., & Jones, E. Y. (2011). Structural and functional studies of LRP6 ectodomain reveal a platform for Wnt signaling. *Developmental Cell*, 21(5), 848–861. <https://doi.org/10.1016/j.devcel.2011.09.007>
- Cheng, Z., Biechele, T., Wei, Z., Morrone, S., Moon, R. T., Wang, L., & Xu, W. (2011). Crystal structures of the extracellular domain of LRP6 and its complex with DKK1. *Nature Structural and Molecular Biology*, 18(11), 1204–1210.
<https://doi.org/10.1038/nsmb.2139>
- Coombs, G. S., Yu, J., Canning, C. A., Veltri, C. A., Covey, T. M., Cheong, J. K., Utomo, V., Banerjee, N., Zhang, Z. H., Jadulco, R. C., Concepcion, G. P., Bugni, T. S., Harper, M. K., Mihalek, I., Jones, C. M., Ireland, C. M., & Virshup, D. M. (2010). WLS-dependent secretion of WNT3A requires Ser209 acylation and vacuolar acidification. *Journal of Cell Science*, 123(19), 3357–3367. <https://doi.org/10.1242/jcs.072132>
- Croce, J. C., & McClay, D. R. (2008). *Evolution of the Wnt Pathways* (Vol. 469, pp. 3–18).
https://doi.org/10.1007/978-1-60327-469-2_1
- Darras, S., Fritzenwanker, J. H., Uhlinger, K. R., Farrelly, E., Pani, A. M., Hurley, I. A., Norris, R. P., Osovitz, M., Terasaki, M., Wu, M., Aronowicz, J., Kirschner, M., Gerhart, J. C., & Lowe, C. J. (2018). Anteroposterior axis patterning by early

- canonical Wnt signaling during hemichordate development. *PLoS Biology*, 16(1).
<https://doi.org/10.1371/journal.pbio.2003698>
- Darras, S., Gerhart, J., Terasaki, M., Kirschner, M., & Lowe, C. J. (2011). β -catenin specifies the endomesoderm and defines the posterior organizer of the hemichordate *Saccoglossus kowalevskii*. *Development (Cambridge, England)*, 138(5), 959–970.
<https://doi.org/10.1242/dev.059493>
- De Robertis, E. M. (2010). Wnt Signaling in Axial Patterning and Regeneration: Lessons from Planaria. *Science Signaling*, 3(127), pe21–pe21.
<https://doi.org/10.1126/scisignal.3127pe21>
- de Vries, W. N., Evsikov, A. V., Haac, B. E., Fancher, K. S., Holbrook, A. E., Kemler, R., Solter, D., & Knowles, B. B. (2004). Maternal β -catenin and E-cadherin in mouse development. *Development*, 131(18), 4435–4445. <https://doi.org/10.1242/dev.01316>
- Debnath, P., Huirem, R. S., & Dutta, P. (2021). *Epithelial – mesenchymal transition and its transcription factors*. 0, 1–29.
- Dijksterhuis, J. P., Baljinnyam, B., Stanger, K., Sercan, H. O., Ji, Y., Andres, O., Rubin, J. S., Hannoush, R. N., & Schulte, G. (2015). Systematic mapping of WNT-FZD protein interactions reveals functional selectivity by distinct WNT-FZD pairs. *Journal of Biological Chemistry*, 290(11), 6789–6798. <https://doi.org/10.1074/jbc.M114.612648>
- Dijksterhuis, J. P., Petersen, J., & Schulte, G. (2014). WNT/Frizzled signalling: Receptor-ligand selectivity with focus on FZD-G protein signalling and its physiological relevance: IUPHAR Review 3. *British Journal of Pharmacology*, 171(5), 1195–1209.
<https://doi.org/10.1111/bph.12364>
- Dillman, A. R., Minor, P. J., & Sternberg, P. W. (2013). Origin and evolution of dishevelled. *G3 (Bethesda, Md.)*, 3(2), 251–262. <https://doi.org/10.1534/g3.112.005314>
- Dong, B., Vold, S., Olvera-Jaramillo, C., & Chang, H. (2018). Functional redundancy of *Frizzled 3* and *Frizzled 6* in planar cell polarity control of mouse hair follicles. *Development*, dev.168468. <https://doi.org/10.1242/dev.168468>
- Duffy, D. J., Plickert, G., Kuenzel, T., Tilmann, W., & Frank, U. (2010). Wnt signaling promotes oral but suppresses aboral structures in *Hydractinia* metamorphosis and regeneration. *Development*, 137(18), 3057–3066. <https://doi.org/10.1242/dev.046631>
- Erwin, D. H., & Davidson, E. H. (2009). The evolution of hierarchical gene regulatory networks. *Nature Reviews Genetics*, 10(2), Article 2. <https://doi.org/10.1038/nrg2499>
- Ettenberg, S. A., Charlat, O., Daley, M. P., Liu, S., Vincent, K. J., Stuart, D. D., Schuller, A. G., Yuan, J., Ospina, B., Green, J., Yu, Q., Walsh, R., Li, S., Schmitz, R., Heine, H., Bilic, S., Ostrom, L., Mosher, R., Hartlepp, K. F., ... Cong, F. (2010). Inhibition of tumorigenesis driven by different Wnt proteins requires blockade of distinct ligand-binding regions by LRP6 antibodies. *Proceedings of the National Academy of Sciences of the United States of America*, 107(35), 15473–15478.
<https://doi.org/10.1073/pnas.1007428107>
- Eubelen, M., Bostaille, N., Cabochette, P., Gauquier, A., Tebabi, P., Dumitru, A. C., Koehler, M., Gut, P., Alsteens, D., Stainier, D. Y. R., Garcia-Pino, A., & Vanhollebeke, B. (2018). A molecular mechanism for Wnt ligand-specific signaling. *Science*, 361(6403). <https://doi.org/10.1126/science.aat1178>
- Favarolo, M. B., & López, S. L. (2018). Notch signaling in the division of germ layers in bilaterian embryos. *Mechanisms of Development*, 154(March), 122–144.
<https://doi.org/10.1016/j.mod.2018.06.005>
- Flack, J. E., Mieszczanek, J., Novcic, N., & Bienz, M. (2017). Wnt-Dependent Inactivation of the Groucho/TLE Co-repressor by the HECT E3 Ubiquitin Ligase Hyd/UBR5.

- Molecular Cell*, 67(2), 181-193.e5. <https://doi.org/10.1016/j.molcel.2017.06.009>
- Fritzenwanker, J. H., & Technau, U. (2002). Induction of gametogenesis in the basal cnidarian *Nematostella vectensis* (Anthozoa). *Development Genes and Evolution*, 212(2), 99–103. <https://doi.org/10.1007/s00427-002-0214-7>
- Galli, L. M., Barnes, T. L., Secrest, S. S., Kadowaki, T., & Burrus, L. W. (2007). Porcupine-mediated lipid-modification regulates the activity and distribution of Wnt proteins in the chick neural tube. *Development*, 134(18), 3339–3348. <https://doi.org/10.1242/dev.02881>
- Gammons, M., & Bienz, M. (2018). Multiprotein complexes governing Wnt signal transduction. *Current Opinion in Cell Biology*, 51, 42–49. <https://doi.org/10.1016/j.ceb.2017.10.008>
- García de Herreros & Duñach. (2019). Intracellular Signals Activated by Canonical Wnt Ligands Independent of GSK3 Inhibition and β -Catenin Stabilization. *Cells*, 8(10), 1148–1148. <https://doi.org/10.3390/cells8101148>
- Genikhovich, G., Fried, P., Prünster, M. M., Schinko, J. B., Gilles, A. F., Fredman, D., Meier, K., Iber, D., & Technau, U. (2015). Axis Patterning by BMPs: Cnidarian Network Reveals Evolutionary Constraints. *Cell Reports*, 10(10), 1646–1654. <https://doi.org/10.1016/j.celrep.2015.02.035>
- Genikhovich, G., & Technau, U. (2017). On the evolution of bilaterality. *Development (Cambridge)*, 144(19), 3392–3404. <https://doi.org/10.1242/dev.141507>
- Gilbert, S. F. (2000). Principles of Development: Life Cycles and Developmental Patterns. In *Developmental Biology. 6th edition*. Sinauer Associates. <https://www.ncbi.nlm.nih.gov/books/NBK10125/>
- Gleason, J. E., Szyleyko, E. A., & Eisenmann, D. M. (2006). Multiple redundant Wnt signaling components function in two processes during *C. elegans* vulval development. *Developmental Biology*, 298(2), 442–457. <https://doi.org/10.1016/j.ydbio.2006.06.050>
- Gong, Y., Bourhis, E., Chiu, C., Stawicki, S., Dealmeida, V. I., Liu, B. Y., Phamluong, K., Cao, T. C., Carano, R. A. D., Ernst, J. A., Solloway, M., Rubinfeld, B., Hannoush, R. N., Wu, Y., Polakis, P., & Costa, M. (2010). Wnt isoform-specific interactions with coreceptor specify inhibition or potentiation of signaling by LRP6 antibodies. *PLoS ONE*, 5(9), 1–17. <https://doi.org/10.1371/journal.pone.0012682>
- Grainger, S., Nguyen, N., Richter, J., Setayesh, J., Lonquich, B., Oon, C. H., Wozniak, J. M., Barahona, R., Kamei, C. N., Houston, J., Carrillo-Terrazas, M., Drummond, I. A., Gonzalez, D., Willert, K., & Traver, D. (2018). EGFR confers exquisite specificity of Wnt9a-Fzd9b signaling in hematopoietic stem cell development Running title: A mechanism for Wnt-Fzd specificity in hematopoietic stem cells. *bioRxiv* 387043; doi: <https://doi.org/10.1101/387043> <https://doi.org/10.1101/387043>
- Grainger, S., & Willert, K. (2018). Mechanisms of Wnt signaling and control. *Wiley Interdisciplinary Reviews: Systems Biology and Medicine*, 10(5). <https://doi.org/10.1002/wsbm.1422>
- Greenfeld, H., Lin, J., & Mullins, M. C. (2021). The BMP signaling gradient is interpreted through concentration thresholds in dorsal–ventral axial patterning. *PLOS Biology*, 19(1), e3001059. <https://doi.org/10.1371/journal.pbio.3001059>
- Guder, C., Pinho, S., Nacak, T. G., Schmidt, H. A., Hobmayer, B., Niehrs, C., & Holstein, T. W. (2006). An ancient Wnt-Dickkopf antagonism in Hydra. *Development (Cambridge, England)*, 133(5), 901–911. <https://doi.org/10.1242/dev.02265>
- Gufler, S., Artes, B., Bielen, H., Krainer, I., Eder, M.-K., Falschlunger, J., Bollmann, A.,

- Ostermann, T., Valovka, T., Hartl, M., Bister, K., Technau, U., & Hobmayer, B. (2018). β -Catenin acts in a position-independent regeneration response in the simple eumetazoan Hydra. *Developmental Biology*, *433*(2), 310–323. <https://doi.org/10.1016/j.ydbio.2017.09.005>
- Gurley, K. A., Rink, J. C., & Alvarado, A. S. (2008). β -Catenin Defines Head Versus Tail Identity During Planarian Regeneration and Homeostasis. *Science*, *319*(5861), 323–327. <https://doi.org/10.1126/science.1150029>
- Hamilton, F. S., Wheeler, G. N., & Hoppler, S. (2001). Difference in XTcf-3 dependency accounts for change in response to β -catenin-mediated Wnt signalling in *Xenopus* blastula. *Development*, *128*(11), 2063–2073. <https://doi.org/10.1242/dev.128.11.2063>
- Hand, C., & Uhlinger, K. R. (1995). Asexual Reproduction by Transverse Fission and Some Anomalies in the Sea Anemone *Nematostella vectensis*. *Invertebrate Biology*, *114*(1), 9–18. <https://doi.org/10.2307/3226948>
- Hannezo, E., & Heisenberg, C. P. (2019). Mechanochemical Feedback Loops in Development and Disease. *Cell*, *178*(1), 12–25. <https://doi.org/10.1016/j.cell.2019.05.052>
- Hayward, P., Kalmar, T., & Arias, A. M. (2008). Wnt/Notch signalling and information processing during development. *Development*, *135*(3), 411–424. <https://doi.org/10.1242/dev.000505>
- Heasman, J., Kofron, M., & Wylie, C. (2000). β Catenin Signaling Activity Dissected in the Early *Xenopus* Embryo: A Novel Antisense Approach. *Developmental Biology*, *222*(1), 124–134. <https://doi.org/10.1006/dbio.2000.9720>
- Hensel, K., Lotan, T., Sanders, S. M., Cartwright, P., & Frank, U. (2014). Lineage-specific evolution of cnidarian Wnt ligands. *Evolution and Development*, *16*(5), 259–269. <https://doi.org/10.1111/ede.12089>
- Hikasa, H., & Sokol, S. Y. (2013). Wnt signaling in vertebrate axis specification. *Cold Spring Harbor Perspectives in Biology*, *5*(1). <https://doi.org/10.1101/cshperspect.a007955>
- Hirai, H., Matoba, K., Mihara, E., Arimori, T., & Takagi, J. (2019). Crystal structure of a mammalian Wnt–frizzled complex. *Nature Structural and Molecular Biology*. <https://doi.org/10.1038/s41594-019-0216-z>
- Hobmayer, B., Rentzsch, F., Kuhn, K., Happel, C. M., von Laue, C. C., Snyder, P., Rothbacher, U., & Holstein, T. W. (2000). WNT signalling molecules act in axis formation in the diploblastic metazoan Hydra. *Nature*, *407*(6801), Article 6801. <https://doi.org/10.1038/35025063>
- Hua, Y., Yang, Y., Li, Q., He, X., Zhu, W., Wang, J., & Gan, X. (2018). Oligomerization of Frizzled and LRP5/6 protein initiates intracellular signaling for the canonical WNT/ β -catenin pathway. *Journal of Biological Chemistry*, *293*(51), 19710–19724. <https://doi.org/10.1074/jbc.RA118.004434>
- Hudson, C., Kawai, N., Negishi, T., & Yasuo, H. (2013). B-Catenin-Driven Binary Fate Specification Segregates Germ Layers in Ascidian Embryos. *Current Biology*, *23*(6), 491–495. <https://doi.org/10.1016/j.cub.2013.02.005>
- Huelsken, J., Vogel, R., Brinkmann, V., Erdmann, B., Birchmeier, C., & Birchmeier, W. (2000). Requirement for β -catenin in anterior-posterior axis formation in mice. *Journal of Cell Biology*, *148*(3), 567–578. <https://doi.org/10.1083/jcb.148.3.567>
- Iglesias, M., Gomez-Skarmeta, J. L., Saló, E., & Adell, T. (2008). Silencing of *Smed- β catenin1* generates radial-like hypercephalized planarians. *Development*, *135*(7), 1215–1221. <https://doi.org/10.1242/dev.020289>
- Isaeva, V. V., & Kasyanov, N. V. (2021). Symmetry transformations in metazoan evolution

- and development. *Symmetry*, 13(2), 1–31. <https://doi.org/10.3390/sym13020160>
- Jackstadt, R., Hodder, M. C., & Sansom, O. J. (2020). WNT and β -Catenin in Cancer: Genes and Therapy. *Annual Review of Cancer Biology*, 4, 177–196. <https://doi.org/10.1146/annurev-cancerbio-030419-033628>
- Janda, C. Y., Waghray, D., Levin, A. M., Thomas, C., & Garcia, K. C. (2012). Structural basis of Wnt recognition by frizzled. *Science*, 336(6090), 59–64. <https://doi.org/10.1126/science.1222879>
- Jumper, J., Evans, R., Pritzel, A., Green, T., Figurnov, M., Ronneberger, O., Tunyasuvunakool, K., Bates, R., Žídek, A., Potapenko, A., Bridgland, A., Meyer, C., Kohl, S. A. A., Ballard, A. J., Cowie, A., Romera-Paredes, B., Nikolov, S., Jain, R., Adler, J., ... Hassabis, D. (2021). Highly accurate protein structure prediction with AlphaFold. *Nature*, 596(7873), 583–589. <https://doi.org/10.1038/s41586-021-03819-2>
- Kakugawa, S., Langton, P. F., Zebisch, M., Howell, S. A., Chang, T.-H., Liu, Y., Feizi, T., Bineva, G., O'Reilly, N., Snijders, A. P., Jones, E. Y., & Vincent, J.-P. (2015). Notum deacylates Wnt proteins to suppress signalling activity. *Nature*, 519(7542), Article 7542. <https://doi.org/10.1038/nature14259>
- Karabulut, A., He, S., Chen, C. Y., McKinney, S. A., & Gibson, M. C. (2019). Electroporation of short hairpin RNAs for rapid and efficient gene knockdown in the starlet sea anemone, *Nematostella vectensis*. *Developmental biology*, 448(1), 7–15. <https://doi.org/10.1016/j.ydbio.2019.01.005>
- Kawakami, Y., Esteban, C. R., Raya, M., Kawakami, H., Martí, M., Dubova, I., & Belmonte, J. C. I. (2006). Wnt/ β -catenin signaling regulates vertebrate limb regeneration. *Genes & Development*, 20(23), 3232–3237. <https://doi.org/10.1101/gad.1475106>
- Kikuchi, Y., Verkade, H., Reiter, J. F., Kim, C. H., Chitnis, A. B., Kuroiwa, A., & Stainier, D. Y. R. (2004). Notch Signaling Can Regulate Endoderm Formation in Zebrafish. *Developmental Dynamics*, 229(4), 756–762. <https://doi.org/10.1002/dvdy.10483>
- Kinney, B. A., Al Anber, A., Row, R. H., Tseng, Y. J., Weidmann, M. D., Knaut, H., & Martin, B. L. (2020). Sox2 and Canonical Wnt Signaling Interact to Activate a Developmental Checkpoint Coordinating Morphogenesis with Mesoderm Fate Acquisition. *Cell Reports*, 33(4), 108311–108311. <https://doi.org/10.1016/j.celrep.2020.108311>
- Kirillova, A., Genikhovich, G., Pukhlyakova, E., Demilly, A., Kraus, Y., & Technau, U. (2018). Germ-layer commitment and axis formation in sea anemone embryonic cell aggregates. *Proceedings of the National Academy of Sciences of the United States of America*, 115(8), 1813–1818. <https://doi.org/10.1073/pnas.1711516115>
- Ko, S. B., Mihara, E., Park, Y., Roh, K., Kang, C., Takagi, J., Bang, I., & Choi, H. J. (2022). Functional role of the Frizzled linker domain in the Wnt signaling pathway. *Communications Biology*, 5(1). <https://doi.org/10.1038/s42003-022-03370-4>
- Koch, S. (2021). Regulation of wnt signaling by fox transcription factors in cancer. *Cancers*, 13(14). <https://doi.org/10.3390/cancers13143446>
- Komekado, H., Yamamoto, H., Chiba, T., & Kikuchi, A. (2007). Glycosylation and palmitoylation of Wnt-3a are coupled to produce an active form of Wnt-3a. *Genes to Cells*, 12(4), 521–534. <https://doi.org/10.1111/j.1365-2443.2007.01068.x>
- Kraus, Y., Aman, A., Technau, U., & Genikhovich, G. (2016). Pre-bilaterian origin of the blastoporal axial organizer. *Nature Communications*, 7(May), 1–9. <https://doi.org/10.1038/ncomms11694>
- Kumburegama, S., Wijesena, N., Xu, R., & Wikramanayake, A. H. (2011). Strabismus-mediated primary archenteron invagination is uncoupled from Wnt/ β -catenin-dependent endoderm cell fate specification in *Nematostella vectensis* (Anthozoa,

- Cnidaria): Implications for the evolution of gastrulation. *EvoDevo*, 2(1).
<https://doi.org/10.1186/2041-9139-2-2>
- Kurayoshi, M., Yamamoto, H., Izumi, S., & Kikuchi, A. (2007). Post-translational palmitoylation and glycosylation of Wnt-5a are necessary for its signalling. *The Biochemical Journal*, 402(3), 515–523. <https://doi.org/10.1042/BJ20061476>
- Kwon, C., Cheng, P., King, I. N., Andersen, P., Shenje, L., Nigam, V., & Srivastava, D. (2011). Notch post-translationally regulates β -catenin protein in stem and progenitor cells. *Nature Cell Biology*, 13(10), 1244–1251. <https://doi.org/10.1038/ncb2313>
- Lai, M. B., Zhang, C., Shi, J., Johnson, V., Khandan, L., McVey, J., Klymkowsky, M. W., Chen, Z., & Junge, H. J. (2017). TSPAN12 Is a Norrin Co-receptor that Amplifies Frizzled4 Ligand Selectivity and Signaling. *Cell Reports*, 19(13), 2809–2822. <https://doi.org/10.1016/j.celrep.2017.06.004>
- Layden, M. J., Johnston, H., Amiel, A. R., Havrilak, J., Steinworth, B., Chock, T., Röttinger, E., & Martindale, M. Q. (2016). MAPK signaling is necessary for neurogenesis in *Nematostella vectensis*. *BMC Biology*, 14(1). <https://doi.org/10.1186/s12915-016-0282-1>
- Lebedeva, T., Aman, A. J., Graf, T., Niedermoser, I., Zimmermann, B., Kraus, Y., Schatka, M., Demilly, A., Technau, U., & Genikhovich, G. (2021). Cnidarian-bilaterian comparison reveals the ancestral regulatory logic of the β -catenin dependent axial patterning. *Nature Communications*, 12(1). <https://doi.org/10.1038/s41467-021-24346-8>
- Lebedeva, T., Boström, J., Mörsdorf, D., Niedermoser, I., Genikhovich, E., Adameyko, I., & Genikhovich, G. (2022). β -catenin-dependent endomesoderm specification appears to be a Bilateria-specific co-option (p. 2022.10.15.512282). *bioRxiv*. <https://doi.org/10.1101/2022.10.15.512282>
- Leclère, L., Bause, M., Sinigaglia, C., Steger, J., & Rentzsch, F. (2016). Development of the aboral domain in *Nematostella* requires β -catenin and the opposing activities of Six3/6 and Frizzled5/8. *Development (Cambridge)*, 143(10), 1766–1777. <https://doi.org/10.1242/dev.120931>
- Lee, P. N., Kumburegama, S., Marlow, H. Q., Martindale, M. Q., & Wikramanayake, A. H. (2007). Asymmetric developmental potential along the animal-vegetal axis in the anthozoan cnidarian, *Nematostella vectensis*, is mediated by Dishevelled. *Developmental Biology*, 310(1), 169–186. <https://doi.org/10.1016/j.ydbio.2007.05.040>
- Lee, P. N., Pang, K., Matus, D. Q., & Martindale, M. Q. (2006). A WNT of things to come: Evolution of Wnt signaling and polarity in cnidarians. *Seminars in Cell and Developmental Biology*, 17(2), 157–167. <https://doi.org/10.1016/j.semcd.2006.05.002>
- Lee, S., & Lee, D. K. (2018). What is the proper way to apply the multiple comparison test? *Korean Journal of Anesthesiology*, 71(5), 353–360. <https://doi.org/10.4097/kja.d.18.00242>
- Liu, H., Yin, J., Wang, H., Jiang, G., Deng, M., Zhang, G., Bu, X., Cai, S., Du, J., & He, Z. (2015). FOXO3a modulates WNT/ β -catenin signaling and suppresses epithelial-to-mesenchymal transition in prostate cancer cells. *Cellular Signalling*, 27(3), 510–518. <https://doi.org/10.1016/j.cellsig.2015.01.001>
- Liu, P., Wakamiya, M., Shea, M. J., Albrecht, U., Behringer, R. R., & Bradley, A. (1999). Requirement for Wnt3 in vertebrate axis formation. *Nature Genetics*, 22(4), 361–365. <https://doi.org/10.1038/11932>
- Logan, C. Y., & Nusse, R. (2004). The Wnt signaling pathway in development and disease.

- Annual Review of Cell and Developmental Biology*, 20, 781–810.
<https://doi.org/10.1146/annurev.cellbio.20.010403.113126>
- Loh, K. M., van Amerongen, R., & Nusse, R. (2016). Generating Cellular Diversity and Spatial Form: Wnt Signaling and the Evolution of Multicellular Animals. *Developmental Cell*, 38(6), 643–655. <https://doi.org/10.1016/j.devcel.2016.08.011>
- Lu, F. I., Thisse, C., & Thisse, B. (2011). Identification and mechanism of regulation of the zebrafish dorsal determinant. *Proceedings of the National Academy of Sciences of the United States of America*, 108(38), 15876–15880.
<https://doi.org/10.1073/pnas.1106801108>
- Lu, Y. (2018). Post-translational modifications and secretion of Wnt proteins. *Biomedical Journal of Scientific & Technical Research*, 9(4).
<https://doi.org/10.26717/bjstr.2018.09.001824>
- MacDonald, B. T., & He, X. (2012). Frizzled and LRP5/6 receptors for wnt/ β -catenin signaling. *Cold Spring Harbor Perspectives in Biology*, 4(12).
<https://doi.org/10.1101/cshperspect.a007880>
- MacDonald, B. T., Hien, A., Zhang, X., Iranloye, O., Virshup, D. M., Waterman, M. L., & He, X. (2014). Disulfide bond requirements for active Wnt ligands. *Journal of Biological Chemistry*, 289(26), 18122–18136. <https://doi.org/10.1074/jbc.M114.575027>
- MacDonald, B. T., Semenov, M. V., Huang, H., & He, X. (2011). Dissecting molecular differences between Wnt coreceptors LRP5 and LRP6. *PLoS ONE*, 6(8).
<https://doi.org/10.1371/journal.pone.0023537>
- Mao, B., Wu, W., Li, Y., Hoppe, D., Stannek, P., Glinka, A., & Niehrs, C. (2001). LDL-receptor-related protein 6 is a receptor for Dickkopf proteins. *Nature*, 411(6835), 321–325. <https://doi.org/10.1038/35077108>
- Martindale, M. Q., & Hejnal, A. (2009). A developmental perspective: Changes in the position of the blastopore during bilaterian evolution. *Developmental Cell*, 17(2), 162–174. <https://doi.org/10.1016/j.devcel.2009.07.024>
- Martinez-Bartolomé, M., & Range, R. C. (2019). A biphasic role of non-canonical Wnt16 signaling during early anterior-posterior patterning and morphogenesis of the sea urchin embryo. *Development (Cambridge)*, 146(24).
<https://doi.org/10.1242/dev.168799>
- Matoba, K., Mihara, E., Tamura-Kawakami, K., Miyazaki, N., Maeda, S., Hirai, H., Thompson, S., Iwasaki, K., & Takagi, J. (2017). Conformational Freedom of the LRP6 Ectodomain Is Regulated by N-glycosylation and the Binding of the Wnt Antagonist Dkk1. *Cell Reports*, 18(1), 32–40.
<https://doi.org/10.1016/j.celrep.2016.12.017>
- Matsui, T., Raya, Á., Kawakami, Y., Callol-Massot, C., Capdevila, J., Rodríguez-Esteban, C., & Izpisua Belmonte, J. C. (2005). Noncanonical Wnt signaling regulates midline convergence of organ primordia during zebrafish development. *Genes & Development*, 19(1), 164–175. <https://doi.org/10.1101/gad.1253605>
- McCauley, B. S., Akyar, E., Rosa Saad, H., & Hinman, V. F. (2015). Dose-dependent nuclear β -catenin response segregates endomesoderm along the sea star primary axis. *Development (Cambridge)*, 142(1), 207–217.
<https://doi.org/10.1242/dev.113043>
- McClay, D. R., Croce, J. C., & Warner, J. F. (2021). Conditional specification of endomesoderm. *Cells and Development*, 167(July).
<https://doi.org/10.1016/j.cdev.2021.203716>
- McGough, I. J., Vecchia, L., Bishop, B., Malinauskas, T., Beckett, K., Joshi, D., O'Reilly, N.,

- Siebold, C., Jones, E. Y., & Vincent, J. P. (2020). Glypicans shield the Wnt lipid moiety to enable signalling at a distance. *Nature*, *585*(7823), 85–90. <https://doi.org/10.1038/s41586-020-2498-z>
- McMahon, A. P., & Moon, R. T. (1989). Ectopic expression of the proto-oncogene int-1 in *Xenopus* embryos leads to duplication of the embryonic axis. *Cell*, *58*(6), 1075–1084. [https://doi.org/10.1016/0092-8674\(89\)90506-0](https://doi.org/10.1016/0092-8674(89)90506-0)
- Medina, A., Reintsch, W., & Steinbeisser, H. (2000). *Xenopus* frizzled 7 can act in canonical and non-canonical Wnt signaling pathways: Implications on early patterning and morphogenesis. *Mechanisms of Development*, *92*(2), 227–237. [https://doi.org/10.1016/S0925-4773\(00\)00240-9](https://doi.org/10.1016/S0925-4773(00)00240-9)
- Mehta, S., Hingole, S., & Chaudhary, V. (2021). The Emerging Mechanisms of Wnt Secretion and Signaling in Development. *Frontiers in Cell and Developmental Biology*, *9*(August), 1–17. <https://doi.org/10.3389/fcell.2021.714746>
- Metcalfe, C., Mendoza-Topaz, C., Mieszczanek, J., & Bienz, M. (2010). Stability elements in the LRP6 cytoplasmic tail confer efficient signalling upon DIX-dependent polymerization. *Journal of Cell Science*, *123*(9), 1588–1599. <https://doi.org/10.1242/jcs.067546>
- Mi, K., & Johnson, G. V. W. (2005). Role of the intracellular domains of LRP5 and LRP6 in activating the Wnt canonical pathway. *Journal of Cellular Biochemistry*, *95*(2), 328–338. <https://doi.org/10.1002/jcb.20400>
- Mirdita, M., Schütze, K., Moriwaki, Y., Heo, L., Ovchinnikov, S., & Steinegger, M. (2022). ColabFold: Making protein folding accessible to all. *Nature Methods*, *19*(6), 679–682. <https://doi.org/10.1038/s41592-022-01488-1>
- Momose, T., Derelle, R., & Houliston, E. (2008). A maternally localised Wnt ligand required for axial patterning in the cnidarian *Clytia hemisphaerica*. *Development*, *135*(12), 2105–2113. <https://doi.org/10.1242/dev.021543>
- Mukherjee, S., Chaturvedi, P., Rankin, S. A., Fish, M. B., Wlizla, M., Paraiso, K. D., Macdonald, M., Chen, X., Weirauch, M. T., Blitz, I. L., Cho, K. W. Y., & Zorn, A. M. (2020). Sox17 and b-catenin co-occupy wntresponsive enhancers to govern the endoderm gene regulatory network. *ELife*, *9*, 1–26. <https://doi.org/10.7554/ELIFE.58029>
- Mulligan, K. A., Fuerer, C., Ching, W., Fish, M., Willert, K., & Nusse, R. (2012). Secreted Wingless-interacting molecule (Swim) promotes long-range signaling by maintaining Wingless solubility. *Proceedings of the National Academy of Sciences of the United States of America*, *109*(2), 370–377. <https://doi.org/10.1073/pnas.1119197109>
- Muncie, J. M., Ayad, N. M. E., Lakins, J. N., Xue, X., Fu, J., & Weaver, V. M. (2020). Mechanical Tension Promotes Formation of Gastrulation-like Nodes and Patterns Mesoderm Specification in Human Embryonic Stem Cells. *Developmental cell*, *55*(6), 679–694.e11. <https://doi.org/10.1016/j.devcel.2020.10.015>
- Murillo-Garzón, V., & Kypka, R. (2017). WNT signalling in prostate cancer. *Nature Reviews Urology*, *14*(11), 683–696. <https://doi.org/10.1038/nrurol.2017.144>
- Newman, S. A. (1974). The interaction of the organizing regions in hydra and its possible relation to the role of the cut end in regeneration. *Development*, *31*(3), 541–555. <https://doi.org/10.1242/dev.31.3.541>
- Niedermoser, I., Lebedeva, T., & Genikhovich, G. (2022). Sea anemone Frizzled receptors play partially redundant roles in the oral-aboral axis patterning. *Development*, *7*. <https://doi.org/10.1242/dev.200785>
- Nile, A. H., & Hannoush, R. N. (2016). Fatty acylation of Wnt proteins. *Nature Chemical*

- Biology*, 12(2), 60–69. <https://doi.org/10.1038/nchembio.2005>
- Nile, A. H., Mukund, S., Stanger, K., Wang, W., & Hannoush, R. N. (2017). Unsaturated fatty acyl recognition by Frizzled receptors mediates dimerization upon Wnt ligand binding. *Proceedings of the National Academy of Sciences of the United States of America*, 114(16), 4147–4152. <https://doi.org/10.1073/pnas.1618293114>
- Owlarn, S., & Bartscherer, K. (2016). Go ahead, grow a head! A planarian's guide to anterior regeneration. *Regeneration*, 3(3), 139–155. <https://doi.org/10.1002/reg2.56>
- Pani, A. M., Favichia, M., Goldstein, B., & Comprehensive, L. (2023). Long-distance Wnt transport in axons highlights cell type-specific modes of Wnt transport in vivo. *bioRxiv* 2023.05.03.539245; doi: <https://doi.org/10.1101/2023.05.03.539245>
- Pani, A. M., & Goldstein, B. (2018). Direct visualization of a native Wnt in vivo reveals that a long-range Wnt gradient forms by extracellular dispersal. *ELife*, 7, e38325. <https://doi.org/10.7554/eLife.38325>
- Park, H. W., Kim, Y. C., Yu, B., Moroishi, T., Mo, J. S., Plouffe, S. W., Meng, Z., Lin, K. C., Yu, F. X., Alexander, C. M., Wang, C. Y., & Guan, K. L. (2015). Alternative Wnt Signaling Activates YAP/TAZ. *Cell*, 162(4), 780–794. <https://doi.org/10.1016/j.cell.2015.07.013>
- Pascual-Carreras, E., Marín-barba, M., Castillo-lara, S., Coronel-córdoba, P., Magri, M. S., Wheeler, G. N., Gómez-skarmeta, J. L., Abril, J. F., Saló, E., & Adell, T. (2023). Wnt / β -catenin signalling is required for pole- specific chromatin remodeling during planarian regeneration. *Nature Communications*, 14, 298 (2023). <https://doi.org/10.1038/s41467-023-35937-y>
- Pei, J., & Grishin, N. V. (2012). Cysteine-rich domains related to Frizzled receptors and Hedgehog-interacting proteins. *Protein Science*, 21(8), 1172–1184. <https://doi.org/10.1002/pro.2105>
- Petersen, C. P., & Reddien, P. W. (2008). Smed- β catenin-1 Is Required for Anteroposterior Blastema Polarity in Planarian Regeneration. *Science*, 319(5861), 327–330. <https://doi.org/10.1126/science.1149943>
- Petersen, C. P., & Reddien, P. W. (2009). Wnt Signaling and the Polarity of the Primary Body Axis. *Cell*, 139(6), 1056–1068. <https://doi.org/10.1016/j.cell.2009.11.035>
- Piao, S., Lee, S. H., Kim, H., Yum, S., Stamos, J. L., Xu, Y., Lee, S. J., Lee, J., Oh, S., Han, J. K., Park, B. J., Weis, W. I., & Ha, N. C. (2008). Direct inhibition of GSK3 β by the phosphorylated cytoplasmic domain of LRP6 in Wnt/ β -catenin signaling. *PLoS ONE*, 3(12). <https://doi.org/10.1371/journal.pone.0004046>
- Pires-daSilva, A., & Sommer, R. J. (2003). The evolution of signalling pathways in animal development. *Nature Reviews Genetics*, 4(1), 39–49. <https://doi.org/10.1038/nrg977>
- Poggi, L., Casarosa, S., & Carl, M. (2018). An eye on the wnt inhibitory factor Wif1. *Frontiers in Cell and Developmental Biology*, 6(DEC), 1–7. <https://doi.org/10.3389/fcell.2018.00167>
- Pond, K. W., Doubrovinski, K., & Thorne, C. A. (2020). WNT/ β -catenin signaling in tissue self-organization. *Genes*, 11(8), 1–18. <https://doi.org/10.3390/genes11080939>
- Port, F., & Basler, K. (2010). Wnt Trafficking: New Insights into Wnt Maturation, Secretion and Spreading. *Traffic*, 11(10), 1265–1271. <https://doi.org/10.1111/j.1600-0854.2010.01076.x>
- Pukhlyakova, E., Aman, A. J., Elsayad, K., & Technau, U. (2018). β -Catenin-dependent mechanotransduction dates back to the common ancestor of Cnidaria and Bilateria. *Proceedings of the National Academy of Sciences of the United States of America*, 115(24), 6231–6236. <https://doi.org/10.1073/pnas.1713682115>

- Raisch, J., Côté-Biron, A., & Rivard, N. (2019). A role for the WNT co-receptor LRP6 in pathogenesis and therapy of epithelial cancers. *Cancers*, *11*(8). <https://doi.org/10.3390/cancers11081162>
- Range, R. C., Angerer, R. C., & Angerer, L. M. (2013). Integration of Canonical and Noncanonical Wnt Signaling Pathways Patterns the Neuroectoderm Along the Anterior-Posterior Axis of Sea Urchin Embryos. *PLoS Biology*, *11*(1). <https://doi.org/10.1371/journal.pbio.1001467>
- Recouvreux, P., Pai, P., Torro, R., Ludányi, M., Méléneq, P., Boughzala, M., Bertrand, V., & Lenne, P. (2023). Establishment of Wnt ligand-receptor organization and cell polarity in the *C. elegans* embryo. *bioRxiv* 2023.01.17.524363; doi: <https://doi.org/10.1101/2023.01.17.524363>
- Rigo-Watermeier, T., Kraft, B., Ritthaler, M., Wallkamm, V., Holstein, T., & Wedlich, D. (2012). Functional conservation of *Nematostella* Wnts in canonical and noncanonical Wnt-signaling. *Biology Open*, *1*(1), 43–51. <https://doi.org/10.1242/bio.2011021>
- Ritthaler, M. (2012). Funktionelle Konservierung der Wnt-Liganden in *Nematostella vectensis*. [Dissertation]. <https://doi.org/10.11588/heidok.00013177>
- Röper, J.-C., Mitrossilis, D., Stirnemann, G., Waharte, F., Brito, I., Fernandez-Sanchez, M.-E., Baaden, M., Salamero, J., & Farge, E. (2018). The major β -catenin/E-cadherin junctional binding site is a primary molecular mechano-transducer of differentiation in vivo. *ELife*, *7*. <https://doi.org/10.7554/eLife.33381>
- Röttinger, E. (2021). *Nematostella vectensis*, an emerging model for deciphering the molecular and cellular mechanisms underlying whole-body regeneration. *Cells*, *10*(10). <https://doi.org/10.3390/cells10102692>
- Röttinger, E., Dahlin, P., & Martindale, M. Q. (2012). A Framework for the Establishment of a Cnidarian Gene Regulatory Network for ‘Endomesoderm’ Specification: The Inputs of β -Catenin/TCF Signaling. *PLoS Genetics*, *8*(12). <https://doi.org/10.1371/journal.pgen.1003164>
- Rulifson, E. J., Wu, C. H., & Nusse, R. (2000). Pathway specificity by the bifunctional receptor frizzled is determined by affinity for Wingless. *Molecular Cell*, *6*(1), 117–126. [https://doi.org/10.1016/S1097-2765\(05\)00018-3](https://doi.org/10.1016/S1097-2765(05)00018-3)
- Salinas-Saavedra, M., Rock, A. Q., & Martindale, M. Q. (2018). Germ layer-specific regulation of cell polarity and adhesion gives insight into the evolution of mesoderm. *ELife*, *7*, e36740. <https://doi.org/10.7554/eLife.36740>
- Schaefer, K. N., Bonello, T. T., Zhang, S., Williams, C. E., Roberts, D. M., McKay, D. J., & Peifer, M. (2018). Supramolecular assembly of the beta-catenin destruction complex and the effect of Wnt signaling on its localization, molecular size, and activity in vivo. *PLoS Genetics*, *14*(4). <https://doi.org/10.1371/journal.pgen.1007339>
- Schaefer, K. N., Pronobis, M. I., Williams, C. E., Zhang, S., Bauer, L., Goldfarb, D., Yan, F., Major, M. B., & Peifer, M. (2020). Wnt regulation: Exploring Axin-Dishevelled interactions and defining mechanisms by which the SCF E3 ubiquitin ligase is recruited to the destruction complex. *Molecular Biology of the Cell*, *31*(10), 992–1014. <https://doi.org/10.1091/mbc.E19-11-0647>
- Schenkelaars, Q., Fierro-Constain, L., Renard, E., Hill, A. L., & Borchiellini, C. (2015). Insights into Frizzled evolution and new perspectives. *Evolution and Development*, *17*(2), 160–169. <https://doi.org/10.1111/ede.12115>
- Schihada, H., Kowalski-Jahn, M., Turku, A., & Schulte, G. (2021). Deconvolution of WNT-induced Frizzled conformational dynamics with fluorescent biosensors. *Biosensors and Bioelectronics*, *177*(November 2020), 112948–112948.

- <https://doi.org/10.1016/j.bios.2020.112948>
- Schulte, G., & Bryja, V. (2007). The Frizzled family of unconventional G-protein-coupled receptors. *Trends in Pharmacological Sciences*, 28(10), 518–525.
<https://doi.org/10.1016/j.tips.2007.09.001>
- Schulte, G., & Wright, S. C. (2018). Frizzleds as GPCRs – More Conventional Than We Thought! *Trends in Pharmacological Sciences*, 39(9), 828–842.
<https://doi.org/10.1016/j.tips.2018.07.001>
- Schwarz, C., & Hadjantonakis, A. K. (2020). Cells under Tension Drive Gastrulation. *Developmental Cell*, 55(6), 669–670. <https://doi.org/10.1016/j.devcel.2020.11.023>
- Scimone, M. L., Lapan, S. W., & Reddien, P. W. (2014). A forkhead Transcription Factor Is Wound-Induced at the Planarian Midline and Required for Anterior Pole Regeneration. *PLOS Genetics*, 10(1), e1003999.
<https://doi.org/10.1371/journal.pgen.1003999>
- Semaan, C., Henderson, B. R., & Molloy, M. P. (2019). Proteomic screen with the proto-oncogene beta-catenin identifies interaction with Golgi coatomer complex I. *Biochemistry and Biophysics Reports*, 19(April), 100662–100662.
<https://doi.org/10.1016/j.bbrep.2019.100662>
- Semenov, M. V., Habas, R., MacDonald, B. T., & He, X. (2007). SnapShot: Noncanonical Wnt Signaling Pathways. *Cell*, 131(7), 1378.e1-1378.e2.
<https://doi.org/10.1016/j.cell.2007.12.011>
- Sherwood, D. R., & McClay, D. R. (2001). LvNotch signaling plays a dual role in regulating the position of the ectoderm-endoderm boundary in the sea urchin embryo. *Development*, 128(12), 2221–2232. <https://doi.org/10.1242/dev.128.12.2221>
- Shook, D. R., Kasprovicz, E. M., Davidson, L. A., & Keller, R. (2018). Large, long range tensile forces drive convergence during *Xenopus* blastopore closure and body axis elongation. *ELife*, 7, e26944. <https://doi.org/10.7554/eLife.26944>
- Sinigaglia, C., Peron, S., Eichelbrenner, J., Chevalier, S., Steger, J., Barreau, C., Houliston, E., & Leclère, L. (2020). Pattern regulation in a regenerating jellyfish. *ELife*, 9, 1–33.
<https://doi.org/10.7554/ELIFE.54868>
- Somorjai, I. M. L., Martí-Solans, J., Diaz-Gracia, M., Nishida, H., Imai, K. S., Escrivà, H., Cañestro, C., & Albalat, R. (2018). Wnt evolution and function shuffling in liberal and conservative chordate genomes. *Genome Biology*, 19(1).
<https://doi.org/10.1186/s13059-018-1468-3>
- Stamos, J. L., Chu, M. L. H., Enos, M. D., Shah, N., & Weis, W. I. (2014). Structural basis of GSK-3 inhibition by N-terminal phosphorylation and by the Wnt receptor LRP6. *ELife*, 2014(3). <https://doi.org/10.7554/eLife.01998>
- Steinmetz, P. R. H., Aman, A., Kraus, J. E. M., & Technau, U. (2017). Gut-like ectodermal tissue in a sea anemone challenges germ layer homology. *Nature Ecology and Evolution*, 1(10), 1535–1542. <https://doi.org/10.1038/s41559-017-0285-5>
- Strittmatter, B. G., Jerde, T. J., & Hollenhorst, P. C. (2021). Ras/ERK and PI3K/AKT signaling differentially regulate oncogenic ERG mediated transcription in prostate cells. *PLOS Genetics*, 17(7), e1009708.
<https://doi.org/10.1371/journal.pgen.1009708>
- Sumanas, S., Strege, P., Heasman, J., & Ekker, S. C. (2000). The putative Wnt receptor *Xenopus* frizzled-7 functions upstream of β -catenin in vertebrate dorsoventral mesoderm patterning. *Development*, 127(9), 1981–1990.
<https://doi.org/10.1242/dev.127.9.1981>
- Swartz, S. Z., Tan, T. H., Perillo, M., Fakhri, N., Wessel, G. M., Wikramanayake, A. H., &

- Cheeseman, I. M. (2021). Polarized Dishevelled dissolution and reassembly drives embryonic axis specification in sea star oocytes. *Current Biology*, 31(24), 5633–5641.e4. <https://doi.org/10.1016/j.cub.2021.10.022>
- Takada, R., Satomi, Y., Kurata, T., Ueno, N., Norioka, S., Kondoh, H., Takao, T., & Takada, S. (2006). Monounsaturated fatty acid modification of Wnt protein: Its role in Wnt secretion. *Developmental Cell*, 11(6), 791–801. <https://doi.org/10.1016/j.devcel.2006.10.003>
- Tamai, K., Semenov, M., Kato, Y., Spokony, R., Liu, C., Katsuyama, Y., Hess, F., Saint-Jeannet, J.-P., & He, X. (2000). LDL-receptor-related proteins in Wnt signal transduction. *Nature*, 407(6803), 530–535. <https://doi.org/10.1038/35035117>
- Tamulonis, C., Postma, M., Marlow, H. Q., Magie, C. R., de Jong, J., & Kaandorp, J. (2011). A cell-based model of *Nematostella vectensis* gastrulation including bottle cell formation, invagination and zippering. *Developmental Biology*, 351(1), 217–228. <https://doi.org/10.1016/j.ydbio.2010.10.017>
- Tang, X., Wu, Y., Belenkaya, T. Y., Huang, Q., Ray, L., Qu, J., & Lin, X. (2012). Roles of N-glycosylation and lipidation in Wg secretion and signaling. *Developmental Biology*, 364(1), 32–41. <https://doi.org/10.1016/j.ydbio.2012.01.009>
- Tao, Q., Yokota, C., Puck, H., Kofron, M., Birsoy, B., Yan, D., Asashima, M., Wylie, C. C., Lin, X., & Heasman, J. (2005). Maternal Wnt11 activates the canonical Wnt signaling pathway required for axis formation in *Xenopus* embryos. *Cell*, 120(6), 857–871. <https://doi.org/10.1016/j.cell.2005.01.013>
- Tsutsumi, N., Hwang, S., Hansen, S., Waghray, D., Wang, N., Glassman, C. R., Caveney, N. A., Jude, K. M., Janda, C. Y., Hannoush, N. & Garcia, K. C. (2022). Structure of the Wnt-Frizzled-LRP6 initiation complex reveals the basis for co-receptor discrimination. *bioRxiv* 2022.10.21.513178; doi: <https://doi.org/10.1101/2022.10.21.513178>
- Tursch, A., Bartsch, N., Mercker, M., Schluter, J., Lommel, M., Marciniak-Czochra, A., Ozbek, S., & Holstein, T. W. (2022). Injury-induced MAPK activation triggers body axis formation in *Hydra* by default Wnt signaling. *Proceedings of the National Academy of Sciences of the United States of America*, 119(35), 1–12. <https://doi.org/10.1073/pnas.2204122119>
- Umbhauer, M., Djiane, A., Goisset, A., & Penzo-me, A. (2000). The C-cytoplasmic Lys-Thr-X-X-X-Trp motif in frizzled receptors mediates Wnt/B-catenenin signaling. *The EMBO journal*, 19(18), 4944–4954. <https://doi.org/10.1093/emboj/19.18.4944>
- van Amerongen, R. (2012). Alternative Wnt pathways and receptors. *Cold Spring Harbor Perspectives in Biology*, 4(10). <https://doi.org/10.1101/cshperspect.a007914>
- Van Itallie, E. S., Field, C. M., Mitchison, T. J., & Kirschner, M. W. (2023). Dorsal lip maturation and initial archenteron extension depend on Wnt11 family ligands. *Developmental Biology*, 493, 67–79. <https://doi.org/10.1016/j.ydbio.2022.10.013>
- Vastenhouw, N. L., Cao, W. X., & Lipshitz, H. D. (2019). The maternal-to-zygotic transition revisited. *Development (Cambridge, England)*, 146(11). <https://doi.org/10.1242/dev.161471>
- Veeman, M. T., Axelrod, J. D., & Moon, R. T. (2003). A second canon: Functions and mechanisms of β -catenin-independent Wnt signaling. *Developmental Cell*, 5(3), 367–377. [https://doi.org/10.1016/S1534-5807\(03\)00266-1](https://doi.org/10.1016/S1534-5807(03)00266-1)
- Villarroel, A., del Valle-Pérez, B., Fuertes, G., Curto, J., Ontiveros, N., Garcia de Herreros, A., & Duñach, M. (2020). Src and Fyn define a new signaling cascade activated by canonical and non-canonical Wnt ligands and required for gene transcription and cell

- invasion. *Cellular and Molecular Life Sciences*, 77(5), 919–935.
<https://doi.org/10.1007/s00018-019-03221-2>
- Voloshanenko, O., Gmach, P., Winter, J., Kranz, D., & Boutros, M. (2017). Mapping of Wnt-Frizzled interactions by multiplex CRISPR targeting of receptor gene families. *FASEB Journal*, 31(11), 4832–4844. <https://doi.org/10.1096/fj.201700144R>
- Wang, Y., Chang, H., Rattner, A., & Nathans, J. (2016). Frizzled Receptors in Development and Disease. In *Current Topics in Developmental Biology* (Vol. 117, pp. 113–139). Academic Press Inc. <https://doi.org/10.1016/bs.ctdb.2015.11.028>
- Wang, Z., Tacchelly-Benites, O., Yang, E., Thorne, C. A., Nojima, H., Lee, E., & Ahmed, Y. (2016). Wnt/Wingless Pathway Activation Is Promoted by a Critical Threshold of Axin Maintained by the Tumor Suppressor APC and the ADP-Ribose Polymerase Tankyrase. *Genetics*, 203(1), 269–281. <https://doi.org/10.1534/genetics.115.183244>
- Warner, J., Amiel, A., Johnston, H., Röttinger, E., Warner, J., Amiel, A., Johnston, H., & Röttinger, E. (2020). Regeneration is a partial redeployment of the embryonic gene network. *HAL Id: Hal-03021512*. <https://doi.org/10.1101/658930>
- Warner, J. F., Guerlais, V., Amiel, A. R., Johnston, H., Nedoncelle, K., & Röttinger, E. (2018). NvERTx: A gene expression database to compare embryogenesis and regeneration in the sea anemone *Nematostella vectensis*. *Development (Cambridge)*, 145(10). <https://doi.org/10.1242/dev.162867>
- Weaver, C., & Kimelman, D. (2004). Move it or lose it: Axis specification in *Xenopus*. *Development*, 131(15), 3491–3499. <https://doi.org/10.1242/dev.01284>
- Whyte, J. L., Smith, A. A., & Helms, J. A. (2012). Wnt signaling and injury repair. *Cold Spring Harbor Perspectives in Biology*, 4(8), 1–13.
<https://doi.org/10.1101/cshperspect.a008078>
- Wijesena, N., Sun, H., Kumburegama, S., & Wikramanayake, A. H. (2022). Distinct Frizzled receptors independently mediate endomesoderm specification and primary archenteron invagination during gastrulation in *Nematostella*. *Developmental Biology*, 481(July 2021), 215–225. <https://doi.org/10.1016/j.ydbio.2021.11.002>
- Wikramanayake, A. H., Hong, M., Lee, P. N., Pang, K., Byrum, C. A., Bince, J. M., Xu, R., & Martindale, M. Q. (2003). An ancient role for nuclear β -catenin in the evolution of axial polarity and germ layer segregation. *Nature*, 426(6965), 446–450.
<https://doi.org/10.1038/nature02113>
- Willert, K., Brown, J. D., Danenberg, E., Duncan, A. W., Weissman, I. L., Reya, T., Yates, J. R., 3rd, & Nusse, R. (2003). Wnt proteins are lipid-modified and can act as stem cell growth factors. *Nature*, 423(6938), 448–452. <https://doi.org/10.1038/nature01611>
- Willert, K., & Nusse, R. (2012). Wnt proteins. *Cold Spring Harbor Perspectives in Biology*, 4(9), 1–13. <https://doi.org/10.1101/cshperspect.a007864>
- Willert, K., Shibamoto, S., & Nusse, R. (1999). Wnt-induced dephosphorylation of Axin releases β -catenin from the Axin complex. *Genes and Development*, 13(14), 1768–1773. <https://doi.org/10.1101/gad.13.14.1768>
- Wu, D., & Pan, W. (2010). GSK3: A multifaceted kinase in Wnt signaling. *Trends in Biochemical Sciences*, 35(3), 161–168. <https://doi.org/10.1016/j.tibs.2009.10.002>
- Wu, G., Huang, H., Abreu, J. G., & He, X. (2009). Inhibition of GSK3 phosphorylation of β -catenin via phosphorylated PPPSPXS motifs of Wnt coreceptor LRP6. *PLoS ONE*, 4(3). <https://doi.org/10.1371/journal.pone.0004926>
- Wu, X., Tu, X., Joeng, K. S., Hilton, M. J., Williams, D. A., & Long, F. (2008). Rac1 Activation Controls Nuclear Localization of β -catenin during Canonical Wnt Signaling. *Cell*, 133(2), 340–353. <https://doi.org/10.1016/j.cell.2008.01.052>

- Wylie, A. D., Fleming, J. A. G. W., Whitener, A. E., & Lekven, A. C. (2014). Post-transcriptional regulation of *wnt8a* is essential to zebrafish axis development. *Developmental Biology*, 386(1), 53–63. <https://doi.org/10.1016/j.ydbio.2013.12.003>
- Xu, Q., Wang, Y., Dabdoub, A., Smallwood, P. M., Williams, J., Woods, C., Kelley, M. W., Jiang, L., Tasman, W., Zhang, K., & Nathans, J. (2004). Vascular Development in the Retina and Inner Ear: Control by Norrin and Frizzled-4, a High-Affinity Ligand-Receptor Pair. *Cell*, Vol. 116, pp. 883–895.
- Yang, J., Tan, C., Darken, R. S., Wilson, P. A., & Klein, P. S. (2002). β -Catenin/Tcf-regulated transcription prior to the midblastula transition. *Development*, 129(24), 5743–5752. <https://doi.org/10.1242/dev.00150>
- Yu, H., Ye, X., Guo, N., & Nathans, J. (2012). Frizzled 2 and frizzled 7 function redundantly in convergent extension and closure of the ventricular septum and palate: Evidence for a network of interacting genes. *Development (Cambridge)*, 139(23), 4383–4394. <https://doi.org/10.1242/dev.083352>
- Zhan, T., Rindtorff, N., & Boutros, M. (2017). Wnt signaling in cancer. *Oncogene*, 36(11), 1461–1473. <https://doi.org/10.1038/onc.2016.304>
- Zhang, X., Abreu, J. G., Yokota, C., MacDonald, B. T., Singh, S., Coburn, K. L. A., Cheong, S.-M., Zhang, M. M., Ye, Q.-Z., Hang, H. C., Steen, H., & He, X. (2012). Tiki1 is required for head formation via Wnt cleavage-oxidation and inactivation. *Cell*, 149(7), 1565–1577. <https://doi.org/10.1016/j.cell.2012.04.039>
- Zheng, X., Lin, J., Wu, H., Mo, Z., Lian, Y., Wang, P., Hu, Z., Gao, Z., Peng, L., & Xie, C. (2019). Forkhead box (FOX) G1 promotes hepatocellular carcinoma epithelial-Mesenchymal transition by activating Wnt signal through forming T-cell factor-4/Beta-catenin/FOXG1 complex. *Journal of Experimental & Clinical Cancer Research*, 38(1), 475. <https://doi.org/10.1186/s13046-019-1433-3>